THE
PHYSICAL REVIEW
A Journal of Experimental and Theoretical Physics
VOL. 44, No. 3 AUGUST 1, 1933 SECOND SERIES

Diffuse Scattering of X-Rays from Sylvine. IV. Scattering at High Temperatures

G. G. HARVEY,* *Ryerson Physical Laboratory, University of Chicago*
(Received June 13, 1933)

Effect of temperature on the diffuse scattering of Mo $K\alpha$ radiation from sylvine.—Intensity measurements have been carried out at 630°K and 1020°K which is about as close to the melting point (1049°K) as it is feasible to work. It is again found that the results are in good agreement with the formula $S=(f^2-F^2)/Z+(1-f^2/Z^2)/(1+\alpha \text{ vers } \phi)^2$ provided experimental values of F are used rather than assuming $F=fe^{-M}$ where M is given by the Debye-Waller formula.

I. INTRODUCTION

THE effect of temperature on the diffuse scattering from crystals has been considered both theoretically and experimentally in a number of papers.[1, 2, 3, 4, 5, 6, 7, 8] Debye, in a paper[1] concerned mainly with the effect of temperature on regular reflection, showed that for a simple cubic crystal consisting of point atoms the intensity of the diffuse scattering should be given by $(1-e^{-M})$ times the scattering from an amorphous substance; M is given by

$$M=\frac{6h^2}{mk\Theta}\left\{\frac{\phi(z)}{z}+\frac{1}{4}\right\}\frac{\sin^2\theta}{\lambda^2} \qquad (1)$$

if the existence of zero-point energy is assumed; if there is no zero-point energy the quantity $\frac{1}{4}$ in Eq. (1) is to be omitted. In this formula h is Planck's constant, k Boltzmann's constant, m the mass of a single atom, Θ the Debye characteristic temperature[9] of the crystal, $z=\Theta/T$ where T is the absolute temperature,

$$\phi(z)=(1/z)\int_0^z ydy/(e^y-1),$$

2θ the angle of scattering and λ the wave-length of the incident radiation. Later work by Waller[10] showed that M should be replaced by $2M$. If we define S as the scattering per electron[11] in terms of the Thomson value[12]

$$I_e=I_0(e^4/2m^2c^4)(1+\cos^2\phi),$$

where I_e is the scattering per unit solid angle in the direction ϕ and I_0 is the intensity of the incident radiation, i.e., if

$$S=I_\phi/ZI_e, \qquad (2)$$

where I_ϕ is the intensity of the scattered radiation and Z the atomic number of the scatterer,

* National Research Fellow.

[1] P. Debye, Ann. d. Physik **43**, 49 (1914).
[2] G. E. M. Jauncey, Phys. Rev. **37**, 1193 (1931).
[3] G. E. M. Jauncey and G. G. Harvey, Phys. Rev. **37**, 1203 (1931).
[4] Y. H. Woo, Phys. Rev. **38**, 6 (1931).
[5] G. E. M. Jauncey, Phys. Rev. **20**, 421 (1922).
[6] W. D. Claus, Phys. Rev. **38**, 604 (1931).
[7] G. E. M. Jauncey and G. G. Harvey, Phys. Rev. **38**, 1925 (1931).
[8] G. G. Harvey, Phys. Rev. **43**, 707 (1933).
[9] P. Debye, Ann. d. Physik **39**, 789 (1912).
[10] I. Waller, *Uppsala Dissertation* 1925; Zeits. f. Physik **17**, 398 (1923).
[11] A. H. Compton, Phys. Rev. **35**, 925 (1930).
[12] J. J. Thomson, *Conduction of Electricity through Gases*, p. 325, 2nd edition.

then according to the Debye theory as modified by Waller the diffuse scattering from a simple cubic crystal consisting of point atoms should be given by

$$S=Z(1-e^{-2M}). \tag{3}$$

Later work by Jauncey and Harvey[2, 3] showed that the scattering from such a crystal consisting of atoms having spatial extension should, on the classical theory, be given by

$$S=(f^2-F^2)/Z+1-\left(\sum_1^Z E_r^2\right)/Z, \tag{4}$$

where f is the atomic structure factor of the atom at rest, F the atomic structure factor including the effect of thermal agitation and E_r the contribution to f due to the rth electron in an atom. If all the electrons are assumed equivalent then $\sum E_r^2=f^2/Z$. If the atoms consist of points then $f=Z$ and since $F=fe^{-M}$ Eq. (4) reduces to Eq. (3), as of course it must. Simultaneously and independently Woo[4] showed that on taking account of the fact that part of the radiation is scattered incoherently due to the Compton effect and hence has its intensity diminished by the Breit-Dirac factor[13, 14] the scattering should be given by

$$S=\frac{f^2-F^2}{Z}+\frac{1-\left(\sum_1^Z E_r^2\right)/Z}{(1+\alpha \text{ vers } \phi)^3}, \tag{5}$$

where $\alpha=h/mc\lambda$. The first term gives the coherent and the second the incoherent part of the scattering.

The experiments of Jauncey[5] on rocksalt and calcite and of Claus[6] on rocksalt showed that the Debye theory was inadequate to account for the observed effect and although Claus found that the Waller modification seemed to work at low temperatures it did not fit the facts at high temperatures and as he points out, it should not be expected to fit since the atoms are not points. Claus found that Eq. (4), (or Eq. (5)), seemed to account for the observed effect at high temperatures but not at low temperatures. Jauncey and Harvey[7] working with sylvine and using the same apparatus and method as used by Claus (inhomogeneous radiation and photographic measurement of intensity) obtained similar results at low temperatures. Results at high temperature were not published as it was felt that the measurements were not reliable. It may be here stated, however, that an apparent increase of about twenty percent in the intensity of the diffuse scattering was found at large angles whereas Eqs. (4) and (5) predict only a small increase. It is to be noted also that Claus found an apparent trend in the same direction for rocksalt. In view of the success of Eqs. (4) and (5) in correlating the scattering from gases[11, 15] and reflexion from crystals[16, 17] with the diffuse scattering from crystals[18, 19] and in predicting the absolute intensity of the diffuse scattering at room temperature[3, 20, 21, 22, 23] the apparent discrepancy with the results at other than room temperature was regarded with some suspicion. That this suspicion was justified, at low temperatures at least, may be seen from more recent work on sylvine at the temperature of liquid air[8] when homogeneous radiation is used and measurements are made with an ionization chamber and electrometer. The theory was there found to fit very closely. Accordingly the present investigation on the diffuse scattering from sylvine at high temperatures was undertaken.

II. Experimental

The apparatus used has been previously[23] described with the exception of the heating chamber. This consisted of a coil of Nichrome wire wound on a refractory core surrounding the steel crystal mounting. The whole was completely

[13] G. Breit, Phys. Rev. **27**, 242 (1926).
[14] P. A. M. Dirac, Proc. Roy. Soc. **A111**, 405 (1926).
[15] E. O. Wollan, Phys. Rev. **37**, 862 (1931).
[16] R. W. James and Elsie M. Firth, Proc. Roy. Soc. **A117**, 62 (1927).
[17] R. W. James and G. W. Brindley, Proc. Roy. Soc. **A121**, 155 (1928).
[18] G. E. M. Jauncey, Phys. Rev. **38**, 1 (1931).
[19] G. E. M. Jauncey and G. G. Harvey, Phys. Rev. **38**, 1071 (1931).
[20] G. G. Harvey, Phys. Rev. **38**, 593 (1931).
[21] G. E. M. Jauncey and P. S. Williams, Phys. Rev. **41**, 127 (1932).
[22] G. E. M. Jauncey and Ford Pennell, Phys. Rev. **43**, 505 (1933).
[23] G. G. Harvey, Phys. Rev. **43**, 591 (1933).

inclosed in an asbestos container one-half inch thick, thin mica windows being provided for the x-rays. Temperatures were measured by a nickel-iron thermocouple beside the crystal just out of the x-ray beam. As the stray scattering from the furnace and crystal mounting was considerable and as Mo $K\alpha$ radiation is rather strongly absorbed in mica it was not deemed feasible to use the balanced filter method as in the previous work since the necessity of taking the difference of comparable currents, both of which are small, and again taking differences to correct for the stray scattering was considered too unreliable. Instead a rather thick ZrO_2 filter was used. This, however, will not effect the results to any appreciable extent, except possibly at small angles, since the radiation penetrating the filter was predominantly Mo $K\alpha$. The experiment then consisted in measuring the ratio, τ, of the ionization current with the crystal at temperature T to that with the crystal at room temperature (295°K) for a fixed scattering angle ϕ and various values of θ the angle between the primary beam and the normal to the crystal face, both above and below $\theta=\phi/2$ and interpolating to obtain this ratio for $\theta=\phi/2$. The values of this ratio, so measured, are given in Table I for 630°K and 1020°K.

TABLE I.

ϕ	$(\sin\phi/2)/\lambda$	$\tau_{630°K}$ D-W	J-B	Exp.	$\tau_{1020°K}$ D-W	J-B	Exp.
10°	0.123	1.37	1.43	1.40	1.77	2.10	2.22
20°	0.245	1.50	1.52	1.57	1.99	2.26	2.30
30°	0.365	1.32	1.35	1.35	1.53	1.64	1.64
40°	0.482	1.24	1.26	1.28	1.35	1.38	1.40
50°	0.596	1.17	1.18	1.18	1.22	1.23	1.27
60°	0.708	1.11	1.12	(1.10–1.15)	1.13	1.13	(1.10–1.15)
70°	0.804	1.07		(1.05–1.10)	1.07		(1.05–1.10)
80°	0.905	1.035		(1.00–1.05)	1.035		(1.00–1.05)
90°	0.995	1.015		(1.00–1.02)	1.015		(1.00–1.02)
100°	1.080	1.005		(1.00)	1.005		(1.00)
110°	1.154	1.00		(1.00)	1.00		(1.00)

III. DISCUSSION

We may write

$$S_1=(f^2-F^2)/Z \tag{6}$$

and

$$S_2=1-\left(\sum_1^Z E_r^2\right)/Z, \tag{7}$$

where S_1 is the coherent scattering factor and $S_2/(1+\alpha \text{ vers } \phi)^3$ the incoherent scattering factor. The sum of S_1 and S_2 will be denoted by $S_{\text{class.}}$, as usual, and gives the classical value of the total scattering. The actual scattering, as given by Eq. (5) may be written

$$S=S_1+S_2/(1+\alpha \text{ vers } \phi)^3. \tag{8}$$

However, neither $S_{\text{class.}}$ nor S is measured directly. What is actually measured is the ionization current produced by the scattered radiation or, in the case of the temperature effect, the ratio of the ionization currents at the two temperatures in question. If this ratio is denoted by τ then

$$\tau=\frac{S_{1,\,(1)}+TS_2(K_\phi/K_0)/(1+\alpha \text{ vers } \phi)^3}{S_{1,\,(2)}+TS_2(K_\phi/K_0)/(1+\alpha \text{ vers } \phi)^3}, \tag{9}$$

wherein it is assumed that F is the only quantity affected by temperature. $S_{1,\,(1)}$ is the value of S_1 at temperature T_1 and $S_{1,\,(2)}$ the value at T_2; the factor T is due to the fact that the incoherent radiation is more completely absorbed in the crystal itself.[24] K_ϕ is the percentage absorption of the incoherent radiation in the ionization chamber and K_0 the same quantity for the coherent radiation. Values of τ were calculated for the two temperatures 630°K and 1020°K with respect to 295°K. In these calculations f values of James and Brindley[25] were used and $\sum E_r^2$ was taken as f^2/Z. However, the values of τ are practically unaltered by making this assumption. In order to obtain values of F at high temperatures the following procedure was used. James and Brindley have measured[17] the integrated reflection from sylvine for a number of spectra at various temperatures and although it was found that the Debye-Waller theory breaks down at high temperatures the values of $(\lambda^2/\sin^2\theta)\log(\rho_T/\rho_{290})$ when plotted against temperature fall on a smooth curve which is approximately a parabola; ρ denotes the integrated reflexion and is given by

$$\rho=\frac{N^2\lambda^3}{2\mu}\frac{e^4}{m^2c^4}(\sum fe^{-M})^2\frac{1+\cos^2 2\theta}{2\sin 2\theta}. \tag{10}$$

Hence from this empirical curve it is possible to obtain experimental values of ΔM, the change in the temperature factor M from 290°K to T°K,

[24] G. E. M. Jauncey and O. K. Defoe, Phil. Mag. **1**, 711 (1926).

[25] R. W. James and G. W. Brindley, Phil. Mag. **12**, 81 (1931).

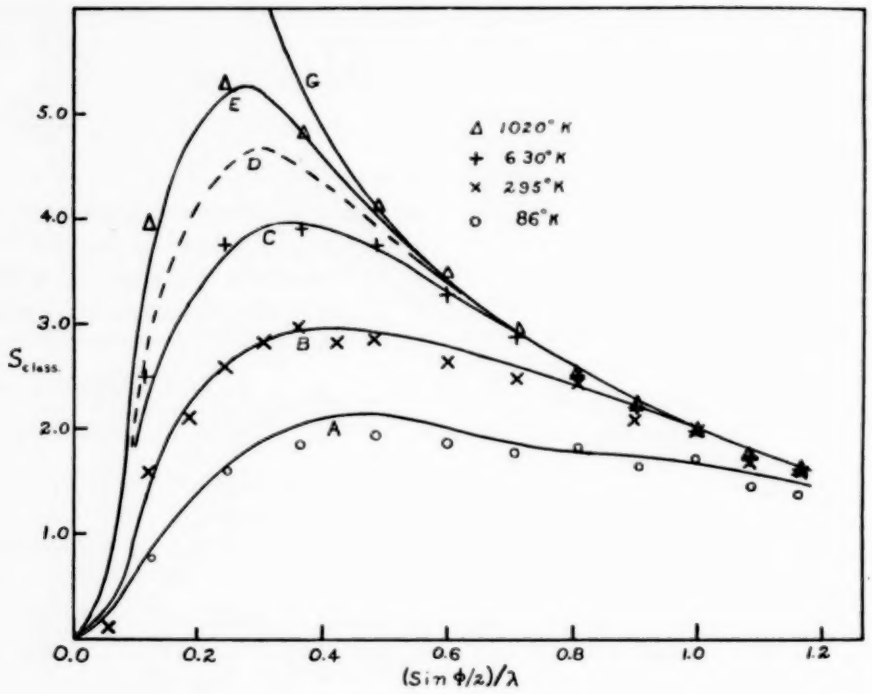

FIG. 1.

and thus values of $F_T = F_{290}e^{-\Delta M}$. James and Brindley's measurements extend only to 936°K and it was necessary to extrapolate to 1020°K. This may introduce considerable uncertainty, especially since the measurements of ρ at high temperature are subject to considerable error due to the extremely weak intensity. Further, sylvine melts at 1049°K and it is doubtful whether an extrapolation up to a temperature so near the melting point is justifiable. The values of the temperature factor τ so calculated are denoted by J–B in Table I. τ was also calculated assuming the Debye-Waller theory to be valid, i.e., by taking M from Eq. (1) and putting $F = fe^{-M}$. These values are also given in Table I, (D–W), together with the experimental ratios. At 630°K it does not make much difference whether M is taken from Eq. (1) or from James and Brindley's data and the experimental ratios cannot be said to distinguish between the two. At 1020°K, however, the difference is quite marked at small angles and here the experimental ratios definitely favor the results of James and Brindley. Fig. 1 shows the results plotted in the form of $S_{class.}$; the curves[8, 23] for 86°K and 295°K are also included for completeness. In obtaining these curves $S_{class.}$ for 295°K has been multiplied by τ_T to obtain $S_{class.}$ at T°K since, as pointed out for the low temperature work,[8] for radiation as soft as Mo $K\alpha$ and with almost complete absorption in the ionization chamber the ratio of the ionization currents is practically identical with the ratio of the $S_{class.}$ values. This fact enables experimental values of $S_{class.}$ to be obtained without making any assumption as to what quantities are affected by temperature. In general, for hard radiation and small absorption in the ionization chamber both TK_ϕ/K_0 and $TK_\phi/K_0(1+\alpha \text{ vers } \phi)^3$ may differ considerably from unity and the only way to obtain the *experimental* ratio of $S_{class.}$ or S values at two temperatures, without assuming that the entire change is due to a change in F, would be to carry out another experiment in which S_1/S_2 or $S_1/(S_1+S_2)$ was determined at the two temperatures, and this is a difficult thing to do with any accuracy.[26] In such a case it would be better merely to compare measured and calcu-

[26] G. E. M. Jauncey and G. G. Harvey, Phys. Rev. **40**, 329 (1932).

lated values of τ as measurement of the diffuse scattering is probably not an accurate method for determining F.

Curve D in Fig. 1 is based on the Debye-Waller value of M at 1020°K while E is based on the results of James and Brindley. At 630°K the Debye-Waller curve is only slightly below the James and Brindley curve C and is omitted. At first sight it would appear that the results are in very close agreement with James and Brindley's values of F. Too much significance should not be attached to this close agreement since, as pointed out above, the F values at 1020°K are rather uncertain and the absolute value of $S_{\text{class.}}$ at small angles might thus be considerably different from that shown in curve E. This, however, can hardly be the case at large angles where any reasonable assumption concerning M leads to insignificant values of F. It is thus satisfactory to find that the large angle points closely follow curve G which is calculated on the assumption $F=0$ and gives the scattering from a monatomic gas[11] consisting of K^+ and Cl^-. At small angles, where the temperature effect is most marked, any reflected radiation present would tend to make the experimental values of τ too near unity so that the experimental points may be too low. The presence of radiation of shorter wave-length would also have the same effect since $\tau \rightarrow 1$ for large values of $(\sin \phi/2)/\lambda$. On the whole, however, it is felt that the experimental results are reasonably accurate and that there is no large discrepancy between the measured values of S and those calculated from Eq. (5).

To what extent the relation[19]

$$S_{\text{gas}} = (S + F^2/Z)_{\text{crystal}} \qquad (11)$$

is verified at various temperatures, S_{gas} being taken as independent of temperature, may be approximately judged from the departure of the experimental points from the theoretical curves in Fig. 1. Jauncey and Pennell[22] have measured a quantity S_{th}, which is related to $S+F^2/Z$ for a powdered crystal, and have found good agreement between calculated and measured values. More recently[27] they have measured this quantity at low temperature and have found a slight decrease of one or two percent at small angles. They have suggested that this may indicate a change in f with temperature. However, as may be seen from their paper[22] S_{th} is equal to S_u plus a correction term involving F, this term being most important at small angles. Thus S_{th} should vary slightly irrespective of a change in f. That $S+F^2/Z$ decreases with decreasing temperature (or increases with increasing temperature) is not inconsistent with the results shown in Fig. 1 but the author would be unwilling to assert that his results are inconsistent with even the opposite conclusion. It would be an extremely difficult matter to measure the diffuse scattering from a single crystal to an accuracy of one percent due to the necessity of using as wide slits as possible in order to obtain a measurable intensity and yet narrow enough so as to be sure that only diffuse scattering is measured.

The author wishes to take this opportunity to express his appreciation to Professor Arthur H. Compton for his interest in the work and the use of the Ryerson Physical Laboratory.

---

[27] Ford Pennell and G. E. M. Jauncey, Bull. Am. Phys. Soc. **8**, No. 4, p. 25 (1933). Paper presented at Chicago meeting, June, 1933.

Scattering of X-Rays from Powdered Crystals at Low Temperatures

G. E. M. JAUNCEY* AND FORD PENNELL, *Department of Physics, Washington University, St. Louis*

(Received June 3, 1933)

Jauncey has suggested that the true atom form factor of a crystal may decrease at low temperatures. With the method of Jauncey and Pennell, x-rays have been scattered from powdered crystals of KCl and NaF at various mean angles ϕ over a fairly wide range of $(\sin \frac{1}{2}\phi)/\lambda$ at each mean angle ϕ with the powdered crystal first at 295°K and then at 103°K. Changes of the order of 1 or 2 percent in the intensity of the scattered rays were observed. Various possible explanations for this change are discussed. It is concluded that from 295 to 103°K the true atom form factors of NaF do not change, while those of KCl either do not change or decrease by very small amounts which are less than, but of the same magnitude as, those indicated in a recent paper by Harvey.

1. INTRODUCTION

IN a recent paper entitled *Remarks on the Scattering of X-Rays by Gases and Crystals*, Jauncey[1] has discussed the possibility that the true atom form factor f may be a function of the temperature. More recently Jauncey and Pennell[2] have shown that, if x-rays are scattered over a fairly wide range of $(\sin \frac{1}{2}\phi)/\lambda$ by a powdered crystal into an ionization chamber set at a mean angle ϕ, the intensity of the scattered x-rays entering the window of the ionization chamber is given by

$$S(\text{powder}) = G - H + L, \tag{1}$$

where

$$G = \int \left\{ \frac{f^2}{Z} + \frac{(1 - f''^2/Z^2) K_\phi T_\phi}{K_0 (1 + \alpha \text{ vers } \phi)^3} \right\} I d\lambda \Big/ \int I d\lambda, \tag{2}$$

$$H = \int (F^2/Z) I d\lambda \Big/ \int I d\lambda \tag{3}$$

and

$$L = \left\{ \frac{1}{4\pi} \sum_r \frac{F_r^2}{Z} \cdot \frac{p_r \lambda_r I(\lambda_r)}{r^4} \right\} \Big/ \int I d\lambda. \tag{4}$$

We shall refer to this paper by Jauncey and Pennell as the previous paper. In this previous paper it has been shown that so long as the scattering angle ϕ is not too small, $L - H$ is small and consequently S(powder) is approximately equal to G. The symbol G refers to the scattering from the fictitious gas obtained by changing the crystal into a gas without disturbing the electron structures of the atoms of the crystal. At room temperature it has been established by Jauncey and Harvey[3,4] that G very nearly equals the S(gas) for the corresponding real gas in the case of sylvine and argon. However, according to Jauncey,[1] it seems that G for the crystal may depart from S(gas) at low temperatures. If this is the case S(powder) may be a function of the temperature. In the present research this point has been tested as regards powdered KCl and powdered NaF.

2. EXPERIMENTAL METHOD

The same experimental method and x-rays with the same spectral distribution of intensity were used as were described in the previous paper. X-rays were scattered from the powdered crystal first at room temperature and then at liquid air temperature into the ionization chamber set at a mean angle ϕ. The crystal in both cases was set so that the normal to the crystal bisected the angle of scattering ϕ and in both cases was mounted in the cooling chamber which is described by Williams.[5] The widths of the defining slits and of the ionization chamber

* The senior author was aided in part by a grant from the Rockefeller Foundation to Washington University for research in science.

[1] G. E. M. Jauncey, Phys. Rev. **42**, 453 (1932).

[2] G. E. M. Jauncey and Ford Pennell, Phys. Rev. **43**, 505 (1933).

[3] G. E. M. Jauncey and G. G. Harvey, Phys. Rev. **38**, 1071 (1931).

[4] G. G. Harvey, Phys. Rev. **43**, 591 (1933).

[5] P. S. Williams, Rev. Sci. Inst. **4**, 334 (1933).

window were such that the variation in the angle of scattering for a given chamber setting was 5°. The "liquid air temperature" of the crystal was found, by means of a nickel-copper thermocouple, to be about 103°K.

3. Experimental Results

The ratio of the ionization current produced by the rays scattered into the ionization chamber set at an angle ϕ when the powdered crystal was at liquid air temperature to the current when the crystal was at room temperature was obtained for each of several values of ϕ. The ratios, together with their probable errors as calculated from the experimental readings, are shown in Table I. It is seen that with certain exceptions

Table I. *Ratio of the scattering from powdered crystals at 103°K to that from crystals at 295°K.*

ϕ	KCl	NaF
12°	0.965±0.006	1.015±0.008
15°	0.985±0.006	0.990±0.006
18°	0.995±0.008	0.960±0.006
21°	0.990±0.010	1.013±0.010
24°	0.972±0.010	
27°	0.998±0.012	
30°	0.996±0.012	
33°	0.983±0.012	
36°	0.974±0.014	

the ratios differ from unity by no more or very little more than the probable error.

4. Discussion

Insofar as the ratios shown in Table I differ from unity by more than the probable error, there is some indication of the difference being real. Any true difference might be due to a change in G, in $L-H$, or to changes in both G and $L-H$ with the temperature.

First, let us consider the possibility of a change in $L-H$. Since, according to Eqs. (3) and (4), both L and H are functions of the F values and since the F values depend upon the temperature, L and H also depend upon the temperature. Also the F_r values used in calculating L are subject to small changes due to the thermal contraction of the crystal on cooling from 295 to 103°K. Using data[6] on the thermal expansion of KCl we find that the grating space of KCl changes from about 3.14A at 295°K to about 3.12A at 103°K. Using James and Brindley's[7] experimental F values for KCl at liquid air temperature, we obtained curves similar to II and III in Fig. 4 of the previous paper. Also by using these F values a curve for H similar to I in Fig. 4 of the previous paper was obtained. Taking differences between the ordinates of the curves similar to III and I, we obtained values of $L-H$ at liquid air temperature. The values of $L-H$ at 103°K and at 295°K are shown in Table II. By referring to

Table II. *Values of $L-H$ for KCl.*

ϕ	103°K	295°K	Ratio
12°	0.65	0.62	1.004
15°	0.06	0.02	1.007
18°	−0.13	0.00	0.974

the previous paper it is seen that S_{exp} at $\phi=12°$ for KCl at 295°K is 7.13. In going from 295 to 103°K the value of $L-H$ changes from 0.62 to 0.65 so that the value of S_{exp} at 103°K should be $7.13+(0.65-0.62)=7.16$. The ratio of S_{exp} at 103°K to that at 295°K should therefore be 1.004. The ratios for other angles are shown in the fourth column of Table II. It is seen that because of the variation of $L-H$ with the temperature the ratios differ somewhat from unity. It must be remarked here that the values of L and H are calculated from F values read off curves drawn through the experimental F values obtained by James and Brindley. These F values naturally are subject to experimental error. We do not believe, therefore, that the changes in the values of $L-H$ shown in Table II should be regarded as exact. Consequently, the ratios shown in Table II should also not be regarded as exact but only as indicating the order of magnitude of the changes in the ratios to be expected due to a change of $L-H$ with the temperature.

In the case of NaF, experimental F values at liquid air temperature were not available and so we calculated the F values both at room and at liquid air temperatures from the wave mechanics f values given in Table III of the previous paper, combined with the Debye-Waller temperature

[6] Int. Crit. Tab. **3**, 43.

[7] R. W. James and G. W. Brindley, Proc. Roy. Soc. **A121**, 155 (1928).

factor. In order to determine this factor, it is first necessary to find the characteristic temperature of NaF. Comparing the values of the molecular heat[8] of NaF at −150, −100 and −50°C with the Debye specific heat function,[9] we find an average characteristic temperature of 427°K. Values of $L-H$ at 103°K and at 295°K can now be found and ratios for NaF calculated. The ratios range from 0.989 to 1.005.

We are of the opinion that, with perhaps the exception of the ratio at $\phi=18°$, the experimental ratios for NaF do not differ from unity by more than the probable error plus the difference in the respective ratios produced by the change of $L-H$ with temperature. We believe that there is no necessity to suppose a change of G with temperature. Hence, there is no definite evidence that the true atom form factors, or f values, of NaF change in going from 295 to 103°K.

In the case of KCl, since all the experimental ratios are less than unity, we believe that a slight change in G with temperature may be indicated. Harvey[10] has recently measured the diffuse scattering of x-rays of wave-length 0.71A from KCl at room and liquid air temperatures and finds that a small decrease in the f values at liquid air temperature may be indicated. A change in G as defined by Eq. (2) is principally dependent upon a change in f and not upon a change in f''. We have therefore used Harvey's f values at room and liquid air temperatures to enable us to calculate the change in G. If now we suppose that the change in S_{exp} with temperature is due to a change in G and not in $L-H$, we obtain the ratios given in Table III. It is seen that our experimental ratios in the range from 15 to 24° as shown in Table I are closer to unity than is indicated by the ratios calculated from Harvey's suggested f values for liquid air temperature.

TABLE III. *Theoretical ratios due to the change of G with temperature—KCl.*

ϕ	Ratio
10°	0.975
15°	0.964
20°	0.972
25°	1.000

5. CONCLUSION

We have observed small changes in the values of S(powder) for KCl and NaF in going from 295 to 103°K. The observed changes can be explained as due to the small changes in $L-H$ (see Eqs. (3) and (4)) plus the experimental error. Depending upon the angle ϕ, the change in $L-H$ is sometimes an increase and sometimes a decrease. In the case of NaF, since the change in S(powder) is an increase at some angles and a decrease at other angles, there is no definite indication of changes in the values of G (see Eq. (2)) and therefore no indication of changes in the true atom form factors of NaF. In the case of KCl, since the change in S(powder) is a decrease at all angles, there is an indication of a decrease in the values of G and therefore an indication of a slight decrease in the true atom form factors of KCl in going from 295 to 103°K. The decreases in the true atom form factors of KCl, if they exist at all, are less than, but of the same order of magnitude as, the decreases suggested recently by Harvey.[10]

[8] Int. Crit. Tab. **5**, 100.
[9] *See* J. K. Roberts, *Heat and Thermodynamics*, p. 404.
[10] G. G. Harvey, Phys. Rev. **43**, 707 (1933).

Structure of the X-Ray *K* Absorption Limits of the Elements Manganese to Zinc

A. H. BARNES, *Physics Laboratory, Columbia University*

(Received April 24, 1933)

The double crystal spectrometer was employed to investigate the main absorption edge of the free elements Mn, Fe, Co, Ni, Cu, and Zn, and the oxides Mn_2O_3, Fe_2O_3, Co_2O_3, Ni_2O_3, CuO, and ZnO. Definite structure was exhibited by all the free elements except Zn, and all the oxides except ZnO. The oxide edges were all displaced toward shorter wave-length. The observed width of the edges varied from 15 volts in the case of Zn to 23 volts for Fe.

PREVIOUS investigations of the x-ray absorption edges have been made for the most part with the single crystal spectrometer, and usually for the purpose of inspecting either the position of the main edge or the secondary structure on the short wave-length side. The principal contributions in this field have been made by Lindh,[1] Coster,[2] Lindsey,[3] and Hanawalt.[4]

Davis and Purks[5] have shown that the greater resolving power of the double crystal spectrometer provides a more effective means of examining absorption limits. With this instrument Hull[6] has recently studied the *L* limits of mercury and its compounds.

In the present work the double crystal spectrometer was employed in an investigation of the *K* absorption edge of the elements Mn, Fe, Co, Ni, Cu, and Zn, together with Mn_2O_3, Fe_2O_3, Co_2O_3, Ni_2O_3, CuO and ZnO.

APPARATUS

The double x-ray spectrometer was of the universal type crystal mounting described by Spencer.[7] This type of instrument has two advantages: first, by making use of the focussing effect and placing the absorption screen at the position of the focus, behind the second crystal, the movement of the x-ray beam across the sample is reduced to a minimum; and, second, by locating the position of certain emission lines on the divided circle the wave-length of any point on the absorption edge can be determined by using these lines as standards of reference.

The ionization chamber was 4 cm in diameter and 9 cm long, and was filled with methyl bromide. The ionization current was amplified by an F.P. 54 Pliotron feeding into a Leeds and Northrup type R galvanometer of sensitivity 10,000 megohms.

Water-cooled tungsten-target x-ray tubes were used throughout the investigation. The x-ray beam passed out of the tube through a thin glass window 3μ thick. To reduce air absorption the crystals and the entire path of the x-ray beam were enclosed by a flexible tube system filled with hydrogen at atmospheric pressure.

It is of importance that the absorbing screen be of uniform thickness throughout. Otherwise the slight shift of the x-ray beam across the screen may cause it to pass through regions of varying thickness and thus introduce a variation in the energy of the transmitted beam. The effect of a possible nonuniformity was overcome by oscillating the absorption screen at right angles to the x-ray beam. The screen was mounted on horizontal guide rods and the motion produced by an electrically driven cam. The screen was thus oscillated several times per second, and since the ionization current readings each extended over a period of 10 seconds or longer, the effect of any irregularities in the screen was completely smoothed out.

Absorption screens were made by coating thin paper with castor oil upon which the absorbing substance was sifted until optimum thickness

[1] Lindh, Zeits. f. Physik **31**, 210 (1925); **63**, 106 (1930).
[2] Coster and Veldkamp, Zeits. f. Physik **74**, 191 (1932); **70**, 306 (1931).
[3] Lindsey and Vorhees, Phil. Mag. **6**, 910 (1928); Lindsey and Kievit, Phys. Rev. **36**, 648 (1930).
[4] Hanawalt, Zeits. f. Physik **70**, 293 (1931).
[5] Davis and Purks, Phys. Rev. **36**, 336 (1928).
[6] Hull, Phys. Rev. **40**, 676 (1932).
[7] Spencer, Phys. Rev. **38**, 618 (1931).

was reached. All the oxides and the free elements Mn, and Co, were used in fine powdered form. The free elements Fe, Ni, Cu, and Zn, were used in thin foils. The possibility of any chemical change in the samples produced by x-radiation was reduced to a minimum by placing the absorber behind the second crystal where the intensity was small.

The slit limiting the beam of x-rays was placed at the ionization chamber. This slit was 1 cm wide and 0.8 cm high. The maximum deviation due to vertical divergence was 0.03 x.u. The effect of the crystals likewise was negligible.

In obtaining the curves the procedure was to make three determinations at each point: one with the free element as absorber, one with the oxide, and one without either absorber, each determination consisting of three or more individual readings. Correction could then be made for variation in the intensity of the spectrum obtained without the absorber, as well as obviating any error which might have been introduced by slight displacements of the apparatus, had the curves been run separately. The curves so obtained were repeated a number of times.

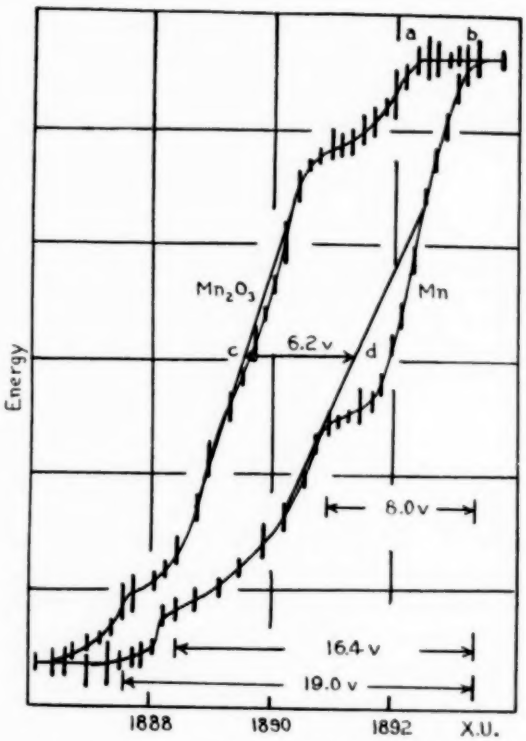

FIG. 1. Absorption edges of Mn and Mn_2O_3.

EXPERIMENTAL RESULTS

Figs. 1 to 6 show the absorption curves obtained for the free elements Mn, Fe, Co, Ni, Cu, and Zn, and the oxides Mn_2O_3, Fe_2O_3, Co_2O_3, Ni_2O_3, CuO, and ZnO. All the curves except those of Zn and ZnO show a definite structure.

The graphs are so plotted that the weight to be attached to the variations in slope is readily apparent. The position of the midpoint of the vertical lines is the mean of the ionization current readings taken at a given setting of the second crystal of the spectrometer. The length of the line has the following significance. Its extension on either side of the midpoint, bears the same relation to the interval from maximum to minimum absorption on the graph, as the average deviation of the ionization current readings from the mean (a. d.), bears to the total change in ionization current corresponding to maximum and minimum absorption. The curves thus plotted are the results of individual runs. They are to be taken as typical of the three or more sets of observations made on each of the sub-

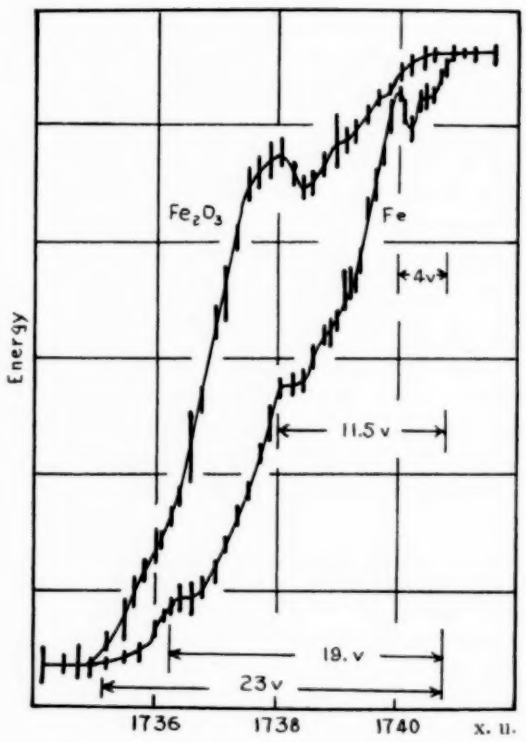

FIG. 2. Absorption edges of Fe and Fe_2O_3.

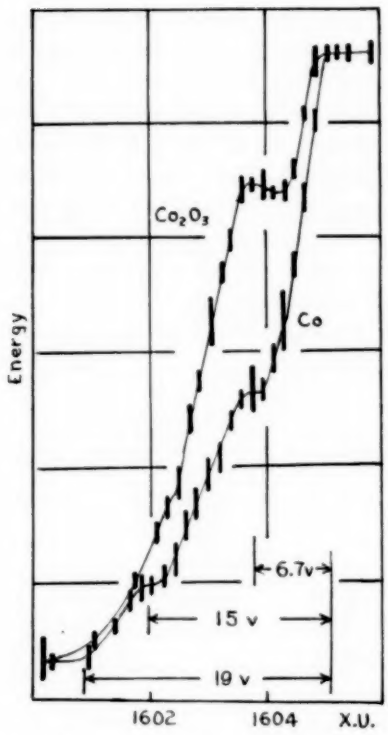

FIG. 3. Absorption edges of Co and Co_2O_3.

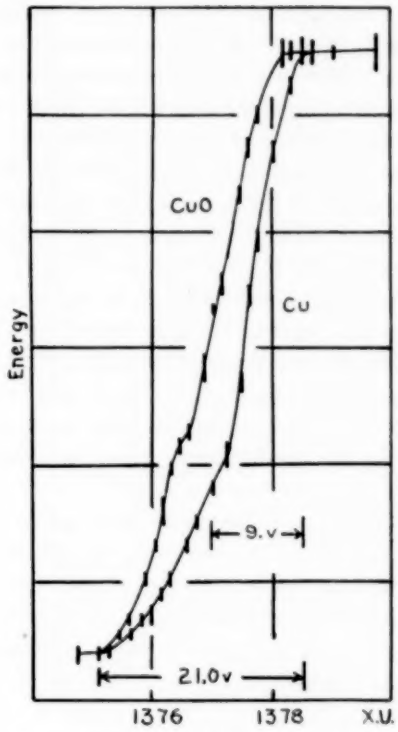

FIG. 5. Absorption edges of Cu and CuO.

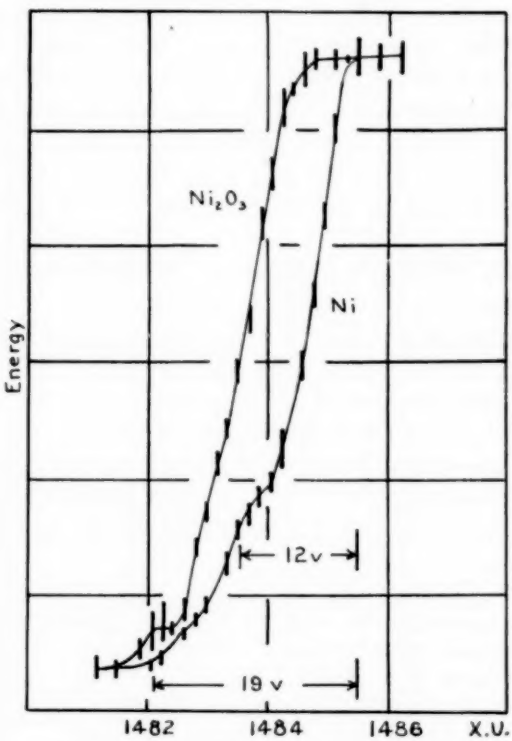

FIG. 4. Absorption edges of Ni and Ni_2O_3.

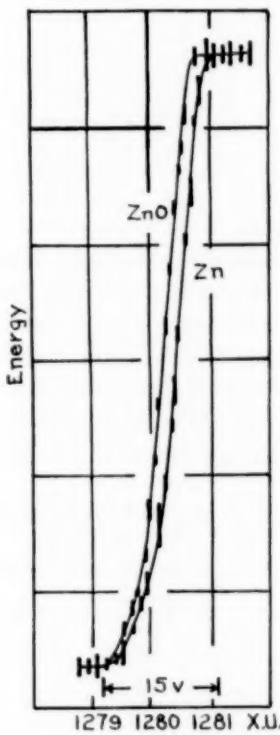

FIG. 6. Absorption edges of Zn and ZnO.

stances investigated. The deviation of the readings taken at any given spectrometer setting varied of course for different runs. The average probable error for all cases varied from 2 percent in the case of Cu to 4 percent for Fe_2O_3.

The wave-lengths in the region of the edges were determined by locating the position of the tungsten L lines and by using them as standards of reference. The lines used were $W_L\beta_1$ at 1279.17 x.u. and $W_L\alpha_2$ at 1484.38 x.u. It was possible to check the precision of the instrument by checking these lines against each other. The measured $d\lambda$ between the two lines agreed with the tabulated value to within a few hundredths of an x.u. The curves have accordingly been plotted with abscissae expressed in x.u.

The displacement of the oxides has been measured in two ways. In the first, the displacement of the position of initial observable increase in absorption has been determined. Values thus obtained are listed in Table I. The estimated precision is also indicated.

TABLE I. *Displacement of oxide edges with position of initial increase in absorption* $(a-b)$.

	x.u.	volts
Mn_2O_3	0.9±0.3	3.3±0.9
Fe_2O_3	0.6±0.3	2.3±1.0
Co_2O_3	0.2±0.2	1.0±1.0
Ni_2O_3	0.7±0.4	4.0±1.5
CuO	0.5±0.3	3.0±1.8
ZnO	0.3±0.2	2.0±1.5

To determine the displacement of the oxide edge as a whole the following construction was made. On each curve lines were drawn through points whose ordinates were $\frac{1}{4}$ and $\frac{3}{4}$ of the value of the maximum ordinate (see Fig. 1). The interval between the midpoints of these lines was then taken as a measure of the displacement of the oxide edge. Values obtained in this manner are listed in Table II. Displacements thus measured should more nearly compare to single crystal photographic determinations.

TABLE II. *Displacement of oxide edges with projected position* $(c-d)$.

	x.u.	volts
Mn_2O_3	1.8	6.2
Fe_2O_3	1.6	6.3
Co_2O_3	0.8	3.7
Ni_2O_3	0.9	4.7
CuO	0.6	3.7
ZnO	0.2	1.6

Table III lists the overall width of the observed edges in x.u. and in volts. The interval taken in each case was from the termination of the region of continuous absorption on the long wave-length side of the curve to the beginning of the region of continuous absorption on the short wave-length side. The oxides have approximately the same width as the free elements and exhibit similar discontinuities.

TABLE III. *Width of edges.*

Element	x.u.	volts
Mn	5.5±0.5	19±1.7
Fe	5.7±0.5	23±2.0
Co	3.9±0.5	19±2.4
Ni	3.2±0.5	19±2.8
Cu	3.4±0.5	21±3.2
Zn	2.1±0.4	15±2.8

This investigation, in agreement with work previously done by others, indicates that the absorption edges are of considerable width. The difficulty arises of deciding which point on the curve is to be taken in specifying the wave-length of the absorption edge. Previously, when the edges appeared to be symmetrical, some arbitrary point either at half or three-quarters of the interval from maximum to minimum absorption, has been used. A point so chosen, however, has no significance as far as electron transitions are concerned.

By referring to a table of wave-lengths of x-ray emission lines it will be seen that the wave-lengths of the $K\beta_2$ [8] lines of the elements Mn to Zn are very nearly the same (within limits of experimental error) as the wave-lengths at which the initial increase in absorption occurs.

The generally accepted theory of the K absorption edge[9, 10, 11, 12, 13] is that it corresponds t the ejection of a K electron to the various u

[8] In notation used by Siegbahn, *Spektroskopie der Roentgenstrahlen*, this would be $K\beta_5$ for elements Mn to Cu.

[9] Kossel, Zeits. f. Physik **1**, 119 (1920),

[10] Stoner, Phil. Mag. **2**, 97 (1926).

[11] Coster and Wolff, Nature **124**, 652 (1929).

[12] Sandstrom, Zeits. f. Physik **66**, 784 (1930).

[13] Kawata, Kyoto Coll. Sci. Mem. **14**, 55 (1931).

occupied levels of the atom. In the usual scheme of arrangement of electrons the outer M level of the atoms Mn, Fe, Co, Ni (and probably Cu in the solid state)[11] is not completely filled. Inspection of the curves reveals that Mn, Fe, Co, Ni, and Cu, show irregularities in the edge, while the curve for Zn is smooth and without observable structure. This might be considered an indication that the uncompleted M shell is responsible for the structure observed.

In conclusion the writer wishes to thank Professor Bergen Davis for suggesting this problem, and for his interest throughout the course of the experiment.

Relative Intensities and Transition Probabilities of the *K*-Series Lines of the Elements 24 to 52 by the Ionization Chamber Method

JOHN H. WILLIAMS,* *Ryerson Physical Laboratory, University of Chicago*

(Received May 25, 1933)

Experiments on the ionization currents produced by x-ray lines of wave-lengths 2.29, 1.93 and 1.66A entering a double ionization chamber filled with methyl iodide, methyl bromide, argon, air, and sulphur dioxide have been carried out. The current ratios obtained when corrected for the fraction of the direct beam absorbed in the front chamber were found not to vary by more than 1.5 percent in these gases. The conclusion is reached that the ionization chamber is a suitable instrument for measuring relative intensities of x-ray lines of different wave-lengths in the region 0.4 to 2.3A. The relative intensities of the *K*-series lines of twenty elements from Cr (24) to Te (52) were examined under controlled conditions and on correction for various factors yield a variation of relative intensity with atomic number. α_2/α_1 remains constant at approximately 0.50 throughout the range. β_1/α_1 rises steeply from a value of 0.161 at Co (27) to 0.274 at Sr (38) then less rapidly to 0.306 at Te (52). β_2/α_1 rises steeply from a value of 0.0036 at Zn (30) to 0.0450 at Zr (40) and then in a more linear fashion to 0.0735 at Te. Equations obtained from measurements on the absorption coefficients of various materials are:

Mica $\mu = 36.56\lambda^{2.76}$	from 0.4 to 2.3A
Cellophane $\mu = 3.52\lambda^{2.66}$	from 0.6 to 2.3A
CH_3Br $\mu/\rho = 19.2\ \lambda^{2.79}$	from 1.1 to 2.3A
CH_3I $\mu/\rho = 65.46\lambda^{2.62}$	from 0.4 to 0.9A.

A treatment is given and discussed for the absorption of the x-rays within the target. The resultant correction is small and on application to the observed relative intensities the ratio of the transition probabilities for the *K*-series lines of these elements is obtained.

PART I

Introduction

THE first part of this paper deals with a test of the method of measuring the relative intensities of x-ray spectrum lines by an ionization chamber in the wave-length region 2.286 to 1.656A.

When one attempts to measure relative intensities by this method the question arises: are the ionic saturation currents caused by the x-rays entering the gas contained in the ionization chamber proportional to the actual intensity of the x-rays? For light gases the principal ionization is caused by the action of the photoelectrons and recoil electrons and it is only in heavier gases excited by a frequency greater than their *K* frequency, or in very heavy gases their *L* frequency, that the fluorescence radiation plays an important rôle. Many experiments[1] have been performed with air and other gases in the wave-length region 0.5 to 1.5A to measure the energy, ϵ, expended by a β-ray in the formation of a pair of ions. These researches lead to various values of ϵ, but all of them show no appreciable variation of ϵ with λ. Any such variation would invalidate measurements of the relative intensity of two x-ray beams of different wave-lengths by the ionization method. However, if ϵ is constant the conclusion is reached that the ionic saturation currents observed in an ionization chamber, where all the x-ray energy is transformed into β-ray energy and all the β-rays reach the end of their ionizing range before striking the boundaries of the chamber, will yield a true measure of the intensities of x-ray beams in the above wave-length region.

Recently Allison and Andrew[2] have attacked this problem in the wave-length region 0.6 to 1.5A, using a double ionization chamber and various gases. As it is not practicable to use such light gases as air because of the small absorption of x-ray energy, one must consider the effects resulting from the use of heavier gases. Fluorescence radiation may be excited in the gas itself or

* National Research Fellow

[1] Stockmeyer, Ann. d. Physik **12**, 71 (1932); O. Gaertner, Ann. d. Physik **3**, 322 (1929); **10**, 825 (1931); Crowther and Bond, Phil. Mag. **6**, 401 (1928), Steenbeck, Ann. d. Physik **87**, 811 (1928).

[2] Allison and Andrew, Phys. Rev. **38**, 441 (1931).

primary radiation may be scattered, and these radiations may escape to the walls of the chamber without being absorbed. Allison and Andrew have restated very clearly the corrections of Martin and Compton[3] to be applied in these cases. Their results showed that an ionization chamber of proper design gives a true measure of the relative intensity of x-ray spectrum lines.

If ϵ is independent of λ the expression for the relative power, $P_{\alpha\beta}$, of two lines α and β can be expressed in the form:

$$P_{\alpha\beta}=I_\alpha F_\beta R_\beta/I_\beta F_\alpha R_\alpha \equiv I_{\alpha\beta}F_{\beta\alpha}R_{\beta\alpha}, \qquad (1)$$

where I is the ionic saturation current,

$$F\equiv(1-e^{-\mu l}), \qquad (2)$$

and

$$R=1-\frac{\tau_K}{\mu}w_K\lambda\sum_i\frac{f_i}{\lambda_i}e^{-\tau_i r}-\frac{\sigma}{\mu}e^{-\tau r}. \qquad (3)$$

From Eq. (2) we see that F is the fraction of the energy removed from the x-ray beam in passing through the chamber of length l when filled with a gas which has an absorption coefficient μ. This factor could be measured experimentally by means of a second chamber placed directly behind the first. In Eq. (3) R is the expression for the loss of energy due to two causes; first, the conversion of energy into fluorescence radiation and the incomplete absorption of this radiation before reaching the boundaries of the chamber, and second, the scattering of the primary radiation and loss of such scattered radiation to the walls. In this equation τ_K is the absorption coefficient of the fluorescence radiation in the gas, w_K is the Auger[4] coefficient, f_i is the fractional part of the total number of quanta emitted having the wave-length λ_i of the ith line of the fluorescence series, r is the effective radius of the chamber, and σ is the scattering coefficient of the gas for the primary wave-length λ.

Allison and Andrew's results showed that even under the most unfavorable conditions, i.e., when the two lines lie on opposite sides of the K absorption limit of the gas filling the chamber, the relative intensities can be accurately determined and checked with those obtained under more favorable conditions.

Measurements

Since the purpose of the present experiment was to measure the relative intensities of x-ray spectrum lines of longer as well as of the same wave-lengths as had been previously examined, it was advisable to test the constancy of ϵ with λ in the region 1.5 to 2.3A. This was done with the apparatus and method of Allison and Andrew.[2] In order to obtain a source of x-rays yielding two lines of comparable intensity and reasonable wave-length separation targets of chromium-iron and iron-nickel alloys were used. The $K\alpha$-lines of wave-lengths 1.656, 1.933 and 2.286A were thus available. By observing the ratio of the intensity of Cr $K\alpha$ to Fe $K\alpha$ and Fe $K\alpha$ to Ni $K\alpha$ one can test whether there is any *significant* change of ϵ with λ by observing if these ratios remain constant when the ionization chamber is filled with different gases and the appropriate corrections are made. As in the work of Allison and Andrew[2] the F values were observed directly by measuring the intensity ratio in the back chamber after the beams had traversed the length of the front chamber when the latter was first filled with the gas at a given pressure and later evacuated.

The results are shown in Tables I and II. All the measurements were made at 25 kv and each result is the average of four determinations.

TABLE I. *Tests with the Kα-lines of Cr and Fe. λ2.286 and 1.933A.*

Gas	Pressure	I_{CrFe}	F_{FeCr}	R_{FeCr}	P_{CrFe}
CH_3Br	15.92 cm	0.9480	0.966	1.00	0.916
Argon	22.55	0.9505	0.960	1.00	0.912
Air	74.40	1.2715	0.721	0.99	0.907
CH_3I	2.85	0.9362	0.9715	1.00	0.909
SO_2	50.18	0.9287	0.9840	1.00	0.914

TABLE II. *Comparison of the Kα-lines of Fe and Ni. λ1.933 and 1.656A.*

Gas	Pressure	I_{FeNi}	F_{NiFe}	R_{NiFe}	P_{FeNi}
CH_3Br	22.55 cm	0.6985	0.9675	1.00	0.676
Argon	43.48	0.6992	0.9685	1.00	0.677
Air	74.88	0.9925	0.6870	0.99	0.675
CH_3I	6.07	0.6912	0.9888	1.00	0.673
SO_2	65.82	0.6927	0.9786	1.00	0.676

[3] Martin, Proc. Roy. Soc. (London) **A115**, 420 (1927); Compton, Phil. Mag. **8**, 961 (1929).

[4] Auger, Ann. de Physique **6**, 183 (1926).

Hicks[5] has disclosed a source of error in ionization chamber measurements due to a faulty design of the front window. If the pressure of the gas is so high that an appreciable fraction of the ions are created in the layer of gas directly behind the window, and these ions are not collected and measured, an error would arise for beams of greatly different wave-lengths. In order to test this point with the present chamber, P_{CrFe}, as in Table I, was examined as a function of pressure. The results are shown in Table III. The results

TABLE III. P_{CrFe} *as a function of pressure of* CH_3Br.

Pressure (cm)	15.92	33.0	51.9	72.5
F_{FeCr}	0.966	0.999	1.00	1.00
P_{CrFe}	0.916	0.897	0.915	0.903

for the higher pressures are for one set of readings only so that the variation is within experimental error. It seems that if the collector is sufficiently close to the charged window that approximately all of the ions formed by the two beams are collected, the effect of the unequal absorption does not introduce an error.

Conclusions

These results were obtained under more favorable conditions than those of Allison[2] in that no fluorescence x-rays of sufficient hardness to reach the walls were excited. Also in no case did the lines investigated overlap any absorption limit of the gas. The most critical test of the method in this wave-length region is the measurements with air where the F factor deviates largely from unity.

Recently Gaertner[1] has determined the energy expended by a β-particle in the formation of a pair of ions. For argon over a range of incident x-rays of wave-lengths 0.345 to 1.38A the energy required per ion pair was constant within the limits of the experiment.

One can therefore conclude that an ionization chamber of proper design will give a true measure of the relative powers of two x-ray beams of different wave-lengths between 0.4 and 2.3A when the appropriate corrections are applied.

[5] Hicks, Phys. Rev. **38**, 572 (1931).

[6] M. Siegbahn and A. Žáček, Ann. d. Physik **71**, 187 (1923); Y. H. Woo, Phys. Rev. **28**, 427 (1926); Duane and Stenström, Proc. Nat. Acad. Sci. **6**, 477 (1920); Allison and Armstrong, Phys. Rev. **26**, 701, 714 (1925).

[7] H.-T. Meyer, Wissenschaftliche Veroffentlichungen aus dem Siemens-Konzern **7**, 108 (1929).

[8] S. K. Allison, Phys. Rev. **30**, 245 (1927).

PART II

Introduction

The second part of this paper deals with measurements on the relative intensities of the K-series lines of twenty elements from atomic numbers 24 to 52 and the calculation of the transition probabilities for these lines from these observations.

Several attempts have been made by many workers[6] to measure the relative intensities of some lines in the K-series of certain isolated elements. These experiments have led to the conclusion that the relative intensity of the doublet α_1, α_2 is two to one, and also indicate that the relative intensity of β_2 to β_1 increases with atomic number. Duane and Stenström[6] give the relative intensities in tungsten of α_2/α_1, β_1/α_1, and β_2/α_1 as 0.50, 0.35, and 0.15, respectively. Allison and Armstrong[6] presented a collection of results on the relative intensity of β_2/β_1 for four elements as measured by Duane and his associates. The value of this ratio in W, Rh, Mo, Cu, is respectively 0.43, 0.15, 0.13, 0.024.

The only comprehensive work on this problem has been done by H.-T. Meyer[7] who photographed the spectra and analyzed the intensities with a microphotometer. The difficulties inherent in the photographic determination of relative intensities and the disagreement with the meager ionization measurements led to the present study of this problem.

Apparatus

Power was supplied by a 5 kva 540 cycle synchronous motor generator to a transformer, kenetrons and condensers. The voltage was measured by an electrostatic repulsion type voltmeter. A tube of the type described by Allison[8] was adapted to facilitate the use of interchangeable targets of standard design. The cathode rays made an angle of 45° with the target and the x-rays observed emerged at right angles to the electron beam. The x-rays left the tube through

a mica window 2.3×10^{-3} cm thick and were collimated by slits 0.08 mm wide and 25.4 cm apart. On reflection from a calcite crystal calibrated for reflecting power (Allison's[9] crystal VB, values of R in Table II) they entered the ionization chamber through a cellophane window 2.5×10^{-3} cm thick. The total air path was 41.5 cm. The ionization chambers were similar to those used by Allison and Andrew[2] and allowed the direct measurement of the fraction of the energy absorbed in the front chamber by measurements of the energy entering the back chamber. The ionization currents were measured by the rate of deflection method with a Compton electrometer.

Measurements

Measurements were made on the relative intensities of the K-series lines of twenty elements from Cr (24) to Te (52). For the elements Cr to Ge methyl bromide at suitable pressures was used in the ionization chamber. For the elements Sr to Pd a chamber 28.1 cm long was filled with methyl iodide to measured pressures in the neighborhood of 20 cm, and for the elements Pd to Te a chamber 56.5 cm long was similarily filled with methyl iodide. In this manner no fluorescence radiation of sufficient hardness to reach the walls of the chamber was excited and the intensities measured were independent of the R factor given by Eq. (3). The F factor as in Eq. (2) for the gas was observed directly by means of the back chamber and as a further check the absorption coefficients for CH_3Br and CH_3I were measured for the appropriate wave-lengths.

The measurements for any one element were obtained at a predetermined voltage (usually kept as low as possible) and consisted in general of four determinations of the ratios α_2/α_1, and β_2/β_1, and seven determinations of β_1/α_1. The value of β_1 includes the unresolved β_3. Readings were taken at 7.5″ intervals over the peak of the lines. The method of determining these ratios was to compare the peak intensities less the base intensities of each line. Since the resolved lines were of the same width, the ordinate of the peak was taken as the measure of the intensity. In the case of the partially resolved lines α_1 and α_2 (totally resolved except for low atomic numbers) these ordinates were corrected by the method suggested by Allison and Armstrong.[6] The angular divergence of the x-ray beam was sufficiently large to give an observed width of line much greater than the natural wave-length widths as observed in recent unpublished work by Allison with a double crystal spectrometer.

Absorption coefficients for mica and cellophane were also obtained for the α_1 and β_1 lines of a number of elements.

Results

The collected results on the observed relative intensities and the calculated corrections to be applied to these results are shown in a logarithmic form in Table IV. The correction factors and the relative intensities refer to α_2/α_1, β_1/α_1, and β_2/α_1. I_λ/I_{α_1} is the observed ratio of intensities F_i, F_a, F_m, F_w, F_c are, respectively, the correction factors for the differential absorption in the gas filling the ionization chamber, the air path, the mica of the tube window, the cellophane of the chamber window, and the ratio of the coefficients of reflection of the calcite crystal. P_λ/P_{α_1} is the resultant ratio of the intensities of two wave-lengths leaving the surface of the target.

As has been previously stated, the F_i factor was observed directly by measurements with the rear chamber and was checked by calculations from the measured absorption coefficients of the gases CH_3Br and CH_3I. The variation of these absorption coefficients with wave-length can be expressed as:

$$CH_3Br\ \mu/\rho = 19.2\lambda^{2.79} \text{ from } 1.1 \text{ to } 2.3\text{A}, \quad (4)$$

and

$$CH_3I\ \mu/\rho = 65.46\lambda^{2.62} \text{ from } 0.4 \text{ to } 0.9\text{A}. \quad (5)$$

These equations are sufficiently accurate to introduce only a negligible error in the resultant correction factors.

The F_a factor was calculated for the 41.5 cm air path from Table 10 in H.–T. Meyer's[7] paper.

The F_m factor was calculated from direct measurements of the absorption coefficients of mica which gave

$$\text{Mica } \mu = 36.56\lambda^{2.76} \text{ from } 0.4 \text{ to } 2.3\text{A}. \quad (6)$$

The F_w factor was similarly calculated from measurements on cellophane which gave

$$\text{Cellophane } \mu = 3.52\lambda^{2.66} \text{ from } 0.6 \text{ to } 2.3\text{A}. \quad (7)$$

TABLE IV.

Element Press. Kv	Line	Log I_λ/I_{α_1}	Log F_i	Log F_a	Log F_m	Log F_w	Log F_c	Log P_λ/P_{α_1}	P_λ/P_{α_1}
Cr (24)	α_2	$\bar{1}.71676$	0	$\bar{1}.99638$	$\bar{1}.99852$	0.00032	0	$\bar{1}.71198$	0.5152
20.00 31.8	β_1	$\bar{1}.48982$	0.00303	$\bar{1}.83803$	$\bar{1}.91819$	$\bar{1}.99211$	0.01072	$\bar{1}.25190$	0.1786
Fe (26)	α_2	$\bar{1}.70243$	0	$\bar{1}.99747$	$\bar{1}.99878$	0.00015	0	$\bar{1}.69883$	0.4998
33.00 26.0	β_1	$\bar{1}.35793$	0.00303	$\bar{1}.89790$	$\bar{1}.94709$	$\bar{1}.99498$	0.02119	$\bar{1}.22212$	0.1668
Co (27)	α_2	$\bar{1}.69966$	0	$\bar{1}.99765$	$\bar{1}.99891$	0.00012	0	$\bar{1}.69634$	0.4970
40.00 26.0	β_1	$\bar{1}.31069$	0.00303	$\bar{1}.91871$	$\bar{1}.95684$	$\bar{1}.99585$	0.02119	$\bar{1}.20559$	0.1605
Ni (28)	α_2	$\bar{1}.69740$	0	$\bar{1}.99819$	$\bar{1}.99900$	0.00010	0	$\bar{1}.69469$	0.4951
50.00 25.0	β_1	$\bar{1}.35334$	0.00363	$\bar{1}.93222$	$\bar{1}.96464$	$\bar{1}.99651$	0.02202	$\bar{1}.27176$	0.1870
Cu (29)	α_2	$\bar{1}.69871$	0	$\bar{1}.99855$	$\bar{1}.99913$	0.00009	0	$\bar{1}.69648$	0.4971
62.00 25.0	β_1	$\bar{1}.35989$	0.00346	$\bar{1}.94660$	$\bar{1}.97128$	$\bar{1}.99717$	0.02160	$\bar{1}.29995$	0.1995
Zn (30)	α_2	$\bar{1}.70329$	0	$\bar{1}.99870$	$\bar{1}.99923$	0.00008	0	$\bar{1}.70130$	0.5027
73.00 25.0	β_1	$\bar{1}.35218$	0.00389	$\bar{1}.95655$	$\bar{1}.97566$	$\bar{1}.99760$	0.02857	$\bar{1}.31550$	0.2068
	β_2	$\bar{3}.59522$	0.00389	$\bar{1}.95352$	$\bar{1}.97388$	$\bar{1}.99750$	0.03203	$\bar{3}.55604$	0.0036
Ge (32)	α_2	$\bar{1}.70001$	0	$\bar{1}.99890$	$\bar{1}.99939$	0.00006	0	$\bar{1}.69836$	0.4993
73.00 31.0	β_1	$\bar{1}.38130$	0.01494	$\bar{1}.97049$	$\bar{1}.98318$	$\bar{1}.99826$	0.02979	$\bar{1}.37796$	0.2397
	β_2	$\bar{2}.12566$	0.01494	$\bar{1}.96918$	$\bar{1}.98166$	$\bar{1}.99820$	0.03282	$\bar{2}.12246$	0.0132
Sr (38)	α_2	$\bar{1}.70346$	$\bar{1}.99896$	$\bar{1}.99946$	$\bar{1}.99965$	0	0	$\bar{1}.70153$	0.5030
19.50 30.5	β_1	$\bar{1}.38543$	0.04493	$\bar{1}.98932$	$\bar{1}.99330$	$\bar{1}.99944$	0.02531	$\bar{1}.43773$	0.2740
	β_2	$\bar{2}.55962$	0.05225	$\bar{1}.98827$	$\bar{1}.99252$	$\bar{1}.99940$	0.02748	$\bar{2}.61954$	0.0416
Zr (40)	α_2	$\bar{1}.70364$	$\bar{1}.99752$	$\bar{1}.99957$	0	0	0	$\bar{1}.70073$	0.5020
19.90 34.0	β_1	$\bar{1}.37107$	0.05918	$\bar{1}.99202$	$\bar{1}.99454$	$\bar{1}.99957$	0.02202	$\bar{1}.43840$	0.2744
	β_2	$\bar{2}.57529$	0.06948	$\bar{1}.99114$	$\bar{1}.99402$	$\bar{1}.99953$	0.02375	$\bar{2}.65321$	0.0450
Cb (41)	α_2	$\bar{1}.70018$	$\bar{1}.99704$	$\bar{1}.99960$	0	0	0	$\bar{1}.69682$	0.4975
20.20 35.5	β_1	$\bar{1}.37291$	0.06521	$\bar{1}.99322$	$\bar{1}.99515$	0	0.01870	$\bar{1}.44519$	0.2787
	β_2	$\bar{2}.60591$	0.07720	$\bar{1}.99242$	$\bar{1}.99476$	0	0.02000	$\bar{2}.69029$	0.0490
Mo (42)	α_2	$\bar{1}.70157$	$\bar{1}.99651$	0	0	0	0	$\bar{1}.69808$	0.4990
20.40 37.0	β_1	$\bar{1}.36736$	0.07262	$\bar{1}.99414$	$\bar{1}.99568$	0	0.01578	$\bar{1}.44558$	0.2790
	β_2	$\bar{2}.62242$	0.08546	$\bar{1}.99342$	$\bar{1}.99538$	0	0.01686	$\bar{2}.71354$	0.0517
Ru (44)	α_2	$\bar{1}.70387$	$\bar{1}.99616$	0	0	0	0	$\bar{1}.70003$	0.5012
20.00 38.0	β_1	$\bar{1}.37658$	0.08207	$\bar{1}.99555$	$\bar{1}.99634$	0	0.01620	$\bar{1}.46674$	0.2929
	β_2	$\bar{2}.64516$	0.09701	$\bar{1}.99498$	$\bar{1}.99610$	0	0.01725	$\bar{2}.75040$	0.0563
Rh (45)	α_2	$\bar{1}.70605$	$\bar{1}.99561$	0	0	0	0	$\bar{1}.70166$	0.5031
20.27 39.0	β_1	$\bar{1}.34635$	0.08955	$\bar{1}.99612$	$\bar{1}.99695$	0	0.01620	$\bar{1}.44517$	0.2787
	β_2	$\bar{2}.64695$	0.10555	$\bar{1}.99560$	$\bar{1}.99679$	0	0.01725	$\bar{2}.76214$	0.0578
Pd (46)	α_2	$\bar{1}.70018$	$\bar{1}.99843$	0	0	0	0	$\bar{1}.69861$	0.4996
20.40 40.0	β_1	$\bar{1}.35218$ / $\bar{1}.39445$	0.09412 / 0.06221	$\bar{1}.99664$	$\bar{1}.99745$	0	0.01452	$\bar{1}.45491$ / $\bar{1}.46527$	0.2850 / 0.2919
	β_2	$\bar{2}.70408$	0.07420	$\bar{1}.99616$	$\bar{1}.99733$	0	0.01542	$\bar{2}.78719$	0.0613
Ag (47)	α_2	$\bar{1}.70114$	$\bar{1}.99712$	0	0	0	0	$\bar{1}.69826$	0.4992
20.57 41.0	β_1	$\bar{1}.38435$	0.07004	$\bar{1}.99708$	$\bar{1}.99787$	0	0.01248	$\bar{1}.46182$	0.2896
	β_2	$\bar{2}.69948$	0.08330	$\bar{1}.99663$	$\bar{1}.99777$	0	0.01328	$\bar{2}.79046$	0.0617
Cd (48)	α_2	$\bar{1}.70209$	$\bar{1}.99585$	0	0	0	0	$\bar{1}.69794$	0.4988
20.52 41.5	β_1	$\bar{1}.39005$	0.07700	$\bar{1}.99739$	$\bar{1}.99826$	0	0.00945	$\bar{1}.47215$	0.2966
	β_2	$\bar{2}.71020$	0.09194	$\bar{1}.99700$	$\bar{1}.99820$	0	0.01002	$\bar{2}.80736$	0.0642
In (49)	α_2	$\bar{1}.70243$	$\bar{1}.99540$	0	0	0	0	$\bar{1}.69783$	0.4987
20.50 42.5	β_1	$\bar{1}.38417$	0.08314	$\bar{1}.99760$	$\bar{1}.99856$	0	0.00860	$\bar{1}.47207$	0.2965
	β_2	$\bar{2}.70742$	0.09892	$\bar{1}.99724$	$\bar{1}.99850$	0	0.00910	$\bar{2}.81118$	0.0647
Sn (50)	α_2	$\bar{1}.70239$	$\bar{1}.99502$	0	0	0	0	$\bar{1}.69714$	0.4979
20.33 42.5	β_1	$\bar{1}.37676$	0.08884	$\bar{1}.99795$	$\bar{1}.99888$	0	0.00945	$\bar{1}.47188$	0.2963
	β_2	$\bar{2}.73469$	0.10546	$\bar{1}.99761$	$\bar{1}.99885$	0	0.00995	$\bar{2}.84656$	0.0702
Sb (51)	α_2	$\bar{1}.70757$	$\bar{1}.99388$	0	0	0	0	$\bar{1}.70145$	0.5029
20.70 44.0	β_1	$\bar{1}.39270$	0.09272	$\bar{1}.99822$	$\bar{1}.99910$	0	0.00903	$\bar{1}.49177$	0.3103
	β_2	$\bar{2}.73314$	0.11059	$\bar{1}.99792$	$\bar{1}.99908$	0	0.00946	$\bar{2}.85019$	0.0708
Te (52)	α_2	$\bar{1}.70329$	$\bar{1}.99344$	0	0	0	0	$\bar{1}.69673$	0.4974
20.65 45.0	β_1	$\bar{1}.38382$	0.09587	$\bar{1}.99843$	$\bar{1}.99930$	0	0.00775	$\bar{1}.48517$	0.3056
	β_2	$\bar{2}.74555$	0.11499	$\bar{1}.99820$	$\bar{1}.99929$	0	0.00810	$\bar{2}.86613$	0.0735

F_c, the ratio of the coefficients of reflection of the calcite crystal VB were measured directly by Allison[9] for several wave-lengths in this region. The values of R given in his Table II were plotted and a smooth curve through the points permitted interpolation to a reasonable accuracy. This application is not strictly correct for the calibration was carried out by means of a partially polarized beam from the first crystal, whereas in the present experiment the beam is unpolarized before reflection. The values of F_c are not changed appreciably by a proper treatment.

There is no significant variation of α_2/α_1 with atomic number, the average value for these twenty elements being 0.5003, in excellent agreement with the theory of Burger and Dorgelo[10] and with all previous experimental work.

The variation of the calculated values of P_{β_1}/P_{α_1} as a function of atomic number is shown graphically by the circles in Fig. 1. The crosses in this figure represent the results of H.–T. Meyer[7] using a gas tube, a rocksalt crystal, and a photographic-microphotometer method. The explanation for the decided lack of agreement between the present work and that of Meyer is perhaps to be found in the rather cumbersome photographic method. In the method of determining relative intensities of x-ray lines from a photographic plate, especially when the lines are very widely separated or lie on opposite sides of the silver or bromine K limit, it is necessary to make some rather bold assumptions which are open to doubt. The internal consistency of the results themselves seems to indicate that the ionization method is preferable.

The variation of β_2/α_1 is shown graphically in Fig. 2, with similar symbols, and it will be noted that the deviation from Meyer's results is in the same direction. His method is, of course, more powerful in the detection of the β_2 line when it almost disappears at Zn. He has continued his measurements on β_2 to lower atomic numbers but this line apparently disappears at Ni (28) and the further observations were on $K\beta_5$.

No attempt was made in this research to measure the relative intensity of any satellite lines.

As far as is known there are no theoretical predictions as to the variations of relative in-

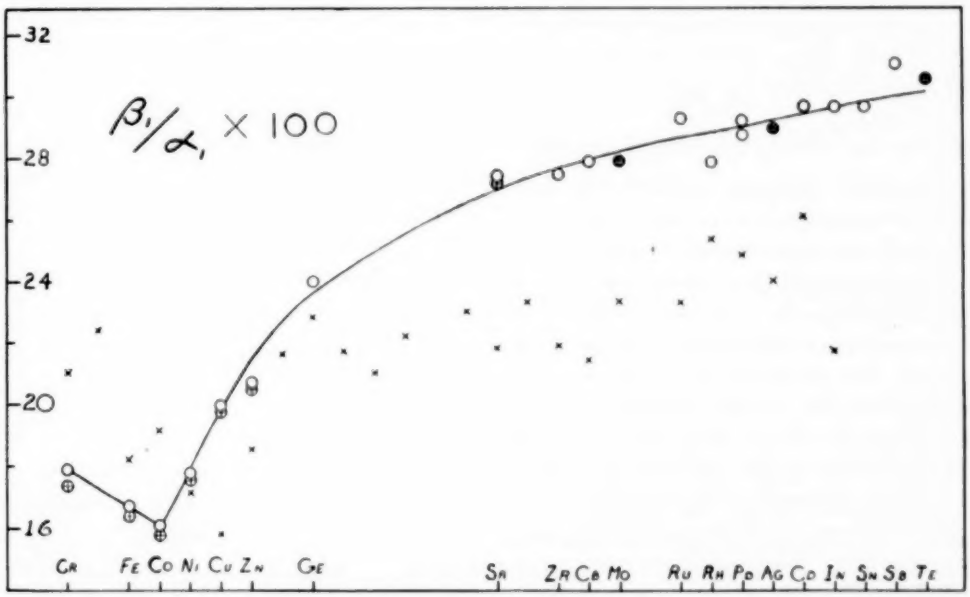

FIG. 1. Variation of the relative intensities and transition probabilities of β_1 to α_1 as a function of atomic number. The open circles are the values of the relative intensities of the two wave-lengths at the surface of the target, the circles containing crosses are the relative transition probabilities, and the crosses are the values of the relative intensities obtained by H.–T. Meyer.[7]

[9] S. K. Allison, Phys. Rev. **41**, 1 (1932).

[10] Burger and Dorgelo, Zeits. f. Physik **23**, 258 (1924).

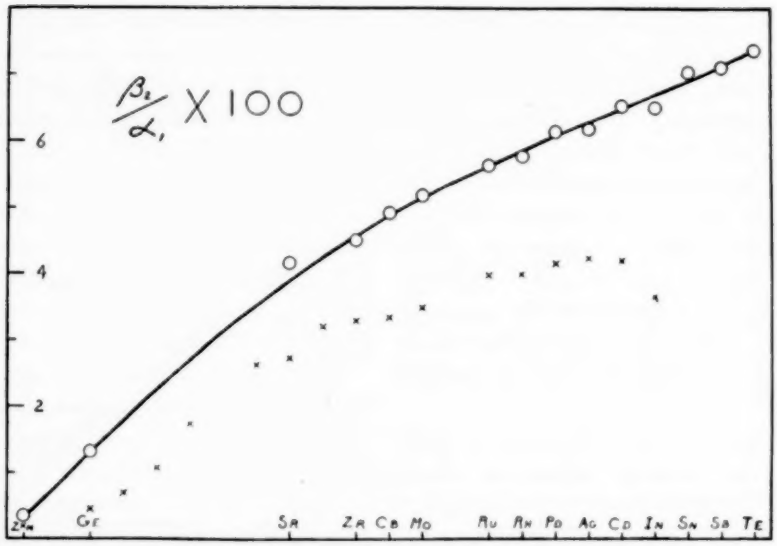

FIG. 2. Variation of the relative intensities of β_2 to α_1 as a function of atomic number. The circles are the present results and the crosses are the values of H.–T. Meyer.[7]

tensity with atomic number. The marked change of β_1/α_1 in the region 27 to 40 is not easily reconciled with the electron population of the M levels. The increased value of the ratio for Fe and Cr is presumably due to the presence of increasingly intense satellites of β_1. However in the case of β_2/α_1 the variation of the intensity ratio in the region 38 to 30 is indicated by the decreasing population of the N_{22} and N_{21} levels.

Corrections for the absorption within the target

The P_λ/P_{α_1} ratios obtained above will yield directly the relative transition probabilities in the various atoms if one can correct for the absorption within the target. As these values are of some theoretical significance it is worth while to attempt an approximate solution to the problem.

Fig. 3 shows the geometrical arrangement of the target with respect to the cathode rays and the observed x-rays. If we assume a perfectly smooth surface of the target material we can set up the following conditions. The intensity dP_λ, of x-rays observed of wave-length λ, arising from primary ionization by the impinging electrons in an element of electron path dx at a depth x is given by:

$$dP_\lambda = c_\lambda F(x) e^{-\mu_\lambda x} dx \qquad (8)$$

where c_λ is a factor including the instrumental constants and the probability of the transition giving rise to the wave-length λ; $F(x)$ is the ionization probability for the impinging electrons at a depth x; and μ_λ is the absorption coefficient of the x-rays in the target material. The total intensity, P_λ, leaving the target at the appropriate angle is

$$P_\lambda = c_\lambda \int_0^{x_0} F(x) e^{-\mu_\lambda x} dx. \qquad (9)$$

The limits of the integration are imposed by the maximum depth to which the electrons can penetrate the target material and yet retain sufficient energy to ionize the level in question. These limits are assumed to be given by the Thomson-Whiddington equation

$$x = (V^2 - V_x^2)/b, \qquad (10)$$

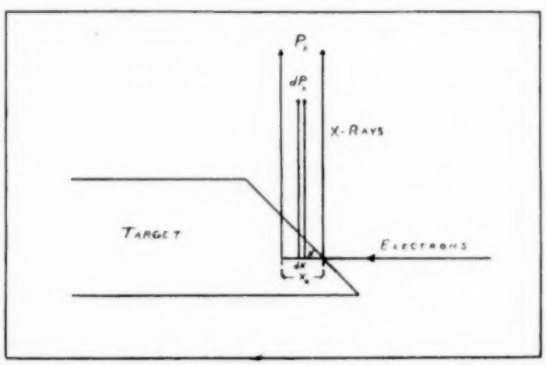

FIG. 3. Geometrical arrangement of the target and cathode beam in the x-ray tube.

where V is the initial voltage of the electrons, V_x is their voltage at the depth x, and V_0 is to be taken as the excitation potential of the level or the voltage at the depth x_0. Substituting from Eq. (10) in Eq. (9), we obtain

$$P_\lambda = \frac{2c_\lambda}{b} e^{-\mu_\lambda V^2/b} \int_{V_0}^{V} V_x F'(V_x) e^{\mu_\lambda V_x^2/b} dV_x. \quad (11)$$

Here $F'(V_x)$ is the ionization probability as a function of the electron voltage, as has been measured by Webster and his associates[11] with thin targets of silver. The best fitting equation given by them is

$$F'(V_x) = \frac{6k_\lambda}{(V_x/V_0)\{[\pi/2\cos^{-1}(V_0/V_x)^{\frac{1}{2}}]^2 - 1\}}. \quad (12)$$

Substituting Eq. (12) in Eq. (11) we obtain

$$P_\lambda = KV_0 \frac{2c_\lambda}{b} e^{-\mu_\lambda V^2/b} \int_{V_0}^{V} \frac{e^{\mu_\lambda V_x^2/b} dV_x}{[\pi/2\cos^{-1}(V_0/V_x)^{\frac{1}{2}}] - 1} \quad (13)$$

or for the ratio

$$\frac{P_\lambda}{P_\alpha} = \frac{c_\lambda'}{c_\alpha'} \frac{e^{-\mu_\lambda V^2/b}}{e^{-\mu_\alpha V^2/b}} \int_{V_0}^{V} \frac{e^{\mu_\lambda V_x^2/b} dV_x}{[\pi/2\cos^{-1}(V_0/V_x)^{\frac{1}{2}}] - 1} \Big/ \int_{V_0}^{V} \frac{e^{\mu_\alpha V_x^2/b} dV_x}{[\pi/2\cos^{-1}(V_0/V_x)^{\frac{1}{2}}]^2 - 1}, \quad (14)$$

where c_λ'/c_α' is the true ratio of the transition probabilities of wave-lengths λ and α.

Since this equation is not integrable by ordinary means it must be evaluated graphically. The limit V is set by the experimental voltage shown in the first column of Table IV and the values of V_0 are taken from Table 225 in Siegbahn.[12] These voltages were transformed to relativistic velocities and the coefficient b became a in the Thomson Whiddington law

$$v^4 - v_x^4 = ax. \quad (15)$$

a was determined from an empirical equation given by Wissak[13]

$$a = 9.6 \times 10^{42} Z\rho/A, \quad (16)$$

where Z is the atomic number, A the atomic weight and ρ the density. μ was determined from Richtmyer's equation

$$\mu = 5.29\rho \times 10^{-4} \lambda^3 Z^{4.3}/A, \quad (17)$$

which holds between the K and L limits and was here presumed to yield absorption coefficients for wave-lengths up to 2.3A although it is known to be rigid only to 1.0A.

With these numerical values the equation has been solved in a graphical manner,[14] for the elements Cr, Fe, Co, Ni, Cu, Zn, Sr, Mo, Ag and Te. The largest correction is for Cr where V/V_0 has the largest value 5.18. The ratio of the integrals comparing the β_1 to the α_1 line is 0.975 and of the exponential factors outside the integral is 1.060. P_{β_1}/P_{α_1} must therefore be multiplied by 0.97 to give the ratio of the transition probabilities for these lines.

The resultant correction factors to be multiplied by P_{β_1}/P_{α_1} to yield $c_{\beta_1}'/c_{\alpha_1}'$ are given in Table V. The resultant values of $c_{\beta_1}'/c_{\alpha_1}'$ are shown graphically by the circles containing crosses in Fig. 1.

TABLE V. *Target corrections to yield ratios of transition probabilities.*

Element	Cr	Fe	Co	Ni	Cu	Zn	Sr	Mo	Ag	Te
F_t	0.97	0.98	0.98	0.99	0.99	0.99	0.99	1.00	1.00	1.00
$c_{\beta_1}'/c_{\alpha_1}'$	0.173	.163	.157	.185	.197	.205	.271	.279	.289	.305

The correction, F_t, to be applied due to the absorption in the target is thus seen to be surprisingly small and to the first approximation measurements on the relative intensities of K-series lines from thick targets of the heavier elements at voltages not much greater than the excitation voltages give the relative transition probabilities.

[11] Webster, Hansen and Duvendack, Phys. Rev. **42**, 141 (1932).

[12] M. Siegbahn, *Spektroskopie der Rontgenstrahlen*, second edition.

[13] Wissak, Ann. d. Physik **5**, 507 (1930).

[14] I am indebted to Mrs. A. T. Monk for carrying out this graphical integration.

The treatment outlined above is very crude and it is perhaps worth while to point out the approximations and examine their effect on the results. A smooth target face is assumed whereas the roughness is large compared to the depth of penetration of the cathode rays (10^{-4} to 4×10^{-4} cm). This is possibly the largest error and might influence the correction factor considerably. Also any deposit on the target face was disregarded, for this was very small for a sufficiently "hard" tube. The treatment takes no account of the indirect production of characteristic radiation; i.e., a cathode ray may first excite a continuous spectrum quanta of shorter λ than the K limit, which in turn will fluoresce line radiation at a different depth within the target. However we know[15] that the ratio of the direct line radiation to the indirect line radiation remains constant at approximately two up to 180 kv in Pd. If it is assumed that the white radiation spreads out spherically from its excitation center and is converted into line radiation within 10^{-4} cm the correction from this source will be of a smaller order of magnitude. Furthermore no account has been taken of the diffusion of the incident electrons within the target, which tends to make the mean depth of penetration less than that calculated by the above method. It is conceivable that the last two factors may to some extent have a balancing effect. The expression for $F'(V_x)$ has been assumed to hold for the excitation function in an element of thickness dx within the target, whereas it is found experimentally to satisfy measurements from a thin surface layer. The values of "a" in the Thomson-Whiddington equation are in doubt since the available experimental values are not in good agreement. Furthermore these values for metals were obtained with the electron beam normally incident on a thin film instead of at 45° as in the present arrangement. E. J. Williams[16] has found the fourth power law to be expressed more accurately as:

$$v^{3.7}-v^{3.7}=ax. \tag{18}$$

The values of the absorption coefficients are supposed to hold for the range of wave-lengths 0.1 to 1.0A and are not accurately true for the longer wave-lengths.

It is felt that nothing very definite can be said about the effect of these assumptions other than that the roughness of the target sets a limit to the accuracy of the correction. In these experiments no attempt was made to polish the target, which was in general machined to a visible smoothness. The cathode beam did not pit the target to any visible extent except in the case of Cd and Sb.

The values in Table IV for P_λ/P_{α_1} may therefore be taken as the ratio of the intensities of the two wave-lengths leaving the surface of the target to within an estimated error of four percent and for the heavier elements they may be accepted as the ratio of the transition probabilities to within a slightly greater error.

In conclusion I wish to express my appreciation to Professor S. K. Allison for the use of his laboratory equipment and for the suggestion of this problem.

[15] Hansen and Stoddard, Phys. Rev. **43**, 701 (1933).

[16] E. J. Williams, Proc. Roy. Soc. (London) **130**, 310 (1930).

Mass Ratio of the Lithium Isotopes from the Spectrum of Li_2

ANDREW MCKELLAR, *Department of Physics, University of California*

(Received May 24, 1933)

Wave-number data.—The blue-green absorption bands of lithium have been photographed in the second order of a 21-foot grating. In the main, Li^7Li^7, system the 2,0, 1,0, 0,0, 0,1 and 0,2 bands and in the isotopic, Li^6Li^7, system the 1,0, 0,0, 0,1 bands and a somewhat incomplete 0,2 band have been measured and analyzed. Wave numbers of the lines of all these bands are tabulated. An unsuccessful attempt was made to identify Li^6Li^6 band lines.

Vibrational constants.—Values of ΔG_v are calculated by least squares and from them are deduced the vibrational constants of the main and isotopic systems. The constants are given by the following equations: $\Delta G_v'' = 351.374 - 5.181\ (v''+\frac{1}{2})$, $\Delta G_v' = 270.941 - 6.266\ (v'+\frac{1}{2})$, $\Delta G_v''^{i} = 365.923 - 5.619\ (v''+\frac{1}{2})$, $\Delta G_v'^{i} = 282.081 - 6.791\ (v'+\frac{1}{2})$. The isotopic mass coefficient $\rho = (\mu/\mu^i)^{\frac{1}{2}} = \omega_e^i/\omega_e$ was calculated for the lower and upper states. The resulting values are, from the $^1\Sigma$ state, $\rho = 1.04141 \pm 0.00008$ (considered the most trustworthy figure) and from the $^1\Pi$ state, $\rho = 1.0411 \pm 0.0002$. These results are shown to correspond to a higher isotopic mass ratio Li^7/Li^6 than that indicated by the mass-spectrograph results of Costa. By employing the Q branch of the 0,2 isotope band, $\Delta G_{1\frac{1}{2}}''^{i}$ was found and the relation $x_e^i/x_e = \rho$ was verified to within the probable error.

Rotational and electronic constants.—From rotational term differences, values of B_v were computed for the main and isotopic systems by least squares. The calculated constants are: $B_v'' = 0.6721 - 0.00708\ (v''+\frac{1}{2})$, $B_v' = 0.5577 - 0.00888\ (v'+\frac{1}{2})$, $B_v''^{i} = 0.7302 - 0.00830\ (v''+\frac{1}{2})$, $B_v'^{i} = 0.6046 - 0.00922\ (v'+\frac{1}{2})$. From the relation $B_e^i/B_e = \rho^2$ are obtained values of ρ which agree to within their probable error (one part in 1500) with the more accurate results obtained from the vibrational constants. The Λ-doubling for the two lowest vibrational levels of the $^1\Pi$ state was investigated and found sensibly equal for the main and isotopic band systems. The origins of the two band systems were computed to be $\nu_e = 20436.25 \pm 0.02$ and $\nu_e^i = 20436.29 \pm 0.04$, indicating no measurable electronic isotope effect.

INTRODUCTION

THE importance of accurate determinations of the mass defects of atoms has been recently emphasized in connection with atomic disintegration experiments and questions of the stability of nuclei. The mass defect of Li^7 is of special interest, for lithium has been disintegrated by bombardment both with protons[1, 2, 3] and with α-particles.[4, 5] From a consideration of the processes taking place certain deductions have been made, based on the Li^7 mass defect; for example, it has been used to establish an upper limit for the mass of the neutron. The only existing determination of the atomic weights of the lithium isotopes by the mass-spectrograph is that of Costa,[6] later modified by Aston.[7] The masses given are $Li^6 = 6.012 \pm 0.002$ and $Li^7 = 7.012 \pm 0.002$. Thus it seems very desirable to obtain a completely independent check on the above results for lithium, using the band spectrum of the diatomic molecule Li_2.

The most accurate determinations of the mass ratio of isotopes from molecular spectra are obtainable with light elements where the proportional difference in mass of the isotopes is large. Thus far the only results from optical methods comparable in accuracy with those from the mass-spectrograph have been obtained by Babcock and Birge[8] on the ratio $O^{18} : O^{16}$ from the atmospheric oxygen bands, and by Jenkins and McKellar[9] on $B^{11} : B^{10}$ from the BO bands. In the case of oxygen, there are no mass-spectrograph data with which to compare the

[1] J. D. Cockcroft and E. T. S. Walton, Proc. Roy. Soc. **A137**, 229 (1932).

[2] E. O. Lawrence, M. S. Livingston and M. G. White, Phys. Rev. **42**, 150 (1932).

[3] M. C. Henderson, Phys. Rev. **43**, 98 (1933).

[4] M. de Broglie and L. Leprince Ringuet, C. R. **194**, 1616 (1932).

[5] I. Curie, F. Joliot and P. Savel, C. R. **194**, 2208 (1932).

[6] J. Costa, Ann. de Physique **4**, 425 (1925).

[7] F. W. Aston, Proc. Roy. Soc. **A115**, 487 (1927).

[8] H. D. Babcock and R. T. Birge, Phys. Rev. **37**, 233 (1931).

[9] F. A. Jenkins and A. McKellar, Phys. Rev. **42**, 464 (1932).

band spectrum value. In the latter case the results by the two methods are in good agreement. The lithium molecular spectrum is, from some points of view, a favorable one with which to work. It yields a value of the isotopic mass coefficient $\rho=(\mu/\mu')^{\frac{1}{2}}$ differing by a greater amount from unity than either of those previously studied and is only exceeded in this respect by possible band systems from the hydrogen isotopic molecules, such as H^1H^2 or H^2H^2 with respect to H^1H^1. The fact that the Li_2 bands are obtained in absorption partially compensates for the rather low abundance ratio of $Li^6 : Li^7$, which is approximately 1 : 11. Furthermore, in the case of lithium, one can evaluate directly the mass ratio Li^7/Li^6 from the experimentally determined value of ρ. This is not so for diatomic molecules composed of two atoms of elements of different atomic number, such as BO, where the absolute mass of one of the isotopes must be assumed to calculate the mass ratio $B^{11} : B^{10}$.

The blue-green lithium bands have been studied by Wurm[10] and by Harvey and Jenkins.[11] They were shown to arise from a $^1\Pi \leftarrow {}^1\Sigma$ electronic transition. Wurm analyzed the rotational structure of the 0,0 and 1,0 bands of the Li^7Li^7 system. Harvey and Jenkins extended the analysis to the 0,1 main band and succeeded in identifying a fairly complete Q branch and a fragmentary P branch in the 0,0 band due to the less abundant isotopic molecule, Li^6Li^7. They also measured the observed alternation of intensities in the Li^7Li^7 band lines, obtaining an intensity alternation ratio of 5/3 which assigns a nuclear spin of $(3/2)(h/2\pi)$ to the Li^7 nucleus. This result was later verified by van Wijk and van Koeveringe.[12] Loomis and Nusbaum,[13] from an examination of the magnetic rotation spectrum under fairly low dispersion, considerably extended the vibrational analysis of this system and calculated a value for the heat of dissociation. In the present work additional rotational analyses of bands of both the Li^7Li^7, hereafter called the *main* system, and of the Li^6Li^7, hereafter called the *isotopic* system, have been carried out and most of the available data have been utilized in applying the theory of the isotope effect to obtain the best value of the mass coefficient.

[10] K. Wurm, Zeits. f. Physik **58**, 562 (1929).

[11] A. Harvey and F. A. Jenkins, Phys. Rev. **35**, 789 (1930).

[12] W. R. van Wijk and A. J. van Koeveringe, Proc. Roy. Soc. **A132**, 98 (1931).

[13] F. W. Loomis and R. E. Nusbaum, Phys. Rev. **38**, 1447 (1931).

Experimental Data

The lithium vapor was enclosed in an electrically heated absorption tube giving an absorbing column about 50 cm long and 3.5 cm in diameter. The ends of the tube were water-cooled to protect the plane glass windows, and the tube contained argon at about 20 mm pressure to retard diffusion of the lithium. Near the completion of the work a longer tube (80 cm) was used in order to identify some of the fainter isotope lines. Plates were taken with various vapor densities corresponding to temperatures of the absorption tube, measured by a thermocouple in contact with it, ranging from 570°C to 950°C. It was found that the bands were most free from underlying structure and exhibited most clearly their rotational structure when the temperature was 630°C. The spectrograms were taken in the second order of the 21-foot concave grating, which is mounted on the Paschen system and gives a dispersion of about 1.33A/mm. With a 500 c.p. Point-o-Lite lamp as a source, well exposed plates were obtained in an exposure time of about 3 hours.

The comparator used in measuring the plates was carefully calibrated for errors in the screw. These amounted at most to 0.002 mm. From independent measurement of the same band on different plates, it is estimated that the absolute accuracy of the measurements is about 0.05 cm^{-1}. Fortunately, with the present mounting, the region from 4800 to 5200A in the second order of the grating gives practically normal dispersion; thus corrections to linear interpolation of wave-lengths were small and never exceeded 0.01A. The 2,0, 1,0, 0,0, 0,1 and 0,2 bands of the main system were measured. No data have heretofore been given for the 2,0 and 0,2 bands. Also, in the Li^6Li^7 isotopic band system quite complete 1,0, 0,0 and 0,1 bands were identified. A somewhat less complete Q branch of the 0,2 isotope band was found but only with con-

siderable difficulty, due to the faintness of the lines and the complexity caused by superposition of the 1,3 and other weak bands. In this identification recourse was had to the graphical method devised by Loomis and Wood[14] and to an examination of microphotometer curves. In all cases the correctness of the analysis was checked by the upper and lower state combination differences. In Tables I to VIII will be found the wave numbers of the band lines obtained in our analysis; the wave-length given for each band being that of its head, formed by the R branch.

TABLE I. 2,0 *Band*, λ4778.618.

K''	R	Q	P	K''	R	Q	P
1	20920.03			24	20864.49	20838.23	20813.13
2	920.73	20917.51		25	858.78	831.49	805.51
3	920.73	916.87		26	852.85	824.56	797.59
4	920.73	915.61	20910.82	27	846.73	817.42	789.38
5	920.73	914.33	908.84	28	840.21	809.95	780.83
6	920.03	912.70	906.28	29	833.34	802.16	772.21
7	919.36	910.82	903.41	30	826.36	794.23	763.20
8	918.31	908.84	900.03	31	819.05	785.91	753.98
9	916.87	906.28	896.62	32	811.54	777.36	744.54
10	915.33	903.41	892.86	33	803.61	768.56	734.81
11	913.41	900.74	888.82	34	795.37	759.55	724.82
12	911.41	897.43	884.54	35	787.14	750.07	714.53
13	908.84	894.01	880.03	36	778.49	740.59	703.96
14	906.28	890.19	875.42	37	769.54	730.83	693.22
15	903.41	886.22	870.42	38	760.35	720.61	682.19
16	900.03	881.89	865.06	39	750.82	710.11	670.89
17	896.62	877.42	859.44	40	741.04	699.39	
18	892.86	872.68	853.60	41	730.83	688.35	
19	888.82	867.52	847.54	42	720.61	677.32	
20	884.54	862.20	841.12	43	710.11	665.87	
21	880.03	856.61	834.67	44	699.39		
22	875.03	850.73	827.67	45	688.01		
23	869.87	844.58	820.50	46	676.30		
				47	664.81		

TABLE III. 0,0 *Band*, λ4900.983.

K''	R	Q	P	K''	R	Q	P
0	20396.49			29	20327.09	20294.65	20263.71
1	397.28	20395.12		30	321.17	287.84	255.78
2	397.91	394.55	20392.42	31	315.03	280.65	247.66
3	398.39	393.92	390.44	32	308.66	273.27	239.32
4	398.39	392.96	388.49	33	302.05	265.62	230.77
5	398.39	391.84	386.34	34	295.20	257.91	221.94
6	398.16	390.44	383.77	35	288.14	249.78	212.95
7	397.67	388.79	381.10	36	280.65	241.53	203.65
8	396.91	386.95	378.13	37	273.27	233.00	194.22
9	395.92	384.96	374.97	38	265.62	224.26	184.53
10	394.55	382.49	371.53	39	257.45	215.30	174.62
11	393.21	379.81	367.92	40	249.15	206.08	164.38
12	391.54	377.25	363.90	41	240.73	196.67	154.16
13	389.69	374.21	359.88	42	231.97	187.07	143.58
14	387.48	370.96	355.68	43	223.05	177.18	132.72
15	384.96	367.52	351.19	44	213.78	167.07	121.76
16	382.49	363.90	346.29	45	204.47	156.74	110.58
17	379.81	359.88	341.31	46	194.68	146.15	099.16
18	376.53	355.68	336.07	47	184.88	135.37	087.51
19	373.19	351.19	330.62	48	174.62	124.35	075.62
20	369.60	346.70	324.92	49	164.38	113.00	063.60
21	365.85	341.85	319.01	50	153.61	101.64	
22	361.82	336.75	312.94	51	142.82	089.99	
23	357.58	331.44	306.52	52	131.67	078.05	
24	353.07	325.87	299.95	53	120.35	065.90	
25	348.35	320.09	293.19	54	108.81	053.49	
26	343.36	314.09	286.13	55	096.98		
27	338.16	307.86	278.87	56	084.83		
28	332.74	301.42	271.39	57	072.65		

[14] F. W. Loomis and R. W. Wood, Phys. Rev. **32**, 223 (1928).

In view of the differences discussed below between the results of the present work and those obtained from mass-spectrograph measurements, we consider it advisable to present all the wave-number data used. Thus we include our measurements of the three previously analyzed bands.[10, 11] Not only has the analysis of these been extended to higher and lower values of K, but the greater resolving power obtained in this investigation has given a considerable improvement in accuracy.

An unsuccessful attempt was made to identify lines due to the Li^6Li^6 molecule in the 0,0 and 1,0

TABLE II. 1,0 *Band*, λ4838.258.

K''	R	Q	P	K''	R	Q	P
0				25	20606.85	20579.10	20552.52
1	20661.69	20659.64		26	601.42	572.61	545.14
2	662.38	659.18	20656.98	27	595.79	565.93	537.39
3	662.84	658.35	655.18	28	589.75	558.93	529.42
4	662.84	657.58	652.99	29	583.58	551.74	521.30
5	662.84	656.24	650.93	30	577.13	544.27	512.82
6	662.38	654.68	648.14	31	570.39	536.63	504.12
7	661.69	652.99	645.38	32	563.47	528.68	495.23
8	660.73	650.93	642.32	33	556.23	520.49	486.07
9	659.64	648.75	638.97	34	548.83	512.02	476.60
10	658.35	646.26	635.38	35	541.06	503.34	467.06
11	656.46	643.52	631.64	36	533.19	494.40	457.18
12	654.68	640.48	627.57	37	524.78	485.24	447.07
13	652.53	637.29	623.14	38	516.32	475.81	436.76
14	650.04	633.81	618.70	39	507.55	466.13	426.15
15	647.42	630.15	613.87	40	498.59	456.22	415.30
16	644.50	626.08	608.84	41	489.32	446.05	404.23
17	641.31	621.80	603.59	42	479.86	435.61	
18	637.86	617.30	598.05	43	470.00	424.95	
19	634.19	612.63	592.25	44	459.98	414.08	
20	630.15	607.65	586.27	45	449.73	402.90	
21	626.08	602.44	580.01	46	439.12		
22	621.80	596.97	573.56	47	428.35		
23	617.02	591.24	566.69	48	417.34		
24	611.91	585.31	559.83	49	405.98		

TABLE IV. 0,1 *Band*, λ4985.556.

K''	R	Q	P	K''	R	Q	P
0				28	19992.29	19961.02	19930.93
1	20051.17	20048.90		29	987.10	954.71	923.74
2	051.81	048.48		30	981.66	948.23	916.26
3	052.37	047.87	20044.62	31	975.96	941.58	908.59
4	052.37	046.96	042.55	32	970.08	934.60	900.66
5	052.37	045.81	040.25	33	963.89	927.50	892.54
6	052.37	044.62	037.90	34	957.54	920.18	884.22
7	051.81	042.89	035.26	35	951.02	912.60	875.70
8	051.17	041.29	032.46	36	944.17	904.89	866.99
9	050.33	039.31	029.33	37	937.13	896.89	858.02
10	049.28	037.10	026.24	38	929.97	888.71	848.92
11	047.87	034.74	022.69	39	922.46	880.30	839.58
12	046.46	032.12	018.95	40	914.81	871.68	830.04
13	044.62	029.33	015.15	41	906.82	862.85	820.26
14	042.89	026.24	011.03	42	898.78	853.80	810.33
15	040.57	022.96	006.67	43	890.41	844.56	800.21
16	038.19	019.45	002.12	44	881.91	835.08	789.87
17	035.57	015.85	19997.33	45	873.12	825.42	779.28
18	032.77	011.95	992.29	46	864.14	815.63	768.52
19	029.76	007.81	987.10	47	854.87	805.41	757.51
20	026.24	003.46	981.66	48	845.43	795.01	746.38
21	022.69	19998.91	975.96	49	835.74	784.57	734.97
22	019.21	994.14	970.33	50	825.89	773.83	723.44
23	015.15	989.16	964.28	51	815.63	762.88	
24	011.03	983.99	958.09	52	805.41	751.71	
25	006.67	978.54	951.60	53	795.01	740.32	
26	002.12	972.93	944.89	54		728.74	
27	19997.33	967.09	938.11	55		716.97	

TABLE V. 0,2 *Band*, λ5071.727 *and* $(0,2)^i$ *Band*, λ5079.

K″	R	Q	Q^i	P	K″	R	Q	Q^i	P
0	19709.08				31	19642.19	19607.80	19570.90	19574.70
1	710.01	19707.94			32	636.50	601.25	563.81	567.14
2	710.76	707.42		19705.01	33	631.08	594.65	556.79	559.71
3	711.26	706.75		703.34	34	624.97	587.81	549.36	551.68
4	711.67	706.11		701.32	35	619.06	580.76		543.77
5	711.67	705.01		699.65	36	612.82	573.52		535.68
6	711.67	703.88		696.83	37	606.38	566.08		527.25
7	711.26	702.40		694.70	38	599.63	558.55		518.62
8	710.76	700.76		692.23	39	592.78	550.62		509.97
9	710.01	699.02		688.95	40	585.63	542.58		500.94
10	709.08	696.83	19666.66	685.92	41	578.38	534.36		491.82
11	707.94	694.70	664.10	682.62	42	570.90	525.99		482.56
12	706.75	692.23	661.85	679.12	43	563.27	517.24		472.95
13	705.01	689.62	659.00	675.27	44	555.44	508.49		463.21
14	703.34	686.77	655.99	671.47	45	547.13	499.46		453.38
15	701.32	683.76	652.68	667.31	46	538.88	490.25		443.25
16	699.02	680.46	648.49	663.01	47	530.33	480.84		432.97
17	696.83	677.04	645.47	658.47	48	521.80	471.34		422.53
18	694.26	673.42		653.78	49	512.63	461.37		411.79
19	691.45	669.57		648.89	50	503.83	451.45		401.06
20	688.46	665.50	633.01	643.71	51	494.54	441.26		389.97
21	685.28	661.24	628.36	638.52	52	485.09	430.85		378.70
22	681.92	656.80	623.46	633.01	53		420.22		367.0
23	678.28	652.17	618.66	627.28	54	465.04	409.40		355.80
24	674.49	647.29	613.11	621.35	55	454.65	398.51		344.28
25	670.47	642.19	607.83	615.31	56		387.31		332.17
26	666.27	636.93	602.05	609.03	57		376.02		319.90
27	661.85	631.58	596.62	602.50	58		364.37		
28	657.26	625.85	590.39	596.00	59		352.63		
29	652.37	620.03		589.03	60		340.52		
30	647.29	614.01	577.53	581.98					

TABLE VI. $(1,0)^i$ *Band*, λ4836.192.

K″	R^i	Q^i	P^i	K″	R^i	Q^i	P^i
1		20668.39		23	20622.43	20594.74	20568.17
2	20671.67	667.87		24	617.02	588.54	560.63
3	671.67	667.03		25		581.80	552.72
4	671.67		20661.37	26	605.44	574.75	
5	671.67	664.76	658.85	27		567.54	535.98
6			655.83	28		559.83	527.56
7		661.16	652.99	29	586.27	552.15	518.93
8	669.81	659.18	649.62	30	579.10	544.27	
9	668.39	656.46	645.80	31		535.68	500.22
10	666.62	653.89	641.96	32	565.06	527.08	490.44
11		650.93	638.21	33	557.36		
12		647.42	633.81	34	548.83	509.04	471.17
13	660.73	644.02		35	541.06	499.66	
14	658.35	640.48	623.89	36	532.09	489.86	
15	655.18	636.22	618.70	37		479.86	
16	651.74		613.24	38	513.66	469.34	
17	648.75	627.37	607.65	39	504.12	459.31	
18		622.43		40	494.40	448.51	
19	641.31	617.30	595.79	41		437.85	
20		611.91	588.54	42	474.19	426.15	
21		606.85	582.60	43	463.85		
22	627.57	600.88	574.75				

TABLE VII. $(0,0)^i$ *Band*, λ4901.296.

K″	R	Q^i	P^i	K″	R^i	Q^i	P^i
1	20395.92			26	20337.27	20305.56	20275.35
2	396.49	20392.96		27	331.44	298.80	267.44
3	397.09	392.07		28	325.47	291.80	259.38
4	397.09	391.17		29	319.46	284.57	251.16
5	397.09	390.04		30	312.94	277.08	242.54
6	396.91	388.49	20381.33	31	306.52	269.28	233.76
7	396.15	386.61	378.13	32	299.55	261.27	224.70
8	395.66	384.65	374.97	33	292.36	253.09	215.30
9	394.34	382.49	371.53	34	284.90	244.63	205.52
10	392.96	379.81	367.92	35	277.60	235.77	196.05
11	391.54	376.88	364.16	36	269.28	226.92	186.10
12	389.69	374.21	359.88	37	261.27	217.79	175.90
13	387.48	370.96	255.10	38	252.78	208.32	165.25
14	385.34	367.15	350.56	39	244.02	198.54	154.65
15	382.49	363.34	345.76	40	235.06	188.60	143.58
16	379.81	359.36	340.44	41	226.17	178.36	132.72
17	376.88	355.10	334.98	42	216.48	167.90	121.11
18	373.19	350.56	329.30	43	207.31	157.23	109.42
19	369.60	345.76	323.47	44	197.31	146.62	097.42
20	365.85	340.78	317.27	45	187.07	135.37	085.53
21	361.44	335.60	310.76	46	176.51	123.68	073.12
22	357.00	330.02	304.20	47	165.69	112.03	
23	352.55	324.26	297.40	48	154.65	100.18	
24	347.64	318.28	290.28	49		087.96	
25	342.58	312.05	282.94	50		075.62	
				51		062.84	

TABLE VIII. $(0,1)^i$ *Band*, λ4989.354.

K″	R^i	Q^i	P^i	K″	R^i	Q^i	P^i
1	20035.67	20033.20		27	19977.46	19944.89	19913.43
2	036.40	032.77		28	972.07	938.11	905.85
3	036.69	032.12	20028.60	29	966.46	931.49	897.96
4	037.10	031.06	026.24	30	960.52	924.43	889.87
5	037.10	029.76	023.78	31	954.36	917.12	881.19
6	036.69	028.60	021.12	32	947.89	909.76	873.12
7	036.40	026.65	018.47	33	940.92	902.14	864.33
8	035.67	024.91	015.15	34	934.60	894.15	855.41
9	034.74	022.96	011.95	35	927.50	885.97	846.15
10	033.61	020.46	008.78	36	919.83	877.56	836.75
11	032.12	017.91	004.73	37	911.95	869.01	827.04
12	030.58	015.15	000.78	38	904.22	860.11	817.24
13	028.60	011.95	19996.54	39	896.45	851.04	807.20
14	026.65	008.78	992.29	40	888.26	841.83	796.90
15	024.22	005.18	987.73	41	879.70	832.33	786.43
16	021.67	001.61	982.71	42	870.48	822.46	775.81
17	018.95	19997.33	977.46	43	861.85	812.54	764.93
18	015.85	993.20	972.07	44	852.49	802.26	753.68
19	012.48	988.74	966.46	45	842.85	791.80	742.12
20	008.78	983.99	960.52	46	833.34	781.01	730.54
21	005.18	979.14	954.36	47	823.34	770.16	719.17
22	001.14	974.06	948.23	48	813.26	758.96	
23	19996.92	968.63	941.58	49	802.78	747.67	
24	992.29	962.84	935.06	50	792.56	736.12	
25	987.73	957.17	928.03	51	781.01	724.06	
26	982.71	951.02	920.79	52	770.16		
				53	758.96		

bands. The low abundance of Li^6, and the complexity of the spectrum prevented the observation of these lines, though a careful search was made by the methods mentioned above. The abundance ratio $Li^7 : Li^6$ has been determined by various observers and the results have varied considerably. Mass-spectrographs have yielded ratios varying from 15 to 10 and the most recent and most consistent of these are the determinations of Bainbridge[15] and Aston[16] which give a ratio of 11. From band spectra the much lower abundance ratio of 7.2 has been found by van Wijk and van Koeveringe[11] from the Li_2 bands and by Nakamura[17] from the LiH bands. Taking as the most favorable case the ratio 7.2 measured by the band spectrum methods, the intensity of the Li^6Li^6 lines relative to the Li^7Li^7 lines should be 1 : 40. One would expect to be able to observe lines of this intensity in absorption but unfortunately the vibrational structure of the band system interferes to such an extent that it makes the task almost impossible. As is evident from the Franck-Condon diagram given by Loomis and Nusbaum,[13] the intense bands of low vibrational quantum number are complicated by the superposition of fainter lines due to bands of higher vibrational energy. Thus even though the absorption is increased at low temperature by

[15] K. T. Bainbridge, J. Frank. Inst. **212**, 317 (1931).
[16] F. W. Aston, Proc. Roy. Soc. **A134**, 571 (1932).
[17] G. Nakamura, Nature **128**, 759 (1931).

increasing the length of the column of lithium vapor, numerous extraneous lines appear in the region where the Li^6Li^6 lines are expected. Also it was found that in order to predict the positions of these lines with sufficient certainty to definitely identify them in the maze of other lines, the rotational constants of the Li^7Li^7 and Li^6Li^7 molecules must be known more precisely than they are known at present. It appears that, with the exception of the possibility of separating Li^6 from Li^7 in fairly large quantities, the most promising method of obtaining Li^6Li^6 band lines is by an examination of the simplified spectrum obtained by magnetic rotation.[13]

Vibrational Isotope Effect

The procedure followed in the evaluation of the mass coefficient ρ from the vibrational constants was essentially that described in previous work on the BO spectrum.[9] By the combination principle, the difference of two terms having the same rotational quantum number, K, and having vibrational quantum numbers, v, differing by unity,

$$\Delta T_{v+\frac{1}{2}}(K) = T_{v+1}(K) - T_v(K), \qquad (1)$$

may be obtained as the wave-number difference of two corresponding lines in a pair of bands suitably chosen. In the present case, three sets of ΔT values can be obtained from each pair, using the lines of the R, Q, and P branches. Those from the R and P branches should be identical, while that from the Q branches may differ slightly if Λ-doubling is present. Thus for example, using two bands $(v',0)$ and $(v',1)$, we may obtain the differences

$$\begin{aligned}\Delta T_{\frac{1}{2}}''(K) &= Q^{v',\,0}(K) - Q^{v',\,1}(K) \\ &= R^{v',\,0}(K) - R^{v',\,1}(K) \\ &= P^{v',\,0}(K) - P^{v',\,1}(K) \cdots. \qquad (2)\end{aligned}$$

The dependence of ΔT on K can be shown[17a] from the equation for the rotational terms in $^1\Sigma$ and $^1\Pi$ states to be given by

$$\begin{aligned}\Delta T_{v+\frac{1}{2}}(K) &= \Delta G_{v+\frac{1}{2}} - (B_v - B_{v+1})(K+\tfrac{1}{2})^2 + \cdots \\ &= \Delta G_{v+\frac{1}{2}} - \alpha_e(K+\tfrac{1}{2})^2 + \cdots,\end{aligned} \qquad (3)$$

where terms in higher powers of $(K+\frac{1}{2})$ are negligible at values of K not too large. When the values of ΔT are fitted by least squares methods to a parabola having its vertex at $K=-\frac{1}{2}$, the constant term in the solution gives the best value of the vibrational term difference ΔG_v. For the $^1\Pi$ state, in which Λ-doubling is observed, the quantities ΔT will not be exactly the same for the Q as for the P and R branches. The ΔG_v should, however, be identical for the two because the difference, which is proportional to the Λ-doubling, is itself a function of $(K+\frac{1}{2})^2$. The vibrational term differences may be represented by the equation

$$\Delta G_v = \omega_e - 2x_e\omega_e(v+\tfrac{1}{2}) + 3y_e\omega_e[(v+\tfrac{1}{2})^2 + 1/12] + \cdots. \qquad (4)$$

From Eq. (4) in conjunction with the values of ΔG_v so obtained, the mass coefficient ρ can be obtained independently from each constant, since

$$\omega_e^i/\omega_e = \rho; \quad x_e^i/x_e = \rho; \quad y_e^i/y_e = \rho^2. \qquad (5)$$

Here the superscript i refers to quantities pertaining to the isotopic molecule Li^6Li^7. As in the case of the BO bands, it was first proved from the observed data that the vertex of the $\Delta T : K$ parabola actually occurs at $K=-\frac{1}{2}$ by making certain that the constant term, ΔG_v, in the solution was unaffected by the introduction of a linear term in $(K+\frac{1}{2})$.

Lower state

The $^1\Sigma$ state is the simpler of the two involved in the production of the blue-green lithium bands and since it is the normal state it should be free from perturbations. It has the added advantage for the precise determination of ρ that the value of ω_e'' is greater than that of ω_e'.

Table IX contains the results of the various least squares solutions for $\Delta G_v''$ and $\Delta G_v''^i$. In the solutions only values of $\Delta T(K)$ up to $K=30$ were used. The probable errors of the resulting average values of $\Delta G_v''$ are calculated on the basis of their external consistency[18] for all cases except that of $\Delta G_{1\frac{1}{2}}''^i$ where this was impossible. Although it is not evident in this particular case, a more conservative estimate of the probable error is obtained by this procedure than by using internal consistency. It will be noted that the

[17a] R. S. Mulliken, Rev. Mod. Phys. **2**, 100 (1930), Eq. (29) on p. 100 with $\Lambda=0$ for $^1\Sigma$ state and $=1$ for $^1\Pi$ state.

[18] R. T. Birge, Phys. Rev. **40**, 207 (1932).

TABLE IX. *Vibrational constants of the* $^1\Sigma$ *state.*

	Branch	*Bands*	$\Delta G_v''$	α''	*Wt.*
Li^7Li^7	*R*	0,0–0,1	346.191	0.00703	3
	Q	0,0–0,1	346.194	0.00713	5
	P	0,0–0,1	346.173	0.00709	1
			Av. 346.193 ±0.003		
	R	0,1–0,2	340.979	0.00728	3
	Q	0,1–0,2	341.022	0.00726	5
	P	0,1–0,2	341.061	0.00735	1
			Av. 341.012 ±0.013		
Li^6Li^7	*R*	0,0–0,1	360.335	0.00844	6
	Q	0,0–0,1	360.299	0.00830	10
	P	0,0–0,1	360.173	0.00814	1
			Av. 360.304 ±0.018		
	Q	0,1–0,2	354.616 ±0.046	0.00828	—

$\omega_e'' = 351.374 \pm 0.014$; $\omega_e''^i = 365.993 \pm 0.058$;
$\rho = 1.0416 \pm 0.0002$
$x_e'' = 0.00737 \pm 0.00002$; $x_e''^i = 0.00777 \pm 0.00007$;
$\rho = 1.05 \pm 0.01$

By assuming that $x_e^i/x_e = \rho$ *and not using the value of* $\Delta G_{1\frac{1}{2}}{}^i$ *(Cf. text page* 160*),*
$\omega_e'' = 351.374 \pm 0.014$ and $\omega_e''^i = 365.923 \pm 0.023$, giving
$\rho = 1.04141 \pm 0.00008$.

probable error of $\Delta G_{1\frac{1}{2}}{}''^i$ is large relative to the others, even though its error was computed by internal consistency, i.e., from the residuals of the least squares solution from which it was obtained. This results from the much smaller degree of accuracy with which the *Q* branch of the 0,2 isotope band could be measured, as previously explained. The items were weighted according to the estimated precision of the measurements for the branches involved. All solutions were carefully examined for any trend in the residuals; this was another determining factor in assigning weights in the one or two cases in which slight evidence of a trend was present. Fig. 1 represents graphically the residuals in the solution from the *Q* branches. Missing points on this figure do not indicate that the corresponding lines were not identified, but that their measurement was regarded as unreliable because of blending.

At the bottom of Table IX are given the values of ρ calculated by Eqs. (4) and (5). Since the data only involve the states $v'' = 0,1$ and 2, they are insufficient for the determination of the $y_e\omega_e$ or higher terms. However, as shown below, this is of no consequence in the present case. The value of ρ obtained from x_e^i/x_e is of course much less accurate than that from ω_e^i/ω_e but agrees with the latter to within its probable error. The second value of ρ given in the table from ω_e^i/ω_e is computed by using in the solution of Eq. (4) only $\Delta G_{1\frac{1}{2}}{}''^i$ and assuming that $x_e''^i/x_e'' \equiv \rho$. This assumption was shown[9] to be justified in the case of BO so in view of the untrustworthiness of the measurements on the 0,2 isotope lines, it is considered that the figure $\rho = 1.04141 \pm 0.00008$, although not as purely experimental as the other, is the more reliable result.

This value of ρ corresponds, as shown below, to a mass ratio Li^7/Li^6 considerably greater than that found by Costa.[6] Therefore the possible sources of error have all been carefully examined and it appears that none of them separately would change the result by more than the probable error. In their study of the lithium band spectrum, Loomis and Nusbaum[13] were able to evaluate a $y_e\omega_e(v+\frac{1}{2})^3$ term in the expression for the vibrational terms of the lower state. Their value of $y_e\omega_e$ was -0.0097. Introducing this into Eq. (4), and solving by means of our experimental ΔG's, a value of ρ was found which differed by only one part in 40,000 from that calculated without this term. Recently Dunham[19] has calculated the energy levels of a rotating vibrator by quantum mechanics, and compared the results with those of the old quantum theory. The correction to be applied to the ratio $\omega_e^i/\omega_e = \rho$ has been evaluated and found to be only one part in 200,000. Since the probable error of the most precise determination of ρ in the present work is one part in 12,000, it is quite evident that neither of the above corrections materially changes the result.

Upper state

The data for the $^1\Pi$ state were obtained earlier than those for the $^1\Sigma$ state, from a set of plates giving slightly less resolution.[19a] They were treated in the same manner as for the normal state. As a consequence of the convention of designating a band line by its lower state value of *K*, it follows that the vertex of the $\Delta T : K$ parabola occurs here at $K = -1\frac{1}{2}$, $-\frac{1}{2}$ and $+\frac{1}{2}$ for the parabolas from the *R*, *Q*, and *P* branches

[19] J. L. Dunham, Phys. Rev. **41**, 721 (1932).
[19a] A. McKellar, Phys. Rev. **43**, 215 (1933).

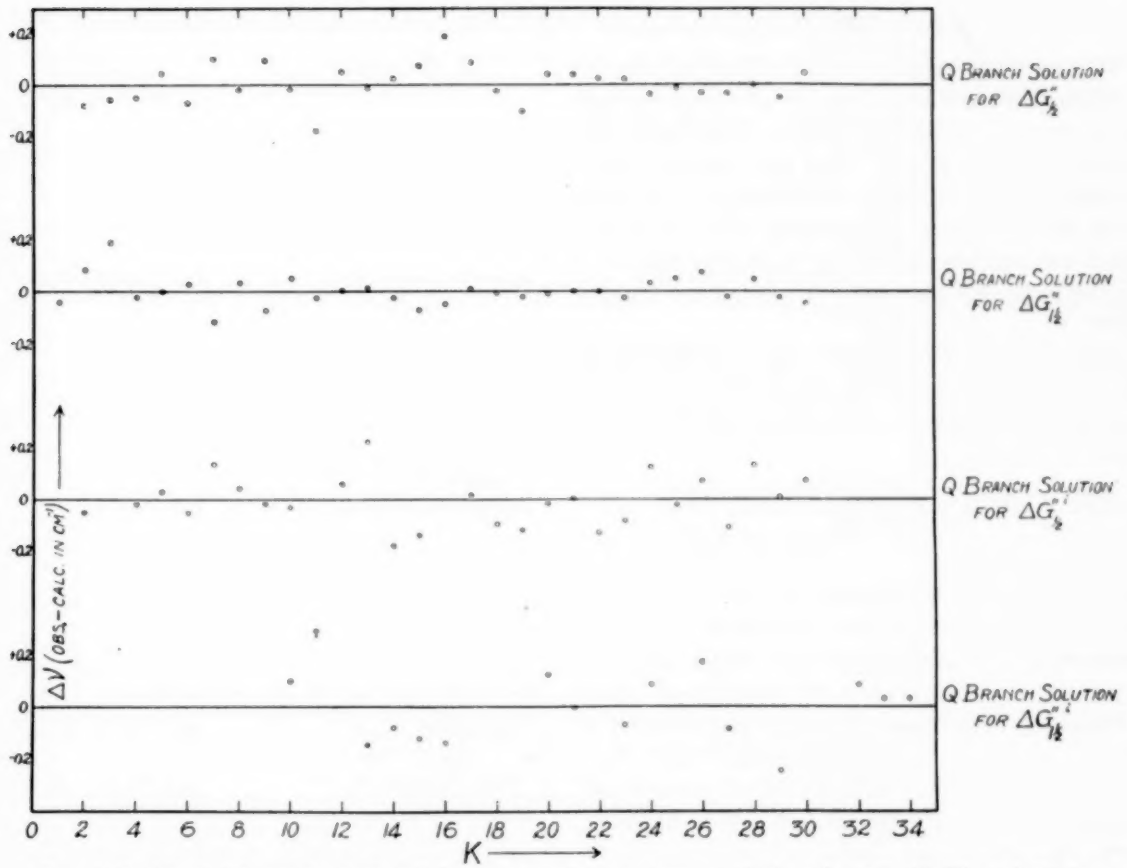
Q BRANCH SOLUTION FOR $\Delta G''_{1/2}$
Q BRANCH SOLUTION FOR $\Delta G''_{1/2}$
Q BRANCH SOLUTION FOR $\Delta G''_{1/2}$
Q BRANCH SOLUTION FOR $\Delta G''_{1/2}$
$\Delta\nu$ (OBS.-CALC. IN CM^{-1})
K

FIG. 1. Residuals (observed-calculated) from adopted least squares solutions for $\Delta T : K$. The relatively large residuals in the single solution for $\Delta G_{1/2}''$, illustrate the unreliability of this determination.

respectively. The highest values of K used in these solutions varied from 30 to 40. The vibrational constants of the upper state calculated by least squares are given in Table X. The results of the three solutions for $\Delta G_{1/2}''$ were given equal weight in this case because, although there were a few more values of ΔT available from the Q branch than from the other two, the residuals in the computations involving the R and P branches appeared to be considerably smaller than those of the Q branch solution. No lines were identified in the 2,0 isotope band so a value of $\Delta G_{1/2}''$ could not be calculated. Therefore it was necessary to assume the theoretical equation $x_e''/x_e' = \rho$ in order to solve Eq. (4) for ω_e''. Although the magnitude of ρ obtained from the upper state is slightly lower than those computed from the $^1\Sigma$ state, the agreement constitutes a satisfactory check on the previous values. In view of the fact that the results from the upper state are less accurate and in general less trustworthy than those from the normal state they should carry much less weight than the latter.

TABLE X. *Vibrational constants of the* $^1\Pi$ *state.*

	Branch	*Bands*	$\Delta G_v'$	α'	*Wt.*
Li^7Li^7	R	1,0–0,0	264.709	0.00896	3
	Q	1,0–0,0	264.663	0.00888	5
	P	1,0–0,0	264.630	0.00882	1
			Av. 264.675 ±0.013		
	R	2,0–1,0	258.450	0.00931	3
	Q	2,0–1,0	258.394	0.00921	5
	P	2,0–1,0	258.364	0.00915	1
			Av. 258.409 ±0.014		
Li^6Li^7	R	1,0–0,0	275.255	0.00905	1
	Q	1,0–0,0	275.399	0.00930	1
	P	1,0–0,0	275.215	0.00926	1
			Av. 275.290 ±0.038		

$\omega_e' = 270.941 \pm 0.029$; $\omega_e'' = 282.081 \pm 0.044$;
$\rho = 1.0411 \pm 0.0002$

Rotational Isotope Effect

It was considered of value to calculate the rotational constants of the main and isotopic molecules since for the latter they have not heretofore been found. They give entirely independent values of ρ for comparison with those from the vibrational constants. The rotational constants are also necessary if an attempt is to be made to detect a possible electronic isotope effect.

The rotational constants were calculated by the same method as that employed by Harvey and Jenkins.[11] The $R-P$ combination differences are given by

$$\Delta_2 F(K) = 4B_v(K+\tfrac{1}{2}) + 8D_v(K+\tfrac{1}{2})^3 + 12F_v(K+\tfrac{1}{2})^5 \cdots \quad (6)$$

in which some negligible terms have been omitted. By means of the well-known relations connecting the vibrational and rotational constants preliminary values of D_v and F_v were calculated. With these, Eq. (6) was reduced to the linear form in $K+\frac{1}{2}$ and so could be solved by least squares for B_v. Such solutions were carried through for the $v'=0,1$ and $v''=0,1$ states of both the main and isotopic systems. Extrapolating to the equilibrium state by means of the relation

$$B_v = B_e - \alpha(v+\tfrac{1}{2}), \quad (7)$$

one obtains the value of ρ by the requirement

$$\rho^2 = B_e^{i}/B_e \cdots. \quad (8)$$

The results of such computations for the lower state are listed in Table XI. In obtaining

Table XI. *Rotational constants of the* $^1\Sigma$ *state.*

Li^7Li^7 Band	B_v''	Li^6Li^7 Band	$B_v''^{i}$
0,0	0.6685	0,0	0.7276
1,0	0.6696	1,0	0.7269
2,0	0.6695		
0,1	0.6606	0,1	0.7166
$\therefore B_e''=0.6721\pm0.0003$ (using $\alpha_e''=0.00708$ from vibrational analysis)		$B_e''^{i}=0.7302\pm0.0007$ (using $\alpha_e''^{i}=0.00830$ from vibrational analysis)	
$D_e''=-0.986\times10^{-5}$		$D_e''^{i}=-1.16\times10^{-5}$	
$F_e''=2.00\times10^{-10}$		$F_e''^{i}=2.4\times10^{-10}$	
$\beta''=-3.86\times10^{-8}$		$\beta''^{i}=-2.1\times10^{-8}$	
$\rho^2=B_e''^{i}/B_e''=1.0863\pm0.0012$; $\rho=1.0422\pm0.0006$			

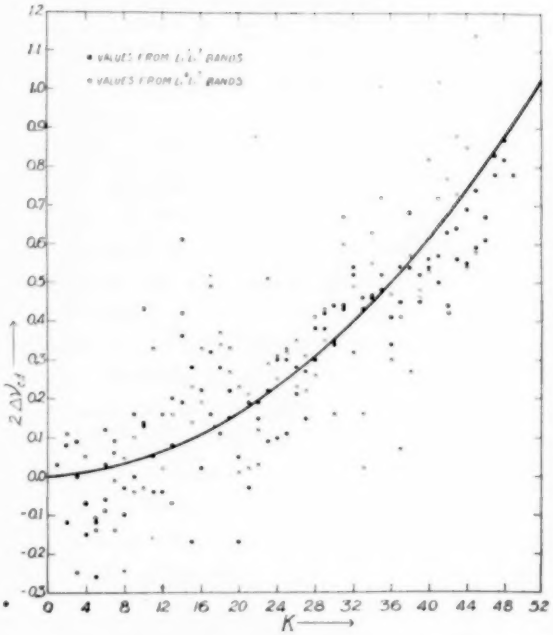

Fig. 2. Λ—doubling in the upper state $v'=0$ for both main (solid points) and isotopic systems (circles). The points of the latter show a somewhat greater scatter due to the smaller degree of accuracy with which the fainter lines could be measured, but the two sets of data appear to fit the same curve. The curve given is the theoretical one

$$\Delta(PQR) = 2\Delta\nu_{dc} = 2(B_d' - B_c')K(K+1),$$

in which $B_d' - B_c' = 0.00018$, as given by Wurm.[9]

$B_e''^{i}$ the data from the 0,1 band were given double weight because the combination differences of the lines of low rotational quantum number in this band were more free from the influence of blends than were those of the other two bands. In calculating both B_e'' and $B_e''^{i}$ the more exact values of α_e'' and $\alpha_e''^{i}$ found from the vibrational analyses were used. The magnitude of ρ obtained from the data in Table XI is seen to be somewhat larger than those computed from the vibrational analysis but agrees with the latter to within its probable error.

Table XII gives the rotational constants calculated for the $^1\Pi$ state. The data were treated in the same manner as for the normal state. Again the resulting ρ is in good agreement with the previous values. The Λ-doubling of the rotational levels of this state, although actually immaterial for the evaluation of ρ, was investigated for the main and isotopic molecules. The doubling in the lowest vibrational state is shown in Fig. 2, from which it appears to be sensibly the same for

TABLE XII. *Rotational constants of the* $^1\Pi$ *state.*

Li^7Li^7 Band	B_v'	Li^6Li^7 Band	$B_v'^i$
0,0	0.5538	0,0	0.6001
0,1	0.5520	0,1	0.5986
0,2	0.5531		
1,0	0.5453	1,0	0.5933
$B_e'=0.5577\pm0.0003$ (using $\alpha'=0.00888$ from vibrational analysis)		$B_e'^i=0.6046\pm0.0007$ (using $\alpha'^i=0.00922$ from vibrational analysis)	
$D_e'=-0.945\times10^{-5}$		$D_e'^i=-1.11\times10^{-5}$	
$F_e'=2.05\times10^{-10}$		$F_e'^i=2.6\times10^{-10}$	
$\beta'=-7.68\times10^{-8}$		$\beta'=-7.5\times10^{-8}$	
$\rho^2=B_e'^i/B_e'=1.0841\pm0.0014$; $\rho=1.0412\pm0.0007$			

both molecules. Although a small difference is to be expected on theoretical grounds, no evidence for this can be found from our data.

ELECTRONIC ISOTOPE EFFECT

Since in BO the origins of the main and isotopic band systems were found to differ slightly[20] indicating an electronic isotope effect, and in view of the relatively large isotope shifts calculated and found[21] in the atomic spectrum of lithium, it is of interest to examine the lithium molecular spectrum in this connection. The origins of the main and isotopic 0,0 bands were computed using the new rotational constants and the equations given by Harvey and Jenkins[22] for the band line frequencies. The results are

$$\nu_0^{(0,0)} = 20395.902\pm0.010;$$
$$\nu_0^{(0,0)^i} = 20394.201\pm0.010.$$

Then, from the relation

$$\nu_e=\nu_0^{(0,0)}-\left[\omega_e'(\tfrac{1}{2})-x_e'\omega_e'(\tfrac{1}{2})^2\right]+\left[\omega_e''(\tfrac{1}{2})-x_e''\omega_e''(\tfrac{1}{2})^2\right]\cdots \quad (9)$$

the two system-origins may immediately be computed with the aid of the vibrational constants from Tables IX and X. The system origins found are

$$Li^7Li^7:\ \nu_e=20436.25\pm0.02;$$
$$Li^6Li^7:\ \nu_e^i=20436.29\pm0.04.$$

[20] Cf. reference 9, p. 483.

[21] D. S. Hughes and C. Eckart, Phys. Rev. **36**, 694 (1930); D. S. Hughes, Phys. Rev. **38**, 857 (1931).

[22] Cf. reference 11, p. 795.

Hence it appears that either the electronic terms of the two molecules are very nearly equal, or they differ by approximately the same amount for the $^1\Sigma$ and $^1\Pi$ states.

DISCUSSION OF RESULTS

A summary of the different determinations of the mass coefficient ρ, with their probable errors, is given in Table XIII. The values derived from the vibrational structure of the bands are somewhat more accurate than those found from the rotational structure. In the last column is included the mass ratio Li^7/Li^6 corresponding to the more exact mass coefficients. From the definition $\rho=(\mu/\mu^i)^{\frac{1}{2}}$, in which μ is the reduced mass of the diatomic molecule $=m_1m_2/(m_1+m_2)$, it follows that

$$Li^7/Li^6=2\rho^2-1. \quad (10)$$

The mass spectrograph results of Costa as modified by Aston[7] are given for comparison at the bottom of the table. It is apparent that the band spectrum values of the mass ratio, although showing considerable variation, are all definitely higher than the mass-spectrograph determination.

There is some uncertainty as to the extent to which the masses of the electrons enter into the

TABLE XIII. *Summary of values of* ρ *and the corresponding mass-ratios* Li^7/Li^6.

Constants used	*Bands used*	ρ	Li^7/Li^6
ω_e''	(0,0)(0,1)(0,2) $(0,0)^i(0,1)^i$	1.04141 ± 0.00008	1.1690 ± 0.0003
ω_e''	(0,0)(0,1)(0,2) $(0,0)^i(0,1)^i(0,2)^i$	1.0416 ± 0.0002	1.1698 ± 0.0008
ω_e'	(0,0)(1,0)(2,0) $(0,0)^i(1,0)^i$	1.0411 ± 0.0002	1.1678 ± 0.0008
B_e''	(0,0)(1,0)(2,0)(0,1) $(0,0)^i(1,0)^i(0,1)^i$	1.0422 ± 0.0006	
B_e'	(0,0)(0,1)(0,2)(1,0) $(0,0)^i(1,0)^i(0,1)^i$	1.0412 ± 0.0007	
Values by Costa[6]. $Li^6=6.012\pm0.002$ (*limit of error*) $Li^7=7.012\pm0.002$ $\rho=1.04075\pm0.00017$		$Li^7/Li^6=1.1663\pm0.0007$	

ratio determined by Eq. (10). It is probably more nearly true to assume that the electrons of each atom vibrate with its nucleus than that the nuclei alone vibrate. On the former assumption, the result from Eq. (10) represents the actual mass ratio of the *atoms* (nuclei+electrons), whereas on the latter, it represents the ratio of the *nuclear* masses, and is to be corrected in obtaining the atomic ratio by the addition of three electrons to each mass. However, when this is done, the ratio is only decreased by one part in 25,000, which is well within the probable error of our most accurate result.

We now have independent evidence from disintegration experiments that the figure 7.012 is definitely low for the atomic weight of Li^7. From experiments in which lithium is disintegrated by the impacts of protons, the mass of the Li^7 atom may be found by considering it as the unknown quantity in the process represented by the equation.

Energy + proton + Li^7 nucleus → 2α-particles +energy. Using the data of Cockcroft and Walton,[23] who found 17.2 million volts as the total energy of the two α-particles produced by bombardment of lithium with 450,000 volt protons, the mass of the Li^7 atom is computed to be 7.015. In consequence of the precision with which the other factors are known, this figure should be accurate to better than ±0.001.

Taking this as the correct mass of Li^7, and using the mass ratio $Li^7/Li^6 = 1.1690$, found from the vibrational constants of the normal state (considered the best value) the mass of Li^6 is 6.001. From the upper state mass ratio $Li^7/Li^6 = 1.1678$, one obtains $Li^6 = 6.007$. On the packing fraction-mass number diagram of Aston,[24] these figures place Li^7 directly upon the upper branch of the curve, occupied by the relatively easily disintegrated atoms. On the other hand, Li^6 is shifted down to a position approximately on the lower branch of the curve upon which are He^4, C^{12} and O^{16}, the more stable atoms. If the Li^6 nucleus is composed of one α-particle, one proton and one neutron and the Li^7 nucleus is obtained by the addition of one neutron, it seems not at all unreasonable that the three entities outside the α-particle for Li^7 should give a greater mass defect than the two for Li^6. However, this does not appear to be so for the boron isotopes. An important difficulty appears if we consider the Li^6 and Li^7 nuclei to be so constituted, since one would expect the *lower* limit to the mass of Li^6 to be the mass of Li^7 minus the mass of a neutron. The mass of Li^6 computed from our best mass ratio is below this value by considerably more than its probable error. Therefore, in view of the unexpectedly high Li^7/Li^6 mass ratio obtained here it would appear very desirable to obtain new mass-spectrograph data on lithium.

In conclusion I wish to express my sincere appreciation of the invaluable assistance rendered by Professor F. A. Jenkins under whose guidance this work has been done. I am deeply indebted also to Professors R. T. Birge and R. H. Fowler for helpful discussions.

Note added in proof, July 17, 1933: K. T. Bainbridge has very recently[25] made accurate measurements of the masses of the lithium isotopes using his mass-spectrograph. His results are $Li^7 = 7.0146 \pm 0.0006$ and $Li^6 = 6.0145 \pm 0.0003$ corresponding to a mass ratio $Li^7/Li^6 = 1.16628 \pm 0.00016$. His value for Li^7 is seen to be in very good agreement with that obtained from disintegration data. The mass ratio found is almost identical with the former mass-spectrograph determination of Costa and is thus considerably lower than that computed from band spectrum data as presented above. In view of the good agreement of the two methods in the cases of boron[9] and hydrogen,[26] this result is very surprising. We are unable to account for the discrepancy at the present time.

[23] Cf. reference 1, p. 236.

[24] Cf. reference 7, p. 511.

[25] K. T. Bainbridge, Phys. Rev. **44**, 56 (1933).

[26] J. D. Hardy, E. F. Barker and D. M. Dennison, Phys. Rev. **42**, 279 (1932).

The Emission Spectrum of Molecular Hydrogen in the Extreme Ultraviolet

C. RULON JEPPESEN, *University of California*

(Received May 9, 1933)

Experimental procedure and results

A new grazing incidence vacuum spectrograph containing a two meter grating, designed by Professor H. E. White and built in the shop of the University of California Physics Department, has been used to photograph more than 2200 lines in the emission spectrum of molecular hydrogen between 1375A and 810A. The known spectrum of this molecule has thus been extended about 200A toward shorter wave-length and more than 1400 new lines have been obtained.

Identification of lines

The $2p^1\Sigma - 1s^1\Sigma$ ($B-A$) band system has been extended so that a number of bands ending on the three lowest vibrational levels of the normal electronic state are now included. A new analysis of the bands of the $2p^1\Pi_{cd} - 1s^1\Sigma$ system has also been made. Observed and calculated wave numbers are given for all identified lines. Except in the case of perturbed lines these two values agree always within the probable error of experiment (about 2 cm^{-1}).

The $1s^1\Sigma$ state

Values of the molecular constants for each observed vibrational level in the normal $1s^1\Sigma$ state have been calculated and tables of the rotational energy function, F, have been constructed. The new values of B fall regularly upon a smooth $B_v : v$ curve, so that it is no longer necessary to assume that a perturbation exists in the $v=0$ vibrational level. This $B_v : v$ curve has, however, a positive curvature for low values of v in contradistinction to the known negative curvature for higher values of v. The new $\Delta G_v : v$ curve is also found to be smooth and of the same general shape as the $B_v : v$ curve.

The $2p^1\Sigma$ state

The available data on the $2p^1\Sigma$ state from bands in the visible spectrum given by Richardson and Davidson have been combined with the ultraviolet data for calculation of the rotational constants. The value of B_0 thus obtained agrees with that given by these authors. The $B_v : v$ curve for this state is found to have a decided positive curvature for low values of v, the curvature becoming much less as v increases. The new and independent values of ΔG_v agree to within 0.4 cm^{-1} with those given by Richardson and Davidson. Tabulated values of the rotational energy function are given.

The $2p^1\Pi_{cd}$ state

Because of the Λ-type doubling in this state we find two "effective" values of each of the rotational constants B, D and F. The true value of B is, in our case, the effective B given by the c component levels. The values of B_v for these latter levels fall quite regularly on a smooth $B_v : v$ curve. On the other hand, the B_v values derived from the d component levels do not lie on any smooth curve. This is due to a number of perturbations in the d component levels. Besides a number of ordinary rotational perturbations there is one apparent *vibrational* perturbation of 10.4 cm^{-1} in the $v=3$ state.

Values of the constants

Values of B_e for the $1s^1\Sigma$ (A), $2p^1\Sigma$ (B) and $2p^1\Pi_{cd}$ (C) states are found to be 60.8715 (60.587), 19.987, and 31.288 (30.065) cm^{-1}, respectively. Similarly the values of ΔG_e for these states are 4417.9 (4371.), 1358.33, and 2468 (2444) cm^{-1}, respectively. The value of ν_e for the $2p^1\Sigma - 1s^1\Sigma$ system is 91,708 cm^{-1} and the frequency of the 0−0 band is $\nu_{00}=90{,}206.1$ cm^{-1}. Corresponding values for the $2p^1\Pi_{cd} - 1s^1\Sigma$ system are $\nu_e=100{,}049$ cm^{-1} and $\nu_{00}=99{,}087.4$ cm^{-1}. These new values differ appreciably in some cases from the best previous results (as given in parentheses above) and these changes are due to many new assignments and reassignments of lines as well as to the reinterpretation of the apparent perturbation in the $v=0$ level of the normal state.

INTRODUCTION

THE secondary or molecular spectrum of hydrogen has been the subject of considerable investigation. The extensive and accurate measurements of wave-lengths in the near infrared, visible and near ultraviolet made by Gale, Monk and Lee have been used by Richardson and his students to obtain extensive information concerning many excited electronic states of hydrogen. In order to evaluate the constants of the normal state of the molecule, the extreme ultraviolet spectrum must be studied.

Many investigators, including Lyman,[1] Wer-

[1] T. Lyman, *The Spectroscopy of the Extreme Ultraviolet* (1914).

ner,[2] Witmer,[3] Hori,[4] Dieke and Hopfield,[5] Schaafsma and Dieke,[6] and Hyman,[7] have searched for hydrogen bands in the extreme ultraviolet until almost a thousand lines distributed among nearly a hundred bands have been photographed.

All these data have led to considerable knowledge concerning the energy states and the molecular constants of hydrogen. However, only one band has been observed, by Hori,[4] having as a final state the lowest vibrational level ($v=0$) of the normal electronic state of the molecule and only six of the analyzed bands are found to have $v=1$ or $v=2$ as their final states. Moreover, in each of these bands the number of lines observed was small, and accurate values of their wavelengths could not be obtained. The more accurate data of Hyman did not include any lines from bands belonging to the three lowest vibrational states of the molecule.

The analysis of previously observed emission bands in the extreme ultraviolet spectrum has been carried out by Hori,[4] Dieke and Hopfield,[5] Schaafsma and Dieke,[6] and Hyman.[7] It has been shown by these investigators that all of the bands are associated with two excited electronic states of the molecule. Dieke and Hopfield[5] tentatively called these the B and C states, the normal level being designated the A state. It is now known[8] that the normal level is a $(1s\sigma)^2S^1\Sigma$ state, and that the B and C levels are respectively $(1s\sigma)(2p\sigma)P^1\Sigma$ and $(1s\sigma)(2p\pi)P^1\Pi_{cd}$ states. The designations of these states are usually abbreviated as follows $1s^1\Sigma$, $2p^1\Sigma$ and $2p^1\Pi_{cd}$. It is to be noted that Richardson and his students have published a long series of papers giving bands in the visible spectrum having the two latter levels as their final states.

The theoretical importance of the hydrogen molecule, as well as certain questions concerning the constants for the lowest vibrational states of the normal electronic level, made it seem worth while to try to obtain new bands in the extreme ultraviolet spectrum. In addition it was thought that bands might be found having different initial electronic states from the two to which all previous bands belonged.

In the investigation here described a large number of new bands was found and the analysis of a number of them has led to much more complete data on the three lowest electronic states of the molecule than have been heretofore available.

Experimental Procedure

The spectrograph

In the vacuum region the method of grazing incidence, applied to the construction of grating spectrographs, has been found to possess several advantages over the older types of mounting which featured nearly normal incidence of the light upon the grating. Chief of these advantages are the comparatively much greater dispersion and the greatly increased reflecting power of the grating.

The spectrograph used in the present investigation was designed by Professor H. E. White and constructed in the shop of the University of California Physics Department. It contains a 2-meter concave grating, having a ruled surface of 8 by 5 cm and approximately 567 ruled lines per mm. The grating was ruled at the National Physical Laboratory and was obtained from Adam Hilger Company. A schematic diagram of the instrument is shown in Fig. 1. The

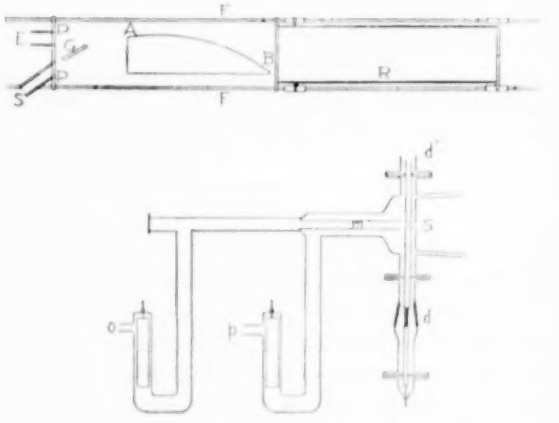

Fig. 1. Schematic diagram of spectrograph and discharge tube.

[2] S. Werner, Proc. Roy. Soc. **A113**, 107 (1926).
[3] E. E. Witmer, Proc. Nat. Acad. Sci. **12**, 338 (1926).
[4] T. Hori, Zeits. f. Physik **44**, 838 (1927).
[5] G. H. Dieke and J. J. Hopfield, Zeits. f. Physik **40**, 299 (1926); and Phys. Rev. **30**, 400 (1927).
[6] A. Schaafsma and G. H. Dieke, Zeits. f. Physik **55**, 164 (1929).
[7] H. H. Hyman, Phys. Rev. **36**, 187 (1930).
[8] See O. W. Richardson, Proc. Roy. Soc. **A126**, 487 (1930).

slit S, the grating G, and the plateholder AB are all placed on the usual Rowland circle. The receiver R is a drawn brass tube 8 inches in diameter and about 36 inches long. As indicated in the diagram, the receiver tube is mounted on wheels fitting a track F so that the tube may easily be fitted against the end plate P. A vacuum-tight connection is made by means of a rubber gasket. The spectrograph is evacuated through the air outlet E by means of a double stage mercury condensation pump backed by a Cenco Hyvac. The design is such that light is incident on the grating at an angle of about 82.5°. Lines having wave-lengths from the very shortest up to about 1375A may be photographed in the first order spectrum.

With the instrument in its best adjustment, remarkably good definition and resolving power can be obtained, as may be seen by examination of the reproductions of two typical spectrograms shown in Fig. 2. The actual resolving power attained in the first order spectrum was about 30,000. The total number of ruled lines on the grating is about 45,000. This last number is not, however, the theoretical resolving power since, as shown by Mack, Stehn and Édlen,[9] the optimum width of a grating at large angles of incidence may be considerably less than the width ordinarily ruled on the grating. The data given by these authors show that in our case the theoretical resolving power of the grating was practically attained. It should be noted also that nonsymmetrical ghosts appeared near each of the very strong lines obtained in this investigation. In accordance with the theory of Mack, Stehn and Édlen, it is now thought that these would not have appeared had the aperture of the grating been reduced to its optimum value.

The source

The best development of the bands in the extreme ultraviolet spectrum of H_2 is found to be attained in a rather long discharge tube (total length about 80 cm), the inside of which is ground rough. As was noted by Hyman,[7] the grinding of the discharge tube serves also to suppress the continuous spectrum of hydrogen.

The design of the tube is indicated in Fig. 1. It may be seen that this design permits the discharge to be brought very near the slit, and thus serves to insure the full surface of the grating being illuminated as well as to reduce absorption in the discharge tube itself. The electrodes are of aluminum and the tube is of Pyrex of inside diameter about 11 mm, except for the constricted portion m near the slit. This is reduced to about 6 mm inside diameter.

In operation there exists a continuous leak of hydrogen from the discharge tube through the very narrow slit into the spectrograph. To compensate for this, a continuous flow of hydrogen is maintained through the tube. The hydrogen flows from an electrolytic generator through a variable leak[10] of the type devised by Hopfield, then through drying tubes of calcium chloride and phosphorus pentoxide, and finally into the discharge tube through the inlet o. A pumping system, separate from that used to evacuate the spectrograph itself, maintains the flow by removing the gas through the tube p.

As a source of power a one kw 25,000 volt transformer was found to be sufficient. The current through the discharge tube may be estimated at about 30 milliamperes. It may be noted that in the previous investigations of Dieke and Hopfield, and of Hyman, current densities up to 10 times that used in the present investigation were employed. It is thought that the greater number of bands observed in the present work, as well as the extension of the spectrum to a shorter wave-length limit, is due jointly to the maintenance of the discharge at a somewhat lower pressure, to the much better vacuum attained in the receiver (certainly lower than 10^{-4} mm of Hg) and to the high reflecting power of the grating at grazing incidence.

The comparison spectrum

Investigations in the extreme ultraviolet region of the spectrum have been handicapped by a deplorable lack of suitable standards. The design of the present spectrograph does not permit of the superposition of orders in the region of this investigation since the long wave-length limit, as before noted, is at about 1375A. The vacuum

[9] Mack, Stehn and Édlen, J. Opt. Soc. Am. **22**, 245 (1932).

[10] J. J. Hopfield, J. Opt. Soc. Am. **12**, 391 (1926).

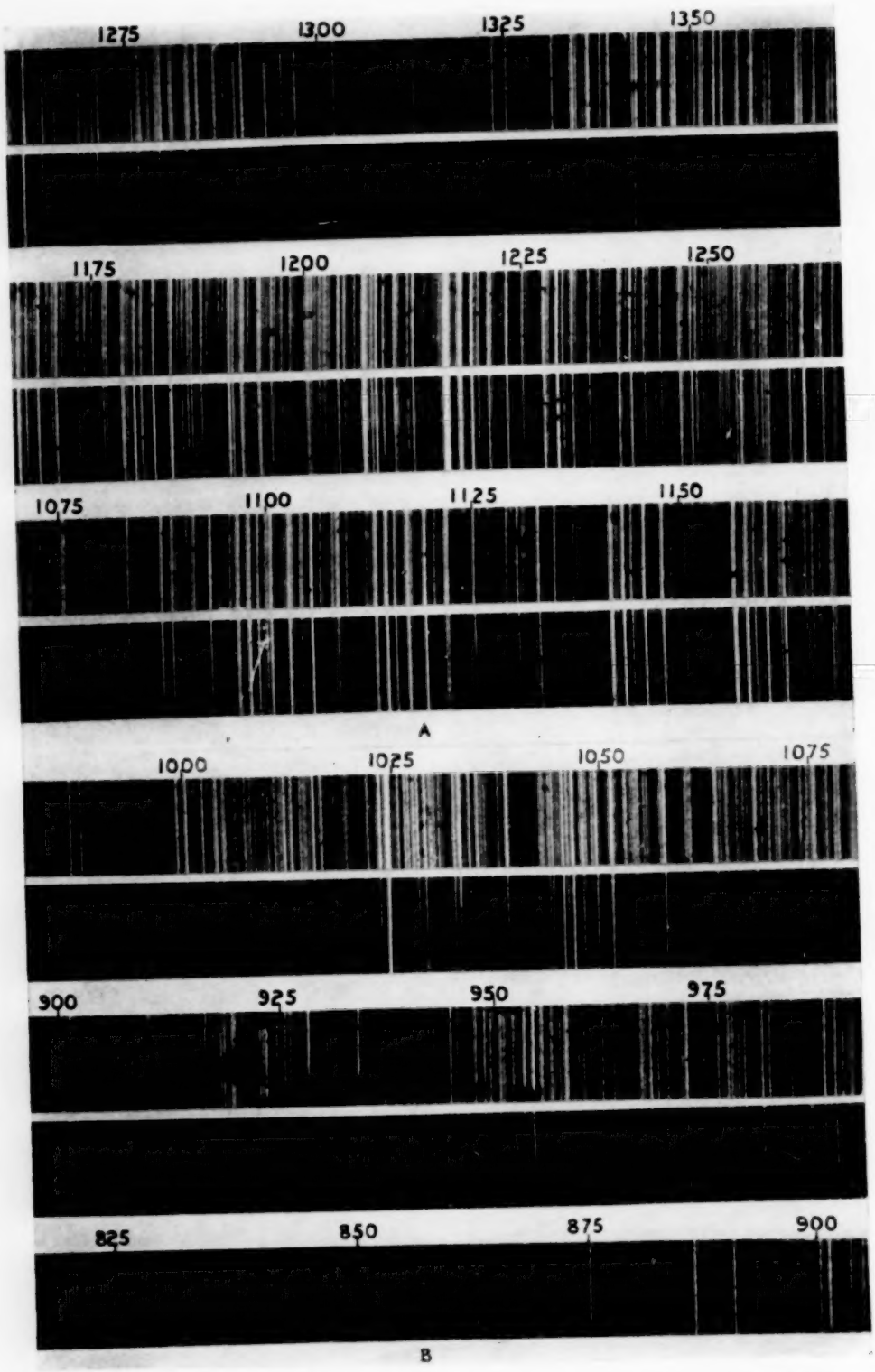

FIG. 2. Enlargements (about 4×) of two spectrograms. Exposure times 45 and 25 minutes, respectively.

spark seemed, then, to offer the best possibilities for the production of a sufficient number of lines of known wave-length. Accordingly, a discharge tube was designed in such a way that a pair of aluminum electrodes could be placed between the tube *m* (Fig. 1) and the slit of the spectrograph. These electrodes are carried in two side tubes, *d*, *d'*, in such a manner that by means of a ground glass joint in each they may be adjusted with respect to each other and may be aligned with respect to the slit. The electrodes are placed in series with an external spark gap and in parallel with condensers of about 0.05 microfarad capacity. An interrupter is arranged so that about 25 discharges occur per minute, the sparking time being about 0.8 second. An intermittent spark is necessary so that overheating of the electrodes can be avoided and so that the necessarily low pressure in the tube may be maintained.

It was found that the spark lines of oxygen in the region under investigation could be obtained by using aluminum electrodes. However, the conditions under which they appeared were not easily reproducible. Under certain conditions the oxygen lines disappeared entirely and the spark lines of silicon were found to be brought out with considerable intensity. The wave-lengths of the latter lines, however, are not known with sufficient accuracy for use as standards. If a small stick of carbon be placed in one of the aluminum electrodes, it is found that not only the lines of ionized carbon but also a number of the spark lines of oxygen are easily made to appear in the discharge. There is a sufficient number of these lines so that between 800 and 1375A there is no gap greater than 75A. Usually the distance between lines is much smaller than this. The wave-lengths of the lines may be found in the tables compiled by MacInnes and Boyce.[11] Besides these lines the second, third and fourth members of the Lyman series were available as standards in the present work. The theoretical values of the wave-lengths of the Lyman series lines have been calculated by Penney.[12] The first member of the Lyman series was usually so overexposed on the plates obtained by the writer that it could not be used as a standard.

For various reasons it was thought best not to superpose the comparison spectrum upon the plates that showed the H_2 spectrum in its best development. Instead, a rather large number of plates were taken, each showing the comparison spectrum but having various different times of exposure of the hydrogen spectrum. From these plates there were determined the wave-lengths of 35 hydrogen lines to be used as auxiliary standards.

Reduction of the plates and experimental results

Measurements of the plates studied were made by use of a 200 mm Gaertner comparator, owned by Professor R. T. Birge. It was found that in a few cases the vacuum spark spectrum was shifted by a small but easily detectable amount with respect to the hydrogen band spectrum. It is thought that this was due to the spark electrodes being in such a position that only part of the grating (and probably not a central part) was illuminated. It would seem necessary in all studies in which such spark spectra are observed to make certain, by measurement of a reasonable number of plates, that the spectrum is not shifted because of unequal illumination of the grating. This effect may be shown to be accentuated considerably by use of the grating at grazing incidence. It may be especially troublesome where, as in the present study, two spectra from different sources are to be superposed.

Another source of possible error in the measurement of wave-length is due to the fact that at grazing incidence not only is the spectrum far from normal, but small irregularities in the curvature of the plate may introduce relatively very large deviations from a smooth dispersion curve. In the present instance it was found that if the dispersion curves were assumed smooth, an error in value of the wave-lengths of more than 0.2A might be made in some cases. It is accordingly thought worthwhile to give a rather detailed description of the method used in reduction of the plates.

For a determination of the wave-lengths of 35 hydrogen lines to be used as auxiliary standards, seven plates showing both vacuum spark and hydrogen discharge spectra were measured. For

[11] J. M. MacInnes and J. C. Boyce, *Wave-lengths of the Extreme Ultraviolet Lines from Gas Discharges* (1930).

[12] W. G. Penney, Phil. Mag. **9**, 661 (1930).

each of these plates tables were constructed of divided second differences of the wave-lengths of spark lines as a function of comparator readings. From these second differences, wave-lengths corresponding to equal intervals of the comparator scale were interpolated. The method of Birge and Shea[13] could then be applied to the calculation of least square polynomials of the second degree giving wave-length as a function of comparator readings. The differences between the known wave-length of each standard line and the wave-length calculated in this way for the particular plate under consideration could then be plotted as a correction curve. From the least squares equation and the correction curve, the wave-length of each of the 35 auxiliary hydrogen standards was obtained. Comparison of the wave-lengths thus calculated from different plates indicates that the probable error of λ in any case should not be greater than 0.05A. Application of the combination principle shows that over small intervals, such as the extent of any one band, the relative wave-lengths have probable errors much smaller than 0.05A but that the probable error of the relative values of λ over great intervals may be as large as 0.05A.

After determination of λ for the auxiliary standards, all the lines were measured on two plates showing the best development of the H_2 spectrum. Correction curves for these plates were made in the same manner as described above and from the resulting least squares equations, wave-lengths were found of a larger number of lines spaced over intervals of 4 mm or less. It may be shown that over intervals no greater than 4 mm along the plate, linear interpolation introduces no appreciable error in the derived values of λ. The determination of the remaining wave-lengths, which includes more than 2200 lines, was then made by direct linear interpolation. The difference in wave-length of the great majority of lines, as determined from the two separate plates, was less than 0.02A.

Two typical spectrograms are reproduced in Fig. 2, with a magnification of about 4×. The exposure times for these plates were 45 minutes and 25 minutes, respectively. The first of the plates contains about 2200 lines (exclusive of ghosts) of which at least 1400 are new. The short wave-length limit is at 810A as contrasted with a former limit of about 1000A.

Rotational Analysis

Identification of lines

Since the approximate positions of all bands in the $2p^1\Sigma - 1s^1\Sigma$ and $2p^1\Pi_{cd} - 1s^1\Sigma$ systems could be determined from previous work, the identification of as many lines as possible was carried out by searching for constant frequency intervals. In accordance with the prevailing notation, these constant frequency intervals may be designated as follows:

$R(K) - P(K) = \Delta_2 F'_K =$ a constant for all bands having the same initial vibrational state $v' =$ constant;

$R(K-1) - P(K+1) = \Delta_2 F''_K =$ a constant for v'' constant;

$Q(K) - P(K) =$ constant for v' constant;

$R(K) - Q(K) =$ constant for v' constant.

The latter two conditions are used only for the $^1\Pi_{cd} - {}^1\Sigma$ system. The rule that the second differences of the frequencies of lines in any branch are approximately constant is also very useful. Because of the extremely large number of lines in this spectrum (see Fig. 2) and the fact that there are no superficially evident regularities, chance agreement of frequency intervals is very frequent and in many cases it is only after applying every known test that one can be certain of the proper identification of the lines of a band.

The $1s^1\Sigma$ state

As has been noted previously, the data given by Hyman[7] have yielded values of the rotational constants of the normal ($1s^1\Sigma$) state for values of v equal to or greater than 3. An extrapolation of these data to smaller values of v has already been made.[14] From Rasetti's data[15] on the Raman effect in gaseous hydrogen, accurate values of the constants for $v=0$ and $v=1$ have been calcu-

[13] R. T. Birge and J. D. Shea, University of California Publications in Math. **2**, No. 5, 67 (1927).

[14] H. H. Hyman and C. R. Jeppesen, Nature **125**, 462 (1930).

[15] F. Rasetti, Phys. Rev. **34**, 367 (1924).

TABLE I. *Average values of* Δ_2F'' (cm^{-1}).

K	$v=0$	1	2	3	4	5
1		336.52 (4)	319.2 (4)	301.70 (7)	285.33 (9)	268.3 (5)
2		558.04 (5)	528.63 (3)	500.74 (7)	473.65 (11)	445.56 (5)
3	812.0 (3)	772.84 (5)	734.0 (4)	695.17 (7)	654.49 (8)	618.46 (3)
4	1034.42 (4)	981.43 (3)	932.03 (3)	882.64 (7)	832.98 (5)	781.66 (3)
6	1452.1 (2)					

lated.[16] Since the Raman effect data had shown an unexplained deviation in the values of the rotational constant B_0 and the vibrational constant $\Delta G_{\frac{1}{2}}$ from the smooth extrapolated $B_v : v$ and $\Delta G : v$ curves[16] it was desirable to obtain complete data from band spectra on the lower vibrational states and to examine critically all the experimental results.

In Table I are given the values of Δ_2F as obtained in the present work.

The figures in parentheses give the number of individual values on which each average is based. The lines from which each individual value is obtained are listed in Table VII.

Since the spectrograph used did not permit observation of the bands having wave-lengths greater than 1375A, these data were supplemented by data of Hyman[7] in order to obtain values of Δ_2F for v larger than 3. By the well-known graphical method[17] preliminary values of B_v were found. B_e is obtained by a simple extrapolation. The value of D_e is now found from the theoretical relation:

$$D_e = -4B_e^3/\omega_e^2 \qquad (1)$$

where $\omega_e = \Delta G_{-\frac{1}{2}}$ except for the (negligible) difference between the value of the finite difference and the derivative.

The values of D_v may be derived from the theoretical relation:

$$D_v = D_e - \beta_e(v+\tfrac{1}{2}) \qquad (2)$$

where[7]

$$\frac{\beta_e}{D_e} = -\frac{\omega_e}{24B_e}\left(\frac{\alpha_e}{B_e}\right)^2 - 5\left(\frac{\alpha_e}{B_e}\right) + 8x_e \qquad (3)$$

$2x_e\omega_e$ is the slope of the $\Delta G : v$ curve at $v=-\frac{1}{2}$ and α_e is the corresponding slope of the $B_v : v$ curve at $v=-\frac{1}{2}$.

[16] R. T. Birge and C. R. Jeppesen, Nature **34**, 463 (1930).

[17] See R. T. Birge, National Research Council Bulletin No. 57, *Molecular Spectra in Gases*, pp. 172–4 (1926).

The value of F_e is given by the expression

$$F_e = (D_e^2/B_e)(2-\alpha_e\omega_e/6B_e^2). \qquad (4)$$

The value of F_e may be seen to be very small, although it is not negligible in the case of the present work. The variation in F_v with v is however so small[18] that the use of F_e for F_v in our work was justified. From these values of D_v and F_v better approximate values of B_v were found.

The preliminary values of all of these rotational constants together with similar constants for the excited B and C states of the molecule allowed the values of the rotational energy functions to be obtained for each of the electronic states under consideration. These, in turn, enabled a rigorous check of the placement of lines in the various bands to be made. Corrections were then made in the values of Δ_2F and the analytic method given by Birge[17] was then used for the final calculation of B_v values. The results of this calculation without smoothing the data, together with the previous best values[7, 14, 16] are given in Table II.

It may be seen that the agreement between the band spectra data of the previous work as given

TABLE II.

v	B_v from present work	B_v from Raman effect data	B_v from previous smooth curve[14]
0	59.396	59.354	59.192
1	56.413	56.4035	56.411
2	53.528		53.630
3	50.697		50.834
4	47.870		48.008
5	44.973		45.138
6	42.094		42.210
7	39.134		39.209
8	36.086		36.120
9	32.712		32.930

[18] The theoretical expression for F_v as a function of v is given by J. L. Dunham, Phys. Rev. **41**, 721 (1932).

in column 3, Table II, and that here obtained is not as good as might be expected. This is due to two factors. In the first place, the placement of a number of lines in the previously analyzed bands[4, 6, 7] has been found to be incorrect. In most cases, it has been found impossible to be certain of the placement of any lines for greater rotational quantum number than $K=5$ or 6. This is due to the fact that for large values of K the constants D and F contribute a very large amount to the value of the rotational energy function and the theoretical values of these constants which must be used in our calculations progressively become less trustworthy as v increases. In the second place, it has been found possible in the present work to proceed entirely, in the final calculations, by the more accurate analytical method.[17]

It should be noted that the results for B_0, B_1 and B_2 in the third column of Table II were obtained largely by linear extrapolation since the more accurate band spectra data previous to the present work did not extend below the $v=3$ level. The fact that the extrapolated value of B_1 agreed with the Raman effect value was considered good evidence for the reliability of the linear extrapolation. However, it is now seen that this agreement was largely accidental and was due to the fact that the accepted values of B_v for v greater than 3 were too large, by small but appreciable amounts. The Raman effect value of B_0, however, did not lie upon the smooth extrapolated curve and this was then believed to denote a perturbation in the moment of inertia for the lowest level.[16]

On the other hand, it may be seen that the values of both B_0 and B_1, as obtained in the present work, are in quite satisfactory agreement with the values obtained[16] from Rasetti's data[15] on the Raman effect. The fact that the agreement between the two values of B_0 is not quite so good as between the B_1 values is due to the lack of data on the $v=0$ state for lower values of the rotational quantum number K, and also to the greater amount of data on the $v=1$ state for nearly all values of K. The Raman effect values have been adopted in this work since they are somewhat more accurate than the values obtained from band spectra.

It is now found that the values of both B_0 and B_1, as well as the value of B_2 which has not previously been determined with any accuracy, all lie on a smooth curve with the new values of B_v for v larger than 2. Hence we have the important conclusion that it is no longer necessary to assume that the value of B_0 is perturbed.

The new $B_v : v$ curve, Fig. 3, is found to have a

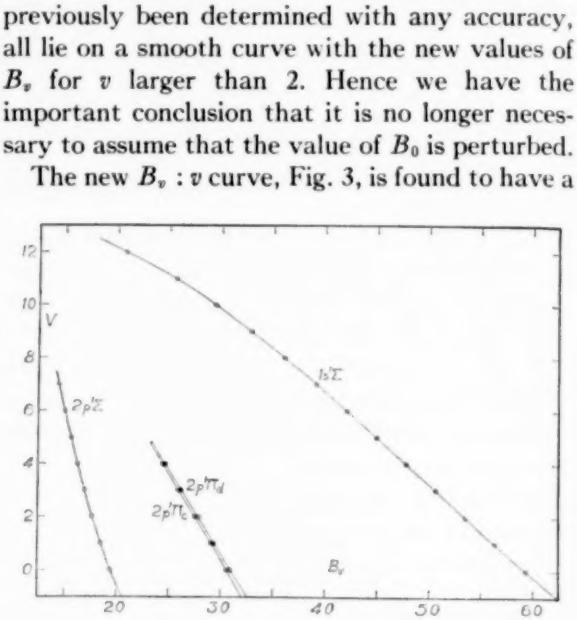

FIG. 3. $B_v : v$ plot for the $1s^1\Sigma$ (A), $2p^1\Sigma$ (B) and $2p^1\Pi_{cd}$ (C) states.

decided positive curvature for low values of v in contrast to the negative curvature for high values. From $v=0$ to $v=4$, the values of B_v are given to well within the probable error by the least squares equation:

$$B_v = 60.8715 - 3.06709(v+\tfrac{1}{2}) + 0.068393(v+\tfrac{1}{2})^2 - 0.0065(v+\tfrac{1}{2})^3. \quad (5)$$

The pronounced positive curvature at $v=0$ and the negative curvature starting at about $v=3$ make the $B_v : v$ function impossible of accurate representation by this type of equation for all values of v. The extrapolated value of B_e (60.8715 cm^{-1}) given by the above equation is the same as that determined by difference tables and also graphically, so that the extrapolation is believed to be trustworthy. The resulting new value of $I_e = 0.45437 \times 10^{-40}$ g cm^2 is less by 0.47 percent than that previously published.[14]

Values of the rotational energy function F for the $1s^1\Sigma$ state are given in Table VI.

The $2p^1\Sigma$ state

For the evaluation of the constants of the $2p^1\Sigma$ state we have, in addition to the data of the present work, the investigations of the ultra-

violet spectrum mentioned previously and the more accurate data published by Richardson and Davidson[19] who have found bands in the visible spectrum having the level $2p^1\Sigma$ as their final state. The Δ_2F values that result from these data on the visible bands were found to be in all cases consistent with the Δ_2F values based on the ultraviolet bands, and the two sets of Δ_2F values have therefore been freely combined to give final, most probable values of the various constants.

Both Richardson and Davidson[19] and Hyman[7] have evaluated the moment of inertia for the $v=0$ level of this state. We wish, however, to evaluate the constants of the molecule for the higher vibrational states so as to be able to give a complete rotational and vibrational analysis of the $2p^1\Sigma - 1s^1\Sigma$ system.

The procedure outlined for the derivation of constants for the $1s^1\Sigma$ state should apply also to the $2p^1\Sigma$ state under consideration. It may be shown, however, that, in the latter case, Eq. (2) cannot be made to give values of D_v that agree with the experimental data, for any constant values of x_e and α_e. While the method about to be described has no obvious theoretical justification, values of D_v for the $2p^1\Sigma$ state may be obtained such that, within the limit of the experimental error of the measurements, entirely satisfactory results are secured. Two rigorous checks are required of the D_v values thus obtained: they must satisfy the analytic method for determination of B_v values by successive approximations, and they must give rotational energy functions such that every line in a band gives the same value of the origin of the band when the rotational term values are subtracted out.

Let us assume

$$D_v = D_{v-1} + \beta_{v-\frac{1}{2}}, \tag{6}$$

where

$$\beta_{v-\frac{1}{2}} = \beta_i = -\frac{1}{6}\frac{\alpha_i^2}{\omega_i} - \frac{20\alpha_i B_i^2}{\omega_i^2} - \frac{32 x_i B_i^3}{\omega_i^2}. \tag{7}$$

Eq. (7) is obtained from Eq. (3) by the substitution of the value of D_e from (1) and the replacing of B_e by $B_{v-\frac{1}{2}}$. The quantities $\alpha_{v-\frac{1}{2}}$ and $x_{v-\frac{1}{2}}$ are not assumed constant; instead they represent the slope of the $B_v : v$ and $\Delta G_v : v$ curves at any designated values of $v-\frac{1}{2}$ and are obtained directly from the experimental data. Since the theoretical equation $D_e = -B_e^3/\omega_e^2$ is true for any kind of binding in the molecule (i.e., independent of the linearity or lack of linearity of the $\Delta G : v$ and $B_v : v$ curves) we first get the true value of D_e and then proceed step by step to obtain each value of D_v from D_{v-1} according to the above equations. Values of x_v and α_v as functions of v, as well as the derived values of D_v are given in Table III.

TABLE III. *Values of x, α and D for the $2p^1\Sigma$ state.*

v	$x_{v-\frac{1}{2}}$	$\alpha_{v-\frac{1}{2}}$ (cm^{-1})	D_v (cm^{-1})
0	0.01516	1.077	−0.015838
1	0.01453	0.962	−0.013571
2	0.01402	0.832	−0.011791
3	0.01373	0.720	−0.010416
4	0.01373	0.662	−0.009243
5	0.01388	0.635	−0.008162
6	0.01404	0.605	−0.007179
7	0.01426	0.575	−0.006298

The extrapolated value of D_e is -0.017188 cm^{-1}. The calculated value of F_e is (from Eq. (4)) 2.916×10^{-5} cm^{-1}, and as already noted F_e may safely be used for F_v in general.

By using these calculated values of D_v and F_v it is possible to obtain values of $4B_v$ from each value of $\Delta_2F/K+\frac{1}{2}$ by use of the well-known expression for the rotational energy of a $^1\Sigma$ state. A weighted average of the resulting values of $4B_v$ for each value of v was thus obtained. These values of $4B_v$ differed by such small amounts from the first values obtained directly from the $(\Delta_2F/K+\frac{1}{2}) : K$ curves that it was deemed unnecessary to calculate new D_v values and to apply a second approximation. The values of B_v obtained, from $v=0$ to $v=7$, are as follows: 19.457, 18.482, 17.652, 16.933, 16.265, 15.626, 15.004, 14.410 cm^{-1}. The extrapolated value of B_e is 19.987 cm^{-1}. The value of B_0 given above, i.e., 19.457, may be compared with Richardson and Davidson's[19] published value of 19.455. Of course these two values are not independent since, as just noted, Richardson and Davidson's data were used in conjunction with the extreme ultraviolet data for the derivation of the results given above. The comparison does, however,

[19] O. W. Richardson and P. M. Davidson, Proc. Roy. Soc. **A123**, 54 (1929); also Proc. Roy. Soc. **A123**, 466 (1929).

show in a simple manner the perfect consistency of the visible and the ultraviolet data for this $2p^1\Sigma$ state.

The B_v values obtained as described lie very well on a smooth curve, the least squares solution of which is:

$$B_v = 20.0245 - 1.195559(v+\tfrac{1}{2}) + 0.1292308(v+\tfrac{1}{2})^2 - 0.0133636(v+\tfrac{1}{2})^3 + 0.00053788(v+\tfrac{1}{2})^4. \quad (8)$$

While this equation fits the data very well from $v=0$ to 6 it does not give a good extrapolated value of B_e. This is due to the pronounced curvature of the $B_v : v$ curve (see Fig. 3) which is such that another form of function than the polynomial is required if one wishes a trustworthy extrapolation.

The $2p^1\Pi_{cd}$ states

The analysis of the $2p^1\Pi_{cd}$ states of H_2 was first carried out by Hori.[4] The more accurate data of the present investigation have shown, however, that a number of his lines were given incorrect quantum assignments. This, together with the fact that his measured wave-lengths are necessarily less accurate, may in part be responsible for his positive values of the rotational constants D_v, as well as for a value of the moment of inertia of the normal $1s^1\Sigma$ state that does not agree well with the one later obtained in this laboratory.[14, 16]

Accordingly, a new analysis of the $2p^1\Pi_{cd} - 1s^1\Sigma$ bands has been made in the present study. The rotational energy function for a $^1\Pi$ state may be written:[20]

$$F = B_v[(K+\tfrac{1}{2})^2 - \Lambda^2 + \bar{G}^2] + \varphi_i(K) + D_v[(K+\tfrac{1}{2})^4 + \cdots] + F_v[(K+\tfrac{1}{2})^6 + \cdots], \quad (9)$$

in which $\varphi_i(K)$ is given by:

$$\varphi_i(K) = \kappa_i + \delta_i(K+\tfrac{1}{2})^2 + \mu_i(K+\tfrac{1}{2})^4 + \cdots \quad (10)$$

where $\delta_i \gg \mu_i \gg \cdots$ and κ_i is of the same order of magnitude as δ_i. The data of the present work show this equation to be correct for the $2p^1\Pi_{cd}$ state of H_2. In this case $\varphi_i(K)$ may be combined with the other terms of Eq. (9) by writing

$$B_i^x = B_v + \delta_i; \quad D_i^x = D_v + \mu_i. \quad (11)$$

Since the constant term $B_v(\bar{G}^2 - \Lambda^2)$ is small and cannot be separated from the electronic energy of the term, we write Eq. (9) in the form

$$F = B_i^x(K+\tfrac{1}{2})^2 + D_i^x(K+\tfrac{1}{2})^4 + F_i^x(K+\tfrac{1}{2})^6. \quad (12)$$

This is identical with the expression giving the rotational energy for $^1\Sigma$ states except that here we have the "effective" B, D and F values, B_i^x, D_i^x and F_i^x in place of the true B_v, D_v and F_v that give the value of the moments of inertia and other constants of the molecule.

Van Vleck[21] has shown that in the case of $^1\Pi$ states the function $\varphi_i(K)$ has the double form:

$$\varphi_c(K) = -2C + (C+C_2)(K+\tfrac{1}{2})^2 \cdots \text{ and}$$
$$\varphi_d(K) = -2C + (C+C_1)(K+\tfrac{1}{2})^2 \cdots. \quad (13)$$

It is also shown by Hill and Van Vleck[22] and by Dieke[23] that in the case of many of the excited states of H_2 and He_2, where the existence of $\varphi_i(K)$ is due mainly to an electron in a large orbit of azimuthal quantum number l, C_2 equals zero and if $l=1$, C also equals zero. It is evident that in the case of the $2p^1\Pi_{cd}$ state of H_2 these conditions are satisfied; hence for this state we have $\varphi_c(K)=0$. One of the two values of B_i^x, namely B_c^x, should then equal the true B_v value for this state, and B_d^x should equal $B_v + C_1$.

This situation is also found in He_2[23] where a series of np states ($n=2$ to 11) is known. In this case B_c^x remains practically constant throughout the series whereas B_d^x decreases steadily with increasing n, due presumably to a variation of C_1 with n.

According to theory, the Q branches of our $^1\Pi - {}^1\Sigma$ bands arise from transitions having the c component levels as their initial states, whereas the P and R branches arise from the d components. Values of the effective constants B_i^x and D_i^x have been derived from the data of the present work and their values are given later in the paper.

For the d component levels $\Delta_2 F_d$ values, derived from the P and R branches, may be obtained from the usual relation:

[20] See R. S. Mulliken, Rev. Mod. Phys. **2**, 100 (1930) and **3**, 102 (1931).

[21] J. H. Van Vleck, Phys. Rev. **33**, 484 (1929).

[22] E. L. Hill and J. H. Van Vleck, Phys. Rev. **32**, 270 (1928).

[23] G. H. Dieke, Zeits. f. Physik **47**, 71 (1929).

$$\Delta_2F'' = R(K) - P(K). \quad (14)$$

The wave numbers of these lines are given in Table VII. For the c components, however, the Δ_2F values cannot be obtained so directly. Our previous analysis has enabled us to get very accurate values of F, the rotational energy function, for the $1s^1\Sigma$ level which is the final state for the bands under consideration. Hence the $\Delta F''$ values are known with considerable accuracy.

From the familiar relation

$$Q(K) = \nu_0 + F_c'(K) - F''(K) \quad (15)$$

we have:

$$Q(K+1) - Q(K) = F_c'(K+1) - F''(K+1) - F_c'(K) + F''(K) \quad (16)$$

and since by definition

$$\Delta F(K+\tfrac{1}{2}) = F(K+1) - F(K)$$

we have at once from Eq. (16):

$$\Delta F_c'(K+\tfrac{1}{2}) = Q(K+1) - Q(K) + \Delta F''(K+\tfrac{1}{2}). \quad (17)$$

Using the observed wave numbers of the Q branch lines as given in Table VII and using $\Delta F''$ values derived from the calculated F values for the normal state of the molecule (Table VI), we are then enabled to obtain ΔF_c values for the $2p^1\Pi_c$ states by means of Eq. (17). The values obtained from Eqs. (14) and (17) are given in Table IV.

TABLE IV.

K	$v=0$	1	2	3	4
	Average $\Delta_2F_d'(K)$ values (cm^{-1})				
2	305.33	290.5	276.67	257.4	244.2
3	426.93	401.07	390.95	360.5	330.1
4	542.8	513.4		457.7	
5	661.7				
	Average $\Delta F_c'(K+\frac{1}{2})$ values.				
1	122.3	115.9	109.7	104.0	96.63
2	180.23	171.8	162.28	153.46	145.13
3	240.45	227.55	214.68	202.95	192.05
4	295.8	282.40	266.37	250.5	235.4

The semi-graphical method, already used in connection with the calculation of preliminary values of B_v in the case of the $2p^1\Sigma$ state, may then be applied to the data of the $2p^1\Pi_{cd}$ states. It was found immediately that the $(\Delta_2F_d/K+\frac{1}{2})$ values did not in some cases fall regularly upon a smooth curve. This, and additional evidence to be presented later, led to the discovery of a number of perturbations in the d component levels. The c levels, however, were found to be quite regular.

After obtaining approximate values of B_i^x in the way just described, preliminary values of D_i^x were calculated by the theoretical Eqs. (1), (2) and (3) given previously. The analytic method described by Birge[17] was then applied to the accurate determination of B_i^x. The values of B_c^x (obtained from $\Delta F_c(K+\frac{1}{2})$ as given in Table IV) were found to fall quite regularly upon a smooth curve, as is shown in Fig. 3. The least squares equation giving B_c^x as a function of v is:

$$(B_c^x)_v = 31.288 - 1.31673(v+\tfrac{1}{2}) - 0.119696(v+\tfrac{1}{2})^2 + 0.0164167(v+\tfrac{1}{2}). \quad (18)$$

As mentioned previously the rotational levels belonging to the d component states contain so many perturbations that accurate values of $(B_d^x)_v$ could not be calculated. While it is not possible to determine the form of the $(B_d^x) : v$ function because of the irregularity of the data, a straight line seemed to offer the best analytic representation of this function. Accordingly, the following linear equation was found:

$$(B_d^x)_v = 31.735 - 1.5702(v+\tfrac{1}{2}). \quad (19)$$

The values of B_i^x as obtained from the data and as calculated from Eqs. (18) and (19) are given together with values of D_i^x in Table V.

The calculated values of F_i^x are, from Eq. (4): $F_c^x = 1.8901\times10^{-5}$ cm^{-1} and $F_d^x = 1.9702\times10^{-5}$ cm^{-1}.

Richardson[24] has found also a number of bands in the visible spectrum having $2p^1\Pi_{cd}$ as the final state. The values of B_i^x for the $v=0$ state as determined from his data may be compared with those of the present investigation. Richardson does not calculate "effective" B values, but when the methods used in this paper are applied to his data one obtains $B_c^x = 30.361$ and $B_d^x = 31.063$ for $v=0$.

The agreement is seen not to be as good as might be expected. In obtaining the above values from Richardson's data the following

[24] O. W. Richardson, Proc. Roy. Soc. **A126**, 487 (1929).

TABLE V. B_i^x *values for* $2p^1\Pi_{cd}$ *states.*

v	Obs. B_c^x	Calc. B_c^x	D_c^x	Obs. B_d^x	Calc. B_d^x	D_d^x
$-\frac{1}{2}$		31.288	−0.020959		31.735	−0.021001
0	30.599	30.602	−0.020545	31.003	30.950	−0.020197
1	29.113	29.099	−0.019718	29.348	29.380	−0.019393
2	27.485	27.505	−0.018891	27.945	27.809	−0.018589
3	25.931	25.917	−0.018064	26.211	26.239	−0.017785
4	24.432	24.435	−0.017236	24.674	24.669	−0.016981

procedure was followed. From the rotational energy function

$$F=B_i^x(K+\tfrac{1}{2})^2+D_i^x(K+\tfrac{1}{2})^4+F_i^x(K+\tfrac{1}{2})^6 \quad (20)$$

we have:

$$\Delta_1 F=(2B_i^x+D_i^x+(3/8)F_i^x)(K+\tfrac{1}{2}) +(4D_i^x+5F_i^x)(K+\tfrac{1}{2})^3+6F_i^x(K+\tfrac{1}{2})^5. \quad (21)$$

Let us write, following the usual analytic method[17]

$$\Delta_1 F^*=\Delta_1 F-(4D_i^x+5F_i^x)(K+\tfrac{1}{2})^3 -6F_i^x(K+\tfrac{1}{2})^5. \quad (22)$$

Richardson's published $\Delta_1 F$ values then yield the following values of $\Delta_1 F^*$:

$K+\frac{1}{2}$	$\Delta_1 F^*$ (c states)	$\Delta_1 F^*$ (d states)
$1\frac{1}{2}$	122.262	124.442
$2\frac{1}{2}$	183.137	186.341
$3\frac{1}{2}$	237.734	247.933

But $2B_i^x=(\Delta_1 F^*/K+\tfrac{1}{2})-D_i^x+(3/8)F_i^x$. (23)

Hence, using each of the above values of $\Delta_1 F^*$, one obtains for B_c^x and B_d^x the following:

$K+\frac{1}{2}$	B_c^x	B_d^x
$1\frac{1}{2}$	30.576	31.121
$2\frac{1}{2}$	30.533	31.068
$3\frac{1}{2}$	29.727	31.002

It is seen that the values of both B_c^x and B_d^x, instead of being constant, show a distinct downward trend as K increases, indicating that the values of D_i^x used are numerically too small. However, the values of D_i^x used are the values calculated by the equations given previously and furthermore, these same D_i^x values lead to entirely consistent results when applied to the data of the present paper. It therefore appears that Richardson's data include some incorrect identifications. Indeed Chalk[25] has published a later paper in which new identifications are made for some of these lines. The data are quite fragmentary in some cases, and in other cases rather doubtful, so that it has been thought better to make the evaluation of the constants for this state independently of the data obtained from the visible spectrum. It is hoped that the present work may lead to a more definite identification of some lines in the visible spectrum.

We now have complete data on the constants of the rotational energy functions for the $1s^1\Sigma$, $2p^1\Sigma$ and $2p^1\Pi_{cd}$ states of the molecule. The values of the rotational function F for all observed vibrational and rotational states in these levels are given in Table VI.

The values of the rotational energy function given in Table VI allow the calculation of the origin of each band in the $2p^1\Sigma-1s^1\Sigma$ and $2p^1\Pi_{cd}-1s^1\Sigma$ systems from the value of the wave number of each line in the band under consideration, by means of the familiar relation:

$$\nu=\nu_0+(F'-F'') \quad (24)$$

where ν is the wave number of the line considered, and ν_0 is the origin of the band to which it belongs.

This calculation has been made for all the observed lines in the two systems above mentioned. The results of the calculation for the bands obtained in the present work are given in Table VII together with observed wave numbers of lines and eye estimates of their intensities. A few bands, the analysis of which is somewhat uncertain, are not included in the table. With the values of the origins of the bands as determined above, calculated values of the wave numbers of all identified lines are given. The agreement

[25] M. L. Chalk, Proc. Roy. Soc. **A128**, 579 (1930).

TABLE VI.

A. Value of $F=B(K+\frac{1}{2})^2+D(K+\frac{1}{2})^4+F(K+\frac{1}{2})^6$ for $1s^1\Sigma$ state.

K	0	1	2	3	4	5	6	7
$v=0$	14.84	133.31	369.19	720.30	1183.55	1754.94	2427.77	3202.82
1	14.10	126.68	350.80	684.36	1124.35	1666.92	2307.53	3041.12
2	13.38	120.22	332.88	649.34	1066.68	1581.18	2188.45	2883.65
3	12.67	133.86	315.24	614.86	1009.91	1496.77	2071.25	2728.68
4	11.96	107.49	297.57	580.34	953.05	1412.25	1953.88	2573.49
5	11.24	101.02	279.64	545.29	895.35	1326.46	1834.74	2415.93
6	10.52	94.49	261.54	509.91	837.07	1239.82	1714.42	2256.80
7	9.78	87.87	243.18	474.03	777.97	1151.94	1592.36	2095.31
8	9.02	81.04	224.24	437.00	716.98	1061.24	1466.37	1928.69
9	8.21	73.74	204.01	397.45	651.83	964.32	1331.68	1750.44
10	7.35	65.99	182.50	355.39	582.57	861.19	1188.33	1560.65
11	6.41	57.56	159.12	309.65	507.14	748.99	1032.31	1353.99
12	5.14	46.12	127.39	247.57	404.72	596.41	819.88	1072.23

B. Value of $F=B(K+\frac{1}{2})^2+D(K+\frac{1}{2})^4+F(K+\frac{1}{2})^6$ for $2p^1\Sigma$ state.

$v=0$	4.86	43.70	120.99	236.02	387.75	574.89	759.98	1049.52
1	4.62	41.52	114.99	224.42	368.94	547.47	758.84	1001.85
2	4.41	39.66	109.87	214.52	352.86	523.99	726.95	960.80
3	4.23	38.05	105.43	205.92	338 86	503.50	699.02	924.71
4	4.07	36.55	101.30	197.91	325.82	484.36	672.89	890.84
5	3.91	35.12	97.35	190.25	313.32	466.02	647.83	858.32
6	3.75	33.72	93.50	182.78	301.13	448.11	623.30	826.44
7	3.61	32.42	89.90	175.78	289.71	431.31	600.28	796.49

C. Value of $F=B_d{}^z(K+\frac{1}{2})^2+D_d{}^z(K+\frac{1}{2})^4+F_d{}^z(K+\frac{1}{2})^6$ for $2p^1\Pi_d$ state.

$v=0$	7.74	69.53	192.62	376.03	618.29	917.57	1271.64	1678.00
1	7.35	66.01	182.84	356.92	386.83	870.82	1206.75	1592.24
2	6.95	62.47	173.05	337.79	555.34	824.02	1141.80	1506.41
3	6.56	58.95	163.26	318.68	523.88	777.27	1076.91	1420.63
4	6.17	55.42	153.49	299.57	492.42	730.52	1012.01	1334.87

D. Value of $F=B_c{}^z(K+\frac{1}{2})^2+D_c{}^z(K+\frac{1}{2})^4+F_c(K+\frac{1}{2})^6$ for $2p^1\Pi_c$ state.

$v=0$	7.65	68.75	190.46	371.82	611.42	907.43	1257.69	1659.71
1	7.27	65.37	181.10	353.53	581.31	862.72	1195.66	1577.79
2	6.88	61.79	171.17	334.14	549.38	815.26	1129.80	1490.75
3	6.48	58.22	161.27	314.80	517.56	767.98	1064.18	1404.04
4	6.11	54.89	152.05	296.77	487.89	723.91	1003.04	1323.29

between the observed and calculated values of each line is the best evidence of the correctness of our calculated F values. In the case of the $2p^1\Pi_{cd}-1s^1\Sigma$ bands, the origins are determined from the lines of the Q branches alone, since these are unperturbed, whereas a considerable number of perturbations appear in the levels associated with the P and R branch lines as shown by the table. Lines known to be blends are indicated in the table by an asterisk.

Perturbations

It may be seen by examination of Table VII that the differences between observed and calculated wave numbers of lines in bands of the $2p^1\Sigma-1s^1\Sigma$ system are in practically every case within the limits of experimental error (about 2 cm^{-1}). This is not so, however, for the lines of the $2p^1\Pi_{cd}-1s^1\Sigma$ band system. But in every case these deviations of observed from calculated wave numbers may be explained by assuming a number of perturbations in the d levels of the $2p^1\Pi_{cd}$ state. The c levels are all found to be regular, as shown by the very good agreement between calculated and observed wave numbers for all Q branch lines.

The most remarkable of the perturbations is found in the $v=3$ level. Here the separation of all the c and d states averages 10.4 cm^{-1} greater than the value calculated by assuming no perturbations to exist. This is evidenced by the fact that

TABLE VII, A. *Bands of the $2p^1\Sigma - 1s^1\Sigma$ system.*

R branches					P branches				
K''	I	Obs.cm^{-1}	Calc.cm^{-1}	$O-C$	K''	I	Obs.cm^{-1}	Calc.cm^{-1}	$O-C$
				3 −0 band ν_0 = 94052.60					
1	2	94027.4	94024.7	2.7	4	0	93075.0	93075.0	0.0
2	00B	93891.1	93889.3	1.8	5	2	92636.3	92636.5	−0.2
3	1	93671.5	93671.2	0.3	6	1	92124.0	92126.3	−2.3
4	0	93372.1	93372.5	−0.4	7	2	91545.2	91548.8	−3.6
5	1	92998.5	92996.7	1.8					
				4 −0 band ν_0 = 95264.98					
0	3	952886	95286.7	1.9	1	00	95136.0	95135.8	0.2
3	3	94869.7*	94870.5	−0.8	4	1	94278.3	94279.4	−1.1
4	0	94566.1	94565.8	0.3	5	2	93835.5	93835.9	−0.4
					6	0	93319.3	93319.6	−0.3
				6 −0 band ν_0 = 97592.84					
2	00	97406.8	97407.4	−0.6	1	1	97460.7	97463.2	−2.5
3	00	97174.2	97176.3	−2.1	4	1	96596.4	96593.0	3.4
4	3	96865.5	96863.1	2.4	5	2	96141.9	96141.7	0.2
5	3	96472.9	96471.8	1.1	6	2	95617.5	95616.9	0.6
					7	3B	95021.9	95023.9	−2.0
				3 −1 band ν_0 = 89895.83					
0	0	89919.6	89919.7	−0.1	1	0	89773.2	89773.3	−0.1
1	1	89873.9	89874.5	−0.6	2	4B	89581.9	89583.0	−1.1
2	1	89750.5	89750.9	−0.4	3	4	89317.4	89316.9	0.5
3	0	89549.7	89550.3	−0.6	4	3	88978.9	88977.4	1.5
4	1	89274.9	89274.9	0.0	5	4	88568.9	88567.7	1.2
				6 −1 band ν_0 = 93430.14					
0	1	93444.2	93449.8	−5.6	1	3	93308.2	93307.3	0.9
1	2	93398.8	93397.3	1.5	2	3	93115.0	93113.2	1.8
2	2	93263.1	93263.2	−0.1	3	4	92841.4	92839.6	1.8
3	2	93049.1	93049.7	−0.6	4	3	92490.3	92489.6	0.7
					5	4	92066.3	92067.1	−0.8
				5 −1 band ν_0 = 92284.56					
0	3	92304.5	92305.6	−1.1	1	3	92161.2	92161.8	−0.6
1	2	92255.2	92255.3	−0.1	2	3	91969.0	91968.9	0.1
2	2	92124.0	92124.0	0.0	3	4	91698.1	91697.6	0.5
3	2	91913.4	91913.6	−0.2	4	5	91349.1	91350.5	−1.4
4	00	91627.0	91626.3	0.7	5	3B	90932.9	90931.0	1.7
				1 −2 band ν_0 = 83440.01					
0	2	82467.7	83468.2	−0.5	1	3	83324.3	83324.4	−0.1
1	2	83435.1	83454.8	0.3	2	4B	83148.2*	83148.7	−0.5
2	2	83331.7	83331.6	0.1	3	3	82908.1	82905.7	0.4
3	2B	83159.7*	83159.6	0.1	4	3D	82598.9*	82597.8	1.1
4	2D	82918.9	82920.8	−1.9	5	0B	82224.5	82227.8	−3.3
5	00	82617.8?	82617.7	0.1					
				2 −2 band ν_0 = 84720.77					
0	2	84748.5	84747.1	1.4	1	4	84606.4	84605.0	1.4
1	5	84708.9*	84710.9	−2.0	2	4	84429.2	84427.6	1.6
2	4	84606.4*	84604.1	2.3	3	5	84183.4	84181.8	1.6
3	4	84425.7*	84428.9	−3.2	4	3	83870.3	83870.3	0.0
					5	3	83494.0	83497.0	−3.0
				0 −3 band ν_0 = 78426.57					
0	3	78455.6	78457.6	−2.0	1	3	78317.1	78317.6	−0.5
1	3	78433.6	78433.7	−0.1	2	3	78155.0	78155.0	−0.0
2	1B	78347.2	78347.4	−0.2	3	6	77932.3	77932.7	−0.4
3	4	98198.2	78199.5	−1.3	4	4	77653.7	77652.7	1.0
4	0	77992.8	77991.6	1.2	5	4	77319.6	77317.6	2.0

TABLE VII, A. *Bands of the $2p^1\Sigma - 1s^1\Sigma$ system.* (*Continued.*)

R branches					P branches				
K''	I	Obs.cm^{-1}	Calc.cm^{-1}	$O-C$	K''	I	Obs.cm^{-1}	Calc.cm^{-1}	$O-C$
				1 −3 band ν_0 = 79744.32					
0	3B	79772.8	79773.2	−0.4	1	2	79634.6	79635.1	−0.5
1	3	79744.8	79745.5	−0.7	2	3	79470.9	79470.5	0.3
2	1	79653.4	79653.5	−0.1	3	4	79244.3	79244.5	−0.2
3	3	79498.1	79498.4	−0.3	4	3	78959.6	78958.8	0.8
				5 −3 band ν_0 = 84666.29					
0	3	84689.1	84688.7	0.4	1	4	84556.5*	84556.3	0.2
1	4	84650.4	84649.8	0.6	2	4	84386.9	84386.2	0.7
2	2	84542.6	84541.4	1.2	3	4	84149.6	84148.8	0.8
4	2	84118.4	84122.4	−4.0	4	3	83847.8	83846.6	1.2
5	2B	83814.6	83817.4	−2.8	5	3	83482.1	83482.8	−0.7
				6 −3 band ν_0 = 85813.15					
0	1	85835.2	85834.2	1.0	1	3	85703.7	85703.0	0.7
1	4	85793.1	85792.8	0.3	2	3	85532.2	85531.6	0.6
2	1	85681.9	85680.7	1.2	3	4	85292.6	85291.8	0.8
3	2B	85500.3	84599.4	0.9	4	3B	84984.3	84986.1	−1.8
5	0	84935.9	84939.7	−3.8	5	3	84620.8	84617.5	3.3
				0 −4 band ν_0 = 74957.19					
0	3	74990.5	74988.9	1.6	1	8	74853.8	74854.6	−0.8
1	6	74972.1	74970.7	1.4	2	5	74702.5	74703.3	−0.8
2	4	74896.7	74895.6	1.1	3	7	74495.4	74497.8	−2.4
				1 −4 band ν_0 = 76278.63					
0	0	76307.5	76308.2	−0.7	1	2	76176.7	76175.8	0.9
1	3	76285.8	76286.1	−0.3	2	2	76022.5	76022.6	−0.1
2	3	76204.5	76205.5	−1.0	3	3	75813.8	75813.3	0.5
3	2	76068.1	76067.2	0.9	4	0	75550.1	75550.0	0.1
					5	1	75235.0	75235.3	−0.3
				2 −4 band ν_0 = 77558.74					
0	1	77586.8	77586.4	0.4	1	4	77455.9	77455.7	0.2
1	4	77561.4	77565.7	0.3	2	2	77301.6	77300.8	0.8
2	00	77475.6	77475.7	0.1	3	5	77088.7	77088.3	0.4
3	3	77331.1	77331.3	0.0	4	1	76821.9?	76819.2	2.7
					5	3	76497.3	76499.4	−2.1
				3 −4 band ν_0 = 78804.51					
0	1B	78830.1	78830.6	−0.5	1	4	78701.5	78701.3	0.2
1	4	78802.0	78802.5	−0.5	2	3	78545.3	78545.0	0.3
2	2B	78712.4	78712.9	−0.5	3	4	78330.1	78329.6	0.5
3	4	78562.9	78563.0	−0.1	4	5	78058.7	78057.4	1.3
4	2B	78353.1	78354.9	−1.8	5	4	77732.0?	77731.1	0.9
				4 −4 band ν_0 = 80016.05					
0	3B	80039.4	80040.6	1.2	1	4	79913.7	79912.6	1.1
1	4	80011.0	80009.9	1.1	2	1	79756.1	79755.0	1.1
2	4	79913.7	79916.4	2.7	3	4	79537.9	79537.0	0.9
3	4B	79762.9	79761.5	1.4	4	4B	79258.0	79260.9	−2.9
				5 −4 band ν_0 = 81196.31					
1	1B	81187.2	81186.2	1.0	1	1B	81093.7	81092.7	1.0
3	3	80929.0	80929.3	−0.3	3	3	80711.3*	80713.3	−2.0
				7 −4 band ν_0 = 83460.92					
0	3	83482.1	83481.4	0.7	1	2	83356.8	83357.0	−0.2
1	2	83443.3	83443.3	0.0	2	3B	83196.0	83195.8	0.2
2	3	83337.5	83339.1	−1.6	3	4	82971.4	82970.5	0.9
3	2B	83170.9	83170.3	0.6	4	0	82684.7	82683.7	1.0
				3 −5 band ν_0 = 75562.73					
0	2	75591.4	75589.5	1.9	1	4	75466.9	75465.9	1.0
1	4	75568.9	75567.1	1.8	2	3	75322.1	75321.1	1.0
2	2	75490.4	75489.0	1.4	3	5	75123.6	75122.9	0.7
3	3	75357.0	75356.3	0.7	4	3B	74870.0	74873.3	−3.3
4	00	75170.7	75170.9	−0.2	5	2	74572.5	74575.1	−2.6
5	00	74933.1	74935.3	−2.1					

TABLE VII, A. *Bands of the* $2p^1\Sigma - 1s^1\Sigma$ *system.* (*Continued.*)

R branches					*P branches*				
K''	I	Obs.cm^{-1}	Calc.cm^{-1}	$O-C$	K''	I	Obs.cm^{-1}	Calc.cm^{-1}	$O-C$
				5–5 band ν_0 = 77956.61					
0	2	77980.2	77980.5	−0.3	1	4	77859.2	77859.5	−0.3
1	4B	77953.1	77952.9	0.2	2	4	77711.6	77712.1	−0.5
2	4	77866.1	77867.2	−1.1	3	5	77508.4	77508.7	−0.3
3	4	77724.8	77724.6	0.5	4	3	77252.5	77251.5	1.0
					5	3	76944.6*?	76943.5	1.1

R branches					*P branches*				
K''	I	Obs.cm^{-1}	Calc.cm^{-1}	$O-C$	K''	I	Obs.cm^{-1}	Calc.cm^{-1}	$O-C$
				6–5 band ν_0 = 79102.37					
0	2	79125.3	79124.9	0.4	1	5	79005.6*	79005.1	0.5
1	4	79095.7	79094.9	0.8	2	4	78857.7*	78856.5	1.2
2	5	79005.6*	79005.5	0.1	3	5	78651.0	78650.9	0.1
3	4	78857.7*	78858.2	−0.5	4	4	78386.7	78389.8	−3.1

TABLE VII, B. *Bands of the* $2p^1\Pi_{cd} - 1s^1\Sigma$ *system.*

Band	ν_0	Branch	K''	I	Obs.cm^{-1}	Calc.cm^{-1}	$O-C$
0–2	91002.24	*R*	0	4	91058.6	91058.4	0.2
			1	6	91075.7	91074.6	0.9
			2	3	91044.2	91045.4	−1.2
			3	4	90973.4?	90971.2	2.3
		P	2	4	90739.2	90738.9	0.3
			3	5	90547.5	90545.5	2.0
			4	3B	90311.4	90311.6	−0.2
			5	4 –	90044.2	90039.4	4.8
		Q	1	7	90950.7	90950.8	−0.1
			2	4	90859.8	90859.8	−0.0
			3	5	90724.3	90724.7	−0.4
			4	5	90547.5	90547.0	0.5
0–3	87308.89	*R*	0	3	87366.2*	87365.8	0.4
			1	7	87388.7	87387.7	1.0
			2	1	87372.4	87369.7	2.7
			3	3	87315.6	87312.3	3.3
			4	00	87218.9	87216.6	2.3
		P	2	5	87065.0	87063.2	1.8
			3	5	86888.0	86886.7	1.3
			4	3	86676.1	86675.0	1.1
			5	3	86433.3	86430.4	2.9
		Q	1	5	87263.8	87263.8	0.0
			2	5	87185.4	87184.1	1.3
			3	5	87065.0	87065.9	−0.9
			4	3B	86910.3	86910.4	−0.1
			5	3	86719.2	86719.6	−0.4
0–4	838401.02	*R*	1	4	83927.5*	83926.2	1.3
			2	4B	83915.9	83919.5	−3.6
			3	2	83881.6	83879.0	2.6
		P	2	1	83612.7	83613.0	0.3
			3	3	83454.3	83453.3	1.0
			4	00	83258.3	83264.0	2.4
			5	0	83050.2	83047.1	3.1
		Q	1	4	83801.9	83801.3	−0.4
			2	3	83733.9	83733.9	0.0
			3	4	83631.6	83632.5	−0.9
			4	3	83494.0?	83499.4	−5.4
			5	2	83337.5*	83336.2	1.3
1–1	97239.72	*P*	1	4B	97298.3	97295.9	2.4
			2	3	96957.1	96954.9	2.2
			3	6	96739.6	96738.2	1.4
			4	3	96472.9	96472.3	0.6
			5	7B	96157.0?	96159.6	−2.6
		Q	2	4	97070.0	97070.0	0.0
			3	5	96909.0	96908.9	0.1
			4	3	96696.6	96696.7	0.1
			5	1	96438.3	96435.5	2.8
1–3	89617.92	*R*	0	6	89671.6	89671.3	0.3
			1	7	89687.6	89686.9	0.7
			2	4	89661.0	89659.6	1.4
			3	3B	89589.3	89589.9	−0.6
			4	2	89479.1	89478.9	0.2
		P	2	4B	89370.0	89368.7	1.3
			3	2	89184.5	89185.9	−1.4
			4	1	88964.8	88964.9	−0.1
			5	2	88709.9	88708.0	1.9
		Q	1	6	89569.8	89569.4	0.4
			2	5	89483.8	89483.8	0.0
			3	5	89356.5*	89366.6	−0.1
			4	5	89188.6	89189.3	−0.7
			5	3	88978.9?	88983.9	0.4
1–4	86147.40	*R*	0	5	86202.1	86201.5	0.6
			1	6	86224.9	86222.8	2.1
			2	3	86208.9	86206.7	2.2
			3	4	86153.9	86153.9	0.0
			4	3	86068.6	86065.2	3.4
		P	2	4	85915.3	85915.8	−0.5
			3	3	85747.8	85749.9	2.1
			4	3	85554.7?	85551.3	3.4
			5	0	85318.4	85322.0	3.6
		Q	1	5	86106.0	86105.3	0.7
			2	5	86031.8	86030.9	0.9
			3	7	85920.2	85920.6	−0.4
			4	1	85776.2	85775.7	0.5
			5	2	85597.3	85597.9	−0.6
			6½	1	85388.0	85389.2	−1.2
1–5	82906.30	*R*	0	3B	82961.9	82961.1	0.8
			1	6B	82989.7	82988.1	1.6
			2	3B	82984.2	82983.6	0.6
			3	2	82947.5*	82947.8	−0.3
			4	3B	82883.2	82881.8	1.4
		P	2	2	82694.2	82692.7	1.5
			3	1	82541.6	82543.9	−2.3
			4	3	82370.3*	82367.9	2.4
			5	4B	82160.5	82166.7	0.5
		Q	1	5	82871.1	82870.7	0.4
			2	4	82808.9	82807.8	1.1
			3	5	82714.3	82714.5	−0.2
			4	3B	82590.9	82592.3	−1.4
2–2	95482.68	*R*	0	6B	95532.6	95532.4	0.2
			1	6B	95536.2	95536.2	0.0
			2	4B	95487.8	95481.5	−6.7
			3	00	95396.4	95389.3	7.1
		P	2	4	95214.0	95212.9	1.1
			3	5	95007.5	95007.0	0.5
			4	3	94747.2	94754.5	−7.3
			5	0B	94464.2	94457.5	6.7
		Q	1	5	95425.4	95424.9	0.5
			2	4	95322.5	95321.6	0.9
			3	5	95168.3	95168.1	0.2
			4	1	94965.3	94966.0	−0.7
			5	1 –	94716.6	94717.4	0.8
2–3	91790.03	*R*	0	4	91839.6	91839.8	−0.2
			1	4	91847.2	91849.2	−2.0
			2	2	91804.4	91812.6	−8.2
			3	5	91737.3	91730.5	6.8

TABLE VII, B. *Bands of the* $2p^1\Pi_{ed} - 1s^1\Sigma$ *system.* (*Continued.*)

Band	ν_0	Branch	K''	I	Obs.cm^{-1}	Calc.cm^{-1}	$O-C$	Band	ν_0	Branch	K''	I	Obs.cm^{-1}	Calc.cm^{-1}	$O-C$
		P	2	2	91538.2	91537.3	0.9	3−6	84111.22	*R*	1	6	84191.2	84180.0	11.2
			3	5	91349.1	91348.1	1.0				2	4	84178.3	84168.4	9.9
			4	3	91110.4	91117.9	−7.5				3	3	84135.6	84125.0	10.4
			5	3	90855.0	90847.6	6.4			*P*	2	4B	83915.9?	83908.6	7.9
		Q	1	5	91737.3	91737.3	0.0				3	3	83775.0	83764.6	10.4
			2	3	91646.2	91645.7	0.5				4	2	82601.9	83592.8	9.1
			3	5	91510.0	91509.5	0.5			*Q*	1	4	83404.4	83395.3	9.1
			4	1	91329.4	91330.4	−1.0				2	4	84075.2	84075.0	0.2
			5	3	91110.4	91110.2	0.2				3	4B	84011.4	84011.0	0.4
2−4	88324.97	*R*	0	2	88377.0	88375.5	1.5				5	1	83915.9	83916.1	−0.2
			1	5	88391.1	88390.5	0.6						83638.9	83639.4	−0.5
			2	1	88358.7	88365.2	−6.5	3−7	81327.89	*R*	0	2	81388.5	81377.1	11.4
		P	2	0	88309.2	88300.0	9.2				1	5	81414.2*	81403.3	10.9
			3	3B	88091.1	88089.9	1.2				2	5	81414.2*	81403.5	10.7
			3	5	87917.2	87917.7	−0.5				3	2	81388.5	81377.8	10.7
			4	1	87702.7	87709.7	−7.0				4	1B	81337.0	81327.2	9.8
		Q	1	4	88280.5	88279.5	1.0			*P*	2	1	81155.8	81143.7	12.1
			2	3	88199.4	88199.1	0.3				3	5	81028.1	81017.1	11.0
			3	5B	88078.7	88079.8	−1.1				4	3	80879.3	80868.6	10.7
			4	2B	87926.7?	87923.0	3.7				5	3	80711.3	80699.8	11.5
			5	00	87731.4	87730.5	0.9			*Q*	1	6	81298.0	81298.2	−0.2
2−5	85080.05	*R*	0	4	85133.0	85132.5	0.5				3	5	81246.1	81246.0	0.1
			1	5B	85153.9	85153.3	0.6				4	2B	81068.6	81068.7	−0.1
			2	4	85133.0	85139.4	−6.4				5	1B	81067.4	81067.5	−0.1
			3	3	85101.5	85091.3	10.2						80944.2*	80943.9	0.3
		P	2	4	84864.7	84864.1	0.6	4−5	89042.67	*R*	0	2B	89087.3	89066.0	1.3
			3	5	84708.9	84709.0	−0.1				1	3	89099.2	89094.5	4.7
			4	4	84516.9	84523.7	−6.8			*P*	2	2B	88818.9	88817.6	1.3
			5	00	84316.5	84310.1	6.4				3	3	88584.1	88650.0	4.1
		Q	1	5	85042.5	85042.0	0.5			*Q*	1	4	88996.1	88995.7	0.4
			2	5	84973.7	84972.8	0.9				2	3	88914.3	88914.2	0.1
			3	5	84869.5	84870.1	−0.6				3	3	88792.8	88793.3	−0.5
			4	2	84734.6	84735.3	−0.7				4	1	88629.1	88634.4	0.6
			5	3	84569.9	84570.1	−0.2				5	00	88438.7	88439.3	−0.6
2−6	82067.48	*R*	0	4	82120.7*	82119.4	1.3	4−7	83240.68	*R*	0	1	83289.5?	83286.3	3.2
			1	5B	82145.8*	82146.0	−0.2				1	2	83311.3	83306.3	5.0
			2	5B	82145.8*?	82142.2	−8.5				2	1	83295.5	83297.1	2.4
			3	4	82120.7*	82110.0	10.7				3	00	83258.3	83259.1	−0.8
		P	2	2	81869.4	81868.4	1.0			*P*	2	0	83050.2	83052.9	−2.7
			3	6	81730.4	81730.6	−0.2				3	2	82936.1	82920.2	5.9
			4	4	81560.5	81568.7	−7.7				4	00	82764.7	82762.3	2.4
			5	2	81388.5	81383.0	5.5				5	1	82036.2	82036.7	0.5
		Q	1	6B	82035.7	82034.8	0.9			*Q*	1	6B	83208.2	83207.7	0.5
			2	4	81978.2	81977.1	1.1				2	4B	83148.2	83149.6	−1.4
			3	5	81891.8	81891.7	0.1				3	3	83064.5	83063.4	1.1
			4	2	81779.3	81779.8	−0.5				4	2	82947.5	82950.6	−3.1
			5	3	81641.3	81642.9	−1.6				5	4	82808.9*	82812.7	3.0
3−4	90368.38	*R*	0	2	90424.7	90415.4	9.8	4−8	80699.29	*R*	0	3	80747.1	80745.2	1.9
			1	3	90433.4	90424.2	9.2				1	6	80774.9*	80771.2	3.7
			2	1	90398.2	90389.5	8.7				2	5	80774.9*	80774.1	0.8
		P	2	00	90141.8	90129.8	12.0			*P*	2	2	80531.8	80529.9	1.9
			3	4	89961.7	89951.3	10.4				3	5	80419.9	80415.3	3.8
			4	2	89744.7	89734.0	10.7				4	1	80287.8	80281.3	−3.5
			5	2	89471.5	89480.0	11.5				5	3	80128.1	80129.9	−1.8
		Q	1	8B	90316.3	90319.1	−2.8			*Q*	1	7	80672.3	80672.6	−0.3
			2	4	90231.5	90232.1	−0.6				2	4	80626.9	80626.6	0.3
			3	4	90102.8	90102.8	0.0				3	4	80558.1	80558.5	−0.4
			4	1	89933.3	89932.9	0.4				4	1	80469.9	80469.7	0.2
			5	00	89724.3	89724.1	0.2				5	2	80361.6	80361.4	0.2

every line in the P and R branches of bands originating on this level gives a value of ν_0 10.4 cm^{-1} (to within the experimental error) greater than the ν_0 given by lines of the Q branches. Since all the other perturbations in the band system are found in the d states, and since, as has been remarked previously, the B_e^z values, in contradistinction to the B_d^z values, when given as a function of v, fall regularly on a smooth curve, it may be assumed that the perturbations exist entirely in the d state. This, then, seems to be a vibrational perturbation, all of the d rotational levels of the $v=3$ state being shifted by 10.4 cm^{-1}.

In the other vibrational states of the $2p^1\Pi_d$ level, most of the rotational levels are either not perturbed or have perturbations scarcely greater than the errors of measurement. There are, however, as is apparent at once from Table VII, a number of rather large perturbations. These perturbed levels, together with the amount of the perturbation in cm^{-1} units, are given in Table VIII. A plus perturbation means an increase in the energy of the state.

TABLE VIII. *Perturbations in rotation levels of $2p^1\Pi_d$ state.*

v	$K=1$	2	3	4	5
0				3.2	
1					
2			−7.4	7.3	
3	10.5	10.5	10.1	10.6	9.8
4		4.5			

The properties of the $2p^1\Sigma$ and $2p^1\Pi_{cd}$ levels of H_2[26] are given in the diagram of Fig. 4. It may be seen that all of the $2p^1\Sigma$ levels and the d levels of the $2p\Pi_{cd}$ state satisfy all the conditions, as given by Dieke,[27] necessary that two different levels may perturb each other. It is therefore quite probable that these two sets of levels are perturbing one another. Unfortunately this cannot be directly verified. The overlapping of the levels of the two states begins at the vibrational level $v=7$ of the $2p^1\Sigma$ state. Schaafsma and Dieke's[6] and Hyman's[7] analyses include a few bands having the initial states $v'=8$ and $v'=9$, but none of these bands yield consistent values of

[26] See R. S. Mulliken, Rev. Mod. Phys. **3**, 149 (1931) and **4**, 78 (1932).

[27] G. H. Dieke, Phys. Rev. **38**, 646 (1931).

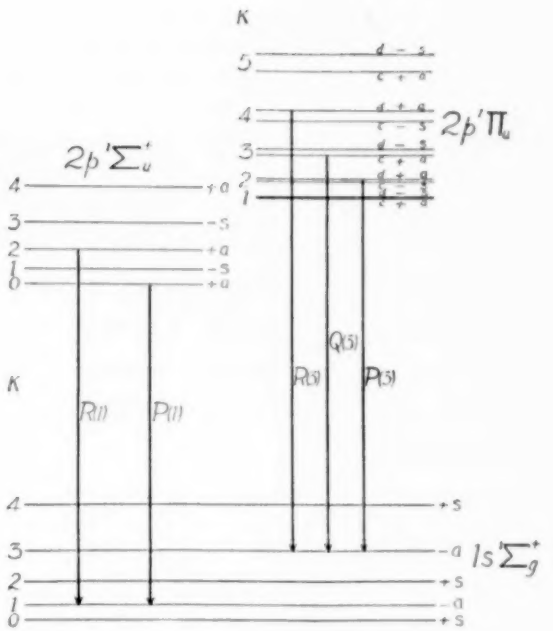

FIG. 4. Schematic energy level diagram showing properties of the states.

Δ_2F'. It has therefore been impossible to calculate values of the molecular constants for these states. It is thought that some of the lines listed by the above authors have been given incorrect quantum assignments. On the other hand many of these levels may have perturbations and some of the Δ_2F' values may, for that reason, deviate from a smooth curve. Richardson has found no bands ending on the $2p^1\Sigma$ state, in the visible spectrum, for which v is greater than 7. It should be remembered that in $^1\Sigma-{}^1\Sigma$ bands there occur only P and R branches, perturbations of both of which may show. Hence it is quite difficult to effect an analysis in case there should be a large number of such perturbations. It is significant that no perturbations are found in the $2p^1\Sigma-1s^1\Sigma$ bands for any values of v less than 7. Several different lines of evidence thus point to the conclusion that the two states in question do perturb each other.

The vibrational and electronic levels

The values of the origins of the bands given in Table VII enable us to obtain the vibrational term differences (denoted by ΔG) for all the observed levels of the three electronic states considered in this investigation. Since the

TABLE IX. ΔG *values* (cm^{-1}).

State v	$1s^1\Sigma$	Δ	$2p^1\Sigma$ Ultra-violet	Richardson	$2p^1\Pi_{cd}$
$\frac{1}{2}$	4161.70		1318.85	1318.586	2309.38
		238.80			
$1\frac{1}{2}$	3922.90		1281.72	1281.676	2171.39
		228.37			
$2\frac{1}{2}$	3694.53		1246.38	1246.715	2044.01
		226.01			
$3\frac{1}{2}$	3468.52		1213.56	1213.184	1914.17
		228.30			
$4\frac{1}{2}$	3240.22		1180.03	1180.102	
		225.54			
$5\frac{1}{2}$	3014.68		1147.86	1147.645	
		231.93			
$6\frac{1}{2}$	2782.75		1115.59	1115.642	
		238.62			
$7\frac{1}{2}$	2544.13				
		250.77			
$8\frac{1}{2}$	2293.36				
		266.20			
$9\frac{1}{2}$	2027.16				
		288.65			
$10\frac{1}{2}$	1738.51				
		320.47			
$11\frac{1}{2}$	1418.04				

spectrograph used in the present work did not permit us to photograph the longer wave-length bands of the $2p^1\Sigma - 1s^1\Sigma$ system our own data have been supplemented by that of Hyman,[7] in determining ΔG values for the $2p^1\Sigma$ and $1s^1\Sigma$ states. The resulting values of ΔG for the three states are given in Table IX. The values for the $2p^1\Sigma$ state as determined from the extreme ultraviolet spectrum are compared, in the table, with those given by Richardson and Davidson[19] in their analysis of the bands in the visible spectrum and are seen to agree well within the limits of experimental error. In obtaining Table IX all possible independent combinations of the ν_0 values were used so as to obtain the best average values of ΔG.

It may be mentioned again that, due to the scarcity of standard lines in the extreme ultraviolet, the relative values of wave-lengths over large intervals may have considerably larger probable errors than do relative wave-lengths within small intervals. It may be seen that the values of ΔG given in Table IX are of the order of ten times the $\Delta_2 F$ values that are used in determining the rotational constants. The probable error in cm^{-1} units of any ΔG value is therefore larger than the probable error of the $\Delta_2 F$ values given previously. It is thought, however, that the probable error in any value of ΔG given in Table IX is in all probability smaller than 2 cm^{-1}. The agreement of the values obtained for the $2p^1\Sigma$ state with those of Richardson and Davidson indicate a definitely smaller probable error than this.

Since the probable error of Rasetti's Raman effect measurements[15] is less than that for the measurements in the extreme ultraviolet, the value of $\Delta G_{\frac{1}{2}}$ given in Table IX for the $1s^1\Sigma$ state is that determined from his data.[16] The value determined in the present investigation is $\Delta G_{\frac{1}{2}} = 4160.83$ cm^{-1}, which differs by less than 1 cm^{-1} from the Raman effect value. This furnishes a check upon the validity of the Raman effect work and entirely substantiates it.

In Table IX are given also the first differences of the ΔG values for the $1s^1\Sigma$ state. It may be seen from these differences, as well as from Fig. 5, that

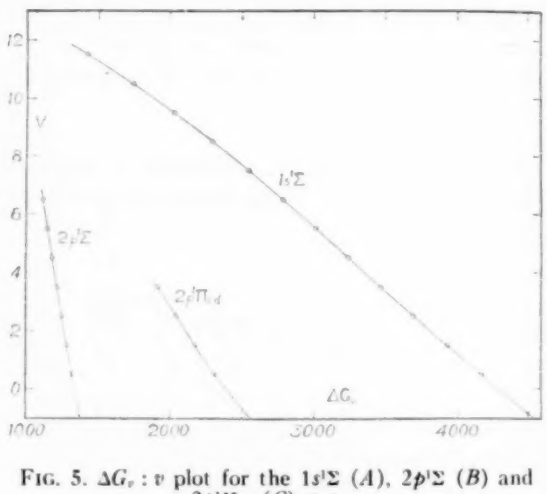

FIG. 5. $\Delta G_v : v$ plot for the $1s^1\Sigma$ (A), $2p^1\Sigma$ (B) and $2p^1\Pi_{cd}$ (C) states.

the $\Delta G : v$ function has a very pronounced positive curvature at the value $v = \frac{1}{2}$. The more fragmentary data available previous to the present work[16] had indicated a large deviation of the value of $\Delta G_{\frac{1}{2}}$ from a $\Delta G : v$ curve which was then assumed to be linear for low values of v. This deviation was at the time of the former work ascribed to a vibrational perturbation. The present data indicate, however, that it is unnecessary to assume such a perturbation.

A least squares equation giving ΔG_v as a function of v designed to fit the data from $v = -\frac{1}{2}$ to $v = 5\frac{1}{2}$ is:

$$\Delta G_v = 4417.19 - 262.63(v+\tfrac{1}{2}) + 9.34619(v+\tfrac{1}{2})^2 - 0.76(v+\tfrac{1}{2})^3 \quad (25)$$

but the extreme positive curvature of the function for small v does not allow an entirely satisfactory fitting of any equation of this type. The greatest difference between observed and calculated values of ΔG when using the above equation is 2.47 cm^{-1}, which is somewhat larger than the probable error in any particular value of ΔG_v.

The extrapolated value of $\Delta G_e = 4417.$ cm^{-1} was obtained by a graphical treatment in combination with difference tables.

The $\Delta G : v$ form of the curve for the $2p^1\Sigma$ state has been discussed by Birge.[28] A least squares equation representing the $\Delta G_v : v$ function for this state is:

$$\Delta G_v = 1357.302 - 39.9307(v+\tfrac{1}{2}) + 1.218487(v+\tfrac{1}{2})^2 - 0.0638888(v+\tfrac{1}{2})^3. \quad (26)$$

The value of $\Delta G_e = 1357.302$ cm^{-1} obtained from the above equation agrees sufficiently well for practical purposes with the value 1358.33 which was determined by use of difference tables. It should be noted that although the difference between observed and calculated values of ΔG_v when using the above equation is in all cases less than 0.3 cm^{-1}, a cubic equation of the type derived is not capable of representing the data to within the experimental error. A graph of $\Delta G_v : v$ for this state is given in Fig. 5.

For the $2p^1\Pi_{cd}$ state $\Delta G_v : v$ is shown graphically in Fig. 5 and a least squares representation is given by the equation:

$$\Delta G_v = 2471.05 - 177.867(v+\tfrac{1}{2}) + 18.375(v+\tfrac{1}{2})^2 - 2.17833(v+\tfrac{1}{2})^3. \quad (27)$$

It is thought that the value $\Delta G_e = 2468$ cm^{-1} obtained by a semi-graphical treatment of the data, is more trustworthy than the extrapolated value 2471 given by the above equation.

The vibrational term value, G_v, may be obtained by integrating Eqs. (25), (26) and (27) from $v = -\frac{1}{2}$ to $v = v$, or more accurately by

$$G_v = G_0 + \sum_{\frac{1}{2}}^{v-\frac{1}{2}} \Delta G_v = G_0 + G_v^* \quad (28)$$

by using for ΔG_v the values listed in Table IX. G_0 represents the vibrational term $v = 0$, using the true electronic level $v = -\frac{1}{2}$ as origin. Investigators often use $v = 0$ as origin, and we write the vibrational term value based on this origin as G_v^* in order to distinguish it from the true vibrational term value G_v. The value of G_0 is given to a very close approximation by $\frac{1}{2}\Delta G_{-1/4}$, where $\Delta G_{-1/4}$ is to be taken from Eqs. (25), (26) and (27). The results are 2176.1, 673.7 and 1213.9 cm^{-1}, respectively. The only remaining data necessary for the calculation of any spectral line are the electronic term values, T_e. But these are merely the origins of the two band systems, ν_e, since by definition $T_e = 0$ for the normal state. To obtain ν_e we first calculate ν_{00}, the origin of the 0−0 band. This is given by

$$\nu_{00} = \nu_0 - [G_v^{*\prime} - G_v^{*\prime\prime}]. \quad (29)$$

Each band origin ν_0 as given in Table VII, used in conjunction with the values of G_v^* obtainable from Table IX, thus gives a value of ν_{00}. The various values thus obtained were found to agree well within the limits of error and accordingly the arithmetic average was adopted as the most probable value. The results are 90,206.1 cm^{-1} for the $2p^1\Sigma - 1s^1\Sigma$ system and 99,087.4 cm^{-1} for the $2p^1\Pi_{cd} - 1s^1\Sigma$ system.

The true origin of each system is then given by

$$\nu_e = \nu_{00} - [G_0' - G_0''] \quad (30)$$

and the numerical results are 91,708 and 100,049 cm^{-1}, respectively.

The wave number of any line may now be obtained from the general equation

$$\nu = \nu_e + G_v' - G_v'' + F'(v, K) - F''(v, K). \quad (31)$$

The values of F' and F'' are given in Table VI and the values of G_v' and G_v'' are obtained from the quantities already used in Eq. (28). It is however simpler in practice to use the relation

$$\nu = \nu_{00} + G_v^{*\prime} - G_v^{*\prime\prime} + F' - F''. \quad (32)$$

In conclusion attention may again be called to the fact that, in order to get a fairer estimate of the accuracy of the rotational functions F' and F'', the calculated values of ν listed in Table VII were obtained from the simpler Eq. (24).

[28] R. T. Birge, Trans. Faraday Soc. **25**, 707 (1929).

Summary

The constants for the three electronic levels considered in this investigation are collected in Table X.

TABLE X.

	$1s^1\Sigma$	$2p^1\Sigma$	$2p^1\Pi_{cd}$
T_e (cm^{-1})	0	91708	100,049
G_e (cm^{-1})	2176.1	673.7	1213.9
$\Delta G_{\frac{1}{2}}[\omega_e]$ (cm^{-1})	4417.9	1358.33	2468
$2x_e\omega_e$ (cm^{-1})	262.63	39.931	177.867
B_e (cm^{-1})	60.8715	19.987	31.288
B_0 (cm^{-1})	59.354	19.457	30.602
D_e (cm^{-1})	−0.04652	−0.017188	0.020959
F_e (cm^{-1})	5.1806×10^{-5}	2.9160×10^{-5}	1.8901×10^{-5}
I_e (g cm^2)	0.45437×10^{-40}	1.38381×10^{-40}	0.88399×10^{-40}
r_e (cm)	0.73949×10^{-8}	1.2905×10^{-8}	1.03145×10^{-8}
a_e (cm^{-1})	3.06709	1.19556	1.31673
	$2p^1\Sigma - 1s^1\Sigma$	$2p^1\Pi_{cd} - 1s^1\Sigma$	
ν_{00}	90206.1	99087.4	

The data of the present investigation seem to indicate conclusively that in the normal state of the H_2 molecule the $B_v : v$ and $\Delta G_v : v$ curves have a quite unmistakable positive curvature for low values of v, changing to a negative curvature for higher values. Until recently, no such phenomenon had been observed in the case of the normal state of any molecule. Professor Birge has, however, found evidence[29] for just such a situation in the case of the oxygen molecule. This situation would seem to lead to the belief that the deviations from straight lines in the values of the above functions are not due to perturbations as was formerly supposed.

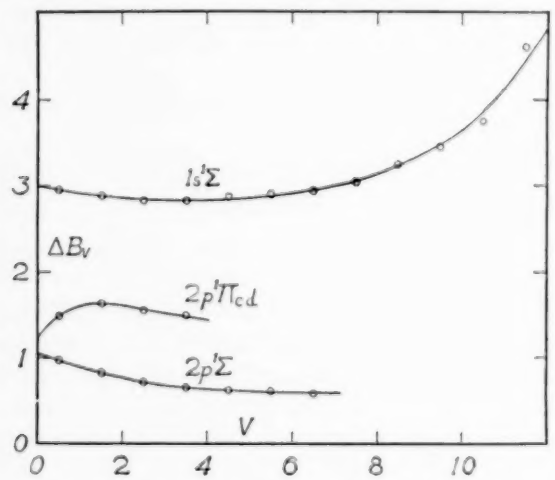

FIG. 6. $\Delta B_v : v$ plot for each of the three states.

[29] R. T. Birge, private communication.

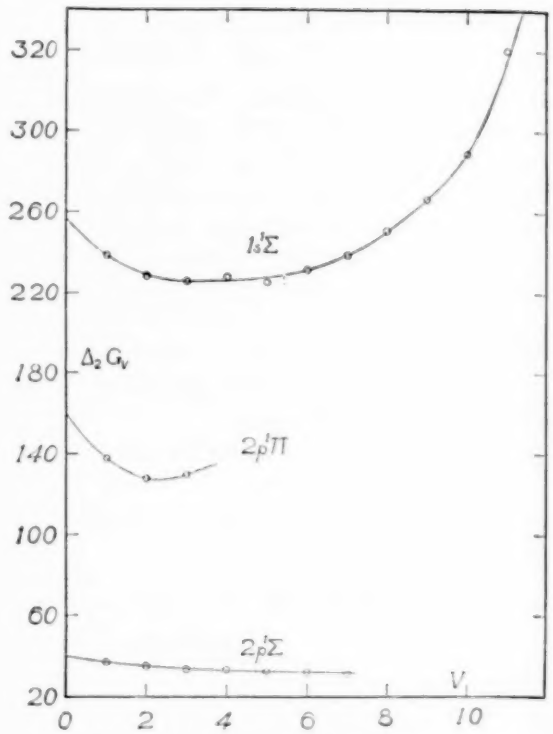

FIG. 7. $\Delta_2 G_v : v$ plot for each of the three states.

On the other hand there are a number of cases in which the $B_v : v$ and $\Delta G : v$ curves for excited states have initial positive curvature. An example of this is the $2p^1\Sigma$ state investigated here. (See Figs. 3 and 5.) In the case of the $2p^1\Pi_{cd}$ state the $\Delta G_v : v$ function also has a positive initial curvature, but the $B_v : v$ curve for the c component levels has for low values of v a negative curvature. (See Figs. 3 and 5.) The nature of the $B_v : v$ and $\Delta G_v : v$ functions is shown very well by curves of $\Delta B_v : v$ and $\Delta_2 G_v : v$ as given in Figs. 6 and 7. These curves also serve to show graphically the accuracy with which the experimental values of B_v and ΔG_v fit smooth $B_v : v$ and $\Delta G_v : v$ curves.

In conclusion, the writer wishes to express his deep appreciation of the many valuable suggestions and the assistance that Professor Birge has so willingly given throughout the course of the investigation.

Resolution of the Two Difference Bands of CO_2 Near 10μ

E. F. BARKER AND ARTHUR ADEL, *University of Michigan*

(Received June 5, 1933)

The rotational structure of two absorption bands of CO_2 at 9.4μ and 10.4μ has been completely resolved. Both bands have positive and negative branches, but no zero branches. They correspond to transitions up to the state ν_3 from the double state $(\nu_1, 2\nu_2)$, and yield the value 102.8 cm^{-1} for the separation of the two levels. From the intensity distribution of the lines it is clear that J must have only even values in the normal molecule. The line separations and convergences provide a very precise value for the moment of inertia, namely 70.6×10^{-40} gram cm^2. The numerical agreement with predictions from formulae based upon previous measurements with other bands is very satisfactory.

THE form and dimensions of the CO_2 molecule are already well known as a result of observations upon infrared absorption bands and Raman spectra. Symmetry and linearity are assured by the vibrational selection rules, and by the character of the rotational fine structure,[1,2,3,4] the latter yielding also the moment of inertia and the interatomic distances. The mechanics of the system, including anharmonic perturbations, rotational and vibrational interactions, and resonance degeneracy has also been very completely treated.[5,6] The observations here recorded fit precisely into this scheme, providing a check upon its quantitative aspect which is very gratifying. They also yield further information regarding one of the anharmonic constants, and a very precise value for the moment of inertia.

The two absorption bands near 10μ were first observed by Schaefer and Philipps[7] with a one-meter cell containing CO_2 at a pressure of 8 atmospheres. They were observed as doublets, and their mean positions were recorded as 9.42μ and 10.42μ. We have examined them with a grating having 2400 lines per inch, using slits only 0.5 cm^{-1} in width, thus obtaining ample resolution for the separation of the rotation lines. The band centers so determined lie at 961.03 cm^{-1} (10.41μ) and 1063.87 cm^{-1} (9.40μ). The absorption cell was a seven meter tube 20 cm in diameter, with windows of thin lacquer films. It was filled by displacement, the concentration of CO_2 being about 80 percent.

The bands are shown graphically in Fig. 1, and the measured positions of the individual lines appear in Tables I and II. The ordinal number N is the initial value of J in the negative branch and the final value in the positive branch, i.e., the larger J in each case. The line frequencies are well represented by the equations

$$\nu = 961.03 \pm 0.7765N - 0.00311N^2 \quad (1)$$

and

$$\nu = 1063.87 \pm 0.7765N - 0.00335N^2 \quad (2)$$

from which the computed values shown in the tables were obtained. The mean of all residuals is less than 0.04 cm^{-1}. The conditions of observation for these bands are advantageous, not only on account of the high resolution available, but because this region is quite free from atmospheric absorption, and the bands are themselves fairly weak, without complications due to superposition of close neighbors as was the case at $15\mu(\nu_2)$.

The two bands arise from absorption by molecules already excited to the double state $(\nu_1, 2\nu_2)$. The initial levels each have a population of about 0.15 percent at room temperature, and their term values are 1285.8 and 1388.4 cm^{-1} respectively. The final state is ν_3, at 2350.1 cm^{-1}. These are the first difference bands to be subjected to high resolution in the infrared. Since the quantum number l is zero both in the

[1] Dennison, Rev. Mod. Phys. **3**, 280 (1931).
[2] Martin and Barker, Phys. Rev. **41**, 291 (1932).
[3] Houston and Lewis, Proc. Nat. Acad. **17**, 229 (1931).
[4] Adams and Dunham, Pub. A.S.P. **44**, 243 (1932).
[5] Dennison, Phys. Rev. **41**, 304 (1932).
[6] Adel and Dennison, Phys. Rev. **43**, 716; **44**, 99 (1933).
[7] Schaefer and Philipps, Zeits. f. Physik **36**, 641 (1926).

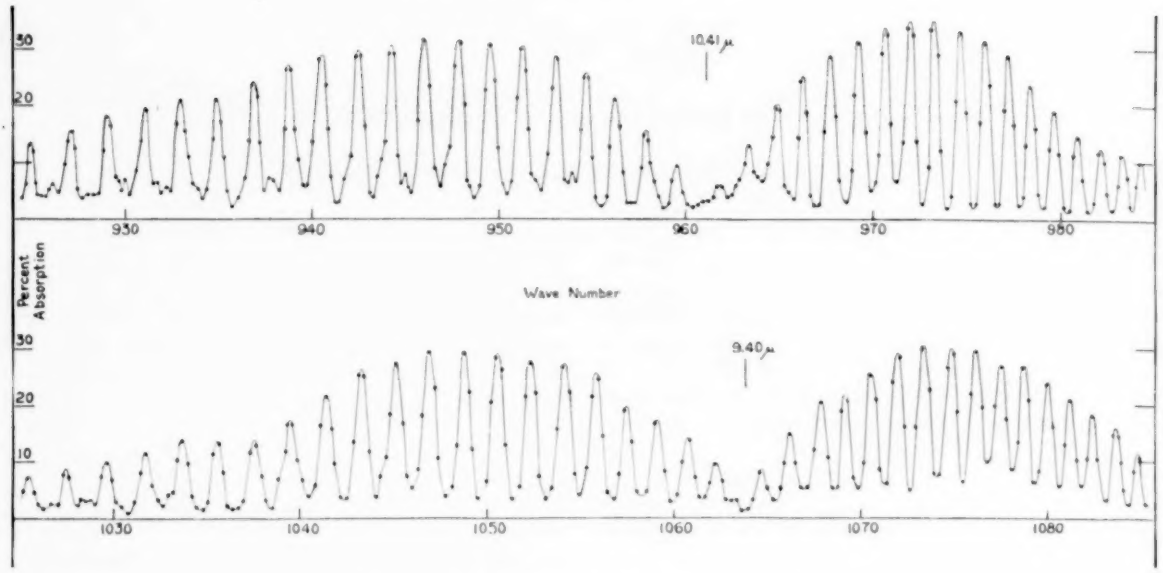

FIG. 1. The CO_2 absorption bands $\nu_3-(\nu_1, 2\nu_2)$.

TABLE I. *The band at 10.41μ.*

	Positive Branch				Negative Branch		
N	ν comp.	ν obs.	dif.	N	ν comp.	ν obs.	dif.
1	961.80	961.76	+0.04	2	959.47	959.43	+0.04
3	963.33	963.33	0	4	957.88	957.79	+0.09
5	964.83	964.87	−0.04	6	956.26	956.20	+0.06
7	966.31	966.34	−0.03	8	954.63	954.61	+0.02
9	967.76	967.78	−0.02	10	952.96	953.03	−0.07
11	969.20	969.24	−0.04	12	951.26	951.25	+0.01
13	970.60	970.68	−0.08	14	949.55	949.53	+0.02
15	971.98	972.00	−0.02	16	947.81	947.85	−0.04
17	973.34	973.30	+0.04	18	946.04	946.06	−0.02
19	974.66	974.68	−0.02	20	944.26	944.28	−0.02
21	975.97	975.98	−0.01	22	942.45	942.47	−0.02
23	977.24	977.20	+0.04	24	940.61	940.56	+0.05
25	978.50	978.43	+0.07	26	938.74	938.76	−0.02
27	979.72	979.71	+0.01	28	936.86	936.90	−0.04
29	980.92	980.93	−0.01	30	934.93	934.94	−0.01
31	982.12	982.12	0	32	932.99	932.98	+0.01
33	983.28	983.30	−0.02	34	931.01	931.04	−0.03
35	984.41	984.39	+0.02	36	929.04	929.07	−0.03
				38	927.02	927.10	−0.08

TABLE II. *The band at 9.40μ.*

	Positive Branch				Negative Branch		
N	ν comp.	ν obs.	dif.	N	ν comp.	ν obs.	dif.
1	1064.65	1064.70	−0.05	2	1062.30	1062.23	+0.07
3	1066.20	1066.17	+0.03	4	1060.71	1060.61	+0.10
5	1067.67	1067.81	−0.14	6	1059.09	1059.03	+0.06
7	1069.14	1069.14	0	8	1057.45	1057.46	−0.01
9	1070.59	1070.55	+0.04	10	1055.77	1055.79	−0.02
11	1072.01	1071.92	+0.09	12	1054.07	1054.15	−0.08
13	1073.41	1073.32	+0.09	14	1052.34	1052.31	+0.03
15	1074.76	1074.77	−0.01	16	1050.59	1050.58	+0.01
17	1076.11	1076.11	0	18	1048.61	1048.76	−0.15
19	1077.41	1077.38	+0.03	20	1047.00	1046.99	+0.01
21	1078.70	1078.69	+0.01	22	1045.16	1045.18	−0.02
23	1079.95	1079.95	0	24	1043.24	1043.28	−0.04
25	1081.19	1081.16	+0.03	26	1041.41	1041.39	+0.02
27	1082.39	1082.37	+0.02	28	1039.51	1039.50	+0.01
29	1083.57	1083.54	+0.03	30	1037.56	1037.57	−0.01
31	1084.72	1084.81	−0.09	32	1035.55	1035.54	+0.01
				34	1033.70	1033.60	+0.10
				36	1031.68	1031.57	+0.11
				38	1029.62	1029.63	−0.01
				40	1027.55	1027.47	+0.08
				42	1025.45	1025.50	−0.05
				44	1023.32	1023.31	+0.01
				46	1021.18	1021.34	−0.16

initial and final levels there are no zero branches, and it is possible to observe the central portion of the pattern, which is completely obscured in the 15μ band. The intensity distribution here makes it perfectly clear that the rotation states have been properly numbered, i.e., that in the upper state ($V_3=1$) the values of J are all odd. They are consequently all even in the unexcited molecule, as determined previously but not so directly.[2]

The interaction between rotation and vibration in the CO_2 molecule has two important consequences. Firstly, it alters the major fine structure interval of the rotation-vibration bands from $h/4\pi^2Ic$ to

$$(h/4\pi^2Ic)[1+\tfrac{1}{2}\{A+2B+C+\sum_i C^2_{\tau t_i}(AV_1+BV_2+CV_3)_i-\sum_j C^2_{\sigma s_j}(AV_1+BV_2+CV_3)_j\}],$$

where the $C_{\tau t_i}$ and $C_{\sigma s_j}$ are respectively the coefficients in the stabilized wave functions of the upper and lower vibrational levels involved in the transition.

$$A=(0.00175+0.000112a),\ B=(-0.00117+0.000037b),\ C=(-0.00033+0.000019c),$$

where $a=-36.2$, $b=72.9$, and $c=-202.1$ cm^{-1} are the coefficients of the cubic anharmonic potential of vibration. The moment of inertia, I, may be computed by equating this expression to the observed fine structure interval. Corresponding to the bands at 1063.87 and 961.03 cm^{-1} we obtain the equations

$$(h/4\pi^2Ic)[1+\tfrac{1}{2}\{1.43A+3.14B+2C\}]=0.7765\ \text{cm}^{-1},$$

$$(h/4\pi^2Ic)[1+\tfrac{1}{2}\{1.57A+2.86B+2C\}]=0.7765\ \text{cm}^{-1}.$$

Both relations yield the value $I=70.6\times10^{-40}$ gram cm^2.

Secondly, the interaction between rotation and vibration produces a convergence of the fine structure depending upon the square of the ordinal number of the line and given by

$$(h/8\pi^2Ic)\{\sum_i C^2_{ri}(AV_1+BV_2+CV_3)_i-\sum_j C^2_{sj}(AV_1+BV_2+CV_3)_j\}N^2.$$

It is thus possible to predict the convergence of the above bands. We find $-0.0034\ N^2$ and $-0.0031\ N^2$ in excellent agreement with the observed values $-0.00335\ N^2$ and $-0.00311\ N^2$.

Variation with Temperature of the Continuous Absorption Spectrum of Diatomic Molecules: Part I. Experimental,* The Absorption Spectrum of Chlorine

G. E. GIBSON AND NOEL S. BAYLISS,† *Department of Chemistry, University of California*

(Received May 4, 1933)

A photographic method was used to investigate the continuous absorption spectrum of chlorine at 18°, 168°, 281°, 426°, 580° and 765°C. The effect of increasing the temperature is to decrease the absorption coefficient at the maximum, and to broaden the region of continuous absorption. The results were analyzed to obtain the contributions of individual vibrational levels to the total absorption. The absorption from the level $v''=0$ has a single maximum, that from the level $v''=1$ has two maxima, and it appears probable that the absorption from the level $v''=2$ has three maxima.

INTRODUCTION

THE interpretation of the continuous spectra of diatomic molecules was first given by Franck.[1] The continuous absorption is caused by transitions from any one of the energy levels of the normal electronic state to one of the continuous series of energy levels which lie above the energy of dissociation of the excited state. A qualitative explanation of the intensity relations between the continuous and band spectra was given by the Franck-Condon principle.[2] Later, Condon[3] showed that the ideas embodied in this principle were too classically precise to explain the breadth of the region of continuous absorption of the halogens. Condon considered only the continuum arising from the lowest vibrational level of the normal state of the molecule and without evaluating the proper functions of the excited state, he was able to give a qualitative explanation of the breadth of the continuous absorption.

It was pointed out by one of us that Condon's reasoning could be extended to account for the temperature variation of the continuous absorption of chlorine by taking into account the absorption from the higher vibrational levels of the normal state.[4]

This paper describes an experimental investigation of the temperature variation of the continuous absorption spectrum of chlorine, and gives a method of obtaining the contributions of the higher vibrational levels which is independent of any wave mechanical theory of the absorption. The theoretical interpretation of our experimental results will be given in Part II.

Chlorine, which absorbs continuously between λλ4300 and 2500, is a particularly suitable substance for the study of this temperature variation. At room temperature, the higher vibrational states contribute little to the absorption, since 93.5 percent of the molecules are in the state $v''=0$. At 765°C, the highest temperature which was reached during the experiments, only 53 percent of the molecules are in the lowest state, so that the contribution of the higher vibrational states is considerable.

The effect of temperature on the continuous absorption spectrum of chlorine has not been studied previously, although Halban and Siedentopf,[5] and Ribaud[6] have published measurements of the absorption coefficient of chlorine at room temperature. Vogt and Koenigsberger[7]

* An account of this work was presented to the New Haven Meeting of the American Physical Society, June, 1932.

† Commonwealth Fund Fellow.

[1] J. Franck, Trans. Faraday Soc. **21**, 536 (1926).

[2] E. U. Condon, Phys. Rev. **28**, 1182 (1926).

[3] E. U. Condon, Phys. Rev. **32**, 858 (1928).

[4] G. E. Gibson, Phys. Rev. **39**, 550 (1932).

[5] H. V. Halban and K. Siedentopf, Zeits. f. physik. Chemie **103**, 71 (1922).

[6] G. Ribaud, Ann. de Physique **12**, 107 (1919).

[7] K. Vogt and J. Koenigsberger, Zeits. f. Physik **13**, 292 (1923).

have investigated the effect of temperature on the continuous absorption of bromine and iodine. In these two cases, the vibrational levels of the normal electronic state are rather too closely spaced to make them suitable substances for the present investigation. However, the general effect of an increase in temperature on the continuous absorption of bromine and iodine is the same as that which we will describe for chlorine; i.e., a decrease in the absorption coefficient at the maximum and a general broadening of the region of absorption.

Apparatus

A photographic method[8] was used to determine the absorption coefficients. The source of continuous ultraviolet radiation was a water-cooled hydrogen discharge tube made according to the specifications of Bay and Steiner.[9] The discharge tube was operated with a current of 0.5–1 amp. at 6000 volts. Before each series of exposures it was run overnight in order that it might reach a steady state and during each run the intensity was kept as constant as possible by maintaining the primary current through the transformer at a constant value. The spectrum of the source was continuous from 4500A down to 2400A. A small amount of structure in the neighborhood of 4000A did not interfere with the measurements. A series of diaphragms in front of the discharge tube cut out stray light which might have been reflected from the wall of the absorption cell.

The light passed through a quartz absorption cell, 10 cm long, with plane windows and filled with chlorine at a pressure of about 5 cm. The chlorine was prepared by heating dry, anhydrous cupric chloride in vacuum and was purified by distillation. Three equal fractions were collected, the first and last being discarded, while part of the middle fraction was used to fill the cell. When the absorption measurements were concluded, the concentration of chlorine was accurately determined by opening the cell under a slightly acid solution of potassium iodide, and titrating the liberated iodine with hundredth normal sodium thiosulphate. The use of solutions of this dilution introduces an error in the end point which was corrected by standardizing the sodium thiosulphate with Merck's purest iodine under identical conditions. The volume of the cell was determined by weighing it full of distilled water.

The absorption cell was contained in a tubular electric furnace 30 cm long. A constant temperature over the whole length of the cell was attained by making the inner tube of the furnace out of heavy copper and by spacing the furnace windings more closely at the ends than in the middle. The temperature of the absorption cell was measured by calibrated chromel-alumel thermocouples. Even at the highest temperature reached, 765°C, the variation in temperature over the whole length of the cell was not more than 3°C.

The absorption cell was fitted with a narrow side tube which projected outside the furnace and into which all the chlorine could be frozen. A small correction was applied to the concentration of gas in the cell to allow for the fact that the side tube was not at the temperature of the furnace. If c is the average concentration of chlorine as determined by analysis, and c_1 is the actual concentration in the cell at a temperature T_1, then $c_1 = cT_2(V_1+V_2)/(T_1V_2+T_2V_1)$, where V_1 is the volume of gas in the furnace at a temperature T_1, and V_2 is the volume of gas in the projecting side tube at a mean temperature T_2.

Wire screens[10] were used to diminish the light intensity by known amounts. The screens were calibrated by two different methods. The first was a visual one, with the use of a two-meter photometer bench with a Lummer-Brodhun head. Later, we were able to make use of a sensitive 1000 junction thermopile which was constructed in this laboratory by Dr. Boris Brüzs. The combination of thermopile and galvanometer responded linearly to light of different intensities. The two methods of calibration agreed to within one part in 200, except for the three screens with the lowest transmission factors. Since visual photometry is apt to be unreliable with light of small intensity, the

[8] A summary of the methods of photographic photometry is given by G. R. Harrison, J. Opt. Soc. Am. **19**, 267 (1929).

[9] Z. Bay and W. Steiner, Zeits. f. Physik **59**, 48 (1929); **45**, 337 (1927).

[10] G. R. Harrison, J. Opt. Soc. Am. **18**, 492 (1929).

values obtained with the thermopile were used in these cases. The screens transmitted respectively 81.5, 69.5, 48.6, 38.0, 33.9, 29.7, 15.6 and 6.6 percent of the incident light. A mechanical "shaker" held the screens normal to the beam of light and moved them with an eccentric circular motion of about 2 cm amplitude. Additional calibration points were obtained by using the screens in pairs, moving 90° out of phase with each other. A preliminary test with the thermopile showed that the transmission factor of a pair of screens used in this way was very closely equal to the product of the transmission factors of the separate screens.

Exposures were timed by means of a shutter placed immediately in front of the slit of the spectrograph. The shutter was controlled electrically so that an exposure of any multiple of five seconds could be repeated with an error not exceeding 0.1 second.

The light was analyzed by a Hilger E3 quartz spectrograph. Eastman Speedway plates were used. Their rather coarse grain is no disadvantage when working with a continuous spectrum and they have the advantage of a long working range between the regions of overexposure and underexposure. They were developed in a metol-hydroquinone developer, even development being obtained by lightly brushing the plates with a camel hair brush.[11] Since the experiments were carried out so that each plate was independent of the others,[12] no particular precautions were observed with regard to time of development or strength of developer. Wave-length calibrations which gave a convenient number of lines in the ultraviolet were obtained from the spectrum of an arc between brass electrodes.

Experimental Procedure

The spectrum of the brass arc was photographed at each side of the plate. In between, a number of spectra were photographed, all with the same exposure. One of these was the absorption spectrum of chlorine and the others were photographs of the source weakened by various screens, the disposition of the apparatus being absolutely unchanged except that the chlorine was frozen out of the cell into the side tube. The absorption spectrum and the calibration spectra were thus taken under identical conditions.

The blackening on the plate was measured with a Zeiss self-recording microphotometer, for the use of which we are indebted to the Physics Department of the University of California. Photometer traces were taken across each plate between identical lines of the brass spectra. The intensity of the light transmitted by chlorine was thus compared directly with the intensity transmitted by the calibrated screens at the same wave-length. A simple graphical interpolation gave the value of the absorption coefficient at each wave-length. At least four plates were taken at each temperature, and a complete series of measurements was made at each of six different temperatures.

Results

The absorption coefficient, ϵ, is defined by the relation

$$I = I_0 10^{-\epsilon c d}$$

where I_0 is the incident intensity, I, the transmitted intensity, d, the length of the absorbing path in cm and c the concentration in mol. liter^{-1}. The results for the six different experimental temperatures are given in Table I and are compared with the theoretical values in Fig. 4 of Part II. The experimental errors inherent in a photographic method are rather difficult to estimate. The exposures used ranged from 15 seconds to 5 minutes so that errors in timing were less than 1 part in 150. The maximum error in the transmission factors of the screens is about 1 part in 200, except where the transmission factor is small. The temperature measurements were correct to within 5°C at the highest temperature, with a correspondingly smaller error at the lower temperatures. It is difficult to estimate the errors introduced by the photographic plate and the photometer. The experimental points lie on smooth curves. The agreement between different plates taken at the same temperature indicates that, in the most favorable region of medium absorption coefficient, the error is less than 2 percent. At the absorption maximum where the

[11] Dobson, Griffiths and Harrison, *Photographic Photometry*, p. 76, Oxford University Press (1926).

[12] G. R. Harrison, reference 8.

TABLE I.

Wave-length A	Absorption Coefficient 18°C 291°K	168°C 441°K	281°C 554°K	426°C 699°K	580°C 853°K	765°C 1038°K	Wave number cm^{-1}
4275	2.3	2.0	3.2	5.0	5.4	7.3	23,385
4023	4.5	6.6	8.3	10.8	11.5	13.8	24,850
3862	9.4	12.2	15.2	17.3	18.5	19.4	25,886
3806	13.7	16.0	17.8	20.5	21.3	23.4	26,267
3741	18.2	19.9	22.2	24.0	24.3	26.8	26,723
3683	24.0	25.0	26.1	28.2	28.3	29.4	27,144
3640	29.0	29.9	29.9	31.1	31.3	31.4	27,465
3573	37.5	38.4	36.3	35.9	35.4	34.5	27,980
3484	50.6	47.5	44.9	43.0	41.5	38.2	28,694
3413	58.2	54.4	49.9	45.2	43.7	41.2	29,291
3381		56.2	52.0	45.9	44.3	42.3	29,569
3346	64.3	58.8	53.5	46.7	45.2	43.1	29,878
3274	64.3	60.6	55.6	47.2	46.4	43.5	30,535
3208	61.3	56.7	53.5	47.0	45.5	42.9	31,163
3174	58.2	53.2	49.9	45.9	48.8	42.5	31,497
3074	44.7	41.9	42.1	41.4	39.7	37.9	32,521
3011	33.3	34.3	34.0	34.6	33.9	34.2	33,202
2961	26.0	27.4	27.2	29.4	28.9	30.2	33,763
2883	15.7	16.5	18.2	20.6	21.4	23.1	34,676
2802	7.9	9.1	10.2	13.4	13.6	15.5	35,678
2722	3.4	3.4	4.0	5.9	6.3	8.9	36,727
2666	2.7	1.8	2.2	3.8	4.4	6.4	37,498
2618		0.9	1.2	2.6	2.7	4.2	38,186

transmission is small and in the region where the absorption coefficient is very small, the errors may be greater. The results of Halban and Siedentopf[5] are plotted in Fig. 4 (Part II). Their measurements were done at fewer points than ours but were carried out with the utmost care. The difference between their results and ours lies well within the limits which we have estimated for our experimental error.

ANALYSIS OF RESULTS

By using the Maxwell-Boltzmann distribution law, the contribution of each vibrational level to the total continuous absorption may be obtained from our experimental results in the following way.

If $N_{v''}$ be the fraction of the total number of molecules which exists in the state with vibrational quantum number v'' at a temperature T, then the total absorption coefficient is given by

$$\epsilon = N_0\epsilon_0 + N_1\epsilon_1 + N_2\epsilon_2 + \cdots \qquad (1)$$

where

$$N_0 + N_1 + \cdots = 1.$$

ϵ_0, ϵ_1, etc., are partial absorption coefficients appropriate to the various vibrational levels. If $E_{v''}$ represents the energy difference between the state v'' and the lowest state $v''=0$, Eq. (1) becomes

$$\epsilon = [\epsilon_0 + \epsilon_1 e^{-E_1/kT} + \epsilon_2 e^{-E_2/kT} + \cdots]/\sum_{v''} e^{-E_{v''}/kT}. \qquad (2)$$

From Elliot's data[13] on the origins of the chlorine bands it is found that

$$E_{v''}/hc = \omega_0 v'' - \omega_1 v''^2 = 560.9v'' - 4.0v''^2.$$

With this formula, the sum (S_T) of the series in the denominator of Eq. (2) was evaluated at each temperature by calculating successive terms until further contributions could be neglected. For a given substance, S_T is a function of the temperature only, and for chlorine it has the following values at our experimental temperatures

$t=$	18	168	281	426	580	765°C
$S_T=$	1.069	1.198	1.314	1.475	1.656	1.882

Then

$$\epsilon S_T = \epsilon_0 + \epsilon_1 e^{-E_1/kT} + \epsilon_2 e^{-E_2/kT} + \cdots. \qquad (3)$$

In order to obtain a convenient interpretation of the experimental results, we regarded the first few vibrational levels in chlorine as equally spaced, and took $\omega = 551$ cm^{-1} as giving a mean value of the energy separation. Eq. (3) becomes

$$\epsilon S_T = \epsilon_0 + \epsilon_1 e^{-hc\omega/kT} + \epsilon_2 e^{-2hc\omega/kT} + \epsilon_3 e^{-3hc\omega/kT} + \cdots, \qquad (4)$$

which has the form

$$\epsilon S_T = \epsilon_0 + \epsilon_1 x + \epsilon_2 x^2 + \epsilon_3 x^3 + \cdots. \qquad (5)$$

At each wave-length, the smoothed experimental

TABLE II.

Wave number	ϵ_0	ϵ_1	Wave number	ϵ_0	ϵ_1
23,500	1.7	2	31,000	66.9	12
24,000	2.0	8	31,500	61.1	16
24,500	2.4	10	32,000	53.9	24
25,000	3.6	26	32,500	45.0	34
25,500	4.7	44	33,000	37.0	36
26,000	8.0	50	33,500	28.6	44
26,500	13.5	48	34,000	21.9	40
27,000	20.5	46	34,500	16.2	36
27,500	28.7	44	35,000	11.8	30
28,000	37.9	38	35,500	8.2	20
28,500	48.8	24	36,000	5.7	12
29,000	58.2	14	36,500	4.0	8
29,500	65.0	8	37,000	2.6	2
30,000	69.8	1	37,500	1.6	2
30,500	69.6	10			

[13] A. Elliot, Proc. Roy. Soc. (London) **A127**, 651 (1930).

results provided a series of absorption coefficients at different temperatures. Each absorption coefficient was multiplied by the appropriate value of S_T, and ϵS_T was plotted against x of Eq. (5). The curves obtained in this way were extrapolated to the point $x=0$, the value of ϵS_T at this point being ϵ_0. The gradient of the curve at this point gives ϵ_1. The values of ϵ_0 and ϵ_1 obtained in this way are given in Table II and are compared with the theoretical values in Fig. 3 of Part II. ϵ_2 would be given by the second derivative of the curve at the point $x=0$. The experimental results are unfortunately not accurate enough to enable values to be assigned to ϵ_2. The general trend of it, however, can be inferred from the curvature of the graphs of ϵS_T against x. ϵ_2 has three maxima in the neighborhood of 24,000, 30,000 and 36,000 cm^{-1} but without experimental data at least ten times as accurate as ours (an accuracy which cannot be attained by present photographic methods), one could draw no further conclusions with regard to it.

One of the authors (N.S.B.) desires to express his thanks to the Commonwealth Fund for a Fellowship which enabled him to engage in this work.

Variation with Temperature of the Continuous Absorption Spectrum of Diatomic Molecules: Part II. Theoretical

G. E. GIBSON, O. K. RICE AND N. S. BAYLISS,* *Chemical Laboratories, University of California and Harvard University*

(Received May 4, 1933)

A method of calculating the matrix components, corresponding to the continuous absorption of light by diatomic molecules in various vibrational and rotational levels of the lower state, is described and applied to the calculation of the absorption of Cl_2 gas at various temperatures. The theory shows that the absorption from a single vibrational level is practically independent of temperature, and that the temperature effect is due to the changing distribution of the absorbing molecules among the various levels. Assuming the Morse function to be approximately correct for the potential energy of the lower state, the theory enables one to calculate the form of the upper potential energy curve. The matrix component of the electric moment corresponding to the absorption from the lower state has been calculated for Cl_2 and found to correspond to the displacement of one electronic charge through 0.016A.

I. THE FUNDAMENTAL EQUATION FOR THE ABSORPTION COEFFICIENT

IN chlorine[1] the transition which gives rise to the continuum at $\lambda = 3300$A is from the normal $^1\Sigma_+$ state to a 0^+ state. At the highest temperature investigated (1038°K) practically none of the 0^+ states are excited. The molecules of the gas are distributed initially among the vibrational and rotational states of $^1\Sigma_+$. The absorption coefficient

$$k_\nu = \frac{\epsilon_\nu \cdot \ln 10}{6.06 \times 10^{20}} = -\frac{1}{N}\frac{d \ln I}{dl}, \qquad (1)$$

where I is the intensity of the incident light, (ϵ has been defined in Part I, the subscript ν merely designating it for light of a particular frequency) N is the number of molecules per cm³ and l in cm is the distance traversed by the light. k_ν is given by the equation

$$k_\nu N = \sum_{\alpha''} \sum_{\alpha'} P_{\alpha''\alpha'} N_{000} e^{-E_{\alpha''}/kT}. \qquad (2)$$

Here, α'', α' are short for the respective sets of quantum numbers $(v''J''M'')$, $(v'J'M')$, N_{000} is the number of molecules per cm³ in the state of lowest energy ($v''=0$, $J''=0$, $M''=0$), $E_{\alpha''}$ is the energy in ergs of the state α'' measured from the state (0, 0, 0), (i.e., $E_{000}=0$), T is the absolute temperature, $k = 1.372 \times 10^{-16}$ ergs/°K and

$$P_{\alpha''\alpha'} = (8\pi^3\nu/3hc)\,|D_{\alpha''\alpha'}|^2 \qquad (3)$$

is the absorption coefficient per molecule,[2] referring to an incident beam of 1 photon crossing unit area per second per unit frequency range. The matrix component in Eq. (3) is defined by the equation

$$D_{\alpha''\alpha'} = \int \varphi''_{\alpha''} \cdot D \cdot \varphi'_{\alpha'} d\tau, \qquad (4)$$

where $\varphi''_{\alpha''}$, $\varphi'_{\alpha'}$ are the eigenfunctions of $^1\Sigma_+$ and 0^+ respectively, and D is the electric moment (a function of all the coordinates). We assume with Born and Oppenheimer[3] that each of these eigenfunctions may be represented as a product of an electronic, a rotational, and a vibrational eigenfunction, and also that in the integration over the electronic coordinates the nuclear separation r is to be regarded as an (approximately) constant parameter. Hence Eq. (4) may be written

* Commonwealth Fund Fellow.

[1] See Part I, of this title, Phys. Rev. **44**, 188 (1933).

[2] Dirac, *Principles of Quantum Mechanics*, p. 168, Eq. (24) (1930). (See also paragraph 61, Eq. (59) and paragraph 71, p. 232.

[3] M. Born and R. Oppenheimer, Ann. d. Physik **84**, 474 (1927).

$$D_{\alpha''\alpha'} = \int P''_{J''M''}(\phi, \theta) F''_{v''J''}(r) \left[\int \varphi_{n''}(\chi) D \varphi_{n'}(\chi) d\chi \right] P'_{J'M'}(\phi, \theta) F'_{E'J'}(r) d\tau$$

$$= \int F''_{v''J''} P''_{J''M''} D_{n''n'} P'_{J'M'} F'_{E'J'} d\tau, \tag{5}$$

where F represents the vibrational eigenfunctions multiplied by r, P_{JM} the rotational eigenfunctions (Tesseral harmonics), $d\tau$ represents the appropriate differential of the nuclear coordinates r, θ, ϕ, and E' is the energy which goes with v'. The integral $D_{n''n'}$ over the electronic variables χ strictly speaking is a function of r, but we shall assume it to be constant over the small range of r for which the eigenfunction $F''_{v''J''}(r)$ has appreciable values.

Integrating Eq. (5) over θ and ϕ and then over r we obtain

$$D_{\alpha''\alpha'} = D_{n''n'} L_{J''J'}^{M''M'} \int_0^R F''_{v''J''} F'_{E'J'} dr = D_{n''n'} L_{J''J'}^{M''M'} \cdot F_{v''E'J''J'} \tag{6}$$

where R is the bounding nuclear separation (Lim $R = \infty$), determined by the size of the containing vessel.

The rotational matrix components $L_{J''J'}^{M''M'}$ have been calculated by Hönl and London[4] and are zero for Cl_2 unless $J' - J'' = \pm 1$, $M' - M'' = \pm 1$ or 0.

They obey the equation

$$\sum_{JM} L_{J''J'}^{M''M'^2} = 2J'' + 1, \tag{7}$$

where the summation includes all possible transitions from the state J''. This relationship will be used later on in carrying out the summations in Eq. (2). Before this can be done, however, we must first evaluate the eigenfunctions $F_{v''J''}$ and $F_{E'J'}$ and calculate the matrix component $F_{v''E'J''J'}$ which occurs in Eq. (6).

II. Evaluation of $F''_{v''J''}(r)$

We shall write, for short, $F'' = F''_{v''J''}(r)$. The Schroedinger equation is

$$\partial^2 F''/\partial r^2 + \kappa^2 (E'' - V'' - J''(J''+1)/\kappa^2 r^2) F'' = 0, \tag{8}$$

where $\kappa^2 = 8\pi^2 \mu_0 / h^2$, where μ_0 is the reduced mass. For $J'' = 0$ the potential energy $V''(\rho)$ (where $\rho = r - r_0$) was taken to be of the form $-(\gamma/\rho) + (\beta/\rho^2)$ and the constants r_0, γ and β were chosen so as to give the best agreement with the Morse curve (lower curve in Fig. 1) in the region near the minimum of $V''(\rho)$. Writing $\kappa^2 E''_{v''} = -a^2 v''$, and $\kappa^2 \beta = m(m-1)$, the quantum condition becomes $\kappa^2 \gamma / 2a_{v''} - m = v''$, where $v'' = 0, 1, 2, \cdots$. Setting $\xi = 2a_{v''}\rho$ and $2m - 1 = \alpha$, the normalized eigenfunctions of Eq. (8) are given by[5]

$$F''_{v''} = [v''!/(2m + 2v'')]^{\frac{1}{2}} [\Gamma(2m + v'')]^{-\frac{1}{2}} e^{-\xi/2} \xi^m L^{\alpha}_{v''+\alpha}(\xi) \tag{9}$$

where $L^{\alpha}_{v''+\alpha}(\xi) = e^{i\pi(\alpha+v'')} \dfrac{\Gamma(\alpha + v'' + 1)}{v''!} \left[\xi^{v''} - \dfrac{(\alpha+v'')v''}{1!} \xi^{v''-1} + \dfrac{(\alpha+v'')(\alpha+v''-1)v''(v''-1)}{2!} \xi^{v''-2} + \cdots \right]$.

---

[4] W. Weizel, *Bandenspektren*, Handb. d. Exp. Phys., p. 167 ff. (1931).

[5] Schroedinger, Ann. d. Physik **80**, 483 (1926).

The four lowest eigenfunctions ($v''=0, 1, 2, 3$) are

$$\text{(a)}\quad F_0''(r)=\frac{(2a_0)^{m+\frac{1}{2}}}{\{\Gamma(2m+1)\}^{\frac{1}{2}}}\rho^m e^{-a_0\rho}$$

$$\text{(b)}\quad F_1''(r)=\frac{(2a_1)^{m+\frac{1}{2}}\cdot 2m}{\{(2m+2)\Gamma(2m+1)\}^{\frac{1}{2}}}\rho^m e^{-a_1\rho}\left[1-\frac{a_1\rho}{m}\right]$$

$$\text{(c)}\quad F_2''(r)=\frac{(2a_2)^{m+\frac{1}{2}}2m(2m+1)}{\{2(2m+4)\Gamma(2m+2)\}^{\frac{1}{2}}}\rho^m e^{-a_2\rho}\left[1-\frac{4a_2\rho}{2m}+\frac{4(a_2\rho)^2}{2m(2m+1)}\right] \tag{10}$$

$$\text{(d)}\quad F_3''(r)=\frac{(2a_3)^{m+\frac{1}{2}}\cdot 2m(2m+1)(2m+2)}{\{3!(2m+6)\Gamma(2m+3)\}^{\frac{1}{2}}}\rho^m e^{-a_3\rho}\left[1-\frac{6a_3\rho}{2m}+\frac{12(a_3\rho)^2}{2m(2m+1)}-\frac{8(a_3\rho)^3}{2m(2m+1)(2m+2)}\right].$$

The data are all for $J''=0$. The effect of J'' will be discussed in paragraph 5. The expression (9) is normalized for integration with respect to ξ instead of r, so (10) differs from (9) by a factor $(2a_{v''})^{\frac{1}{2}}$. In addition the factor $e^{-i\pi\alpha}$ has been dropped from (10) since α was taken to be an even integer in our calculations.

III. Evaluation of $F'_{v'J'}(r)$ for $J'=0$

The Schroedinger equation is

$$\frac{\partial^2 F'}{\partial r^2}+\kappa^2\left(E'-V'-\frac{J'(J'+1)}{\kappa^2 r^2}\right)F'=0. \tag{11}$$

We are concerned here with the potential energy $V'(r)$ in the neighborhood of $r=2$Å since it is only in this region that the eigenfunctions F'' have appreciable values. As an empirical formula for $V'(r)$ which leads to a convenient solution when substituted in (11) we have chosen[6]

$$V'(r)=V_\infty'+[(\omega^2-\tfrac{1}{4})/\kappa^2\rho^2], \tag{12}$$

where $\rho=r-r_0$ as in paragraph 2 and V_∞' and ω are constants to be determined later by comparing the calculated and observed absorption coefficients. This expression cannot be used for $\rho<0$, that is $r<r_0$. This, however, is of no practical importance, as the eigenfunction will already be very small (the approximate one actually zero) at this point. We may extend all our integrals from $\rho=0$ to $\rho=R$ instead of from $r=0$ to $r=R$.

Taking again the case of zero rotation ($J'=0$) the normalized integral of Eq. (11) with $V'(r)$ as given by Eq. (12) is

$$F_{v'}'(r)=(\pi b'/R)^{\frac{1}{2}}\rho^{\frac{1}{2}}J_\omega(b\rho), \tag{13}$$

where $b=\kappa(E'-V_\infty')^{\frac{1}{2}}$ and $J_\omega(b\rho)$ is the Bessel function of order ω and argument $b\rho=b(r-r_0)$. The normalizing factor is $(\pi b'/R)^{\frac{1}{2}}$ where

$$b'=\kappa(E'-E_D')^{\frac{1}{2}} \tag{14}$$

and R, it will be remembered, is the bounding nuclear separation. The energy of the 0^+ molecule when dissociated into atoms at rest is E_D'. This is not equal to V_∞' since Eq. (12) only holds for a limited range of r, and is untrue when $r=\infty$. Were $E_D'=V_\infty'$, then b would naturally occur instead of b' in Eq. (13) and the ratio of the amplitude of the oscillations of Eq. (13) at a point in the important range of r (where $V'=V_a'$, say) to the amplitude at infinite r would be $(E_\infty'-V_\infty')^{\frac{1}{2}}(E'-V_a')^{-\frac{1}{2}}$. In the actual case the ratio of amplitudes is $(E'-E_D')^{\frac{1}{2}}\times(E'-V_a')^{-\frac{1}{2}}$. So we must multiply Eq. (13) (if b instead of b' were in it) by

$$(E'-E_D')^{\frac{1}{2}}(E'-V_a')^{-\frac{1}{2}}/(E'-V_\infty')^{\frac{1}{2}}(E'-V_a')^{-\frac{1}{2}}$$

to give us Eq. (13) as it stands.

IV. Evaluation of the Vibrational Matrix Component $F_{v''E'J''J'}$

Taking $J''=0$, $J'=1$ for which the effect of rotation is certainly negligible, we have, combining Eqs. (6), (10a), and (13), and writing $m+3/2=\mu$

$$F_{0E'01}=A_0\int_0^R \rho^{\mu-1}e^{-a_0\rho}J_\omega(b\rho)d\rho \tag{15}$$

[6] C. Zener, Phys. Rev. **37**, 556 (1931).

where

$$A_0=(\pi b'/R)^{\frac{1}{2}}(2a_0)^{m+\frac{1}{2}}/\{\Gamma(2m+1)\}^{\frac{1}{2}}. \tag{16}$$

Writing $I_0/a_0{}^\mu=F_{0E'01}/A_0$ we have for the integral in Eq. (15)*

$$I_0/a_0{}^\mu=\frac{(\frac{1}{2})^\omega}{a_0{}^\mu}\frac{\Gamma(\mu+\omega)}{\Gamma(\omega+1)}x_0{}^{\omega/2}(1+x_0)^{-\mu+\frac{1}{2}}{}_2F_1\left(\frac{\omega-\mu+1}{2},\ \frac{\omega-\mu}{2}+1;\ \omega+1;\ -x_0\right), \tag{17}$$

where

$$x_0=b^2/a_0{}^2=\kappa^2(E'-V_\infty')/a_0{}^2 \tag{18}$$

and ${}_2F_1$ is the hypergeometric function of parameters and variable indicated.

In a similar manner, using Eqs. (10b, c and d) we obtain the matrix components $F_{1E'01}$, $F_{2E'01}$, $F_{3E'01}$. Before evaluating these, however, we shall discuss the effect of rotation, and carry out the summations indicated in Eq. (2).

V. The Dependence of the Vibrational Matrix Components $F_{v''E'J''J'}$ on the Rotational Quantum Number J''

We return to the Schroedinger Eqs. (8) and (11). To each of the potential energies $V''(r)$ and $V'(r)$ we have to add the term $[J(J+1)]/\kappa^2r^2$. The average value of J'' at 1000°K is about 50 and $2.1>r>1.9$A is the region where the three lowest eigenfunctions $F''_{v''}(r)$ have values large enough to contribute noticeably to the matrix component. Apart from a slight distortion (around ±50 cm^{-1} at the limits of the important range of r for $J=50$), each potential energy curve is therefore raised by the same amount (about 1000 cm^{-1} when J'' goes from 0 to 50) since $J'=J''\pm1\leqq J''$.

The eigenvalues of the lower state are $E''_{v''J''}-E''_{v''0}=[J''(J''+1)]/\kappa^2r_0{}^2$ while in the continuum the eigenvalues are independent of J'. We are concerned with the value of the matrix component $F_{v''E'J''J'}$ for a given value of $h\nu=E'_{J'}-E''_{J''}$. Since the two potential energy curves are raised by practically the same amount, the value of $F_{v''E'J''J'}$ is affected only by the slight distortion of the curves and we shall make a very small error if we take it to be independent of J.

The chief effect of this distortion is to shift the minimum of the potential curve very slightly to the right, so that it is under a slightly lower part of the V' curve. For $J=50$ the minimum is shifted by about 4×10^{-3}A and the value of V'' is only about 200 cm^{-1} lower at that point than it is at the minimum for $J=0$. It is readily seen that the effect on the final curves of Fig. 4 is entirely negligible.

VI. Summation Over α', α'' and Final Formula for k_ν

Since α' is in the region of continuous eigenvalues we have a large number $Z_\nu\Delta\nu$ of transitions $\alpha''\rightarrow\alpha'$ of practically equal probability $P_{\alpha''\alpha'}$ in any small region $\Delta\nu$. In our case Z_ν can readily be shown to have the value

$$Z_\nu=h\kappa^2R/2b'\pi. \tag{19}$$

Since $P_{\alpha''\alpha'}$ in Eq. (3) is defined for a single transition per unit frequency range, the summation over α' is equivalent to multiplication by Z_ν. Hence, combining Eqs. (2), (3), (6), (7) and (19) we have

$$k_\nu N=\sum_{v''J''}(8\pi^3\nu/3hc)D^2_{n''n'}(2J''+1)N_{000}F^2_{v''E'J''J'}e^{-E_{v''J''}/kT}\cdot h\kappa^2R/2b'\pi, \tag{20}$$

where the vibrational matrix component, $F_{v''E'J''J'}$ was shown in Part V to be practically independent of J'', when E' is chosen so that $E'-E''=h\nu$. Each of these matrix components contains the square of the normalizing factor $(\pi b'/R)^2$. By writing

$$(\pi b'/R)\mathfrak{F}^2_{v''E'}=F^2_{v''E'J''J'} \tag{21}$$

* See Watson, *Bessel Functions*, p. 385.

Eq. (20) becomes

$$\frac{3c}{4\pi^3\nu_K^2 D^2_{n''n'}} k_\nu N = \sum_{v''J''} \bar{\mathfrak{S}}^2_{v''E'}(2J''+1)N_{000}e^{-E_{v''J''}/kT} = \sum_{v''} \bar{\mathfrak{S}}^2_{v''E'} N_{v''}, \tag{22}$$

where $N_{v''}$ is the number of molecules in the state v''. Writing $(4\pi^3\nu_K^2 D^2_{n''n'}/6hc)\bar{\mathfrak{S}}^2_{v''E'} = k_{v''}$ we obtain an equation equivalent to the Eq. (1) used in Part I to calculate the values of $\epsilon_{v''}$ from the experimental values.

VII. Determination of ω and V_∞' by Comparison with Experiment

The calculation of the hypergeometric function ${}_2F_1$ in (17) is somewhat laborious. For this reason the approximate expression

$${}_2F_1 \cong [1-[(\omega-\mu+2)/2(\omega+1)]x_0]^{-(1-\mu+\omega)/2} \tag{23}$$

was substituted in Eq. (17), and used to obtain provisional values of ω and V_∞'. To do this we calculated the approximate half widths of the function (17) for various values of ω and interpolated graphically to find the value of ω which gave the half width in agreement with experiment. This gave $\omega \cong 150$. Substituting this value in the exact Eq. (17) and evaluating ${}_2F_1$ by actual summation of the series we obtained a half width differing slightly from the correct value. From the amount of this difference we were now able to estimate the value of ω which, substituted in (17), would give the correct half width. In this way we found the value $\omega = 162$, which was used in the final calculations. Substituting now in Eq. (18) for x_0 the value which corresponds to the maximum of (17) and for E_0' the experimental value of the energy at the absorption maximum of ϵ_0 we can solve (18) for V_∞'. This gives $V_\infty' = 3617$ cm^{-1}.

VIII. Calculation of the Matrix Components for the Vibrational States $v'' = 1, 2, 3$

In place of Eq. (15) we have now, from (6), (9) and (13)

$$F_{v''E'01} = \bar{A}_{v''} \int_0^R \rho^{\mu-1} e^{-a\rho} L^\alpha_{v''+\alpha}(2a\rho) J_\omega(b\rho) d\rho \tag{24}$$

where $\bar{A}_{v''}$ is a constant depending on μ, ω and $a(=a_{v''})$. By writing

$$I_p/a^{\mu+p} = \int_0^R \rho^{\mu-1+p} e^{-a\rho} J_\omega(b\rho) d\rho, \tag{25}$$

Eq. (24) becomes (omitting the J quantum numbers)

$$F_{v''E'} = \sum_{p=0}^{p=v''} C_p I_p/a^{\mu+p}, \tag{26}$$

where the C_p are again constants depending on a, μ and ω. The matrix component is therefore a linear aggregate of expressions of the form (17) with $\mu+p$ in place of μ.

We note that

$$(\partial^p/\partial a^p)(I_0/a^\mu) = (-1)^p I_p/a^{\mu+p} \tag{27}$$

and since $x = b^2/a^2$

$$(\partial/\partial a) = -(2x/a)(\partial/\partial x). \tag{28}$$

With the aid of (27) and (28) we can express $F_{v''E'}$ in terms of I_0/a^μ and its differential coefficients with respect to x. Much labor was saved in the numerical calculations by noting that the logarithm of ${}_2F_1$ in (17) is approximately linear in x, and could therefore be expressed with amply sufficient accuracy by the interpolation formula

$$\log {}_2F_1 + 10 = 6.78302 - 12.797\eta - 9.711\eta^2 - 13.02\eta^3, \tag{29}$$

where $\eta = x - 0.3$. The error introduced by the use of (29) is well within the accuracy of the experimental determinations of the absorption coefficients.

Performing the necessary algebra we obtain from (26), (27), (28) and (29) the following formulas for the matrix components.

$$\begin{aligned}
&\text{(a)} \quad v''=0, \quad F_{0E}=B_0,\\
&\text{(b)} \quad v''=1, \quad F_{1E}=B_1Q,\\
&\text{(c)} \quad v''=2, \quad F_{2E}=B_2[2\mu-15-4Q+Q^2+16x^2(dP/dx)]=B_2S,\\
&\text{(d)} \quad v''=3, \quad F_{3E}=B_3[3S(2\mu-1)+(2\mu-3)(2\mu-2)(2\mu-1)-8U],
\end{aligned} \tag{30}$$

where

$$\text{(a)}' \quad B_{v''}=\left(\frac{\pi b'}{R}\right)^{\frac{1}{2}}\frac{2^{\mu-\omega-1}\Gamma(\mu+\omega)}{a_{v''}\Gamma(\omega+1)[\Gamma(2\mu-3+v'')v''!(2\mu-3+2v'')]^{\frac{1}{2}}}x^{\omega/2}(1+x)^{-\mu+\frac{1}{2}}\cdot{}_2F_1,$$

$$\begin{aligned}
&\text{(b)}' \quad P=\omega/2x-[(\mu-\tfrac{1}{2})/(1+x)]+[d\ln F/dx]=d\ln I_0/dx,\\
&\text{(c)}' \quad Q=-3-4xP,\\
&\text{(d)}' \quad R'=(-Q+2\mu+1)/2,\\
&\text{(e)}' \quad U=R''^3+3R''^2-3(\mu^2+\mu/2+9/2)R'+2(\mu+2)+3(\mu+\tfrac{1}{2})(\mu-\tfrac{1}{2})(\mu-1)\\
&\qquad\qquad +12R'(R'+1)x^2(dP/dx)+8x^3(d^2P/dx^2).
\end{aligned} \tag{30}'$$

IX. Comparison of Theory with Experiment

In Eq. (22) there are three constants which may be fixed arbitrarily, *viz.*, $D_{n''n'}$, ω (the order of the Bessel function), and V_∞'. The unknown electric moment, $D_{n''n'}$ appears in all the results as a constant factor. The position of the upper potential curve with respect to the lower and hence the energies of the transitions, are determined by V_∞'. The slope and curvature of the upper potential energy curve, and the width of the curve representing ϵ_0 depend on the value of ω. As explained in paragraph 7, V_∞' was fixed by making the maxima, and ω by making the widths, of the theoretical and experimental ϵ_0 curves coincide. The value of $D_{n''n'}$ was determined by making the actual values of the ordinates of the theoretical and experimental curves coincide at the maximum of ϵ_0. This done, the rest of the calculations proceeded with no further assumptions. Our values of the various constants were

$$\begin{aligned}
&D_{n''n'}=(4.77\times10^{-10})\times(0.016\times10^{-8})\text{ e.s.u. cm.}\\
&\left.\begin{aligned}\beta&=74{,}574.6\\ \gamma&=154{,}292\end{aligned}\right\}\text{in the units to give the potential energy curve in cm}^{-1}\text{ and A.}\\
&\omega=162,\ \mu=281,\ m=279.5,\ V_\infty'=3617\text{ cm}^{-1}.\\
&r_0=1.009\text{A},\ a_0=2.881\times10^{10}\text{ cm}^{-1}.\\
&\left.\begin{aligned}E_0''&=-79{,}517\text{ cm}^{-1}\\ E_1''&=-78{,}951\text{ cm}^{-1}\\ E_2''&=-78{,}391\text{ cm}^{-1}\\ E_3''&=-77{,}837\text{ cm}^{-1}\end{aligned}\right\}\text{given by the formula}\\
&E''_{v''}=-(\kappa^2\gamma^2/4m^2)[v''/m+1]^{-2}.
\end{aligned}$$

We used Birge's[7] values for h, c, etc. The value of $D_{n''n'}$ corresponds to the displacement of one electronic charge through a distance of 0.016A, which seems to be a reasonable result.

The heavy broken curve in Fig. 1, lying just above the upper Morse curve, is the upper

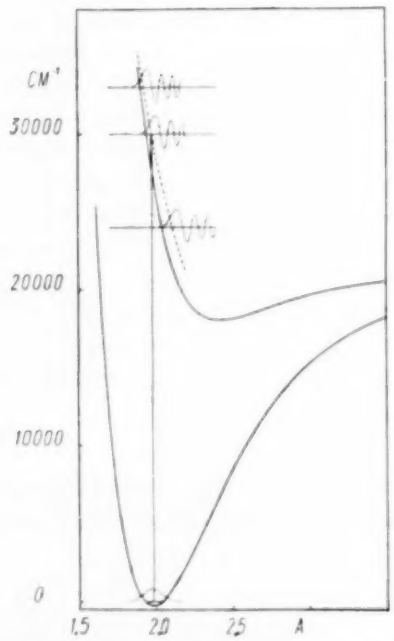

Fig. 1. The heavy continuous curves are the Morse curves for the Cl_2 molecule. The heavy broken curve is our upper potential energy function. The light oscillating curves are the corresponding eigenfunctions and the light dotted curves represent the eigenfunction for $v''=0$.

[7] R. T. Birge, Phys. Rev. Sup. **1**, 1 (1929).

potential curve which was determined by our values of ω and V_∞'. The oscillating curves are three of the corresponding proper functions, $F'_{E'}(r)$, and at each energy we have repeated $F_0''(r)$ (shown dotted). The amount of overlapping of F' and F'' gives one a pictorial representation of the amount of absorption from the level $v''=0$ at different parts of the spectrum. At 24,000 cm^{-1} the overlap is small and ϵ_0 has only 1/100 of its maximum value. At 30,000 cm^{-1}, where the overlap is considerable, ϵ_0 is almost a maximum. At 33,000 cm^{-1} the overlapping is greater still but there is also considerable cancellation because of the negative part of F'. At this point, ϵ_0 has $\frac{1}{2}$ of its maximum value.

The values of the squares of the matrix components for the transitions from the levels $v''=0$, 1, 2 and 3 are drawn in Fig. 2, the vertical

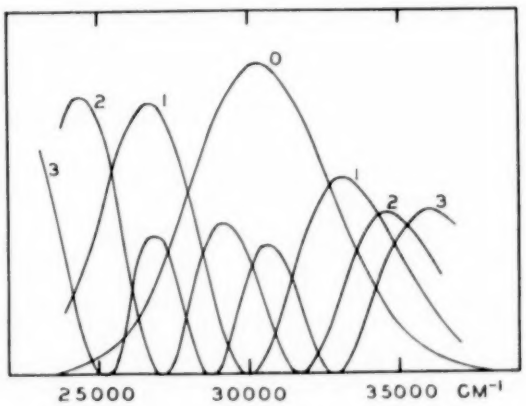

FIG. 2. The squares of the matrix components for transition from the levels $v''=0$, 1, 2 and 3.

scale being arbitrary. In Fig. 3, we have compared the theoretical and experimental values of ϵ_0 and ϵ_1. The check is excellent for ϵ_0 and less good for ϵ_1 but it must be remembered that the experimental values of ϵ_1 were very rough.

A better comparison of the theory with the experimental data is given in Fig. 4. The curves are the theoretical values of ϵ at our extreme temperatures, 291 and 1038°K, calculated by means of Eq. (22), by using the theoretical values of the absorption from the first four vibrational levels of the normal state of the molecule. The points are the experimental values taken from Table I of Part I. The check at 291°K is excellent.

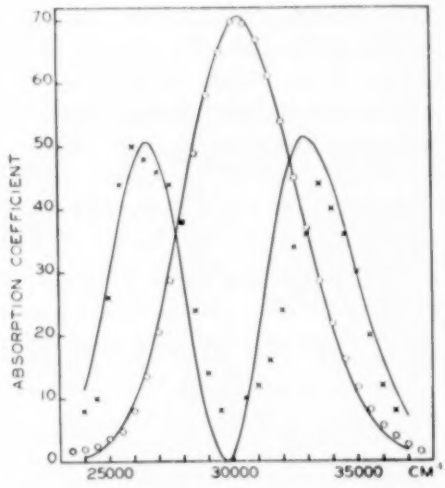

FIG. 3. A comparison of the experimental (points) and theoretical (curves) values of ϵ_0 and ϵ_1. The circles are the experimental values of ϵ_0, and the crosses those of ϵ_1, taken from Table II of Part I.

In discussing the check at 1038°K, it should be borne in mind that only the first four vibrational levels were used, leaving five percent of the molecules unaccounted for. One would therefore expect that the theoretical curve would be a few percent too low.

In a recent paper Stueckelberg[8] has calculated the continuous absorption curve of O_2, by a method which is in principle the same as ours. He uses the Hermitic eigenfunctions (simple

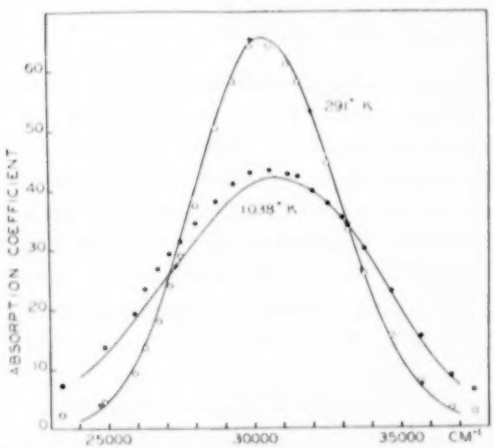

FIG. 4. A comparison of the experimental and theoretical values of the absorption coefficient of Cl_2 at the extreme experimental temperatures. The curves are theoretical; the circles, our experimental result from Table I of Part I, and the crosses are the results of Halban and Siedentopf at room temperature.

[8] E. C. G. Stueckelberg, Phys. Rev. **42**, 522 (1932).

harmonic oscillator) for the lower state and the Kramers approximations for the eigenfunctions of the upper state, which involves the approximation that the potential energy curve for the upper state is linear over the important range of r. There is an error in his calculation of the rotational effect: His Eq. (13) on page 522 should not contain the temperature factor. The author informs us that he is publishing a correction.

X. Validity of the Franck-Condon Principle

Our determination of the upper potential energy curve enables one to see how closely the classical Franck-Condon principle is obeyed. The heavy vertical line in Fig. 1 represents the most probable transition, according to this principle, from the level $v''=0$. The point at which it cuts the upper potential curve should give the energy of the maximum of ϵ_0. It cuts the Morse curve at 27,500 cm^{-1}, and our potential curve at 30,000 cm^{-1}, the actual maximum of ϵ_0 being at 30,300 cm^{-1}. Assuming our potential function to be the correct one, it is seen that the Franck-Condon principle is in error by only 300 cm^{-1}, which is a surprising result when one considers the broad maxima of the upper and lower proper functions and the nature of the integration.

XI. An Alternative Form of $V''(r)$

In the preceding calculations we have assumed the validity of the Morse formula for the lower potential energy V''. This assumption is certainly a good approximation to the truth in the region of our calculations. It seemed desirable, however, to investigate the effect of a slight change in the form of the lower potential energy curve. For this purpose we assumed the eigenfunction to be of the form

$$\psi_0'' = \rho^m e^{-a^2\rho^2}. \tag{31}$$

It is then easy to find the form of V'' which substituted in the Schroedinger equation will give Eq. (31) as a solution. We find

$$V'' = \beta/\rho^2 + \gamma\rho^2 \tag{32}$$

with $\kappa^2\beta = m(m-1)$ and $\kappa^2\gamma = 4a^4$ so that the Schroedinger equation is

$$d^2\psi/d\rho^2 + \kappa^2(E'' - \beta/\rho^2 - \gamma\rho^2)\psi = 0. \tag{33}$$

The potential energy curve (32) is more symmetrical than the Morse curve.

The eigenvalues of (33) are given by

$$\kappa^2 E''_{v''} = 2a^2(2m+1+2v''), \tag{34}$$

$E''_{v''}$ being referred to a different zero from that of the previous case.

It is interesting to note that the energies are equally spaced like those of the simple harmonic oscillator.

The eigenfunctions are given by

$$\psi''_{v''} = \rho^m e^{-a^2\rho^2} \Lambda_{v''}(\rho^2), \tag{35}$$

where $\Lambda_{v''}(\rho^2)$ is a polynomial of degree v'' in $\rho^2 = (r-r_0)^2$.

We have not troubled to find the general form of $\psi''_{v''}$, but have calculated the absorption coefficient for $v''=0$.

The matrix component

$$F_{0E} = \int \rho^{m+\frac{1}{2}} e^{-a^2\rho^2} J_\omega(b\rho) d\rho \tag{36}$$

can also be expressed in terms of a hypergeometric function (Watson, p. 393) which, however, does not converge rapidly enough to make the calculation feasible in the case of chlorine. We therefore evaluated the integral (36), by a method (summation of ordinates) equivalent to graphical integration. We shall omit the details of the calculation and merely mention that the experimental results for the absorption from $v''=0$ are given equally well by the new formula for $V''(\rho)$. The only effect of the change is to raise the curve for $V'(\rho)$ in Fig. 1 by about 600 cm^{-1} relative to the minimum of $V''(\rho)$.

The Franck-Condon principle thus gives a value lying midway between the values obtained from the two formulas for $V''(\rho)$.

The Application of the FP-54 Pliotron to Atomic Disintegration-Studies

L. R. HAFSTAD, *Department of Research in Terrestrial Magnetism, Carnegie Institution of Washington, and Johns Hopkins University*

(Received May 8, 1933)

The possibility of utilizing the high inherent sensitivity of the FP-54 Pliotron in nuclear disintegration-studies, particularly in connection with the problem presented by the discrepancies in present experimental results on resonance-disintegration of aluminum, has been investigated. The usable sensitivity of the tube is found to be limited only by a residual fluctuation of about $\pm 3\times 10^{-5}$ root-mean square volt. A theoretical consideration shows that this fluctuation is of the order of magnitude to be expected from shot-effects and thermal effects in the grid-circuit.

Disintegration-Experiments on Aluminum.—Preliminary observations on the disintegration of aluminum when using a thick target gave the following results. The yield was about 20 protons, of ranges between 30 and 50 cm per 10^8 α-particles, in good agreement with the results of Pose. Groups with ranges of about 30 cm and 60 cm were found to show the abrupt drop in the absorption-curve characteristic of Pose's results. (The present series of observations failed for purely technical reasons to give a conclusive result in the range 45 to 50 cm.) A "differential" curve neglecting the smallest deflections gave a maximum in the region 45 to 50 cm, suggesting the presence of a strong group of about this range. A discussion of other discrepancies in experimental data on the basis of FP-54 results must await further observations with a more suitable α-particle source.

INTRODUCTION

QUANTUM-MECHANICS as applied to the nucleus by Gurney and Condon[1] and by Gamow[2] has successfully accounted for the principal features of nuclear phenomena such as radioactive decay and the Geiger-Nuttall relation. To explain these effects it is only necessary to assume a potential barrier (U_r) surrounding the nucleus and compute by means of Schroedinger's equation the relative amplitude of the ψ-waves as a function of r. Since the probability of finding a particle at any point is, according to wave mechanics, proportional to the square of the amplitude of the ψ-wave at that point, this may be interpreted for the case of many nuclei as representing a large number of α-particles within the barrier with a few particles moving out through the barrier in numbers and with energies depending on the size and shape of the potential barrier. The form of the barrier, that is of U_r, for actual nuclei is given sufficiently well by observations on the scattering of α-particles for the above theory to give results in good agreement with experiment when applied to such nuclei.

By a slight extension of the above ideas the case of a nucleus bombarded by α-particles, that is, ψ-waves, incident on the potential barrier can be considered. It is found that the wave is partly transmitted and partly reflected and, as above, the probability of penetration of the barrier by an α-particle may be obtained from the relative amplitudes of the transmitted and reflected ψ-waves. However, because of the form of the solution within the barrier, two cases arise, each equally valid. In the ordinary case the reflected wave is large, giving a small probability of penetration and a correspondingly small yield of disintegration-protons. In the other case, which arises when the energy of the incident α-particle is nearly equal to that of one of the eigen values of the nucleus, the reflected wave is very small. Hence most of the impinging α-particles must penetrate the barrier, giving a yield of disintegration-protons far in excess of that produced by α-particles of other energies. This is the case of resonance-disintegration pointed out by Gurney.[3]

Experimental evidence which seemed to prove the reality of this effect was first obtained by Pose.[4] By bombarding an aluminum target with a heterogeneous beam of α-particles and by using a Hoffmann electrometer to detect the disinte-

[1] Gurney and Condon, Nature **127**, 439 (1928).
[2] Gamow, Zeits. f. Physik **51**, 204 (1938).
[3] Gurney, Nature **128**, 565 (1929).
[4] Pose, Zeits. f. Physik **64**, 1 (1930).

gration-protons, an absorption-curve was obtained which showed the presence of several groups of protons with definite ranges. By varying the ranges of the incident α-particles, it was possible to show that two of these groups were produced only by α-particles of definite ranges in agreement with the theory outlined above. However, Meitner,[5] de Broglie and Leprince-Ringuet,[6] and Chadwick and Constable and Pollard[7] in repeating this work, using other methods, failed to observe resonance. Consequently, considerable doubt was thrown on Pose's work and his results have been to a large extent ignored.[8] Recently Chadwick and Constable[9] have found indications of resonance but with energy-values differing from Pose. Steudel,[10] on the other hand, obtained evidence on the basis of which he denies the existence of resonance, while Diebner[11] working under Pose checked Pose's work in every detail.

Development of Apparatus

Up to the present time the three instruments which have been used in this work, namely, the point-counter, the linear amplifier, and the Hoffmann electrometer, have been the only ones with a sensitivity great enough to detect individual disintegration-protons. The possibilities of each of these methods have been fairly well covered by the above investigations, so that observations by an entirely independent method seems the most likely to lead to an explanation of the discrepancies. The possibility of developing such new instrument was suggested by the announcement of the FP-54 Pliotron, as a comparison of the constants in Table I will indicate. However, with the usual circuit nothing even approaching the sensitivity implied by the above constants can be obtained over the extended periods of observation required in disintegration-experiments. The single-tube circuit, for instance, was originally recommended only for currents greater than 10^{-14} ampere and the two-tube balanced circuit gives full sensitivity only for a few minutes immediately after opening the key. It was evident that radical changes in operating conditions were needed to adapt the Pliotron to the stringent requirements of artificial disintegration-studies.

Table I. *Comparison of Hoffmann duant and FP-54 Pliotron.*

	Hoffmann duant	FP-54 galvanometer
Capacity	3 cm	3 cm
Voltage-sensitivity	20,000 mm/v	250,000 mm/v
Period	30 sec.	5 sec.

The single-tube circuit as used by DuBridge,[12] shown in Fig. 1 was chosen for study since its

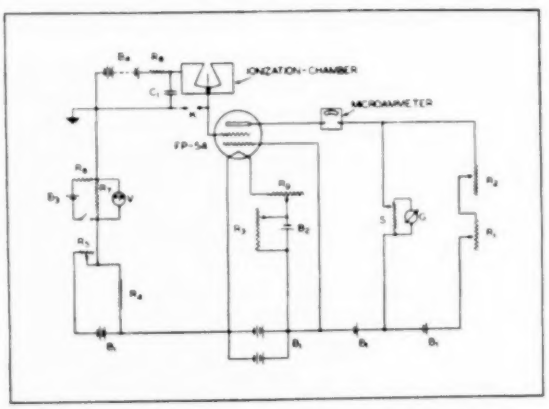

Fig. 1. Single-tube circuit used by DuBridge.

sensitivity is inherently twice that of the balanced circuit. The most serious limitations of the original single-tube circuit were the erratic drifts (closed key) attributed to batteries, and the short-period fluctuations (open key) due to unknown causes.

It was found that the closed-key drifts were primarily due to two things. The first cause was the erratic voltage-change in the batteries due to major readjustments of the circuit being made at intervals less than the time required for the batteries to reach equilibrium. This was overcome by running the tube continuously so that only

[5] Meitner, Phys. Zeits. **32**, 661 (1931).

[6] M. de Broglie et L. Leprince-Ringuet, C.-R. Acad. sci. **193**, 132 (1931).

[7] Chadwick, Constable and Pollard, Proc. Roy. Soc. **A130**, 463 (1931).

[8] Hoffmann, Zeits. f. Physik **73**, 578 (1932).

[9] Chadwick and Constable, Proc. Roy. Soc. **A135**, 48 (1932).

[10] Steudel, Zeits. f. Physik **77**, 139 (1932).

[11] Diebner, Zeits. f. Physik **75**, 753 (1932).

[12] DuBridge, Phys. Rev. **37**, 392 (1931); see also Ortner und Stetter, Zeits. f. Physik **54**, 468 (1929); Rasmussen, Ann. d. Physik **2**, 357 (1929).

minor readjustments were necessary after the first day. As it was found possible to run the tube for two months on a single battery-charge, continuous operation introduces no serious inconvenience. In fact, the fluctuations appear to decrease continuously for the first week. The second cause for closed-key drift was the variation in battery-voltage with room-temperature. This effect was eliminated by placing the apparatus in a constant-temperature room. It was then found that the drifts could be sufficiently reduced to permit preliminary observations of the short-period fluctuations (open key) to be made.

In order to take full advantage of the high input-resistance of the FP-54 tube, attempts were first made to operate the tube with the grid floating at its rated voltage, the open-key drift being compensated by balancing out the grid-current. Though this method had been used by Loveridge[13] at low sensitivities, the method failed because of the usual polarization-effects of the resistances in this work where the highest possible sensitivity is required.

Efforts were then transferred to the operation of the tube with the grid floating at its equilibrium-potential.* The input-impedance of the tube in this condition was considerably reduced, but this disadvantage was offset by the great gain in stability, the rate of drift being exactly the same with the key open as with the key closed. It was immediately evident that the expected residual ionization in the air about the tube was producing very large fluctuations. These were eliminated by evacuation of the case surrounding the tube.

Observations were next made by recording photographically the remaining fluctuations in order to determine the limits set by discontinuous emission, etc., in the tube itself. It appeared that sensitivities comparable to those of the two-tube balanced set could be obtained by this method. The above observations were repeated by Dr. Loveridge and the conclusions as to the limiting sensitivities checked by many measurements with different tubes and batteries and with altered operating conditions. The final conclusions reached, based on evidence then available, were communicated to Dr. Hull in connection with the symposium on electronic devices at Cambridge and were published by him in *Physics*.[14]

On the basis of these results, the writer attempted the photographic registration of pulses due to disintegration-protons in a manner similar to that used by Pose. This work requiring continuous runs of many consecutive hours, it was soon learned that the low drift-rates in the earlier work were of a temporary nature only, and that after the first several hours the rate of drift at a sensitivity of 50,000 mm per volt was always about 30 cm per hour in the direction of decreasing current. This represented a change in plate-current of 3 microamperes per week and corresponded roughly to that which would be expected because of the running down of the filament-batteries. To test this hypothesis a countercell—B_2 in Fig. 1—was inserted in the filament-circuit and a resistance across it so adjusted that the electromotive force of the countercell dropped at a rate just sufficient to keep the plate-current constant, as indicated by zero-drift of the galvanometer.[15] It was then found that the filament-voltage instead of remaining constant was gradually increasing, thus indicating that an appreciable part of the drift was due to a deactivation of the filament. This is an effect which cannot be compensated for in the usual bridge-circuits, so that the countercell-method of drift-compensation has distinct advantages when highest sensitivities are required.

Details of Apparatus

In Fig. 1 the batteries marked B_1 are ordinary lead-cells of about 100 ampere-hour capacity. New batteries were used, for it has been found that they are usually free from the spasmodic voltage-changes which are often, though erroneously,[16] attributed to "bubbling" of the batteries. The battery B_3 is a 1.5-volt dry-cell, while B_4 is a 144-volt Burgess *PL* battery. For the countercell, the battery B_2 in the figure, an Edison cell of 75 ampere-hours with a load-resistance of about 20 ohms was finally used. This cell is particularly

[13] Loveridge, *Dissertation*, University of California.

* I am indebted to Dr. A. E. Ruark for emphasizing the advantages of this method.

[14] Hull, Physics **2**, 409 (1932).

[15] Hafstad, Phys. Rev. **40**, 1044 (1932).

[16] Jaeger and Kussmann, Phys. Zeits. **28**, 645 (1927).

suitable for this purpose, for its discharge-curve (voltage *vs.* ampere-hours) is somewhat steeper than that for a lead-cell, so that a given rate of change of voltage can be maintained with a small drain on the battery.

A dry-cell has an even steeper discharge-characteristic, but cannot be used in the filament-circuit because of the relatively large currents flowing. It is very convenient, however, to compensate for the drift by using a dry-cell loaded with 20 to 30 ohms to balance out the plate-current in the galvanometer-circuit. In this case, the rate of fall of potential of the dry-cell can be adjusted so that the balancing current is always equal to the gradually falling plate-current and the galvanometer-drift is nil. While this method is satisfactory for most purposes, there is a gradual change in sensitivity corresponding to the gradual change in plate-current, so that when constant sensitivity over periods of weeks is desired the filament-circuit compensation has decided advantages.

The resistances R_1 and R_5 in the figure are General Radio decade-boxes (1 to 10,000 ohms) and were chosen in the original design to reduce contact-troubles. No trouble has been experienced from this cause, however, and any good variable resistance, such as the General Radio 371-A, should be satisfactory. In case the decade-boxes are used, it is advisable to mount them on insulating supports, as the insulation provided is not sufficient to prevent leakage-currents from affecting a sensitive galvanometer. The resistances R_2 and R_4 are General Radio units, type 510, giving 10,000 to 100,000 ohms, in steps of 10,000 ohms. These were used in order to give great flexibility while studying the circuit. R_3 and R_9 are ordinary filament-rheostats, while R_6 and R_7 are fixed resistors chosen to give a reading of about one millivolt on the meter when the key is closed. $R_8(50\times10^6$ ohms) and $C_1(4\times10^{-6}f)$ form a filter to reduce fluctuations in B_4. The galvanometer is a Leeds and Northrup type R of sensitivity 2600 megohms, with a period of about 10 seconds.

The ionization-chamber is of copper, made with a conical hole to reduce the volume and with a rounded end to permit each particle which enters to produce ionization along exactly 1.5 cm of path. No special treatment was found which would reduce the number of residual counts of the chamber below that obtained by cleaning with steel wool and mounting in place in the apparatus in a stream of commercial CO_2 with as little exposure to air as possible. The lowest residual-count obtained of pulses greater than 4000 ions was 0.5 particle per hour. This corresponds to about 6 particles per 100 sq. cm of exposed surface per hour, and is in good agreement with the value given by Ziegert[17] for clean copper.

The details of the mounting for the ionization-chamber and electrometer may be seen in Fig. 2. In the early stages of the investigation when frequent changes were necessary, all seals were made with ordinary soft red universal wax. This proved a great convenience, for no heating was necessary. Slow leaks were prone to develop, however, so picein was finally used and it was then found possible to hold a vacuum of less than one millimeter for over a month. By test it was found that pressures up to 2 or 3 millimeters gave no fluctuations due to residual ionization.

The lead for the collecting potential shown to the right of the tube in the figure is in reality behind the tube, that is, rotated through 90° into the paper, so as to avoid interfering with the grounding-key. A similar conductor was brought into the case on the opposite side of the tube to provide a connection for a grid-leak which, when used, was mounted on a key similar to but opposite the grounding-key. The high resistance leaks used were from 10^{10} to 10^{12} ohms and were purchased from the S. S. White Dental Supply Company, 152 West 49th Street, New York, N. Y. The thin foils used for the target and for the absorbers were obtained from the American Platinum Works, Newark, N. J. Information as to the stopping power of different metals was taken from Meyer-Schweidler, *Radioaktivität*, page 103.

Study of the Limits of Sensitivity Set by Residual Fluctuations

Before using the FP-54 under these conditions for recording pulses it was thought advisable to investigate its possibilities and limitations as a current-measuring device. Since by the counter-

[17] Ziegert, Zeits. f. Physik **46**, 677 (1928).

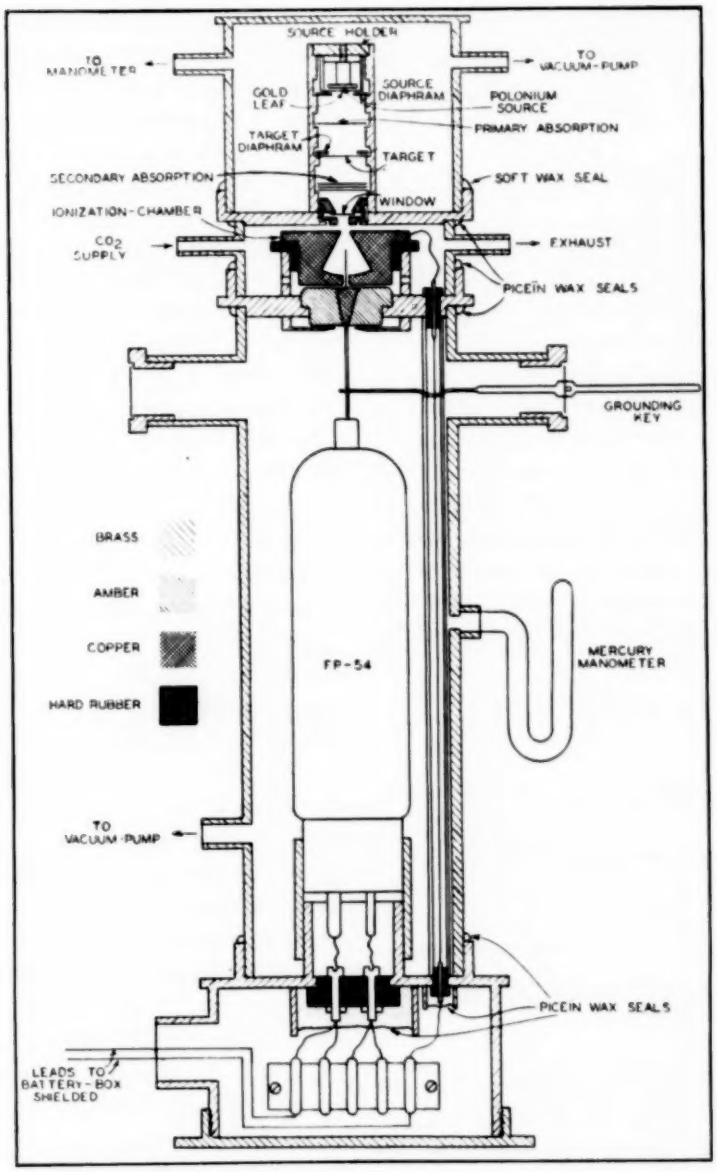

FIG. 2. Ionization-chamber and electrometer-mounting.

cell-method the plate-current may be made to increase or decrease at will, it is possible (with reasonable care and patience) to reduce the drift to any required degree. Furthermore, it has always been found that the fluctuations with the key open are greater than with the key closed, as shown by the two traces in Fig. 3. So long as this is true the fluctuations due to the batteries are smaller than those due to other causes and may be neglected insofar as limiting sensitivity is concerned.

The residual fluctuations might be attributed to any one of a multitude of causes, and a great deal of effort was spent in trying to eliminate them. Different tubes and different mountings in two completely independent sets of apparatus, one of Johns Hopkins University and one at the Department of Terrestrial Magnetism, however, gave approximately the same final value of the residual fluctuations. Most of the possible explanations of these fluctuations, such as mechanical vibration, stray electric or magnetic

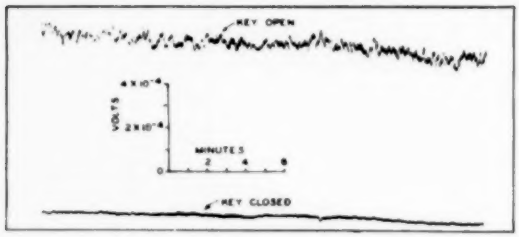

FIG. 3. Record showing fluctuations key open and key closed.

fields, charges on exposed insulators, etc., having been eliminated by direct tests, shot-effects or thermal effects seemed the only possible means of explanation. To check this possibility, traces were taken at a sensitivity of 250,000 millimeters per volt with the tube isolated in vacuum, that is, with no connection whatever to the grid. A short section of a representative trace is shown in Fig. 4. In justice to the tube it must be empha-

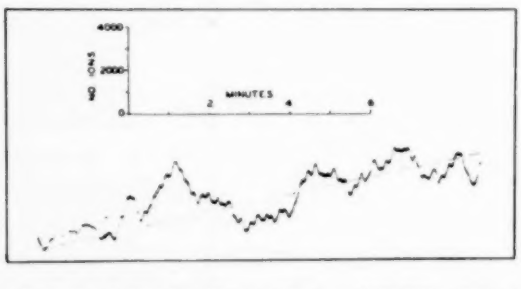

FIG. 4. Record showing fluctuations at 250,000 millimeters per volt.

sized that this ragged trace was obtained at the extreme charge-sensitivity of 80 electrons per millimeter, since the capacity is 3 cm, or for convenience of comparing with other claims, a current-sensitivity of 4×10^{-20} ampere per millimeter, since the input-resistance is about 10^{14} ohms.

The proper way of obtaining the mean-square deviation $\overline{\sigma^2}$ for this curve would be to obtain $(1/T)\int_0^T S^2 dt$ for this curve, where S is the deflection from the mean after correcting for the remaining drift.[18] A sufficiently good approximation for our purpose (order of magnitude only) may be obtained by scaling ordinates, measured from an arbitrary "mean" line at frequent intervals giving $(1/N)\Sigma^N{}_{K=1}S^2{}_K=\overline{\sigma^2}$. In the present case, ordinates were taken at 30-second intervals for a period of 40 minutes, giving $\overline{\sigma^2}=60$ mm, or a root-mean-square (r.m.s.) fluctuation of $\sigma=\pm8$ mm $\leqq\pm3\times10^{-5}$ volt. This then is the experimentally determined value of the standard deviation to be compared with that predicted from theory on various possible hypotheses.

The usual formulas for shot-effect[19] and Johnson effect[20] give values which suggest that while the fluctuations might well be due to either shot-effect or Johnson effect in the grid-circuit, the disagreements in numerical values indicate that the ordinary formulas were used improperly, as will be clear from a discussion given below.

It occurred to the writer that an independent estimate of the magnitude of the shot-effect could be obtained in the following way. With the grid floating at its equilibrium-potential, it is known that the grid-current, which is zero by definition, is really composed of two components[21] equal in magnitude but opposite in sign. For the FP-54 each of these is about 10^{-15} ampere,[14] so that on the average a certain number of ions, say N, of each sign reach the grid every second. As this number varies due to shot-effect, there will be corresponding changes in the potential of the grid and consequently a similar variation in the plate-current as indicated by the galvanometer. The problem may be stated as follows. Suppose the grid to be the insulated electrode of an electrometer of sensitivity S mm/volt, with a capacity C, a negligible leak, and negligible period. What will be the root-mean-square deviation of the indicator from its mean position over any arbitrary length of time t?

This problem is identical with that raised by Von Schweidler's theory of the fluctuations in α-particle ionization with two identical sources, and has been treated at length by Campbell[22] and Kohlrausch.[23]

For the case assumed

$$\sigma=a(2Nt)^{\frac{1}{2}},$$

[18] Campbell, Cambridge, Proc. Phil. Soc. **15**, 126 (1910).

[19] Williams and Vincent, Phys. Rev. **28**, 1250 (1926).
[20] Johnson, Phys. Rev. **32**, 97 (1928).
[21] Nottingham, J. Frank. Inst. **209**, 287 (1930).
[22] Campbell, Cambridge, Proc. Phil. Soc. **15**, 521 (1910).
[23] Kohlrauch, Ergebn. Exakt. Natw. **5**, 192 (1926).

where σ = root-mean-square deviation and a = deflection of electrometer per electron. It is seen from this formula that σ increases indefinitely with t, as it should in the absence of leakage.

However, insulation-leakage and all other effects which tend to decrease the deflections with a velocity proportional to the deflection may be taken into account by imposing the additional condition that

$$ds/dt = -\beta s,$$

where s is the deflection.

If the question is then asked, what is the probability (w) of finding the galvanometer-spot between some deflection s and $s+ds$ at the time t, the equation

$$\partial w/\partial t = a^2 N(\partial^2 w/\partial s^2) + \beta(\partial(S \cdot w)/\partial s)$$

is finally obtained. This, however, is an equation which was solved by Smoluchowski[24] in a study of the Brownian movement of a particle in a viscous medium bound to its equilibrium-position by elastic forces.

The solution is

$$w(s_0, s, t)ds = \left[\frac{2\pi a^2 N}{\beta}(1-e^{-2\beta t})\right]^{-\frac{1}{2}} \exp\left[-\frac{(s-s_0 e^{-\beta t})^2}{(2a^2N/\beta)(1-e^{-2\beta t})}\right]ds,$$

where s_0 is the mean deflection. From this equation the deviation from the mean may be obtained and can be shown to be $\sigma^2 = a^2NRC(1-e^{-2t/RC})$ for our case where essentially $\beta = 1/RC$. When t is large this reduces to

$$\sigma^2 = a^2NRC = (e^2NR/C)S^2,$$

whence $\sigma = \pm 18$ mm $\leqq \pm 7\times10^{-5}$ volt.

On the basis of this result, we are led to believe that the residual fluctuation is caused by shot-effect in the grid-circuit, and it becomes of interest to consider more closely the failure of the ordinary formulas to give a correct answer in this case. Reference to the original sources shows that the ordinary formulas were derived for the general case of a tuned circuit containing both L and C, and which therefore responds only to a narrow band of frequencies in such a way that the input-impedance may be assumed constant over the band. In the present case, the variation of the input-impedance with frequency must be taken into account.*

The input-circuit may be considered as a resistance R and a capacity C in parallel. Following Schottky,[25] the grid-current may be expressed as

$$i = \sum_{k=0}^{\infty} B_k \sin(\omega_k t + \varphi_k),$$

where $\overline{B_k^2} = 4ie/T$ and where T is the time of the observation.

For the above combination of resistance and capacity in parallel, the conductance is $1/R$ and the susceptance is ωC, so that the impedance will be given by

$$Z = [R^2/(1+\omega^2C^2R^2)]^{\frac{1}{2}},$$

hence the voltage across the impedance due to a current i will be $v = iZ$ and

$$\overline{v_s^2} = \overline{i^2}R^2/(1+\omega^2C^2R^2)$$

$$= \sum_{k=0}^{\infty} \overline{B_k^2}\,\overline{\sin^2(\omega_k t+\varphi_k)}R^2/(1+\omega^2R^2C^2).$$

Then since $\omega_k = (2\pi/T)k$, $\Delta\omega_k = 2\pi/T = d\omega$ (when $\Delta\omega$ is sufficiently small), and the summation may be expressed as

$$\overline{v_s^2} = (4ei/T)(1/2\pi)\int_0^{2\pi} \sin^2(\omega t+\varphi)d\omega \int_0 [R^2/(1+\omega^2C^2R^2)]d\omega/\Delta\omega = eiR/2C.$$

* We are indebted to Dr. G. Breit for the derivations which follow.

[24] Smoluchowski, Ann. d. Physik **48**, 1105 (1915).

[25] Schottky, Ann. d. Physik **68**, 157 (1922).

Returning to the actual case, we have two currents statistically independent, hence

$$\overline{v_s^2}=\overline{v_{s1}^2}+\overline{v_{s2}^2}=eiR/C=e^2NR/C$$

in agreement with the previous calculation. This then is the proper formula for calculating shot-effect under the specified conditions.

Turning to the thermal effect, Nyquist[26] has calculated that the square of the voltage across a resistance R_v, at the temperature T, contributed by a frequency-interval dv is

$$\overline{v_T^2}(v)dv=4R_vkTdv=4R_vkT(d\omega/2\pi),$$

where k is Boltzmann's constant. For the grid-circuit as assumed above, the complex impedance is

$$z=R/(1+j\omega CR)=R(1-j\omega C)/(1+\omega^2C^2R^2)$$

and the real part of this is

$$R_v=R/(1+\omega^2C^2R^2).$$

Since the indicator (the galvanometer in this case) will respond to frequencies higher than the circuit itself, the observed fluctuations will be due to a summation of all frequencies permitted by the circuit; hence

$$\overline{v_j^2}=\int_0^\infty v_T^2(v)dv$$

$$=(2kT/\pi)\int_0^\infty[R/(1+\omega^2C^2R^2)]d\omega=kT/C.$$

Whence for the actual case $v_j=\pm3\times10^{-5}$ volt and $\sigma=\pm8$ mm.

A comparison of the values of fluctuation calculated by means of these new formulas with the observed fluctuation is given in Table II.

TABLE II.

Fluctuation	Volt	σ (mm)
Observed	3×10^{-5}	8
Computed, $v_s=(eiR/C)^{\frac{1}{2}}$	7×10^{-5}	18
Computed, $v_j=(kT/C)^{\frac{1}{2}}$	3×10^{-5}	8

From this comparison, the writer believes that there is sufficient evidence for attributing the residual fluctuations to either shot-effect or Johnson effect, or both, and that the limiting sensitivity for the present tube has been attained.

It is important to note that the formula for the Johnson effect is independent of the resistance and applies to the Hoffmann electrometer as well as to the FP-54. Since in any case the accuracy of a measurement is given by the ratio of the mean deflection to the fluctuation it is possible from the above formulas to determine the direction which further efforts to increase sensitivity must take. For steady deflection methods it appears from this ratio that there can be no gain in a further reduction in C contrary to reports in the literature. For rate-of-charge methods however the accuracy increases with $C^{-\frac{1}{2}}$. Vacuum-tube circuits and designs offer new possibilities in this direction.

CURRENT-MEASUREMENTS

For the measurement of moderately small currents it has been customary to use an input-resistance of the order of 10^{10} ohms. The stability of the present circuit has made it possible to use a resistance of 10^{12} ohms with a corresponding increase in sensitivity. It has always been found that in this case as well as in the case of the floating grid, the fluctuations are greater with the key open than with the key closed. Traces showing this effect are given in Fig. 5, the upper

FIG. 5. Record showing fluctuations with resistance in circuit.

trace being taken with the key closed while the lower was taken with the key open. The sensitivity attainable in this way reaches the maximum which is useful in measuring ionization-currents produced by x-rays, β-rays, etc., since in such cases the unit of charge is really about 300ϵ (the average charge produced by a single particle) and the natural fluctuations are correspondingly large. The possibilities and limitations of the

[26] Nyquist, Phys. Rev. **32**, 110 (1928).

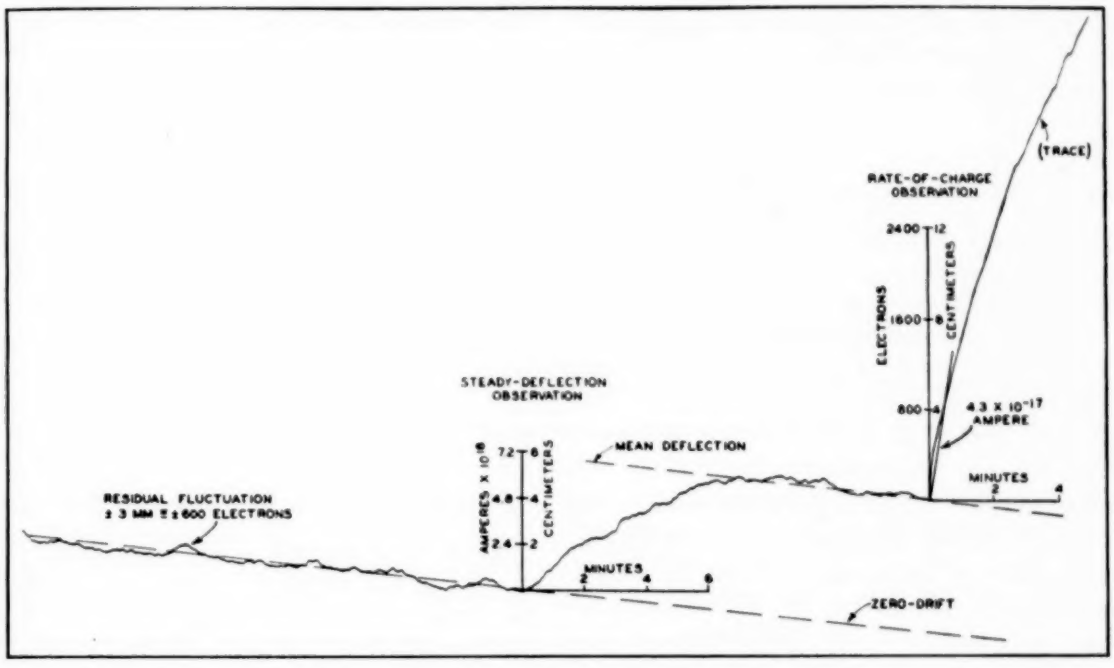

FIG. 6. Record showing deflection due to small steady current.

FP-54 for such measurements have been investigated by Bearden.[27]

In the case of photoelectric currents, however, the fluctuations depend only on ϵ and much higher sensitivities such as may be obtained with a floating grid are useful.

With the magnitude of the residual fluctuations known, it becomes possible to specify the smallest steady currents which can be measured. If we take as the criterion for detection a displacement of the mean equal to the observed root-mean-square deviation, then for the case shown in Fig. 4, $R=10^{14}$ ohms, $C=3$ cm, and $V=250{,}000$ v/mm, a current of 3×10^{-19} ampere or 2 electrons per second could be detected. The time-constant of the grid-circuit being 300 seconds, such a current could be detected in a time of several minutes. This may be taken as the practical limit of the present tube as set by the fluctuations themselves.

As an example of a small current-measurement, an observation was made by producing a current in the "evacuated" space surrounding the tube by gamma-ray ionization at an ordinary recording-sensitivity, no effort being made to attain maximum sensitivity. The resulting trace is shown in Fig. 6. In this case $C\cong3\mu\mu f$ and $R\cong10^{14}$ ohms from the time-constant for the curve and the voltage-sensitivity was 85,000 mm/volt. As calculated from these constants, the current-sensitivity and the charge-sensitivity are 1.2×10^{-19} ampere/mm and 200 electrons/mm, respectively. Two measurements are shown, one using a steady-deflection (galvanometer) observation and the other a rate-of-charge (electrometer) observation. In the first case, the deflection of 6 cm represents a current of 7.2×10^{-18} ampere or 45 electrons per second. The fluctuations are roughly ±3 mm so that this current may be measured to ±5 percent in a time of several minutes. It is significant that the

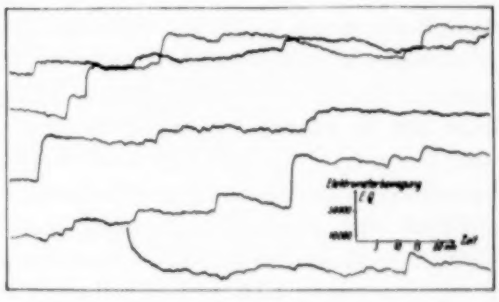

FIG. 7. Specimen record by duant electrometer (after Pose).

[27] Bearden, in preparation.

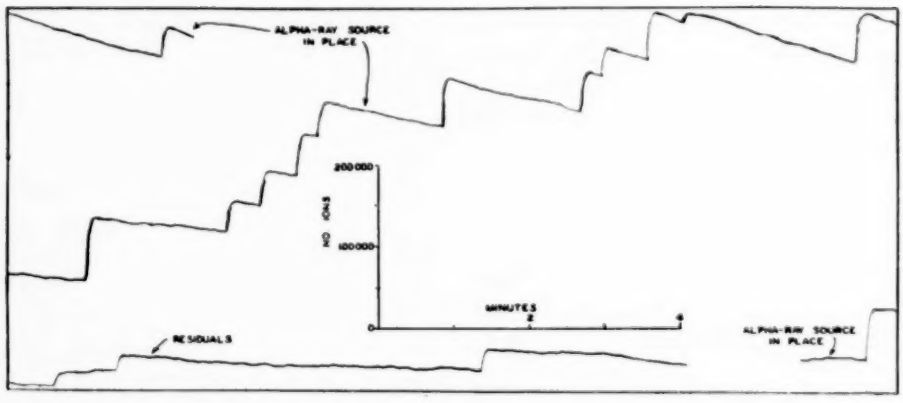

FIG. 8. Record showing alpha-particle deflections by FP-54.

fluctuations of ± 3 mm $\cong \pm 600$ electrons in this trace taken April 2, 1933, are the same as those in Fig. 4 taken on September 5, 1932, for this is independent evidence that the fluctuations represent an absolute limit independent of the state of the batteries, etc., and in agreement with the value predicted from theory.

In view of the above discussion, it might be questioned as to whether it is ever permissible to use the FP-54 as an electrometer for rate of deflection-observation. This obviously is entirely a question of the time-constants involved.

In general, for an electrometer used with a leak the deflection s at any time t will be

$$s = s_f(1 - \epsilon^{-t/RC}),$$

where s_f is the final deflection. This reduces to

$$s = (s_f/RC)t$$

when t is very much smaller than RC, that is, the deflection is strictly proportional to the time, and electrometer-methods may be used, so long as this condition is satisfied. The second measurement in Fig. 6 shows an observation of this kind. The deflection of 41 mm in 30 seconds represents a current of 4.3×10^{-17} ampere, while the magnitude of the fluctuations gives the accuracy as about 7 percent.

An immediate measure of the effectiveness of the FP-54 for pulse-measurements may be obtained by a direct comparison of traces secured with this instrument with those obtained by Pose using the Hoffmann electrometer (Figs. 7 and 8).

PREPARATION OF RADIOACTIVE SOURCE

Until very recently there has been little interest in the preparation of strong α-particle sources in this country and as a result both the highly specialized technique of their production and the material from which they might be prepared are largely confined to European laboratories. Because of this situation a really suitable source comparable in strength and purity to those used in Europe has not as yet been obtained, and it has been necessary to begin observations with such sources as it was possible to prepare with imperfect technique from a limited amount of material.

The writer was particularly fortunate in obtaining a considerable quantity of dead radon-bulbs from various hospitals,* from which sufficiently strong polonium sources for preliminary measurements could be obtained. Such bulbs are originally filled with radon and used for clinical

* The present work, as well as the program of nuclear disintegration-studies, when using radioactive sources, undertaken by the Department of Terrestrial Magnetism of the Carnegie Institution of Washington, was made possible only by the generous cooperation of the following individuals and institutions, for which grateful acknowledgment is made: Dr. C. F. Burnham and Dr. F. West, Kelly Hospital, Baltimore, Maryland; Dr. G. Failla, Memorial Hospital, New York, New York; Dr. J. L. Weatherwax, Philadelphia General Hospital, Philadelphia, Pennsylvania; Dr. M. C. Reinhard, State Institute for the Study of Malignant Disease, Buffalo, New York; Dr. Carl E. Nurnberger, University Hospitals, Minneapolis, Minnesota; Dr. Otto Glasser, Cleveland Clinic Foundation, Cleveland, Ohio; and Dr. Roscoe W. Teahan, Jeanes Hospital, Philadelphia, Pennsylvania.

purposes. Because of the short life of radon and the succeeding products—RaA, RaB, RaC—the radon quickly decays into RaD which has a half-life of 25 years. As RaD decays, RaE and finally RaF are formed in minute quantities of the order of 10^{-7} to 10^{-8} gram per bulb. The latter substance is polonium, which emits only α-particles and forms an almost ideal source for atomic disintegration-studies. It is this material which must be extracted from the bulbs, freed from impurities, particularly from the relatively large amount of mercury which is usually trapped in sealing off the bulb, and concentrated on as small an area as possible to approximate a point-source for the disintegration-experiments.

In order to avoid contamination of the laboratory in which the observations were to be made, permission was obtained to carry out the chemical reductions in an attic room at the Bureau of Standards in Washington. To further insure against spreading the highly active material and thus increasing the residual counts of the observing apparatus, a complete change of clothes was made when working in the chemical laboratory, rubber gloves were worn throughout the manipulations, and finally a direct test for contamination on fingers and clothes was made by means of a point-counter before entering the observing laboratory.

The procedure followed in the chemical purification was that given by I. Curie,[28] in which the final source is obtained by electrochemical deposition on silver without current, though some sources were also made using the electric-current technique.[29] The purification-process proved to be extremely tedious, since the β-ray activity of each beaker, filter-paper, precipitate, and solution (after evaporation to dryness) was measured after each step in the process and followed for several days thereafter to insure against loss of the minute quantities of active material present.

After several weeks of work a source of about 1.1×10^8 alpha-particles per second was obtained which was moderately free from β-rays. The strength of this source was measured by placing it at one end of a long evacuated tube and recording photographically by means of a linear amplifier like that of Wynn-Williams and Ward[30] the number of α-particles which passed through a small hole in the other end.

Resonance-Disintegration of Aluminum

The procedure in the study of disintegration-protons from aluminum was identical with that used by Pose. The first question to be settled was whether or not an absorption-curve for protons from a thick target obtained with this instrument would agree with those of Pose and Diebner. Obtaining such curves is an exceedingly slow process. Many protons must be counted for each point in order to keep statistical errors small so that several days of observation may be required to obtain a single point on the curve. Fortunately, the instrument runs without attention (except for changing traces), so that usually ten or more hours of usable records can be obtained each day. From these records, graphs were made for each of a number of different amounts of secondary absorption. These graphs in turn gave the yield in protons per hour. Data were obtained in this way for proton-ranges up to 50 cm, at which stage the series of observations was brought to an abrupt stop by an accident whereby the evacuated source-chamber was filled with pump-oil.

The data already obtained, however, were reasonably good. The statistical error should be small, for about 200 protons were counted for each point; the angles were small and well defined, since any point on target could "see" the ionization-chamber; and the strength of the source was quite accurately known. Under these conditions, a calculation could be made of the number of protons produced per 10^8 α-particles incident on the target in order to obtain a direct comparison with the yields given by Pose. The results of this calculation are shown by graphs *a* of Fig. 9. It will be noted that the yield for the range from 30 to 50 cm is in almost perfect agreement with that obtained by Pose. Furthermore, the pronounced maximum at about 45 cm in the lower curve, in which only deflections greater than 8000 ions are counted, suggests the

[28] I. Curie, J. chim. Phys. **22**, 471 (1925).

[29] Rutherford, Chadwick and Ellis, *Radiations from Radioactive Substances*, 554 (1930); Erbacher, Naturwiss. **20**, 390 (1932).

[30] Wynn-Williams and Ward, Proc. Roy. Soc. **A131**, 391–404 (1931).

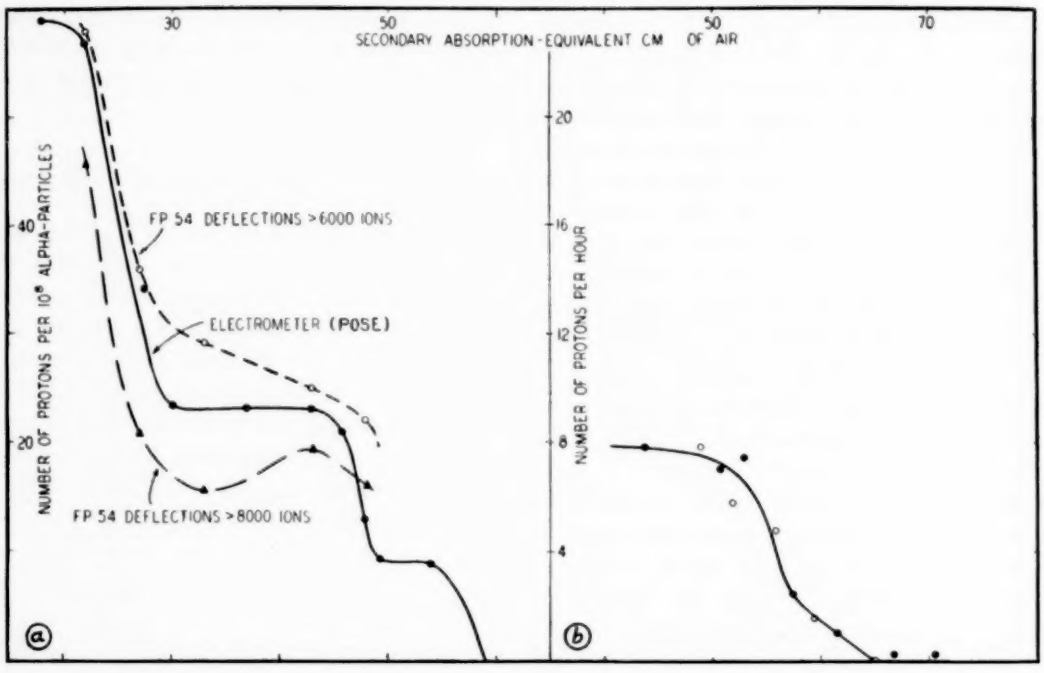

FIG. 9. (*a*) Comparison of disintegration-yields; (*b*) Absorption-curve for disintegration-protons.

presence of a strong group of about this range, since the larger deflections are due to slow protons near the end of their path. Both of these results are in direct contradiction to Steudel, who finds only a very weak group of range 49 cm and a yield many times smaller than that of Pose. In addition to these results we may also note that the absorption-curve taken with FP-54 shows the abrupt drop at 30 cm characteristic of Pose's results rather than the more gradual drop of Steudel's curve. In making this comparison two points must be emphasized. The first is that the scale of ordinates in Steudel's curve is quite arbitrary, since only Pose and Diebner give their results in terms of absolute yields, that is, number of protons per 10^8 α-particles, and that in view of the diversity of sources and angles used by the different investigators it is practically impossible to make comparison on any other basis. The other point is that the FP-54 curve *a* in Fig. 9 for deflections greater than 6000 ions may be too high, because of sudden displacements of the trace caused by β-rays which can be mistaken for protons, but is certainly not too low, for such deflections are greater than 6 mm and cannot be accidentally ignored. This statement, of course, does not deny that protons producing only 2000 or 4000 ions might be missed. The important fact is that for sensitivities comparable to those used by Pose the yield is the same as his. At higher sensitivities the yield might be greater but certainly would not be less as found by Steudel.

In order to complete the curve the chamber was cleaned, the source washed in benzol, and a new series of observations begun. It was found, however, that the proton-yield was so much reduced, presumably due to absorption of the α-particles by hydrocarbons on the surface of the emitter that an arrangement with larger solid angles was required. Unfortunately, in increasing the solid angles to give greater proton-yields, the solid angle subtended by the ionization-chamber at the source was so much increased that β-ray troubles became very serious and observations below 50 cm could not be made. The form of the absorption-curve for ranges beyond 50 cm is shown by *b* in Fig. 9. Two sets of observations were made as indicated by the circles and dots in the figure. While the conditions under which these observations were taken obviously were not as good as for the first series, the two sets of points are still fairly consistent, and it must be concluded that there is an abrupt drop beyond

50 cm, again in agreement with Pose and contrary to Steudel. In this case, a calculation of the yield may be expected to give a low result, since no doubt many of the α-particles leaving the source have energies greatly reduced by absorption on the source itself. As a further check of the yields, however, the strength of the source was again measured and a rough calculation gave 13 protons per 10^8 α-particles at 50 cm secondary absorption compared to 22 for Pose and perhaps about 3 for Steudel.

The above work having shown the necessity of using a better source, before attempting to study such questions as the sharpness of resonance, the observations were stopped and efforts directed toward obtaining a source both stronger and more free from β-rays. A new supply of radon-bulbs was acquired through the courtesy of the hospitals listed above and the chemical reduction is now under way.

This work was begun at the Department of Terrestrial Magnetism of the Carnegie Institution of Washington in the spring of 1931, carried forward at the Johns Hopkins University where the writer was in residence during the academic year 1931–1932, and brought to completion in 1933 at the Department of Terrestrial Magnetism. The writer wishes to take this opportunity for acknowledging his indebtedness to the many whom he has consulted regarding various phases of this problem. The following should be especially mentioned: Professor J. A. Bearden, under whose immediate direction the work at the Johns Hopkins University was done; Dr. L. F. Curtiss of the United States Bureau of Standards, for generous assistance in connection with the preparation of sources; Dr. M. A. Tuve, for continuous advice and encouragement; and Acting Director J. A. Fleming of the Department of Terrestrial Magnetism, whose active support has made the work possible.

Charge Distributions in Fluorine and Neon

F. W. BROWN, *University of Illinois*

(Received May 8, 1933)

Hartree fields (modified to take account of exchange between $2p$ electrons) have been obtained for F, F^-, Ne. The energy parameters of the $1s$, $2s$ and $2p$ electrons are found to be 53.08, 2.40 and 1.09 for F; 52.38, 1.50 and 0.14 for F^-; and 65.68, 2.75, and 1.51 for Ne. The use of the fields for F and F^- enable one to test the wave equation of the "hole" given by Heisenberg and Dirac. This equation is found to be equivalent to the Hartree equation for the corresponding electron and to give the wrong sign for the electron affinity of F. The $1s$, $2s$ and $2p$ functions have been represented by analytic expressions of the Slater type.

I. INTRODUCTION

IN order to carry out any detailed atomic calculations accurate wave functions are essential. Good approximate functions can be obtained from antisymmetric combinations of products of single electron functions.

There are two general methods of obtaining the single electron functions. The variational method, developed mainly by Zener,[1] consists essentially in setting up wave functions with adjustable parameters for each electron, obtaining the energy expression for the entire atom in terms of these parameters and adjusting them to make the energy a minimum. The accuracy of the method depends on the form chosen for the single electron functions and the number of parameters at one's disposal.

The method of self-consistent fields was developed by Hartree[2] and refined to take account of exchange effects by Slater[3] and Fock.[4] The functions obtained by this method are more accurate but are available only in the form of a set of numerical values. It would be much more convenient to have these functions represented by analytic expressions of not too great complexity. The analytic functions[5] given by Slater are the best available at present.

Heisenberg[6] and Dirac[7] have set up a wave equation to describe the holes in a closed shell of an atom. For atoms containing almost closed shells the equation would appear to be much simpler than the equation for the electrons since it involves fewer coordinates.

Most of the work discussed in this paper was done to see if any practical use could be made of the wave equation of the hole for the determination of the energy levels and wave functions of atoms with almost closed shells. The necessary calculations have been carried out for the normal fluorine atom which lacks one electron of having all closed shells. As a further check on the accuracy of the work a self-consistent field for Ne was found.

II. SELF-CONSISTENT FIELDS

General method

In setting up the equation of the self-consistent field the method of Fock[4] has been used with slight modifications as suggested by Slater.[3] The wave function of the atom (in the case of F, F^- and Ne) is written in the determinant form, and it is assumed that the single-electron wave functions may be written in the form

[1] C. Zener, Phys. Rev. **36**, 51 (1930).
[2] D. R. Hartree, Proc. Camb. Phil. Soc. **24**, 89 and 111 (1928).
[3] J. C. Slater, Phys. Rev. **35**, 210 (1930).
[4] V. Fock, Zeits. f. Physik **61**, 126; **62**, 795 (1930).
[5] J. C. Slater, Phys. Rev. **42**, 33 (1932).
[6] W. Heisenberg, Ann. d. Physik **10**, 888 (1931).
[7] P. A. M. Dirac, Ann. de l'Inst. H. Poincare **1**, Pt. 4, 391 (1929).

$$u(n/xyz) = R(n/r)\,Y(\theta, \varphi), \tag{1}$$

which amounts to saying that they are the solutions of central field problems. The energy is then calculated by the method of Slater[8] and minimized with respect to the radial functions, subject to the condition of normality and orthogonality. This leads to a set of linear differential equations for the radial functions of each group of electrons with the same total and azimuthal quantum numbers. These equations are the Euler equations of the above variational problem. The radial functions are the factors which are varied, the coefficients of the arbitrary variations of each function separately being set equal to zero. The auxiliary conditions are taken account of by Lagrangian parameters in the Euler equations.

The notation of Slater's article is used as far as possible and the atomic units of Hartree are used throughout.

The Hamiltonian operator for a many-electron atom, neglecting relativity and all spin interactions, is

$$L = \sum_{k=1}^{N} H_k + \sum_{i>k=1}^{N} (1/r_{ik}), \qquad H_k = -\tfrac{1}{2}\Delta_k - (N/r_k). \tag{2}$$

Here Δ_k is the Laplacian operator acting on the coordinates of the kth electron, r_k is the distance of the kth electron from the nucleus, r_{ik} is the distance between electrons i and k and N is the atomic number.

A diagonal element of the energy matrix can be written in the form

$$E = \sum(n\text{'s})I(n) + \sum(\text{pairs of } n\text{'s})J(n; n') - \sum(\text{pairs of } n\text{'s} \parallel \text{spins})K(n; n'), \tag{3}$$

where

$$I(nlm_lm_s) = \int u^*(nlm_lm_s/k)H_k u(nlm_lm_s/k)dv_k. \tag{4}$$

On making the substitution (1) this reduces to

$$I(nlm_lm_s) = \int_0^\infty R(nl/r)[-\tfrac{1}{2}R''(nl/r) + (1/r)R'(nl/r) + (l(l+1)/2r^2)R(nl/r) - (N/r)R(nl/r)]r^2dr, \tag{5}$$

and, on the further substitution

$$f(nl/r) = rR(nl/r) \tag{6}$$

to

$$I(nlm_lm_s) = \int_0^\infty f(nl/r)[-\tfrac{1}{2}f''(nl/r) + \tfrac{1}{2}(l(l+1)/r^2)f(nl/r) - (N/r)f(nl/r)]dr,$$

which can be written in the form

$$I(nlm_lm_s) = \int_0^\infty \{\tfrac{1}{2}[f'(nl/r)]^2 + f(nl/r)[\tfrac{1}{2}(l(l+1)/r^2)f(nl/r) - (N/r)f(nl/r)]\}dr. \tag{7}$$

The integral J has the value

$$J(nlm_lm_s; n'l'm_l'm_s') = \int u^*(nlm_l/k)u^*(n'l'm_l'/j)(1/r_{kj})u(nlm_l/k)u(n'l'm_l'/j)dv_kdv_j$$

$$= \sum_k a^k(lm_l; l'm_l')F^k(nl; n'l'), \tag{8}$$

---

[8] J. C. Slater, Phys. Rev. **34**, 1293 (1929).

where the a^k come from integration over the angular parts and are given in Slater's[8] tables. We can write

$$F^k(nl; n'l') = \int_0^\infty f^2(nl/r)(2k+1)F_k^{nl;\,n'l'}dr, \tag{9}$$

where

$$F_k^{nl;\,n'l'}(r) = \int_0^\infty f(nl/r')f(n'l'/r')(1/(2k+1))(r^k(a)/r(b)^{k+1}). \tag{10}$$

The expression for the integral K is

$$K(nlm_lm_s; n'm_l'm_s') = \delta(m_s; m_s')\int u^*(nlm_l/k)u^*(m'l'm_l'/j)(1/r_{kj})u(nlm_l/j)u(n'l'm_l'/k)dv_kdv_j$$

$$= \sum_k b^k(lm_l; l'm_l')G^k(nl; n'l'), \tag{11}$$

where the b^k are given in the tables and

$$G^k(nl; n'l') = \int_0^\infty f(nl/r)f(n'l'/r)F_k^{nl;\,n'l'}(2k+1)dr. \tag{12}$$

These formulae allow one to obtain the energy of the atom in terms of radial integrals and are in a form especially convenient for carrying out the variational process.

Equations for atoms containing all closed shells

For the case of atoms with closed shells the equation for the radial functions can be immediately set down.

Heisenberg[6] and Shortley[9] have derived closed formulae for expressions of the type

$$\sum_{m_s'}\sum_{m_l'=-l'}^{l'}[J(nlm_lm_s; n'l'm_lm_s') - \delta(m_s; m_s')K(nlm_lm_s; n'l'm_l'm_s')]. \tag{13}$$

In the form given by Shortley the expression (16) is equal to

$$2(2l'+1)F^0(nl;\ n'l') - \frac{2l'+1}{2l+1}\sum_k C_{l'k}{}^lG^k(nl; n'l'), \tag{14}$$

where

$$C_{l'k}{}^\lambda = \frac{2\lambda+1}{2}\int_0^\pi P_\lambda(\cos w)P_{l'}(\cos w)P_k(\cos w)\sin w dw = \frac{2\lambda+1}{(2l'+1)^{\frac{1}{2}}(2k+1)^{\frac{1}{2}}}\{b^\lambda(l'0; k0)\}^{\frac{1}{2}}. \tag{15}$$

The energy of the atom can then be written in the form

$$E = W_1 + W_2, \tag{16}$$

where

$$W_1 = \sum(n's)I(n) \tag{17}$$

and

$$W_2 = \sum_{nlm_lm_s}\sum_{n'l'}2(2l'+1)F^0(nl; n'l') - \sum_{nlm_lm_s}\frac{1}{2l+1}\sum_{n'l'}(2l'+1)\sum_k C_{l'k}{}^lG^k(nl; n'l'). \tag{18}$$

The energy is to be minimized subject to the conditions

[9] G. H. Shortley, Phys. Rev. **40**, 185 (1932).

$$\delta_{ll'}\int_0^\infty f(nl/r)f(n'l'/r)dr=\delta_{nl;\,n'l'}. \tag{19}$$

The variation of W_1 is carried out quite simply. In varying the integral W_2 we must note that the function to be varied also appears in the $F_k^{nl;\,n'l'}$. We can carry out two types of variation; a complete variation δW_2 in which both the $f(nl/r)$ and the $F_k^{nl;\,n'l'}$ are varied, or a partial variation $\delta' W_2$ in which only the $f(nl/r)$ are varied. It is easy to see that

$$W_2=2\delta' W_2. \tag{20}$$

Carrying out the variation and setting the coefficient of $f(nl/r)$ equal to zero, we have

$$-(2l+1)f''(nl/r)+2(2l+1)[-(N/r)f(nl/r)+(1(l+1)/2r^2)f(nl/r)+\sum_{n'l'}2(2l'+1)F_0^{n'l';\,n'l'}f(nl/r)$$
$$-\sum_{n'l'}[(2l'+1)/(2l+1)]\sum_k C_{l'k}{}^lG_k^{nl;\,n'l'}f(n'l'/r)]=\sum_{n'l'}\lambda_{nl;\,n'l'}\delta_{ll'}f_{(n'l'/r)}, \tag{21}$$

where the $\lambda_{nl;\,n'l'}$ are Lagrangian parameters.

Equations for F, F^-, Ne

For the normal electron configurations of F^- and Ne we can immediately write down the equations from the expression (21). If we write f_1, f_2, f_3 in place of $f(10/r), f(20/r), f(21/r)$, the equations become

$$-f_1''+2(-(N/r)+F_0^{11}+2F_0^{22}+6F_0^{33})f_1-2F_0^{22}f_2-6F_1^{31}f_3=\lambda_{11}f_1+\lambda_{22}f_2, \tag{22a}$$

$$-f_2''+2(-(N/r)+2F_0^{11}+F_0^{22}+6F_0^{33})f_2-2F_1^{12}f_1-6F_1^{32}f_3=\lambda_{12}f_1+\lambda_{22}f_2, \tag{22b}$$

$$-3f_3''+6(-(N/r)+1/r^2+2F_0^{11}+2F_0^{22}+5F_0^{33}-2F_2^{33})f_3-6F_1^{23}f_1=\lambda_{33}f_3. \tag{22c}$$

For normal F_1

$$W_1=\int_0^\infty\left[\left(\frac{df_1}{dr}\right)^2+\left(\frac{df_2}{dr}\right)+\frac{5}{2}\left(\frac{df_3}{dr}\right)^2+\frac{5}{r^2}f_3^2\right]dr-\int_0^\infty(2f_1^2+2f_2^2+5f_3^2)\frac{9}{r}dr \tag{23}$$

and

$$W_2=\int_0^\infty[\tfrac{1}{2}(2f_1^2+2f_2^2+5f_3^2)(2F_0^{11}+2F_0^{22}+5F_0^{33}-f_1^2F_0^{11}-f_2^2F_0^{22}-(5/2)f_3^2(F_0^{33}+(8/5)F_2^{33})$$
$$-2f_1f_2F_0^{12}-5f_1f_3F_1^{13}-5f_2f_3F_1^{23})]dr. \tag{24}$$

The variation equations, imposing the conditions

$$\int_0^\infty f_i^2dr=1\quad(i=1,2,3),\qquad\int_0^\infty f_1f_2dr=0 \tag{25}$$

are

$$-f_1''+2(-(9/r)+F_0^{11}+2F_0^{22}+5F_0^{33})f_1-2F_0^{21}f_2-5F_1^{31}f_3=\lambda_{11}f_1+\lambda_{21}f_2 \tag{26a}$$

$$-f_2''+2(-(9/r)+2F_0^{11}+F_0^{22}+5F_0^{33})f_2-2F_0^{12}f_1-5F_1^{32}f_3=\lambda_{12}f_1+\lambda_{22}f_2 \tag{26b}$$

$$-(5/2)f_3''+5(-(9/r)+1/r^2+2F_0^{11}+2F_0^{22}+4F_0^{33}-(8/5)F_2^{33})f_3-5F_1^{13}f_1-5F_1^{23}f_2=\lambda_{33}f_3. \tag{26c}$$

By multiplying (26a, b, c) by f_1, f_2, f_3, respectively, integrating over all r, and adding, one easily verifies that

$$\lambda_{11}+\lambda_{22}+\lambda_{33}=W_1+2W_2;$$

hence

$$E=\lambda_{11}+\lambda_{22}+\lambda_{33}-W_2. \tag{27}$$

In the solution of the Eqs. (22) and (26) the terms F_1^{ik}, $\lambda_{ik}(i\neq k)$ were neglected. The equations

remaining after this simplification are essentially the Hartree equations except that enough of the exchange integral remains to make the equation for f_3 independent of the magnetic quantum number of the $2p$ electron under consideration. If this was not done the coefficient of F_2^{33} would be changed. In the method as originally developed by Hartree the coefficient of F_2^{33} will be zero in any case because of the method he used for averaging over the radius.

For other p electron configurations there is more than one state and the coefficient of F_2^{33} depends on the state chosen, the variation from state to state being as great as the value of the coefficient for some of the states. Hence, unless one wishes to go through separate calculations for the radial functions for each state of a configuration, it is just as well to neglect the coefficient entirely.

The order of magnitude of the change in the energy parameter of the equation for f_3, for the atoms on which calculations have been made, due to neglecting F_2^{33} would be around 0.05. For the case of F^- this would be an error of 35 percent. The change in the function itself would, however, be comparatively small. No estimate has been made of the other exchange terms, although Fock found that for Na they amounted to 3 percent of the total energy. With the solutions of the simplified equations at our disposal, it would not be difficult to get the accurate solutions.

Method of solution of equations

For convenience all equations are thrown into the form

$$f''=[\epsilon-2v+[1(1+1)/r^2]]f, \tag{28}$$

where $-v$ is the potential of the central field acting on the electron and ϵ is the energy parameter which gives the energy as a multiple of the ionization potential of hydrogen. The methods used in integration of this equation are essentially those described by Hartree.

Probably the only place in which any details further than those given by Hartree need be described is in the calculation of the potential. It is convenient to use the quantities

$$Z_{Vl}{}^{ik}=rF_l{}^{ik} \tag{29}$$

and

$$Z_l{}^{ik}=-r^2(dF_l{}^{ik}/dr). \tag{30}$$

The only cases to be considered are those for which $i=k$. For Hartree's method of averaging the only quantities entering would be those for which $1=0$, and the quantities (29) and (30) would then represent the charges which, when placed at the nucleus, would produce the same potential and field strength, respectively, as would be produced by the charge distribution of an electron.

For the case $1=0$

$$Z_0{}^{ii}(r)=\int_0^r f_i^2dr \Big/ \int_0^\infty f_i^2dr \tag{31}$$

and $Z_{v0}{}^{ii}$ can be obtained by numerical integration of

$$dZ_{v0}{}^{ii}/dr=(Z_0{}^{ii}-Z_0{}^{ii})/r. \tag{32}$$

The integration of (32) is started inward from a large radius where the deviation from a coulomb field is neglible, with the initial values

$$Z_{v0}{}^{ii}=Z_0{}^{ii}, \quad dZ_{v0}{}^{ii}/dr=0. \tag{33}$$

For $1=2$, $Z_{v2}{}^{ii}$ can be obtained by successive numerical integration of

$$d\beta/dr=dZ_0{}^{ii}/dr-2\beta/r \tag{34}$$

and

$$dZ_{v2}{}^{ii}/dr=(3Z_{v2}{}^{ii}-5\beta/r), \tag{35}$$

where the integration of (34) is started at $r=0$ with initial values

$$\beta=0, \quad \beta'=0$$

and the integration of (35) is started inward at a large radius with the initial values

$$Z_{v2}{}^{ii}= \ , \quad dZ_{v2}{}^{ii}/dr=0. \tag{36}$$

The successive approximations were carried out until the maximum variations of $\Sigma Z_0{}^{ii}$ were 0.06, 0.06 and 0.05 for Ne, F, F^-, respectively.

Results

The results of the calculations are given in Tables I to IV inclusive. In the first three tables the normalized radial functions, the total effective nuclear charge and effective nuclear charge for potential, and total charge density are given for Ne, F and F^-. There is no differ-

TABLE I. *Effective nuclear charges, total charge distribution, and normalized radial functions for F.*

r	Z	Z_v	f_1	f_2	f_3	$-(dZ/dr)$
0	9.00	9.00	0	0	0	0
0.01	9.00	8.73	0.475	0.105	0.002	0.473
0.02	8.99	8.48	0.866	0.195	0.006	1.576
0.03	8.97	8.23	1.189	0.266	0.015	2.970
0.04	8.93	7.99	1.450	0.314	0.026	4.406
0.06	8.82	7.55	1.818	0.401	0.053	6.946
0.08	8.66	7.16	2.035	0.437	0.088	8.703
0.10	8.48	6.80	2.131	0.442	0.126	9.552
0.12	8.29	6.49	2.150	0.421	0.167	9.722
0.14	8.10	6.20	2.112	0.383	0.212	9.438
0.16	7.91	5.95	2.028	0.332	0.259	8.781
0.18	7.74	5.71	1.919	0.269	0.303	7.969
0.20	7.60	5.49	1.796	0.202	0.348	7.138
0.25	7.29	5.00	1.466	0.044	0.456	5.002
0.30	7.06	4.56	1.150	−0.176	0.553	4.236
0.35	6.85	4.16	0.881	−0.354	0.637	3.832
0.40	6.66	3.79	0.660	−0.507	0.709	3.899
0.5	6.25	3.13	0.359	−0.752	0.809	4.661
0.6	5.74	2.55	0.187	−0.908	0.862	5.434
0.7	5.17	2.07	0.091	−0.984	0.881	5.834
0.8	4.58	1.67	0.047	−1.003	0.877	5.862
0.9	4.02	1.34	0.024	−0.985	0.856	5.605
1.0	3.48	1.08	0.004	−0.942	0.819	5.129
1.2	2.56	0.69		−0.815	0.742	4.081
1.4	1.84	0.44		−0.677	0.653	3.049
1.6	1.31	0.28		−0.548	0.569	2.220
1.8	0.93	0.18		−0.437	0.490	1.543
2.0	0.64	0.12		−0.334	0.423	1.076
2.5	0.26	0.03		−0.185	0.285	0.474
3.0	0.10	0.01		−0.095	0.190	0.198
3.5	0.05			−0.048	0.126	0.084
4.0	0.02			−0.024	0.082	0.035
4.5	0.01			−0.011	0.052	0.014
5.0				−0.006	0.034	0.006
5.5				−0.003	0.021	0.002
6.0				−0.001	0.014	0.001
7.0					0.006	0
8.0					0.002	
9.0					0.001	

TABLE II. *Effective nuclear charges, total charge distribution and normalized radial functions for F^-.*

r	Z	Z_v	f_2	f_3	$-(dZ/dr)$
0	9.00	9.00	0	0	0
0.01	9.00	8.73	0.106	0.002	0.474
0.02	8.99	8.48	0.195	0.005	1.576
0.03	8.97	8.23	0.266	0.014	2.970
0.04	8.93	7.98	0.315	0.024	4.407
0.06	8.82	7.53	0.401	0.049	6.948
0.08	8.66	7.13	0.437	0.080	8.703
0.10	8.48	6.77	0.443	0.114	9.553
0.12	8.29	6.44	0.412	0.155	9.728
0.14	8.10	6.15	0.383	0.195	9.442
0.16	7.92	5.88	0.332	0.237	8.783
0.18	7.73	5.64	0.270	0.277	7.971
0.20	7.60	5.41	0.202	0.318	7.139
0.25	7.29	4.90	0.044	0.417	5.006
0.30	7.06	4.45	−0.176	0.506	4.243
0.35	6.86	4.03	−0.354	0.573	3.772
0.40	6.67	3.64	−0.508	0.647	3.899
0.5	6.25	2.93	−0.752	0.731	4.595
0.6	5.76	2.31	−0.899	0.794	5.469
0.7	5.20	1.77	−0.972	0.815	5.891
0.8	4.61	1.33	−0.981	0.813	5.895
0.9	4.03	0.95	−0.974	0.797	5.710
1.0	3.50	0.64	−0.932	0.772	5.313
1.2	2.52	0.17	−0.801	0.706	4.274
1.4	1.73	−0.16	−0.678	0.637	3.354
1.6	1.11	−0.38	−0.554	0.571	2.570
1.8	0.65	−0.54	−0.447	0.510	1.960
2.0	0.30	−0.66	−0.356	0.456	1.501
2.5	−0.26	−0.82	−0.201	0.348	0.807
3.0	−0.57	−0.90	−0.106	0.266	0.447
3.5	−0.74	−0.94	−0.060	0.207	0.264
4.0	−0.83	−0.96	−0.030	0.164	0.163
4.5	−0.90	−0.98	−0.018	0.130	0.102
5.0	−0.93		−0.010	0.105	0.066
5.5	−0.95	−0.99	−0.005	0.083	0.041
6.0	−0.96		−0.003	0.068	0.028
7	−0.97		−0.001	0.045	0.012
8	−0.98	−1.00		0.030	0.005
9	−0.99			0.020	0.002
10				0.013	0.001
11	−1.00			0.009	

ence between the functions f_1 for F and F^-, hence it is listed only once. A comparison of the approximate x-ray term values and ionization potentials as calculated by the method of self-consistent fields with the observed values, where those are known, is given in Table IV. Graphs of the functions and total charge distributions are given in Figs. 1, 2, 3. The value of the electron affinity of fluorine from this table is +0.14. The electron affinity of fluorine was also calculated, the difference in the functions of the atom and ion being taken into account by using the relation (32) (without exchange terms). The value obtained was −0.13. It seems strange that it should be negative. There are no measurements with which to compare it but the value obtained by extrapolation methods[10] is +0.25. One cannot be certain whether the polarization energy is actually so large or whether the discrepancy is due to inaccuracy in the method.

The energy of the K level of F was taken from the measurements of Södermann.[11] The ionization potentials are taken from the spectrographic data tabulated by Noyes and Beckman.[12]

[10] J. H. Bartlett, Jr., Nature **125**, 459 (1930).
[11] M. Södermann, Zeits. f. Physik **52**, 795 (1929).
[12] A. A. Noyes and A. D. Beckman, Chem. Rev. **5**, 85 (1928).

TABLE III. *Effective nuclear charges, total charge distributions and normalized radial functions for Ne.*

r	Z	Z_v	f_1	f_2	f_3	$-(dZ/dr)$
0	10.00	10.00	0	0	0	0
0.01	10.00	9.69	0.541	0.124	0.002	0.616
0.02	9.99	9.39	0.996	0.224	0.008	2.085
0.03	9.95	9.10	1.352	0.303	0.020	3.842
0.04	9.91	8.82	1.636	0.363	0.035	5.624
0.06	9.77	8.31	2.016	0.438	0.071	8.542
0.08	9.57	7.85	2.208	0.464	0.114	10.259
0.10	9.36	7.45	2.275	0.453	0.164	10.897
0.12	9.15	7.09	2.248	0.415	0.219	10.739
0.14	8.94	6.76	2.164	0.358	0.274	10.073
0.16	8.74	6.46	2.041	0.287	0.329	9.145
0.18	8.57	6.18	1.895	0.206	0.382	8.142
0.20	8.42	5.93	1.743	0.119	0.437	7.250
0.25	8.11	5.35	1.363	−0.105	0.550	5.552
0.30	7.84	4.83	1.016	−0.321	0.668	4.936
0.35	7.59	4.34	0.745	−0.511	0.756	5.061
0.40	7.31	3.90	0.534	−0.672	0.826	5.567
0.5	6.67	3.11	0.264	−0.897	0.916	6.773
0.6	6.00	2.46	0.128	−1.013	0.952	7.523
0.7	5.22	1.94	0.057	−1.049	0.950	7.618
0.8	4.48	1.52	0.028	−1.032	0.922	7.231
0.9	3.81	1.19	0.001	−0.983	0.881	6.590
1.0	3.22	0.93		−0.916	0.829	5.801
1.2	2.24	0.57		−0.761	0.718	4.251
1.4	1.55	0.36		−0.610	0.607	2.955
1.6	1.08	0.22		−0.478	0.508	2.005
1.8	0.74	0.13		−0.369	0.413	1.301
2.0	0.52	0.09		−0.283	0.349	0.891
2.5	0.20	0.03		−0.143	0.214	0.316
3.0	0.07	0.01		−0.069	0.130	0.111
3.5	0.03			−0.033	0.076	0.037
4.0	0.01			−0.015	0.045	0.012
4.5				−0.007	0.026	0.004
5.0				−0.003	0.015	0.001
5.5				−0.001	0.009	0.000
6.0					0.005	
7.0					0.002	
8.0					0.001	

TABLE IV. *Comparison of term values obtained from self-consistent field with the observed values.*

	F		F⁻		Ne	
Level	ϵ	$\frac{\nu}{R}$ obs.	ϵ	$\frac{\nu}{R}$ obs.	ϵ	$\frac{\nu}{R}$ obs.
K	53.08	49.74	52.38	—	65.68	—
L	2.40	—	1.50	—	2.75	—
Ionization potential	1.09	1.248	0.14	—	1.51	1.587

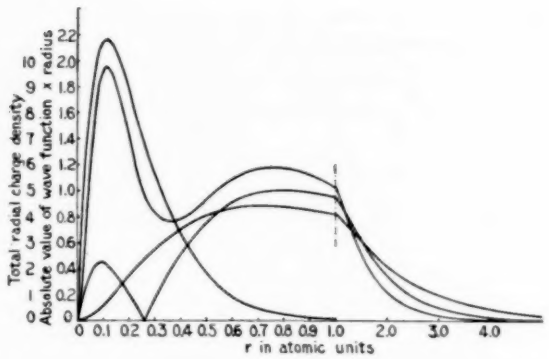

FIG. 1. Total radial charge density and absolute value of functions f_1, f_2, f_3 for F.

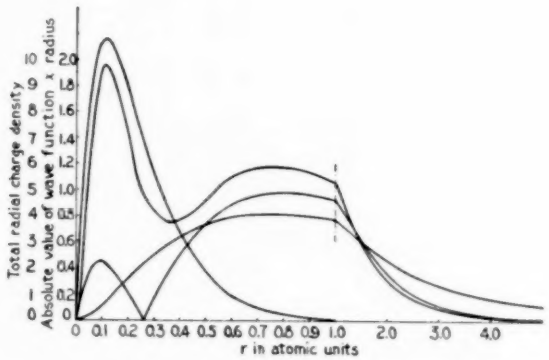

FIG. 2. Total radial charge density and absolute value of functions f_1, f_2, f_3 for F^-.

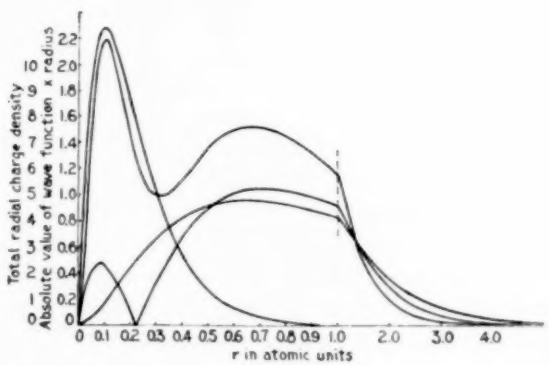

FIG. 3. Total radial charge density and absolute value of functions f_1, f_2, f_3, for Ne.

The Wave Equation of the Hole

The method used by Heisenberg to derive a wave equation describing the holes in a closed shell will be described briefly. Starting from the energy operator of an atom in terms of the non-commutative amplitudes a_i as given by Jordan and Wigner[13]

$$E=\sum_{i,\ k=1}^{k} a_i^* a_k(\delta_{ik}E_i+H_{ik})+\tfrac{1}{2}\sum_{ikrs} a_i^* a_k^* a_r a_s H_{ik;\ rs} \tag{37}$$

where

$$a_i a_i^* = N_i \text{ (number of electrons in state } i=0,\ 1), \tag{38}$$

K is the total possible number of states an electron may have, the E_i are the unperturbed energy levels of the single electrons, and the other matrix elements are defined by

$$H_{ik}=\int u_i^*(l)Hu_k(l)dv_l \tag{39}$$

$$H_{ik;\ rs}=\int u_i^*(l)u_k^*(m)(1/r_m)u_r(m)u_s(l)dv_l dv_m, \tag{40}$$

and making the assumption that the probability of transitions to states outside a closed shell are negligible (i.e., $K=n$, where n is the number of electrons in a closed shell), he transforms to a new set of amplitudes a_i' obeying the same commutation relations as the a_i and satisfying the relations

$$a_i'^* a_i' = (1-N_i) = N_i' \text{ (number of holes in state } i=0,\ 1) \tag{41}$$

$$a_i' = a_i^*, \tag{42}$$

to obtain a new energy operator

$$E=\sum_{i=1}^{n}(H_{ii}+E_i)+\tfrac{1}{2}\sum_{i,\ k=1}^{n}(H_{ik;\ ki}-H_{ik;\ ik})-\sum_{i,\ k=1}^{n} a_i'^* a_k'[\delta_{ik}E_i+H_{ki}$$

$$+\tfrac{1}{2}\sum_{r}(H_{kr;\ ri}-H_{rk;\ ri}-H_{kr;\ ir}+H_{rk;\ ir})]+\tfrac{1}{2}\sum_{ikrs=1}^{n} a_i'^* a_k'^* a_r' a_s' H_{rs;\ ik}. \tag{43}$$

The H^l can be any perturbation on acting on the lth electron. A special case would be the spin-orbit interaction for a single electron.

The essential difference between (37) and (43) is in the factor of $a_i'^* a_k'$ which represents the perturbation energy acting on a hole. The sign is reversed and there are additional terms which arise from the interactions of the electrons and represent the difference in the central fields acting on the electrons and holes. The matrix element H_{ik} becomes H_{ki}. There is also an added term

$$\sum_{i}(E_i+H_{ii})+\tfrac{1}{2}\sum_{i,\ k}(H_{ik;\ ki}-H_{ik;\ ik})=A, \tag{44}$$

which represents the energy of the closed shell.

If we set $H_{ik}=H_{ki}$ and $H_{ik;\ rs}=H_{rs;\ ik}$ the wave equation of the hole becomes

$$\left\{\sum_{l=1}^{n-N}\tfrac{1}{2}\Delta^l+U^l+\sum_{l>m}\frac{1}{r_{lm}}+A-E\right\}\psi=0. \tag{45}$$

U^l is a central field which we shall later discuss in detail. If one wishes to use the equation to calculate the term values of the lowest states of atomic spectra, the perturbation H can be considered as the

[13] P. Jordan and E. Wigner, Zeits. f. Physik **47**, 631 (1928).

interaction between spin and orbit for each electron. For the remaining discussion we shall neglect the spin-orbit interaction.

For the case of one hole in a closed shell there is only one a_i' different from zero in the energy expression (43), hence $i=k$ and the expression which represents the energy due to the additional central field

$$\tfrac{1}{2}\sum_r (H_{kr;\ ri}-H_{rk;\ ri}-H_{kr;\ ir}+H_{rk;\ ir})$$

reduces to

$$\sum_r (H_{ir;\ ri}-H_{ri;\ ri})=\sum_{n'} J(n;n')-\sum_{n'} K(n;n'), \tag{46}$$

where n' is summed over the closed shells.

Making use of the relation (14) and neglecting the exchange terms for which $n,\ l\neq n',\ l'$ we see immediately that the added central field

$$\sum_{n'l'} 2(2l'+1)F_0{}^{n'l';\ n'l'}-\sum_K C_{Kl}{}^l G_K{}^{nl;\ nl} \tag{47}$$

and the equation for the radial part of the function of the hole is

$$f''+2\left[\frac{N}{r}-\frac{l(l+1)}{2r^2}+\sum_{n'l'} 2(2l'+1)F_0{}^{n'l';\ n'l'}-\sum_K C_{lK}{}^l G_K{}^{nl;\ nl}\right]f=2(E-A)f. \tag{48}$$

Neglecting the exchange terms for which $n\neq n'l'$ in (21) we obtain

$$f''(nl/r)+2[(N/r)-l(l+1)/2r^2-\sum_{n'l'} 2(2l'+1)F_1{}^{n'l';\ n'l'}+\sum_k C_{lk}{}^l G_k{}^{nl;\ nl}f(nl/r)]=\lambda f(nl/r),$$

which is exactly equivalent to (48).

From this it is seen that the equation of the hole in a closed shell is exactly equivalent to the equation of an electron in the closed shell when one neglects the exchange terms for which $nl\neq n'l'$. If one takes into account all the exchange terms, expression (46) does not represent an energy due to a central field alone, but also includes exchange terms of the same form as those entering into Fock's modified Hartree equations. From the method of deviation it is not, however, obvious how these added terms enter into the equation of the hole. In Heisenberg's derivation of the wave equation of the hole these exchange terms did not enter because he considered only one (nl) group.

The term value obtained from a solution of the wave equation of the hole is then correct to the extent to which the energy parameters in the Hartree equations actually represent the term values. There is no account taken of the difference of the wave functions of the electrons in the closed shell and those in a shell lacking one electron. For fluorine this difference was found to be large enough to change the sign of the electron affinity.

If there is more than one hole present in the closed shells one can carry out a process of obtaining a self-consistent field for the holes in the same manner as for electrons. For the holes, however, the field U^l would be used as the basic field to which the potentials due to the charge distribution of the holes would be added, whereas in the case of electrons the potentials due to the charge distributions of the electrons are subtracted from (N/r). The radial parts of the hole functions would again be the same as those of the electrons except that the polarization of the part of the atom not included in the particular (nl) group containing the hole would not be taken into account.

Heisenberg has shown that in order for the multiplets to be inverted in cases where there are fewer holes than electrons in a configuration the angular part of the hole function must be the complex conjugate of that for the electron. Hence we can say that the wave functions of the holes in a closed shell are simply the complex conjugates of the functions of the electrons.

It is obvious that there is no particular advantage in using the wave equation of the hole to calculate the term values, since it is equivalent to the Hartree method.

IV. The Analytic Expressions for the Functions

The functions obtained from the self-consistent field can be represented approximately by the following expressions

$$\text{F: } 1s: f_1 = 51.77re^{-8.75r},$$

$$2s: f_2 = 11.30[re^{-7.25r} - r^2(1.00e^{-3.31r} + 0.341e^{-1.98r})],$$

$$2p: f_3 = 13.76r^2(e^{-3.85r} + 0.202e^{-1.66r}),$$

$$\text{F}^-\text{: } 1s: f_1 = 51.77re^{-8.75r},$$

$$2s: f_2 = 11.55[re^{-7.25r} - r^2(1.03e^{-3.33r} + 0.300e^{-1.90r})],$$

$$2p: f_3 = 13.57r^2(e^{-3.86r} + 0.133e^{-1.36r}),$$

$$\text{Ne: } 1s: f_1 = 60.70re^{-9.73r},$$

$$2s: f_2 = 13.60[re^{-8.22r} - r^2(1.08e^{-3.69r} + 0.350e^{-2.15r})],$$

$$2p: f_3 = 20.13r^2(e^{-4.48r} + 0.198e^{-1.91r}),$$

which are of the form suggested by Slater. The curves were fitted by the method outlined by Slater. The analytic expressions for f_1 and f_2 are not exactly orthogonal. The values of the integrals of their products are 0.0000203 for Ne, 0.0000251 for F, and 0.0000292 for F^-. The agreement between the curves and the analytic expression is good for ranges in which the functions are large but in other ranges the discrepancy may be as much as 0.02.

The functions as given are probably not accurate enough for many calculations. To get an accurate fit would probably require several more exponentials. It seems to be just as convenient to carry out the numerical integrations as to use the analytic expressions, if great accuracy is desired.

In conclusion the author wishes to thank Professor J. H. Bartlett, Jr., for suggestions and assistance in this research.

Application of Liouville's Theorem to Electron Orbits in the Earth's Magnetic Field

W. F. G. SWANN, *Bartol Research Foundation of the Franklin Institute*

(Received June 3, 1933)

It is pointed out that in the application of Liouville's theorem to the problem of cosmic-ray intensities, Lemaitre and Vallarta have implicitly taken the electron momentum as that corresponding to a free particle. Calling this momentum p' the particle momentum, we have to realize that Liouville's theorem is usually based upon the Hamiltonian equations in which the momentum p associated with an electron is not the same as p', but is connected with it by the relation $p=p'+eU/c$, where U is the vector potential determining the magnetic field. The Hamiltonian equations are not valid in terms of momenta of the type p', and, it is not, therefore, clear that Liouville's theorem is valid when expressed in terms of these momenta. The object of the paper is to show that a theorem the equivalent of Liouville's theorem is, in fact, true in terms of the coordinates and the momenta p', so that the ultimate validity of the use of the theorem by Lemaitre and Vallarta is substantiated. It is to be observed, moreover, that the validity of this extended form of Liouville's theorem is true even in the presence of an electric field

LIOUVILLE'S theorem states that, if q's refer to coordinates and p's to momenta of a system satisfying the Hamiltonian equations

$$\dot{p}_r=-\partial\mathcal{H}/\partial q_r, \quad \dot{q}_r=\partial\mathcal{H}/\partial p_r \tag{1}$$

then

$$\int\int\int\cdots\int \delta q_1\delta q_2\cdots\delta p_1\delta p_2\cdots = \text{constant with the time}, \tag{2}$$

where the δq's and δp's refer to variations in the coordinates and momenta between two different dynamical paths, and the integral is taken over some region conveniently thought of as infinitesimal in its practical application. In an analytically equivalent form, the theorem states that if in a generalized space representing as coordinates the coordinates and momenta of a dynamical system, we plot a group of points representing different possible states of the system and forming a density τ of such points in a certain vicinity of the space and if we follow the motion of the points in the generalized space, the density τ will remain constant with the time, i.e.,

$$D\tau/Dt=0. \tag{3}$$

This theorem has received a very beautiful application in the hands of Lemaitre and Vallarta[1] to the problem of electron motion in the earth's magnetic field. The system considered is a single electron and the generalized (phase) space is one of six dimensions. The different points in the phase space represent different possible states of the electron; and they may be extended in their meaning to apply to different electrons having different positions and velocities so long as the electrons are mutually non-interacting.

Let us mark out in the actual three dimensional space an elementary cone of solid angle $d\omega$ and of length dl, parallel to the direction of motion of the electron at that point, with its apex pointing in the direction of the resulting velocity of the particle. Let us truncate the apex of this cone by an element of area dS (perpendicular to dl) so as to cut off a length near the apex, small compared with dl. Consider the number δn of electrons which lie within this cone, which have component momenta between p_1 and p_1+dp_1 parallel to the axis of the cone and whose direction of motion is such that they travel through the base of the cone and through its truncated apex dS. Let us divide δn by the volume of the truncated cone, also by dS and by the product of dp_1 and dp_2dp_3 where dp_2 and dp_3 represent the mutually perpendicular infinitesimal ranges of momenta perpendicular to dl, which serve to specify the limits of momenta specified by the cone.[2] The result obtained is the density of the

[1] G. Lemaitre and M. S. Vallarta, Phys. Rev. **43**, 87 (1933).

[2] For purposes of description it is convenient to think of a cone with a rectangular cross section.

points in the phase space corresponding to the position of dS and to the vectorial magnitude of the momenta specified by the absolute magnitude thereof and by the direction of the cone. This is the quantity which, when multiplied by $dp_2dp_3/d\omega$ and also by the velocity corresponding to the momentum p_1, determines the intensity of electron flux per unit range of p_1 in the direction of p_1, i.e., the number of electrons per unit range of momentum p_1 passing per second through unit area perpendicular to dl, per unit solid angle.

In order that equality of density in the phase space along a dynamical path shall imply equality of intensity in the above sense, it is necessary that $dp_2dp_3/d\omega$ shall be constant. If du_2 and du_3 are the velocity ranges corresponding to $d\omega$ and u_1 is the velocity corresponding to p_1, constancy of $dp_2dp_3/d\omega$ implies constancy of $u_1^2dp_2dp_3/du_2du_3$. For convenience of discussion we shall use the term, particle momentum, to designate the quantity p' defined as

$$p' = m_0u/(1-u^2/c^2)^{\frac{1}{2}} \tag{4}$$

where u is the velocity. Now if in the foregoing discussion we could regard the momentum as p', the constancy of $u_1^2dp_2dp_3/du_2du_3$ would be provided for in the case of motion in a pure magnetic field, since in that case u^2 is constant, and so p' is vectorially proportional to u. It is to be observed, however, that the p's which occur in (2) are the p's which occur in (1); and, in its application in (1) p is not the same as p', but is given by

$$p = m_0\mathbf{u}/(1-u^2/c^2)^{\frac{1}{2}} + (e/c)\mathbf{U}, \tag{5}$$

where $\mathbf{U}$ is the vector potential which determines the magnetic field. For, the relativistic Lagrangian function for the electron is

$$L = -m_0c^2(1-u^2/c^2)^{\frac{1}{2}} + (e/c)(\mathbf{U}\cdot\mathbf{u}) - e\varphi, \tag{6}$$

where φ is the scalar potential and p is defined as

$$p = \partial L/\partial u,$$

which leads to (5). This is the p which occurs in the Hamiltonian function $\mathfrak{H}$, given by

$$\mathfrak{H} = m_0c^2\{1+(1/m_0^2c^2)[(p_x-(e/c)U_x)^2 + (p_y-(e/c)U_y)^2+(p_z-(e/c)U_z)^2]^{\frac{1}{2}}\} + e\varphi. \tag{7}$$

The quantity $(e/c)\mathbf{U}$ in (5) is not a small term. It is comparable with the whole magnitude of p and, of course, varies with the position of the electron in its path, since it is the quantity whose curl determines the magnetic field. Thus although $|u|$ remains constant in the path, $|p|$ does not. It is the presence of $\mathbf{U}$ in (6) which through the Lagrangian equations leads to the very term $\mathbf{u}\times\mathbf{H}/c$ which in the equation of motion

$$\frac{d}{dt}\left[\frac{m_0\mathbf{u}/e}{(1-u^2/c^2)^{\frac{1}{2}}}\right] = E + \frac{\mathbf{u}\times\mathbf{H}}{c} \tag{8}$$

represents the action of the magnetic field on the electron.[3]

The point here raised is not something concerned merely with the theory of relativity. For the only effect of neglecting relativity is to replace (5) by

$$p = m_0\mathbf{u} + e\mathbf{U}/c.$$

It is *only* with p understood in this sense that even the nonrelativistic equations assume the Hamiltonian form in their story of the action of the magnetic field on the electron.

In order therefore that the conclusions of Lemaitre and Vallarta may be substantiated, it is necessary to show that although (1) is most assuredly not true for the p''s, nevertheless (2) is true with the p's replaced by p''s. To this end we make, through (4) and (5) the mathematical transformation

$$p = p' + e\mathbf{U}/c, \tag{9}$$

$$q = q'. \tag{10}$$

Expression (2) then yields

$$\int\int\int\cdots\int J\delta q_1\delta q_2\cdots\delta p_1'\delta p_2'\cdots = \text{constant with time}, \tag{11}$$

[3] Or if we speak in terms of the Hamiltonian equations, it is the presence of $\mathbf{U}$ in (7) which leads through (1) to the $\mathbf{u}\times\mathbf{H}/c$ in (8).

where J, the Jacobian of the transformation is given by

$$J=\begin{vmatrix} 1 & 0 & 0 & 0 & 0 & 0 \\ 0 & 1 & 0 & 0 & 0 & 0 \\ 0 & 0 & 1 & 0 & 0 & 0 \\ \dfrac{\partial U_x'}{\partial q_x} & \dfrac{\partial U_x'}{\partial q_y} & \dfrac{\partial U_x'}{\partial q_z} & 1 & 0 & 0 \\ \dfrac{\partial U_y'}{\partial q_x} & \dfrac{\partial U_y'}{\partial q_y} & \dfrac{\partial U_y'}{\partial q_z} & 0 & 1 & 0 \\ \dfrac{\partial U_z'}{\partial q_x} & \dfrac{\partial U_z'}{\partial q_y} & \dfrac{\partial U_z'}{\partial q_z} & 0 & 0 & 1 \end{vmatrix}$$

where $\mathbf{U}'$ is written in short for $e\mathbf{U}/c$. Hence the Jacobian J is unity, and a theorem analogous to Liouville's theorem also holds for the q's and p''s, which justifies the ultimate conclusions of Lemaitre and Vallarta. It will be seen, moreover, that the validity of this extended form of Liouville's theorem is not limited to the case where an electric field is absent but is quite general. Absence of electric field is, of course, necessary in the application to the cosmic-ray problem.

The foregoing argument tends perhaps to conceal the mathematical mechanism of the process. The establishment of the result at one blow by utilization of the properties of the Jacobian seems to imply that it should be obvious. For this reason and in view of the importance of a clear realization of what is happening, we shall establish the result in a way in which the $\mathbf{U}$ in (5) plays a more conspicuous rôle, a rôle comparable with its importance in determining the dynamical paths, for example, and in which it only disappears finally by a sort of accidental cancellation to yield in terms of the q's and p''s a theorem which is the equivalent of Liouville's.

We shall discuss the method along the line which seeks to prove that the density of the points in the phase space does not change with the time.

Following precisely the usual method, as, for example, that given by Jeans[4] we arrive at

$$(D\tau/Dt)+\tau\sum_1^3\{(\partial\dot{p}_r/\partial p_r)+(\partial\dot{q}_r/\partial q_r)\}=0, \quad (12)$$

where τ is the density of the points in the multidimensional space, which in our problem is a six dimensional space, with coordinates q_x, q_y, q_z, p_x, p_y, p_z.

Up to this point no dynamics has been used. If at this stage, however, we assume (1), the curly bracket in (12) vanishes and we find that τ is constant with the time. If we use the quantities p' and q' defined by (9) and (10), the Hamiltonian equations do not hold, however, and it is necessary to find what equations do hold. We have

$$d\mathfrak{H}=\frac{\partial\mathfrak{H}}{\partial q_x'}dq_x'+\frac{\partial\mathfrak{H}}{\partial q_y'}dq_y'+\frac{\partial\mathfrak{H}}{\partial q_z'}dq_z'+\frac{\partial\mathfrak{H}}{\partial p_x'}dp_x'+\frac{\partial\mathfrak{H}}{\partial p_y'}dp_y'+\frac{\partial\mathfrak{H}}{\partial p_z'}dp_z'.$$

Hence, by using (9) and (10)

$$\frac{\partial\mathfrak{H}}{\partial q_x}=\frac{\partial\mathfrak{H}}{\partial q_x'}-\frac{e}{c}\left(\frac{\partial U_x}{\partial q_x}\frac{\partial\mathfrak{H}}{\partial p_x'}+\frac{\partial U_y}{\partial q_x}\frac{\partial\mathfrak{H}}{\partial p_y'}+\frac{\partial U_z}{\partial q_x}\frac{\partial\mathfrak{H}}{\partial p_z'}\right),$$

$$\frac{\partial\mathfrak{H}}{\partial p_x}=\frac{\partial\mathfrak{H}}{\partial p_x'},$$

with similar expressions for the y and z coordinates and momenta. Hence, substituting in (1), and again using (9) and (10) we find

$$\dot{p}_x'+\frac{e}{c}\left(\frac{\partial U_x}{\partial t}+\dot{q}_x\frac{\partial U_x}{\partial q_x}+\dot{q}_y\frac{\partial U_x}{\partial q_y}+\dot{q}_z\frac{\partial U_x}{\partial q_z}\right)$$
$$=-\frac{\partial\mathfrak{H}}{\partial q_x'}+\frac{e}{c}\left(\frac{\partial U_x}{\partial q_x'}\frac{\partial\mathfrak{H}}{\partial p_x'}+\frac{\partial U_y}{\partial q_x'}\frac{\partial\mathfrak{H}}{\partial p_y'}+\frac{\partial U_z}{\partial q_x'}\frac{\partial\mathfrak{H}}{\partial p_z'}\right); \quad (13)$$

also

$$\dot{q}_x'=\partial\mathfrak{H}/\partial p_x', \quad (14)$$

with similar expressions for the other directions.

Hence, substituting in (13) from (14) and from the corresponding expressions for $\dot{q}_y'$ and $\dot{q}_z'$ and further observing that $q=q'$ and $\partial U/\partial q_z=\partial U/\partial q_z'$, we have

$$\dot{p}_x'=-\frac{\partial\mathfrak{H}}{\partial q_x'}+\frac{e}{c}(\dot{q}_y'H_z-\dot{q}_z'H_y)-\frac{e}{c}\frac{\partial U_x}{\partial t}, \quad (15)$$

$$\dot{q}_x'=\partial\mathfrak{H}/\partial p_x', \quad (16)$$

[4] J. H. Jeans, *The Dynamical Theory of Gases*, 4th Edition, pp. 70–71, Cambridge University Press.

in which we have observed that the magnetic field $\mathbf{H}$ is given by $\mathbf{H}=\text{curl }\mathbf{U}$.[5] Returning then to (12), when p' and q' are used instead of p and q and when (15) and (16) and their corresponding expressions in y and z are used, (12) becomes

$$-\frac{D\tau}{Dt}=\tau\sum_1^3\left(\frac{\partial\dot{p}_r'}{\partial p_r'}+\frac{\partial\dot{q}_r'}{\partial q_r'}\right)=\tau\sum_1^3\left(\frac{\partial^2\mathfrak{K}}{\partial q_r'\partial p_r'}-\frac{\partial^2\mathfrak{K}}{\partial p_r'\partial q_r'}\right)-\tau\frac{e}{c}\frac{\partial}{\partial t}\left(\frac{\partial U_x}{\partial p_x'}+\frac{\partial U_y}{\partial p_y'}+\frac{\partial U_z}{\partial p_z'}\right)$$

$$+\frac{e\tau}{c}\left\{\frac{\partial}{\partial p_x'}(\dot{q}_y'H_z'-\dot{q}_z'H_y')+\frac{\partial}{\partial p_y'}(\dot{q}_z'H_x-\dot{q}_x'H_z)+\frac{\partial}{\partial p_z'}(\dot{q}_x'H_y-\dot{q}_y'H_x)\right\}. \quad (17)$$

The first term on the right-hand side vanishes and the mechanism of its vanishing is representative of what is the whole story in the case of equations of Hamiltonian form. Here, however, we have the additional terms shown. Since $\mathbf{U}$ and $\mathbf{H}$ are expressible entirely in terms of the q's and so of the q''s, they are independent of the p''s, so that (17) becomes

$$-\frac{D\tau}{Dt}=\frac{e\tau}{c}\left\{H_x\left(\frac{\partial\dot{q}_z'}{\partial p_y'}-\frac{\partial\dot{q}_y'}{\partial p_z'}\right)+H_y\left(\frac{\partial\dot{q}_x'}{\partial p_z'}-\frac{\partial\dot{q}_z'}{\partial p_x'}\right)+H_z\left(\frac{\partial\dot{q}_y'}{\partial p_x'}-\frac{\partial\dot{q}_x'}{\partial p_y'}\right)\right\}.$$

In view of (16), each of the parentheses vanish, and we are left with

$$D\tau/Dt=0.$$

Hence, although the equations of electron motion are not of Hamiltonian form in terms of the spacial coordinates and the particle momenta p', Liouville's theorem extends to apply with these coordinates and momenta also. It will be observed that our proof is in no way limited to the case where there is no electric field.

---

[5] This relation is not fundamentally germane to the discussion and is introduced simply for convenience of notation.

The Absolute Saturation of Cubic Cobalt

ROBERT I. ALLEN* AND F. W. CONSTANT, *Duke University*

(Received May 12, 1933)

With an ellipsoid of cobalt, quenched so as to be in the cubic state, and Weiss' method of extracting the ellipsoid from the field of a powerful electromagnet, the magnetization was measured for a given temperature but increasing field strengths. With Weiss' formula for the approach to saturation the magnetization for infinite field was calculated. The Weiss formula fitted the upper half of the experimental curve within 0.03 percent. When the saturation magnetizations, J_{ST}, obtained for 13 temperatures were plotted against the square of the absolute temperature a straight line was obtained. When this was extrapolated to absolute zero the saturation intensity (J_{SO}) was found to be 1418. By plotting J_{ST}/J_{SO} against $(\mathbf{T}/\theta)^2$, θ being the Curie point, the line obtained coincided with that for iron and nickel, but not with the curve for hexagonal cobalt nor the line found for orthorhombic crystals. It is indicated that crystal structure plays an important part in ferromagnetism.

THE purpose of this investigation was to determine the absolute saturation intensity of magnetization for cubic cobalt and the law of approach to saturation as a function of the magnetic field and the absolute temperature. It was also of interest to discover if cubic cobalt shares the same reduced-saturation-*vs.*-reduced-temperature curve with the cubic crystals, iron and nickel, or with the "pseudo-cubic" group such as magnetite and cementite. This problem was suggested by Dr. Francis Bitter.[1]

The method adopted was a slight modification of that employed by Weiss and Forrer[2] in determining similar data for several other substances—particularly iron, nickel, magnetite and cementite. It consisted of a repeated extraction of the substance in the form of an ellipsoid of revolution from a system of coils placed in the field of a powerful electromagnet having conical pole pieces and the measurement of the magnetization by the deflection of a ballistic galvanometer which had been calibrated in terms of a known magnetic moment. Before each extraction the ellipsoid was immersed in a pentane bath of known temperature previously cooled with liquid air. The range of temperatures investigated was from the boiling point of liquid air to that of boiling water. The extraction was accomplished by means of the mechanism indicated in Fig. 1. Operation of a trigger released a brass rod (R), to the lower extremity of which the ellipsoid was secured by a Bakelite clamp (B), thus permitting a tightly stretched spring (S) suddenly to jerk the ellipsoid out of the center of the field, the induction coils (C, C, C', C'), and the Dewar flask (F) containing the pentane (P). An air cushion was arranged to stop the rapid movement of the rod. The throw of the ellipsoid was about 20 cm. Weiss and Forrer used a throw of only 11.8 cm and estimated that the error introduced for failure to extract to infinity amounted to only 0.1 percent in a field of 20,000 gauss.

The ellipsoid of cobalt was obtained from Ward's Natural Science Establishment, Inc. of the University of Rochester and showed the following analysis (in percent): cobalt, 98.00; nickel, 0.75; iron, 0.48; sulphur, 0.10; silicon, 0.05; carbon, 0.25; aluminum, 0.25. To make sure that the cobalt was in the cubic crystalline form, the ellipsoid was very carefully heated above its Curie point (θ) (1413°A) and quenched in oil, precautions being taken to prevent oxidation and other injury.

The dimensions of the ellipsoid were: major axis, 1.00 cm; minor axis, 0.42 cm; volume, 0.0924 cc. The ellipsoidal shape was preferable because of the greater ease afforded for magnetizing it uniformly as well as calculating its demagnetizing effect upon the magnetic field.

* Part of a dissertation presented for the degree of Doctor of Philosophy in the Graduate School of Arts and Sciences of Duke University.

[1] Bitter, Phys. Rev. [2] **39**, 337 (1932); also personal correspondence.

[2] Weiss and Forrer, Ann. de Physique [10] **12**, 279 (1929).

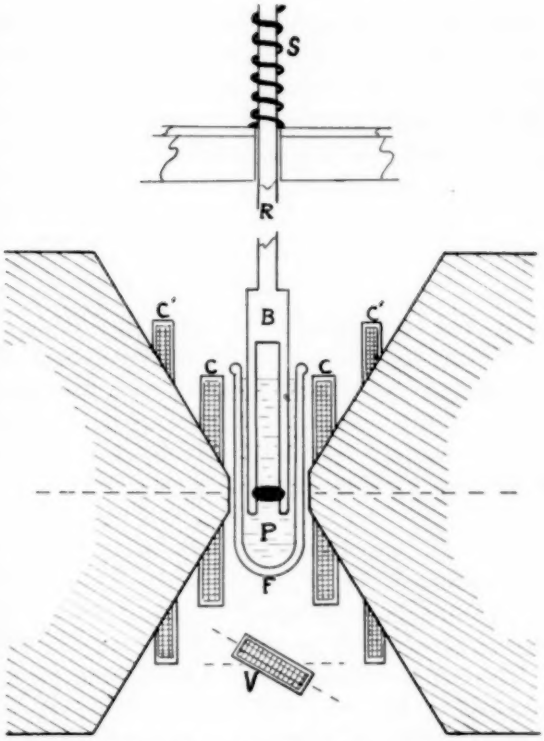

FIG. 1. Experimental arrangement.

Measurements accompanying extraction were possible at the rate of about one in every two minutes, simultaneous readings being taken of the exciting field current, the temperature, and the galvanometer deflection. Over 1500 extractions were observed.

The thirteen temperatures at which extractions were made are as follows: 93, 130, 137, 156, 180, 196, 202, 222, 240, 257, 273, 306, and 373° absolute. These were measured by means of a copper-constantan thermocouple which had been calibrated at the following temperatures: boiling liquid air, carbon dioxide snow and ether, melting ice, room temperature, and boiling water. The "null method" was used in determining the thermocouple readings. The contact junction was mounted in the pentane bath very near the position occupied by the ellipsoid before extraction. Convection in the pentane was sufficient to fully refrigerate both the ellipsoid and thermocouple.

The field strength of the electromagnet was adjusted by a rheostat which regulated the exciting current. Extractions of the ellipsoid were made at the following settings of field current: 0, 4, 9, 12, 14, 16, 17, 18, 19, 20, 21, 22, 23, 24, 25, 26, 27, 28, 29 and 30 amperes. By means of a previously calibrated bismuth spiral these amperes of field current were converted into gauss of field strength. It was found that the latter was a linear function of the current between 16 and 30 amperes.

It was necessary to correct these values of the field strength ($\mathbf{H}_0$) on account of the demagnetizing effect of the ellipsoid, by using the following relation given by Ewing:[3]

$$\mathbf{H}_e = \mathbf{H}_0 - \mathbf{N}\mathbf{J},$$

where $\mathbf{H}_e$ is the effective magnetizing force, $\mathbf{J}$ the intensity of magnetization and $\mathbf{N}$ the demagnetizing factor found from the equation:

$$\mathbf{N} = 4\pi\left(\frac{1}{\mathbf{e}^2} - 1\right)\left(\frac{1}{2\mathbf{e}}\log\frac{1+\mathbf{e}}{1-\mathbf{e}} - 1\right).$$

Here $\mathbf{e}$ is the eccentricity of the ellipsoid. The value thus obtained for $\mathbf{N}$ is 1.79, the demagnetizing factor. The corrected values of the field strength for the ellipsoid at room temperature are shown in Table I, column 4. These values approximated closely those for other temperatures as $\mathbf{J}$ did not vary over 1 percent.

INDUCTION COILS AND COMPENSATION SYSTEM

The induction coils to which the ballistic galvanometer was connected are represented by *C*, *C* in Fig. 1. These were in the form of two thin disks, each mounted on opposite pole pieces near the center of the field, their axes being in line with the latter. They were of sufficiently large diameter so that when the small ellipsoid was placed lengthwise in the field and then extracted the change in induction would produce a galvanometer deflection proportional to the magnetic moment of the ellipsoid.

If it had been found possible to maintain the exciting field current perfectly constant, coils *C*, *C* would have constituted a sufficient induction system; but due to slight fluctuations of the field, the water pressure in the cooling system of the electromagnet, the high sensitivity of the induction coils and galvanometer and other

[3] Ewing, *Magnetic Induction in Iron and Other Metals*, Chapter I.

causes, the resulting effect would produce a continual drifting of the zero position of the galvanometer even though the ellipsoid remained fixed. To overcome this difficulty it was found necessary to use an additional pair of "compensation coils" (C', C'), similar to C, C, except larger and farther away from the ellipsoid. These two compensation coils, their axes being coincident with the main flux, were connected in opposition to the induction coils (C, C) so as to exactly balance out any change of flux caused by the effect just described. On the other hand, due to the relatively close proximity of the interior coils (C, C) to the ellipsoid, any change in flux due to its extraction would produce a predominating influence only upon C, C.

On account of the unequal approach to saturation in different parts of the pole pieces the compensation coils (C', C') were insufficient to give perfect compensation except for a single excitation. It was therefore necessary to connect in series with the coil system and galvanometer a small "vernier compensation coil" (V). This was mounted in one edge of the main field, near the other coils, upon a horizontal axis in such a manner that its effect would add to or subtract from the effect of the compensation coils (C', C'). Table I, column 2, shows the angular settings (as read upon a divided scale attached to the shaft comprising the axle) for complete compensation corresponding to the various values of main flux used. The compensation was adjusted by observing whether any galvanometer deflection accompanied the lowering of the field current by one or two percent, the correct adjustment being that position for which no deflection was obtained.

TABLE I.

Field current (Amp.)	Position of compensation coil (Degrees)	Image correction coefficient	Effective magnetic field ($\mathbf{H}_e$) (Gauss)
0	0	1.000	25
4	0	1.000	1580
9	18	1.118	6500
12	47	1.441	8290
14	59	1.625	9053
16	69	1.773	9525
17	74	1.840	9722
18	79	1.902	9890
19	84	1.952	10045
20	89	2.000	10200
21	94	2.042	10350
22	96	2.085	10500
23	98	2.115	10692
24	99	2.140	10845
25	100	2.155	11005
26	101	2.165	11180
27	101	2.171	11330
28	102	2.175	11500
29	102	2.178	11675
30	102	2.180	11825

Magnetic Images

As the pole pieces of the electromagnet approach saturation their permeability diminishes to a marked extent causing the sensibility of the measuring apparatus to decrease proportionately. It was therefore necessary to determine experimentally the sensibility as a function of the excitation, and accordingly correct all galvanometer deflections for each extraction of the ellipsoid. Weiss termed this effect, "magnetic images," by analogy with the electrical images of Lord Kelvin.[4]

This study was made by substituting for the ellipsoid a definite magnetic moment in the form of a little coil which occupied approximately the same volume as the former. Instead of extracting the "image coil," a current of 1.800 amperes was reversed, thereby doubling the resulting galvanometer deflection. By starting with a deflection of 474.0 mm when the magnet was not excited, the deflection decreased to 217.4 mm for the maximum excitation of 30 amperes. Table I, column 3, gives this important "image correction" in the form of a ratio:

$$\frac{\text{image deflection for zero excitation of electromagnet}}{\text{image deflection for specific excitation of electromagnet}}$$

for each value of the exciting current used. These coefficients show the averages of more than 1000 observations of the "image effect."

The image coil consisted of 114 turns, wrapped upon a copper rod 4 mm in diameter. Its length was 1.0 cm and its outer diameter about 6 mm. It was mounted inside a glass tube through which a water current circulated to prevent noticeable rise in temperature during the brief period of time required for commutation of 1.800 amp.

[4] Weiss, Ann. de Physique [10] **5**, 171 (1926).

Obviously, to correct a given galvanometer deflection produced by the extraction of the ellipsoid, it is only necessary to multiply by the "image effect coefficient" corresponding to the particular field excitation used. Fig. 2, curve *B*, is

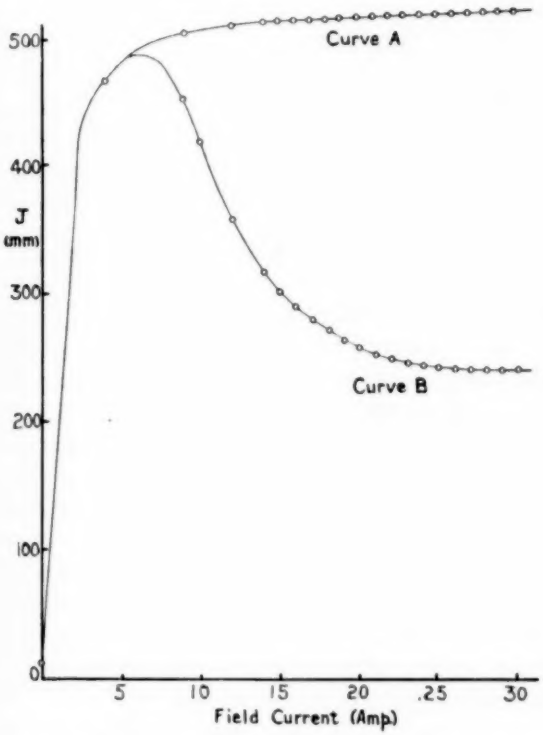

FIG. 2. Typical magnetization curve; Curve *A* corrected and curve *B* uncorrected, for image effect.

a typical case giving the relation at room temperature between the field excitation and the galvanometer deflection as actually observed when the ellipsoid was extracted. Curve *A* of this same figure shows the same data *after* correcting for the image effect. Similar curves were obtained for the thirteen different temperatures investigated.

ABSOLUTE CALIBRATION

The curves last mentioned were plotted in terms of the image-corrected galvanometer deflection as a function of the excitation. It now remains to determine the constant ratio by which the *Y*-axis may be calibrated in terms of ordinary c.g.s. units of intensity of magnetization (**J**). The calibration of the *X*-axis in terms of **H** has already been mentioned.

With the coil system and other physical conditions kept constant, and with a current of 9 amperes in the electromagnet, the ellipsoid was replaced at the center of the field by a small coil similar to that used in studying the image effect. This "absolute calibration coil" consisted of 395 turns and had an effective area of 101.300 cm^2. When a current of 1.000 ampere was reversed in this coil there resulted a galvanometer deflection of 73.3 mm. Correcting for the image effect (1.118), the deflection amounted to 81.9 mm. Thus, since a known magnetic moment of 20.260 c.g.s. units produced a deflection of 81.9 mm, the ratio obtained is 0.247 c.g.s. units per mm. Now, dividing this ratio by the volume of the ellipsoid (0.0924 cc), the necessary coefficient for calibrating the galvanometer deflections in terms of the desired intensity of magnetization units is determined to be 2.67 c.g.s. units per mm per cc.

EFFECTIVE AREA OF CALIBRATION COIL

In the previous paragraph the effective area of the calibration coil was given as 101.300 sq. cm. This calculation was accomplished by comparing this coil with a larger coil of known area, the latter consisting of three turns wound closely upon a hollow Bakelite cylinder 6.994 cm in diameter, hence 115.257 sq. cm in total area. The small calibration coil was carefully mounted in the center of the larger coil, the two axes being coincident. These two coils were placed in the center of, and with axes coincident to, a uniform and intense magnetic field, the latter being produced by a large solenoid 133 cm long and 9.48 cm in diameter, and wound upon a hollow smooth cardboard cylinder. With the two coils connected in opposition to each other, a current of 16 amperes was commutated in the large solenoid which caused a deflection of 57.6 mm upon a ballistic galvanometer connected in series with the two coils. Again, with the two smaller coils connected in the same sense, a deflection of 893.34 mm resulted. The larger coil had the bigger effective area. From these two deflections and the area of the larger coil that of the calibration coil was obtained.

Results and Discussion

According to the recent theory of ferromagnetism advanced by Weiss,[5] Heisenberg,[6] Bitter[7] and others an unmagnetized sample of cobalt is regarded as made up of numerous regions each containing many atoms. Each region is supposed to be magnetized to saturation by a large "internal" or "molecular field," but the direction of this magnetization varies at random from block to block so that the specimen as a whole appears unmagnetized. Application of an external field merely tends to line up the directions of magnetization of the blocks, saturation being reached when they are all parallel. This saturation magnetization $\mathbf{J}_{ST}$ depends on the temperature $\mathbf{T}$, and investigation of its variation with $\mathbf{T}$ is equivalent to a study of the behavior of the atoms of a single region. Such data should be more valuable in checking theories as to the nature of ferromagnetism than results based on the statistical behavior of many regions, such as hysteresis curves.

It was first necessary to calculate $\mathbf{J}_{ST}$ for each temperature investigated. Although saturation could not be obtained experimentally Weiss and Forrer have established that the approach to saturation at a given temperature is represented very well by the equation

$$\mathbf{J}_{HT}=\mathbf{J}_{ST}(1-\mathbf{a}/\mathbf{H}),$$

where $\mathbf{J}_{HT}$ is the magnetization at the field $\mathbf{H}$, and $\mathbf{a}$ is a constant for a given temperature which measures the magnetic hardness. It was possible in this work to assign such values to $\mathbf{a}$ and $\mathbf{J}_{ST}$ that $\mathbf{J}_{HT}$ would fit the experimental curves within 0.03 percent between field currents of 16 and 30 amperes in the electromagnet. This verified Weiss and Forrer's formula for cubic cobalt. Fig. 3 shows in more detail the portion for high fields of curve *A* of Fig. 2, and similar curves for three other typical temperatures. It was to curves such as these that Weiss and Forrer's formula was applied to obtain $\mathbf{J}_{ST}$ for each of the thirteen temperatures.

The thirteen values of $\mathbf{J}_{ST}$ obtained were

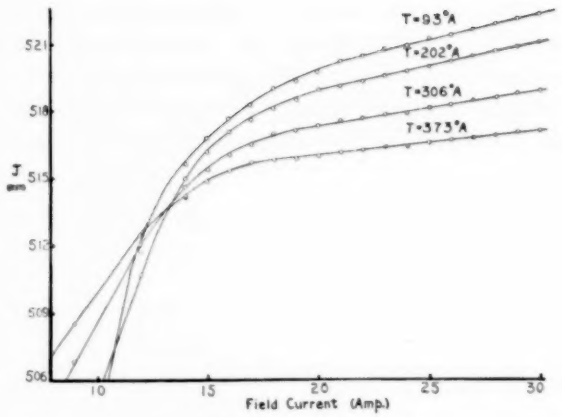

Fig. 3. Typical magnetization curves in region where Weiss and Forrer's formula could be applied.

plotted as a function of the square of the absolute temperature. As in the case of the materials previously investigated a straight line was obtained which was extrapolated to absolute zero, giving $\mathbf{J}_{SO}$, the absolute saturation of cubic cobalt, which was found to be 1418 c.g.s. units per cc. With the weight of the ellipsoid (0.8180 g) and the density of cobalt (8.9) the value obtained was 1426. The error in these values is estimated at 2 percent, due chiefly to the absolute calibration. The error in the points of Fig. 4, which do not involve this calibration, is estimated at less than 0.5 percent.

According to Honda and Masumoto[8] the absolute saturation should be the same for cubic

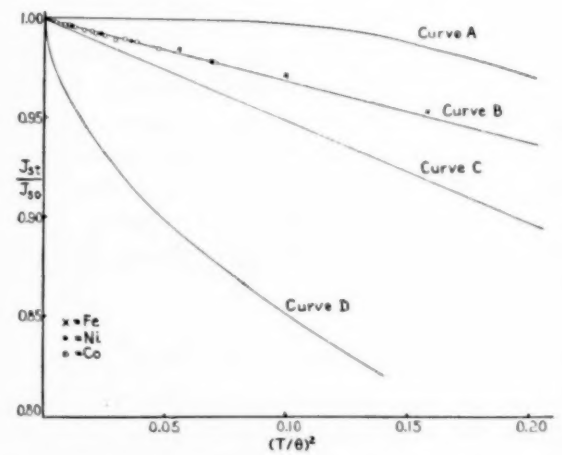

Fig. 4. Reduced magnetization ($\mathbf{J}_{ST}/\mathbf{J}_{SO}$) *vs.* square of reduced temperature ($\mathbf{T}/\theta$).

[5] P. Weiss and G. Foex, Le Magnetisme, 101 (A. Collin, 1926).

[6] W. Heisenberg, Zeits. f. Physik **49**, 619 (1928).

[7] F. Bitter, Phys. Rev. **42**, 697 (1932).

[8] K. Honda and H. Mazumoto, Sci. Reports of Tohoku U. **20**, 323 (1931).

and hexagonal cobalt. A summary of the values of the saturation magnetization found by previous observers, who probably used a mixture of the two forms, is given in Table II for comparison. As most of these values are for room temperature it must be remembered that saturation at absolute zero is about 1 percent higher.

TABLE II. *Saturation values for cobalt.*

Observer	J	t
Ewing, 1889	1310	20°C
Weiss, 1910 (162, 8.9)	1442	17°C
Stifler, 1911	1421	20°C
Williams, 1915	1504	20°C
Barker, 1916 (from Kerr Effect)	1398	20°C
Honda and Masumoto, 1931 (single crystals)	1446	−273°C

Finally, the reduced saturation intensity ($\mathbf{J}_{ST}/\mathbf{J}_{SO}$) was plotted against the square of the reduced temperature ($\mathbf{T}/\theta$), where θ is the Curie point for cobalt, taken as 1413°A. This curve should be the same for all ferromagnetic substances. Fig. 4 shows the results obtained in this work on cobalt together with that of others for other materials. It will be seen that cubic cobalt lies on the same line (curve *B*) as the cubic crystals, iron and nickel, but that the orthorhombic crystals, magnetite, cementite and Fe_2B, fall on another line (curve *C*), while hexagonal cobalt gives a still different curve. Curve *A* is the one obtained from Langevin's classical formula,

$$\mathbf{J}_{ST}/\mathbf{J}_{SO}=\coth \mathbf{x}-1/\mathbf{x},$$

and curve *D* represents the formula obtained theoretically when quantum modifications are included, i.e.,

$$\mathbf{J}_{ST}/\mathbf{J}_{SO}=\tanh \mathbf{x}.$$

Some modification of the present theories is obviously called for, and it is evident that crystal structure is an important factor which will have to be taken into account in future theories.

Erratum

Theory of Continuous Absorption of Oxygen at 1450A

E. C. G. STUECKELBERG, *University of Zürich, Switzerland*

(Phys. Rev. **42**, 518, 1932)

Drs. G. E. Gibson, O. K. Rice and N. S. Bayliss[1] have called the author's attention to a mistake in the above paper.

The first formula for the absorption coefficient α_ν on page 522 is correct.[2] In this formula the sum $\sum_J JN_J$ (or to be valid for all values of J, $\frac{1}{2}\sum(2J+1)N_J$) occurs. The number N_J stands for the pure Boltzmann factor

$$N\cdot\exp\,(B_0J(J+1)/kT)$$

and not for "the number of molecules in the state J" (which is equal to the Boltzmann factor multiplied by $(2J+1)$), because the summation over the sublevels $M(-J<M<+J)$ was taken care of in formula (2).

The value of the sum is therefore $\sum_J JN_J = N/2$ and Eq. (13) reads

$$\alpha_\nu = \frac{64\pi^{9/2}}{3}\cdot\frac{N\mu}{h^2\gamma a}\left(\frac{\nu}{c}\right)M^2(r_1)f\ \text{cm}^{-1}.$$

The calculations in Part II are obviously not affected by this change in (13), with the exception of $M(r_1)$. The correct value of $M(r_1)$ is

$$(4.77\times10^{-10}\ \text{g}^{\frac{1}{2}}\ \text{cm}^{\frac{1}{2}}\ \text{sec.}^{-1})\times0.50\times10^{-8}\ \text{cm}),$$

corresponding to the displacement of one electronic charge over 0.50A.[3]

[1] Gibson, Rice and Bayliss, Phys. Rev. **44**, 193 (1933). I am indebted to Drs. Gibson, Rice and Bayliss for seeing the manuscript of their paper before publication.

[2] The formula contains a typographical error. Read $\pi^{9/2}$ instead of $\pi^{9/8}$.

[3] This value is not very far off from the value given in the paper. This is due to the fact that a numerical mistake happened to cancel the error in formula (13).

LETTERS TO THE EDITOR

Prompt publication of brief reports of important discoveries in physics may be secured by addressing them to this department. Closing dates for this department are, for the first issue of the month, the twentieth of the preceding month; for the second issue, the fifth of the month. The Board of Editors does not hold itself responsible for the opinions expressed by the correspondents.

Dependence of the Absorption of Neutrons on Their Velocity

The purpose of this experiment was to see if the penetrating power of neutrons changes with their velocity. The absorption of neutrons obtained in three different ways was determined: (1) neutrons ejected in the forward direction from Be, (2) neutrons ejected backward from Be, (3) neutrons ejected forward from B. In all cases the alpha particles from polonium were used to produce the neutrons.

J. Chadwick[1] has found the maximum velocity of the neutrons in these three cases to be as shown in Table I. The average velocity of the neutrons emitted in these three cases will probably vary roughly as their maximum velocities.

An ionization chamber filled with hydrogen at 20 atmospheres pressure was used and the radiation was filtered by 2.5 cm of iron before entering the ionization chamber. Hydrogen was used since it gives a high ionization for neutrons but very little ionization for gamma-rays.[2] Diminution of the ionization current was determined when six centimeters of lead were interposed. The geometrical arrangement of the absorbers was the same in each of the three cases. The results are shown in Table I. It will be seen that over this range of velocities the faster neutrons are more easily absorbed by lead than the slower ones. It is suggested that this may correspond to the Ramsauer effect in electron absorption by inert gases where there is a similar range of velocities in which the penetrating power increases with decrease in velocity. It is likely that the absorption coefficient will decrease again for velocities higher than those here studied.

TABLE I.

Neutron group	Maximum velocity (Chadwick) (cm/sec.)	Decrease in ionization in 6 cm of lead (percent)
Be, forward	3.3×10^9	43.2 ± 1.8
Be, backward	2.7×10^9	36.1 ± 1.9
B, forward	2.5×10^9	32.0 ± 2.4

The different penetrating powers of the neutrons emitted from the other elements are probably due to their different velocities but measurements of their velocities have not been made. If we assume then that there is one velocity for which there is a maximum absorption and a decrease in absorption for either faster or slower neutrons, then for the extremely penetrating neutrons from fluorine[3] we see that there are two possibilities: (1) that these neutrons are even slower than those from boron or (2) that they are much faster than those from Be in the forward direction; the former possibility seems the more likely of the two. Similarly the easily absorbed neutrons from lithium[3] would probably be faster than those from Be.

T. W. BONNER

The Rice Institute,
Houston, Texas,
June 20, 1933.

[1] J. Chadwick, Proc. Roy. Soc. **A136**, 692 (1932).
[2] T. W. Bonner, Phys. Rev. **43**, 871 (1933).
[3] I. Curie and F. Joliot, Comptes Rendus **196**, 397 (1933).

The Heat Capacity of Gadolinium Sulfate Octahydrate Below 1° Absolute

A series of adiabatic demagnetizations has been carried out on $Gd_2(SO_4)_3\cdot 8H_2O$ for the purpose of determining the heat capacity below 1°K. The substance was repeatedly cooled from a common initial temperature to different final temperatures by the reduction to zero of various initial magnetic fields. From the value of the applied field and the initial temperature, the entropies at the lower temperatures were calculated in terms of the entropy at a standard temperature. The entropy of magnetization has been tabulated by Giauque and Clark.[1] 51.5 g of $Gd_2(SO_4)_3\cdot 8H_2O$ were used in the measurements. The heat capacity of the glass container was neglected. The measurements extend from 1.7°K to 0.287°K. The apparatus and method of temperature measurement were the same as that previously mentioned.[2] The magnetic field used ranged to 8000 gauss.

The experimental results are shown graphically in Fig. 1. They are compared with a theoretical curve obtained by considering the interaction of two gadolinium ions, treated as simple magnets. For simplicity in calculation the magnets were assumed to have clockwise and counterclockwise directions along the interatomic direction and along three symmetrically placed lines, making an angle of 60° with the interatomic direction. The single unknown in the equation

[1] Giauque and Clark, J. Am. Chem. Soc. **54**, 3135 (1932).
[2] Giauque and MacDougall, Phys. Rev. **43**, 768 (1933).

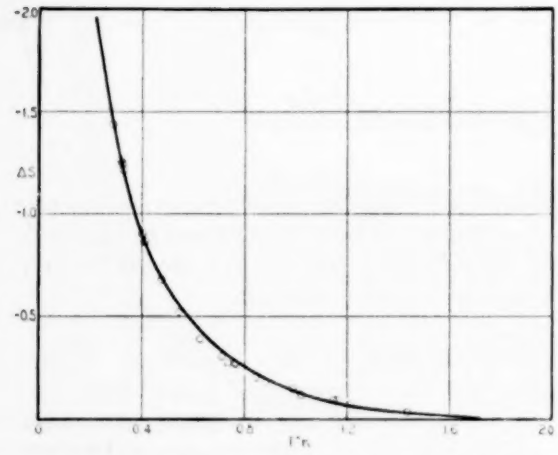

FIG. 1. Decrease in entropy below 1.7°K for $\frac{1}{2}$ mole of $Gd_2(SO_4)_3 \cdot 8H_2O$. The curve is calculated.

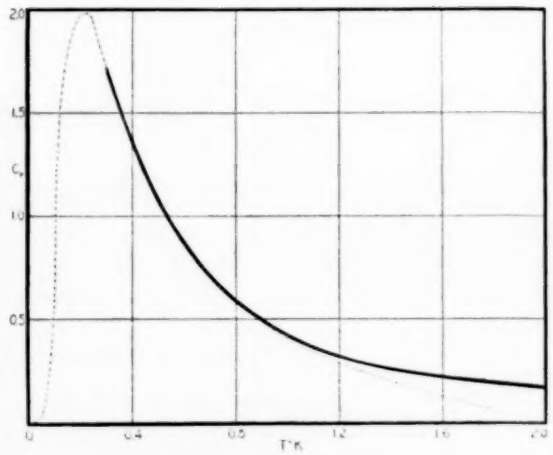

FIG. 2. Heat capacity in calories per degree for $\frac{1}{2}$ mole of $Gd_2(SO_4)_3 \cdot 8H_2O$.

was the distance between the coupled pair of gadolinium atoms. From the experimental data this was evaluated to be 3.5×10^{-8} cm. This is a reasonable order of magnitude since the distance would be 5.9×10^{-8} cm if uniform distribution of gadolinium atoms in $Gd_2(SO_4)_3 \cdot 8H_2O$ were assumed. The agreement shown by Fig. 1 is quite good but this should certainly not be taken as indicating that our geometrical assumptions are even approximately correct.

It is our purpose merely to show that any reasonable interaction theory will give an equation approximating the form indicated by our data. With the above assumption 64 states result from the possible couplings of the eight states known to exist in the case of a free gadolinium ion.

The data are also in quite good agreement with an equation proposed by Kürti.[3] Kürti assumed eight equally spaced levels with each atom acting independently. However, we believe that the extensive investigations of Kamerlingh Onnes and his associates on the effect of magnetic dilution on susceptibility measurements, demonstrate that the interaction mechanism is responsible for the observed heat capacity.

Heat capacities obtained from the data by means of the relation $dS/dT = C_p/T$ are in reasonably close agreement with those given by the theoretical equation. This is evident from Fig. 1. We have therefore shown that theoretical heat capacity curve in Fig. 2. The dotted portion below 0.28°K represents extrapolation. Above 1°K the dotted theoretical curve gives results that are too low. The upper solid curve above 1°K represents a junction of our experimental curve with that of Kürti, who has made calorimetric heat capacity measurements down to a temperature of 1.6°K. Our results near 1.6°K are lower than those of Kürti near this temperature, which probably marks the region of lowest accuracy in both investigations.

In connection with the theoretical equation it should be pointed out that an *a priori* weight of two is given to the lowest energy level by the assumption of isolated pairs of atoms. This leads to a zero point entropy of $\frac{1}{2}R\ln 2$ per gram atom of gadolinium. The consideration of more extensive atomic coupling would reduce this, until as a limit the zero point entropy would disappear from the expression. This would cause the heat capacity curve to drop off less rapidly on the low temperature side of the maximum.

It may be of interest to mention that the lower temperatures were measured with a precision of about three tenthousandths of a degree. The principal uncertainty in the results was caused by fluctuations in the current available for the magnet.

The above results are preliminary and the work will be repeated and extended under more favorable experimental conditions. The temperatures which have been obtained from an extrapolation of magnetic data will be placed on the thermodynamic scale.

A rough estimate shows that with a field of 8000 gauss and a starting temperature of 1°K, $Gd_2(SO_4)_3 \cdot 8H_2O$ should produce a temperature slightly below 0.2°K. With a field of 20,000 gauss at 1°K, the final temperature should be about 0.1°K. With increasing magnetic dilution, it should be possible to extend these estimates to still lower temperatures.

W. F. GIAUQUE
D. P. MACDOUGALL

Department of Chemistry,
University of California,
Berkeley, California,
June 29, 1933.

[3] Kürti, Zeits. f. physik. Chemie **20**, 305 (1933).

Disintegrations of Neon Nuclei by Fast Neutrons

Thirteen disintegrations of neon nuclei have been obtained in 3200 pairs of photographs of a Wilson cloud chamber through which neutrons were passing. In at least four of these the neutron seems to have been captured. The energy relations of these events were calculated on the basis of the assumption that the reaction which occurs is:

$$Ne^{20} + n^1 \rightarrow O^{17} + He^4$$
$$(19.9967 \pm 0.0009) + (1.0067 - E) \rightarrow (17.0032 - E' \pm 0.003) + (4.00216 \pm 0.0004).$$

Here E represents the energy converted into a γ-ray in the formation of a neutron from boron and E', the similar value for the formation of O^{17} from N^{14} by the capture of an alpha-particle by the latter. If E and E' are both zero, then 0.002 unit of mass or 1.9×10^6 electron-volts must be supplied. Since E is probably larger than E', the amount of energy which must be supplied is probably greater than 2×10^6 electron-volts.

The velocity v_n of the neutron, its kinetic energy KE_n, the kinetic energy $-\Delta KE$ which disappears in the reaction, and the energy which presumably escapes in the form of a γ-ray are given in Table I.

TABLE I.

	1	2	3	4
$v_n\times10^{-9}$ cm/sec.	3.9	4.5	5.3	5.1
$KE_n\times10^{-6}$ e.v.	7.8	10.6	14.5	13.4
$-\Delta KE\times10^{-6}$ e.v.	5.0	5.9	10.6	6.9
Energy of γ-ray $\times10^{-6}$ e.v.	3.1	4.0	8.7	5.0

The average energies in millions of electron-volts of the neutrons which have been found to disintegrate light nuclei are 5.8 for nitrogen, 7.0 for oxygen, and 11.6 for neon. The value for oxygen is taken from the work of Feather. The number of disintegrations from which the averages were taken is 19 for nitrogen but only 4 each for oxygen and neon. While the number is too small to show definitely what the relations are, it seems probable that the energy necessary for disintegration increases rapidly in the order N^{14}, O^{16}, Ne^{20}. The mass values indicate that the energy needed to supply mass in each of the reactions increases in this order. The actual values are uncertain but those now accepted indicate that the change of mass is equivalent to a decrease of 1.4×10^6 e.v. for nitrogen, a conservation of mass for oxygen, and an increase of $1.9\times10^{+6}$ e.v. for neon.

The kinetic energy which disappears in the disintegration of neon varies from 5.0 to 10.6×10^6 e.v. Of this, from 3.1 to 8.7×10^6 e.v. is presumably converted into a γ-ray. It is of interest that neon seems to follow the rule found for nitrogen and oxygen, which is that in every disintegration by capture kinetic energy is found to disappear, except that with nitrogen it may occasionally be conserved. In no case is there an increase of kinetic energy.

The range-energy relations for O^{17} in neon are somewhat uncertain, and so the values given above should in this respect be considered as preliminary.

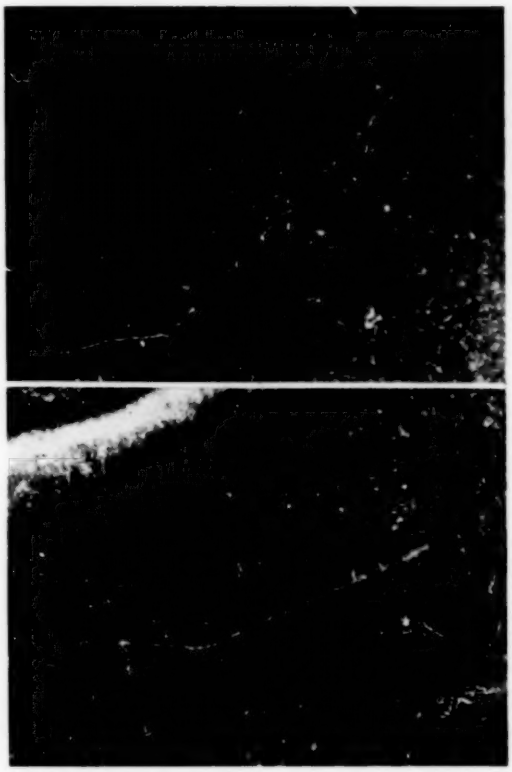

FIG. 1. Stereoscopic views of the disintegration of a neon nucleus by capture of a neutron.

The figure is a reproduction of a photograph of the disintegration of a neon nucleus by a neutron.

WILLIAM D. HARKINS
DAVID M. GANS
HENRY W. NEWSON

George Herbert Jones Chemical Laboratory,
University of Chicago,
June 29, 1933.

On The Production of Positive Electrons by Electrons

The experimental discovery of the positive electron makes possible, as has recently been observed by Oppenheimer and Plesset,[1] a consistent development of Dirac's theory of the electron, in which the appearance of pairs (electron and anti-electron) plays an important part. It appears that, in the experimental production of the pairs, the Coulomb fields, especially those of nuclei, are most important. In this case the theory shows that radiation of energy greater than $2mc^2$ is required for their production. Oppenheimer and Plesset have made a preliminary study of the production of pairs by γ-rays; we have carried through the analogous work for their production by high energy electrons (and positives). For γ-rays it appears, both from OP and from the experiments of Anderson, that the production of pairs becomes increasingly important as the energy of the γ-rays is increased; we have wanted to see whether this

[1] J. R. Oppenheimer and M. S. Plesset, Phys. Rev. **44**, 53 (1933) (hereafter referred to as OP).

is also true for electrons of high energy and to estimate the relative numbers of pairs produced by the two radiations. We shall see that for electrons of sufficiently high energy the production of pairs is as important as for γ-rays; and we believe that these processes will prove essential to an understanding of the behavior of the corpuscular component of the cosmic rays, in particular their absorption curves and the multiple tracks observed in cloud chambers.

We consider, then, a primary electron (or positive) of high energy passing through the Coulomb field of a nucleus; the primary may lose part of its energy and eject a pair. This process is similar to the photoelectric production of pairs in that a nucleus must take up a small recoil momentum, and differs from it in that the pair need not, and in general does not, receive all the energy of the primary radiation. We have treated the case in which the primary loses but a small part of its energy; this makes it possible to neglect the effect of interchange of primary and secondary and the effect of the nuclear field on the primary. When so formulated the calculation is altogether analogous to that of OP for the photoelectric production of high energy pairs. This parallelism between the two cases was maintained throughout the work. To this approximation primary electrons and primary positives behave alike and our results are equally applicable to both.

We have followed OP in using wave functions for the particles of the pair, correct to the first order only, in the field of the nucleus. This approximation is known to be invalid when these particles have very high energies and for this reason the OP results are unreliable for γ-rays of too high energy. The approximation appears, however, to be just sufficient to answer the question which we have put as to the relative importance of production of pairs for the two radiations. For the absolute number of pairs produced our results, too, are untrustworthy. Nevertheless, in our calculation it is only when the energy of the pair is too large that the results are invalid; the energy of the primary may be as great as one wishes.

On this basis the calculation can be made by a straightforward application of the quantum electrodynamics, which is formally analogous to the problem of the interaction of two electrons in an external field. For the case when the kinetic energies of the particles of the pair are large compared to their proper energies and still small compared to the energy of the primary, the differential cross section for production of a pair is:

$$\sigma d\epsilon_+ d\epsilon_- = (\pi/2)(Z\alpha)^2(e^4/m^2c^4)\{\epsilon_+^2+\epsilon_-^2+(8/\pi^2)\epsilon_+\epsilon_-\}(\epsilon_++\epsilon_-)^{-4}\ln(\epsilon_0^2/\epsilon_+\epsilon_-)d\epsilon_+ d\epsilon_-. \quad (1)$$

Here ϵ_0, ϵ_+, ϵ_- are the energies of the primary, positive, and electron in units mc^2, and Ze is the nuclear charge. The distribution in relative energies of positive and negative is of the same general sort as in the photoelectric case, there being a tendency toward unequal energies. The distribution in angle is also similar, the mean angles for positive, negative and deflected primary being of orders of magnitude $1/\epsilon_+$, $1/\epsilon_-$, $1/\epsilon_0$, respectively. Formula (1) shows that most of the pairs have small fractions of the primary energy, which justifies our having regarded this as the important case.

To get the total cross section for production of pairs one should integrate the differential cross section over all ϵ_+ and ϵ_-. We can get a lower limit on the total cross section by integrating (1) over the region for which it is valid. For very large ϵ_0 the result is

$$\int\sigma d\epsilon_+ d\epsilon_- \gtrsim \pi(Z\alpha)^2(e^4/m^2c^4)\ln\epsilon_0\cdot\ln\bar{\epsilon}. \quad (2)$$

Here $\bar{\epsilon}$ is the highest energy of a particle of the pair for which the first order calculation can be applied and is of the order of magnitude $(2\pi^2/Z\alpha)$. (In the case when $\epsilon_0 \gg 1$ but $\epsilon_0 < \bar{\epsilon}$, one must replace $\ln\bar{\epsilon}$ in (2) by $(\ln\epsilon_0)/2$.)

The cross section (2), which gives a lower limit to the production of pairs by high energy electrons (or positives), differs from the OP formula for the case of γ-rays by a factor of about

$$\begin{cases} \pi\alpha\ln\epsilon_0\cdot\ln\bar{\epsilon}, & \epsilon_0 > \bar{\epsilon} \\ (\pi\alpha/2)(\ln\epsilon_0)^2, & \epsilon_0 < \bar{\epsilon}. \end{cases} \quad (3)$$

For primary particles of energy 10^8 volts this factor is roughly 0.3; for 10^{10} volts it is about 1.2. Thus for the range of energies of the cosmic rays the production of pairs is surely as important for electrons and positives as it is for γ-rays.

We wish to thank Professor Oppenheimer for suggesting this problem to us and for much helpful advice.

W. H. Furry*
J. F. Carlson

California Institute of Technology,
Pasadena, California,
July 1, 1933.

* National Research Fellow.

The Relative Abundances of Elements of Even and Odd Mass Number and Atomic Number

In matter which is in equilibrium[1] as regards transmutations, the particles which obey the Fermi-Dirac statistics should be, as a rule, less abundant than the particles which obey the Einstein-Bose statistics; this should hold, whatever the ultimate particles are, of which nuclei are composed. The mean number of particles $\overline{X}_s$ of the sort s is always a monotonic increasing function[2] of μ_s for any particular value of the temperature T but there is a marked difference between the dependence of $\overline{X}_s$ upon μ_s in the case of Fermi particles on the one hand and in the case of Einstein particles on the other. For the former, it can be shown that as μ_s increases from 0 to infinity, $\overline{X}_s$ increases from 0 to infinity. For the latter, as μ_s increases from 0, $\overline{X}_s$ increases at first in the same way as before, but as μ_s approaches 1,

[1] T. E. Sterne, Phys. Rev. **43**, 585, 768, 1056 (1933); M.N.R.A.S. in press.

[2] The parameter μ_s defines the distribution of particles of the sort s in the Einstein or Fermi statistics. It always contains the factor $\exp[c^2M_s(f_H-f_s)/10{,}000RT]$. c is the velocity of light, R is the gas constant, M_s is the mass number, f_H and f_s are the packing fractions of hydrogen atoms and atoms s.

$\overline{X}_s$ approaches infinity; μ_s can never exceed unity for any Einstein particle when the assembly is in equilibrium. It follows, other things being equal, that particles of the latter type will be more numerous than particles of the former type, as is indicated in the approximate curves below, Fig. 1 (the vertical scale depends upon T and M_s). Other things are not equal, since different particles will have in general different μ's; nevertheless, the Einstein particles should be more numerous than the Fermi particles, *as a rule*, for matter in equilibrium.

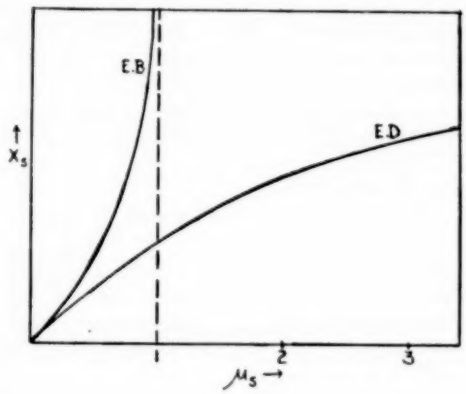

FIG. 1.

From studies of the band spectra of homonuclear molecules it appears that nuclei of even mass number obey the Einstein-Bose statistics while nuclei of odd mass number obey the Fermi-Dirac[3] statistics. One should, accordingly, expect to find a general preponderance of particles of even mass number, a preponderance due to the differences between the statistics. One should also, of course (for temperatures which are not too high) expect a general preponderance of particles of even *atomic* number, since μ is a decreasing function of the packing fraction, while the packing fractions of the lighter even numbered elements are smaller as a rule than the packing fractions of the lighter odd numbered elements.[4] This effect may well be greater than the effect of the differences between the statistics; together the effects lead one to predict a general preponderance of nuclei of even mass number and even atomic number, regardless of other details of nuclear constitution. The abundances in the lithosphere given in Table I are derived from a table compiled by Harkins;[5] it will be seen that nuclei of even mass number in fact predominate, as well as nuclei of even atomic number.

This is what one would expect if the matter of which the Earth is now made had once been in (or nearly in) equilibrium (the heavier elements are badly handicapped in showing themselves in the Earth's crust but the separation can hardly discriminate, in general, between even and odd atomic or mass numbers).[6]

The predicted preponderance of even mass numbers and atomic numbers was noted empirically by Harkins,[7] who also noted the comparative rarity, in the lithosphere and in meteorites, of elements of greater atomic number than nickel. The latter observation is in agreement with the predictions of the equilibrium theory; calculations have yielded a moderately complete "cut-off" of the elements beyond a certain mass number, depending upon the known shape of the packing fraction curve. The place where the cut-off starts depends to some extent upon the density and temperature but is usually beyond mass 56 and not far beyond it. It also depends upon theories of nuclear constitution (and thus differs from the other results mentioned in this letter), although not markedly.

TABLE I. *Abundances in the lithosphere.*

Element	Atomic number	Mass number	Percentage by Weight: Atomic number even	Atomic number odd	Mass number even	Mass number odd
O	8	16	47.33		47.33	
Si	14	28, 30	27.74*		>24.88	
		29				< 2.86
Al	13	27		7.85		7.85
Fe	26	56, 54	4.50		4.50	
Ca	20	40, 44	3.47		3.47	
Na	11	23		2.46		2.46
K	19	39, 41		2.46		2.46
Mg	12	24, 26	2.24*		> 1.52	
		25				< 0.72
Ti	22	48	0.46		0.46	
Totals			85.74	12.77	>82.16	<16.35

* This number includes all the isotopes.

T. E. STERNE*

The Jefferson Physical Laboratory,
Cambridge, Massachusetts,
July 7, 1933.

[3] See, for instance, Mullikan, Rev. Mod. Phys. **3**, 148, 149 (1931).

[4] Rutherford, Chadwick and Ellis, *Radiations from Radioactive Substances*, p. 530, Cambridge University Press.

[5] Rutherford and others, reference 4, p. 526. The limits for Si and Mg are calculated from Harkins' values and the chemical atomic weights.

[6] Urey and Bradley, Phys. Rev. **38**, 718 (1931), studied the abundances of isotopes in the Earth's crust and concluded that the observed ratios were not consistent with equilibrium at any temperature. It is sufficient to point out that they used the classical and not the quantum statistics and that the abundances in the Earth's crust cannot be typical of the whole interior (see H. Jeffreys, *The Earth*, 2nd ed., pp. 129, 137, 210, 217–220, 231, Cambridge University Press). Owing to the separation of certain materials to the center and possible changes of the Earth's total composition since its matter was last in equilibrium, the present traces of a former equilibrium constitution might well be of the sort discussed in this letter.

[7] Harkins, Phil. Mag. **42**, 305 (1921).

* National Research Fellow.

The Isotopic Constitution of Lithium in the Sun

Recent experiments on the disintegration of Li^7 nuclei by impact with comparatively slow protons (possible disintegration has been observed at as low as 13,000 volts) suggest that this process might occur thermally at the temperature of the interior of the sun. If the temperature were 100,000,000°C, the mean kinetic energy of agitation would be equivalent to 10,000 volts and Li^7, in the presence of hydrogen, would be disintegrated with sufficient rapidity to have completely disappeared from the sun unless it is being continually replaced by some other process. The presumably more stable isotope, Li^6, on the other hand, should not be disintegrated and one might expect to find the relative abundance of this isotope greater than it is on the earth (6 percent).

An opportunity for deciding this question is offered by the large isotope shift of 0.15A in the resonance lines of neutral lithium at λ6707.8, which has been investigated by Hughes.[1] These lines, which form a very narrow doublet, are the only lithium lines found in the sun and occur there only in the spot spectrum. They are split by the magnetic field of the spot into a pattern which is between a Zeeman and a Paschen-Back effect and is therefore unsymmetrical; this splitting has been carefully investigated by Kent.[2] The wave-lengths of the zero-field Li^7 doublet have been accurately measured by King[3].

The microphotometer curve shown in Fig. 1 was made from a plate taken in the first order of the 75-foot grating on Mount Wilson and very kindly lent to the author by Dr. King. The plate has two exposures of the spot spectrum, both of which were microphotometered to make sure that none of the details of the line shape were caused by a chance defect in the emulsion. The spot was very near the center of the sun's disk; therefore the line of sight was nearly parallel to the magnetic field and only the perpendicular components of the Zeeman pattern had to be considered.

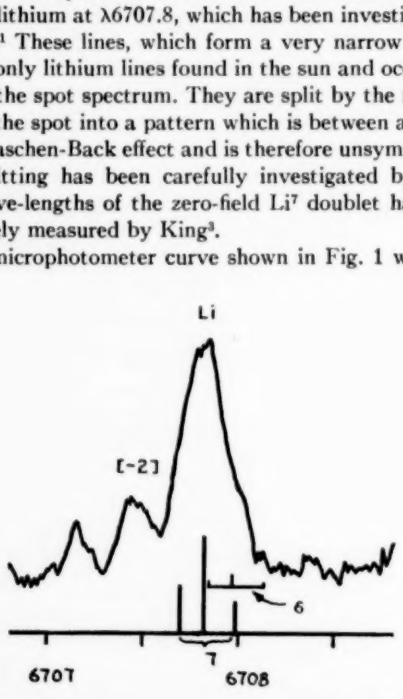

FIG. 1. Microphotometer curve of the lithium line λ6707.8 in the sun spot spectrum. Positions of Li^7 and Li^6 lines are shown below. No line is found in the disk spectrum at the position of the Li line.

The vertical lines drawn upward from the lower border of the figure are the components of the Li^7 line in a field of 3555 gauss, as observed by Kent. (The pattern is theoretically more complicated but it appeared as three lines with his resolving power, which is sufficient for our purpose. The fields of sun spots range from 3000 to 4000 gauss.) The components of the Li^6 line are shown above and to the right, their lengths relative to those of Li^7 being in the ratio of the terrestrial abundances.

It is immediately obvious that the whole observed line can be accounted for by the presence of Li^7 alone. The only evidence for the existence of Li^6 is a tiny hump in the position of the component farthest to the red, but this is no larger than the irregularity of the background, and may not be real. While we cannot definitely confirm the presence of Li^6, we can by assuming that this hump is due to Li^6, set an upper limit to its abundance. By a consideration of the Rowland intensities of the lines and from the calibration of the Rowland scale by Russell, Adams, and Moore,[4] we conclude that the abundance of Li^6 is less than 12 percent.

This result, that the relative abundance of Li^6 on the sun is certainly not much greater than on the earth, seems to indicate that the temperature of the sun's interior is lower than 100,000,000°C, that the low-velocity disintegration results are wrong, or that there is some other process producing Li^7 in the sun.

EDWIN MCMILLAN*

Department of Physics,
University of California,
July 17, 1933.

[1] Hughes, Phys. Rev. **38**, 857 (1914).
[2] Kent, Astrophys. J. **40**, 337 (1914).
[3] King, Astrophys. J. **44**, 169 (1916).
[4] Russell, Adams and Moore, Astrophys. J. **68**, 1 (1928).
* National Research Fellow.

Inability of X-Rays to Decompose Water

Measurements by Risse[1] did not show any decomposition of air-free water by x-rays. We have re-examined this problem with more accurate methods of analysis. Carbon dioxide, oxygen and hydrogen were determined by means of a Van Slyke apparatus, and hydrogen peroxide by electrometric titration, both methods being sensitive to about 1 micromol per liter. Air-free water was irradiated in glass sealed 20 cc Pyrex flasks with dosages up to 150 kiloroentgen. Hydrogen peroxide and oxygen were not found. A few micromols/liter of carbon dioxide and hydrogen were usually produced, but this amount did not depend on the dosage above a few kiloroentgen, and is ascribed to organic impurities. This view has been confirmed by a study of the action of x-rays on solutions of organic substances. It is concluded that pure air-free water is not decomposed by x-rays. This result, by its contrast to observations with radioactive rays, raises an interesting problem which we expect to investigate using α- and β-rays from radon under our experimental conditions.

HUGO FRICKE
E. R. BROWNSCOMBE

The Walter B. James Laboratory for Biophysics,
The Biological Laboratory,
Cold Springs Harbor, L. I., N. Y.,
July 22, 1933.

[1] O. Risse, Zeits. f. physik. Chemie **A140**, 133 (1929).